NAVAL POSTGRADUATE SCHOOL
Monterey, California

THESIS

DEVELOPMENT AND VERIFICATION OF AN AERODYNAMIC MODEL FOR THE NPS FROG UAV USING THE CMARC PANEL CODE SOFTWARE SUITE

by

Stephen J. Pollard

September 1998

Thesis Advisor: Max F. Platzer
Co-Advisor/Second Reader: Kevin D. Jones

Approved for public release; distribution is unlimited.

REPORT DOCUMENTATION PAGE

Form Approved
OMB No. 0704-0188

1. AGENCY USE ONLY *(Leave blank)*	2. REPORT DATE	3. REPORT TYPE AND DATES COVERED
	September 1998	Aeronautical Engineer Thesis

4. TITLE AND SUBTITLE
DEVELOPMENT AND VERIFICATION OF AN AERODYNAMIC MODEL FOR THE NPS FROG UAV USING THE CMARC PANEL CODE SOFTWARE SUITE

5. FUNDING NUMBERS

6. AUTHOR(S)
Pollard, Stephen J.

7. PERFORMING ORGANIZATION NAME(S) AND ADDRESS(ES)
Naval Postgraduate School
Monterey, CA 93943-5000

8. PERFORMING ORGANIZATION REPORT NUMBER

9. SPONSORING / MONITORING AGENCY NAME(S) AND ADDRESS(ES)

10. SPONSORING / MONITORING AGENCY REPORT NUMBER

11. SUPPLEMENTARY NOTES
The views expressed in this thesis are those of the author and do not reflect the official policy or position of the Department of Defense or the U.S. Government.

12a. DISTRIBUTION / AVAILABILITY STATEMENT
Approved for public release; distribution is unlimited.

12b. DISTRIBUTION CODE

13. ABSTRACT *(maximum 200 words)*

The CMARC panel-code is evaluated for the development of an aerodynamic model of the Naval Postgraduate School FROG Unmanned Air Vehicle (UAV). CMARC is a personal computer hosted panel-code software suite for solving inviscid, incompressible flow over complex three-dimensional bodies. A panel model of the NPS FROG UAV is developed to obtain stability derivative data at the cruise flight condition. Emphasis is placed on comparing the CMARC data to aerodynamic models obtained from classical design techniques and parameter estimation. Linearized longitudinal and lateral-directional state-equation models are used to compare the dynamic response of each data set. In addition, CMARC is used to generate static-source and angle-of-attack sensor position corrections. Position corrections are provided in look-up table and curve-fit formats. The aerodynamic model obtained with CMARC demonstrated higher fidelity dynamic longitudinal response than the classical design model. Dynamic lateral-directional response is similar to that obtained from classical design techniques. Adjustment through comparison with flight-test data is still required to optimize the CMARC model. Future studies should concentrate on improving CMARC modeling of fuselage side force through the addition of wake separation lines. Additionally, the propeller disk should be modeled in an attempt to capture the effects of increased dynamic pressure over the horizontal and vertical tail surfaces.

14. SUBJECT TERMS
Unmanned Aerial Vehicles, UAV, CMARC, Panel Method Ames Research Center, PMARC, Panel Code, Stability Derivatives, Boundary Layer Code, Aircraft Dynamic Response

15. NUMBER OF PAGES
195

16. PRICE CODE

17. SECURITY CLASSIFICATION OF REPORT	18. SECURITY CLASSIFICATION OF THIS PAGE	19. SECURITY CLASSIFICATION OF ABSTRACT	20. LIMITATION OF ABSTRACT
Unclassified	Unclassified	Unclassified	UL

NSN 7540-01-280-5500

Standard Form 298 (Rev. 2-89)
Prescribed by ANSI Std.

Approved for public release; distribution is unlimited

DEVELOPMENT AND VERIFICATION OF AN AERODYNAMIC MODEL FOR THE NPS FROG UAV USING THE CMARC PANEL CODE SOFTWARE SUITE

Stephen J. Pollard
Commander, United States Navy
M.S., Naval Postgraduate School, 1997

Submitted in partial fulfillment of the
requirements for the degree of

AERONAUTICAL AND ASTRONAUTICAL ENGINEER

from the

NAVAL POSTGRADUATE SCHOOL
September 1998

Author: Stephen J. Pollard

Approved by: Max F. Platzer, Thesis Advisor

Kevin D. Jones, Co-Advisor/Second Reader

Gerald H. Lindsey, Chairman
Department of Aeronautics and Astronautics

ABSTRACT

The CMARC panel-code is evaluated for the development of an aerodynamic model of the Naval Postgraduate School FROG Unmanned Air Vehicle (UAV). CMARC is a personal computer hosted panel-code software suite for solving inviscid, incompressible flow over complex three-dimensional bodies. A panel model of the NPS FROG UAV is developed to obtain stability derivative data at the cruise flight condition. Emphasis is placed on comparing the CMARC data to aerodynamic models obtained from classical design techniques and parameter estimation. Linearized longitudinal and lateral-directional state-equation models are used to compare the dynamic response of each data set. In addition, CMARC is used to generate static-source and angle-of-attack sensor position corrections. Position corrections are provided in look-up table and curve-fit formats. The aerodynamic model obtained with CMARC demonstrated higher fidelity dynamic longitudinal response than the classical design model. Dynamic lateral-directional response is similar to that obtained from classical design techniques. Adjustment through comparison with flight-test data is still required to optimize the CMARC model. Future studies should concentrate on improving CMARC modeling of fuselage side force through the addition of wake separation lines. Additionally, the propeller disk should be modeled in an attempt to capture the effects of increased dynamic pressure over the horizontal and vertical tail surfaces.

TABLE OF CONTENTS

I. INTRODUCTION

A. BACKGROUND

Computational fluid dynamics (CFD) is increasingly used as a design and analysis tool. As the price of computer hardware drops and computational power increases, CFD becomes more attractive to a larger audience. CFD tools range from the high-end three-dimensional (3D) Navier-Stokes solvers for compressible, viscous fluids to potential flow solvers for incompressible, inviscid flows. This paper discusses the development of an aerodynamic model of the Naval Postgraduate School (NPS) Fiber Optic Guided (FROG) Unmanned Air Vehicle (UAV) using a personal computer hosted panel code.

Validation of the Personal Simulation Works panel code software and initial FROG UAV modeling was completed in June 1997. Results are reported in Ref. [1]. This study expands on the modeling effort to include the development of a complete aerodynamic model at the trim flight condition. Stability derivative data are obtained from the panel code and then compared to data from classical design calculations and parameter estimation. A linearized state space simulation is used to extract the air vehicle dynamic modes and to model control response. Results are compared for all three data sets.

The Personal Simulation Works software suite, consisting of LOFTSMAN, CMARC and POSTMARC, is used for all aspects of the study. The software provides for panel model development, input file processing and the visualization of results. Emphasis is placed on verifying both the accuracy and suitability of the CFD programs for aerodynamic modeling.

Until recently, personal computers (PC) did not have the computational power or memory to be practical for panel code CFD programs. Things have changed with the introduction of the Pentium class PC and low cost RAM. AeroLogic capitalized on the power of the Pentium class PC and developed Personal Simulation Works (PSW). PSW is based on the 3D, low order, inviscid potential flow solver named CMARC. CMARC is a re-hosted version of NASA's Panel Method Ames Research Center (PMARC). PMARC was re-written in the C language and compiled for IBM compatible PCs. CMARC runs under the DOS operating system. It will also run in a DOS window under the WINDOWS 3.x, 95 or NT operating systems. Enhanced capabilities include; improved memory management, an expanded set of command line switches and

provisions for expanded boundary layer post-processing capabilities. However, the core processing algorithms remain the same as implemented in PMARC.

LOFTSMAN, the PSW pre-processing program, is used to mesh complex 3D bodies and create input file patches. The program runs under the Windows operating system and allows the user to loft conics based 3D surfaces. The program automatically creates CMARC, PMARC or VSAERO input patches based on desired panel densities and distribution.

POSTMARC is used for flow visualization and integration of resultant forces. It runs under the Windows 3.x, 95 and NT operating systems. POSTMARC reads CMARC or PMARC output files and provides for the visualization of model geometry, wake stepping, on and off-body streamlines and surface phenomena.

B. REQUIREMENTS

The Naval Postgraduate School Aeronautics Department is integrating UAV hardware and software to demonstrate autonomous flight, trajectory tracking and automatic landing. Closed-loop flight control development requires a valid aerodynamic truth model for the UAV airframe. The introduction of each new airframe requires the development of a new aerodynamic truth model. Most recently, Papageorgiou [Ref. 2] developed and tested an aerodynamic model for the NPS FROG UAV based on classical methods. His model produced a close match to flight test results in the longitudinal axis. However, the lateral-directional axis required modifications based on measured flight test data to produce acceptable results. With the availability of low cost panel code CFD capabilities, it is suggested that a panel code model of the FROG UAV will provide more refined stability derivative data for an initial aerodynamic model.

In addition to a valid truth model, accurate pitot-static and angle-of-attack sensors are required for highly augmented flight control systems. CMARC is well suited for solving on-body static pressure distributions and off-body flow velocities over the predominately attached flow fields of a fuselage forebody. This proves particularly useful for generating pitot-static and angle of attack correction curves and look-up tables.

C. STATEMENT OF OBJECTIVES

The Naval Postgraduate School Aeronautics Department has both active CFD research and avionics development programs. The primary purpose of this investigation

is to verify the accuracy and suitability of the PSW software suite for developing an aerodynamic model of the NPS FROG UAV. Specific objectives are as follows:

- Demonstrate panel code modeling, processing and visualization on a Pentium PC using the PSW software package.
- Develop and analyze a panel code model for the NPS FROG UAV using PSW to obtain a complete set of stability derivatives at the cruise trim condition.
- Verify the aerodynamic model through comparison to data obtained from classical design calculations and parameter estimation.
- Demonstrate techniques for producing angle-of-attack vane and pitot-static correction curves.
- Develop a user guide that outlines PSW panel code modeling for the extraction of stability derivatives.

II. OVERVIEW OF PERSONAL SIMULATION WORKS

A. GENERAL

Personal Simulation Works is a PC based software suite that provides for the three primary CFD requirements; 3D modeling of an aircraft (LOFTSMAN), panel code flow solver (CMARC), and post-processing of the computed flow field (POSTMARC). The software package contains three applications hosted on the IBM compatible personal computer. Each software program is discussed separately.

B. LOFTSMAN

LOFTSMAN is a Windows hosted 3D modeling tool that generates surface panel distributions for CMARC or PMARC input files. The program is based on conics, which allows rapid lofting of streamlined bodies such as aircraft fuselages and engine nacelles. In addition, wing and control surfaces can be designed with the extensive library of airfoil templates or with user specified coordinates. The software is well documented, including a tutorial, in the Personal Simulation Works User Guide [Ref. 3]. LOFTSMAN is primarily designed for creating new objects, but an existing airframe can be matched quite closely with just a detailed three-view drawing that includes frame cross sections. Appendix A outlines the development of the FROG UAV model.

1. Streamlined Bodies

LOFTSMAN functionality is divided into Body Objects and Wing Objects. In general, they remain separate unless the intersection between a wing and body is required.

Body Objects are created using a family of curves called second-degree conics. Circles, ellipses, parabolas and hyperbolas are among this group. An entire fuselage is described by specifying just four lines. These are the top waterline (TW), bottom waterline (BW), the maximum breadth line (MB) and the waterline of the maximum breadth line (WW). For each line, the beginning, ending and a few points along the line are specified. Control points are also specified with a curvature factor that allows LOFTSMAN to generate a smooth conic between the points. The power of conic lofting will become evident when discussing the modeling of the complex FROG UAV fuselage in Chapter V.

2. Wings and Control Surfaces

Wings and control surfaces are easily specified in LOFTSMAN using a short input file created with any text editor. The file specifies root, intermediate and tip rib section, location, axis, chord and incidence. LOFTSMAN then fairs a smooth surface through the rib sections. Washout is specified by varying the incidence of the root and tip ribs. Sweep-back is controlled by staggering the tip rib location with respect to the root rib. Once the general wing surface is specified, control surfaces such as ailerons, flaps and elevators can be deflected and meshed.

3. Patches

LOFTSMAN automatically meshes 3D surfaces and creates patches for CMARC/PMARC input files. The distinction between a mesh and a patch is important. A mesh is a set of quadrilateral and triangular panels that represent the surface of a wing or body. When the set of panels is organized and formatted to create a sub-component portion of a CMARC or PMARC input file, it is called a patch.

A body or wing surface is first meshed at a density specified by the user. Panel compression options include cosine and half-cosine spacing. After meshing the object, one saves it to a text file as a formatted patch. One then opens the patch file with any text editor and copies/pastes the patch text into the appropriate location in the CMARC input file.

Each control surface deflection requires a separate mesh and formatted patch. For instance, to evaluate roll performance one needs to separately mesh an upward aileron deflection on the right wing and a downward deflection on the left wing. If multiple deflections of a single control surface are required, each deflection must be meshed separately.

C. CMARC

CMARC is the C version of PMARC low-order, 3D panel code. Inviscid, irrotational, incompressible, potential flow is assumed. Low-order means that source and doublet strength distribution is constant across a panel. There is no attempt to match the source or doublet strength of an adjacent panel at a common edge. Advanced features include internal flow modeling and time stepping wake models.

PMARC version 12.19 was released as FORTRAN 77 source code in 1992. CMARC was rewritten in the C language and compiled for hosting on IBM compatible personal computers by AeroLogic, Inc. The program runs under the DOS operating system. It will also run in a DOS window from Windows 3.1, 95 or NT. Enhanced features include command-line options and flexible memory management. Command line options simplify batch processing by adding an extensive set of switches that can be set external to the CMARC input file. Flexible memory management provides for the automatic sizing of arrays without having to recompile the source code.

D. POSTMARC

POSTMARC is a Windows post-processing program for the visualization of CMARC and PMARC output files. Capabilities include body geometry, wake stepping, surface pressure and streamline visualization. POSTMARC also provides the capability to integrate pressure and skin friction forces over the model geometry. This proves particularly useful when one desires to recalculate loads around a different center of gravity.

An interesting feature for design work is the integration of panel surface area to obtain total wetted area. After lofting a new geometry in LOFTSMAN, a quick check of geometry is made by running CMARC with the -g command line toggle. The total wetted area is then checked in POSTMARC. This function is particularly useful when working to reduce skin friction drag.

Versions 1.17.3 and later of POSTMARC include the capability to integrate skin friction drag coefficient over the model geometry. It is important to note that a key piece of the drag equation is missing from a POSTMARC solution. CMARC provides induced drag from the surface pressure distribution and skin friction drag from the 2D boundary layer code. Skin friction is only calculated up to the point of boundary layer separation. Pressure drag due to separation, a major portion of the drag equation, is missing from a CMARC/POSTMARC solution.

In fact, if one isn't careful, POSTMARC drag calculations can be misleading. Take for instance two similar model configurations with only minor geometry differences that do not affect wetted area. It is possible for the model with more flow separation to have less skin friction drag because there is no CMARC output for skin friction coefficient after the boundary layer code predicts separation. During iterative design

work, this could lead to the incorrect conclusion that the design team is reducing overall drag. Perhaps a better function for LOFTSMAN than integrated skin friction drag would be a function that predicts the percentage of attached flow and laminar flow. Iterative design changes could be made that maximize laminar flow and minimize separated flow.

III. CMARC PANEL CODE THEORY

A. POTENTIAL FLOW PANEL CODE THEORY (CMARC/PMARC)

Potential flow theory involves the superposition of sources and doublets to generate the desired flow field around a 3D body. It assumes inviscid, irrotational and incompressible flow. As such, valid solutions are only obtained at low Mach numbers and for flow fields without large areas of separation.

The basic concept of panel methods, as outlined by Bertin and Smith [Ref. 4], requires the modeling of the desired 3D configuration with a large number of quadrilateral and triangular panels representing the surface of the aircraft. A series of sources, doublets and vortices is then distributed on each panel. Superposition allows the simultaneous computation of the singularity strengths required to satisfy flow tangency on the surface. The inviscid, irrotational and incompressible flow field represented by the superposition of sources and doublets satisfies the Laplace equation:

$$\nabla^2\Phi = 0 \qquad 3.1$$

Using Green's Theorem, the potential at any point P in the flow is represented by:

$$\Phi_P = \frac{1}{4\pi}\iint_{S+W}(\Phi - \Phi_i)\bar{n}\nabla\left(\frac{1}{r}\right)dS - \frac{1}{4\pi}\iint_{S+W}\left(\frac{1}{r}\right)\bar{n}\cdot(\nabla\Phi - \nabla\Phi_i)dS \qquad 3.2$$

Where $(\Phi - \Phi_i)$ represents the potential from the doublet distribution and $\bar{n}\cdot(\nabla\Phi - \nabla\Phi_i)$ represents the potential from the source distributions.

CMARC is a low order panel code that assumes constant source and doublet strength distributions across each panel. Figure 3.1 shows a panel layout for a generic 3D wing fuselage configuration. It is important to note that for a 3D solution, there is an equivalence to surface doublet and surface vortex distributions. CMARC implements source and doublet distributions.

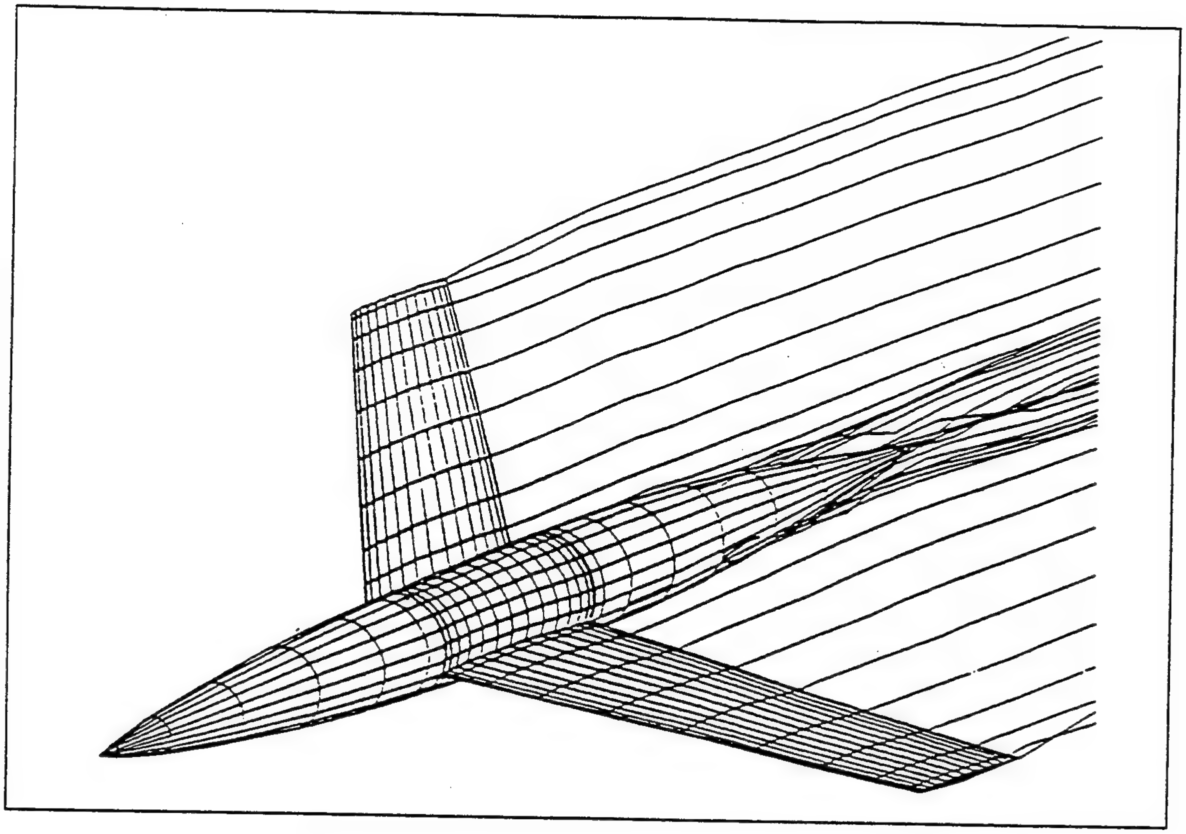

Figure 3.1 Typical Wing/Body Panel Code Configuration, from Ref. [5].

As mentioned previously, the general boundary condition imposed is tangential flow at the surface. CMARC, as outlined in Ref. [3], allows the modification of this boundary condition on individual panels or groups of panels. A normal surface velocity distribution may be specified to simulate flow into or out of ducts.

In order to produce lift, a potential flow panel code requires a method to implement the Kutta condition. As noted in Anderson [Ref. 6], the Kutta condition at the trailing edge implies that the circulation, Γ, around an airfoil is such that the flow exits the trailing edge smoothly. In addition, the velocities leaving the top and bottom surfaces are finite and equal in magnitude and direction.

Panel codes impose the Kutta condition by the shedding of wake panels along the trailing edges or separation lines. Wake panels are similar to a surface panel with only a doublet distribution. The doublet strength of the attached wake panel equals the difference in doublet strengths of the two adjacent surface panels.

The CMARC core panel code processing engine is functionally equivalent to the PMARC panel code module. The implemented equations are well documented by Ashby et al. [Ref. 5]. The PMARC documentation includes a wing-body combination, shown in Figure 3.1, evaluated by PMARC with good correlation to experimental data. The results are shown in Figures 3.2 and 3.3. In addition, Lambert [Ref. 7] compared PMARC panel code results to several theoretical and experimental test cases with good correlation at low angle-of-attack. Sensitivity to wake placement is highlighted by his studies.

Wake positioning can have a large influence on potential flow solutions. A wake is obviously attached to the trailing edge of wings and control surfaces with sharp, thin trailing edges to produce the Kutta condition. However, wake positioning on streamlined fuselages, missile airframes and nacelles is more of an art than science. Recently, Tuncer and Platzer [Ref. 8] investigated generalized wake placement techniques for cylindrical bodies of revolution with good correlation to experimental data at up to 20 degrees angle-of-attack. The techniques were used with success by this author in Ref. [1] for the verification of CMARC calculations for flow over an inclined 6:1 prolate spheroid.

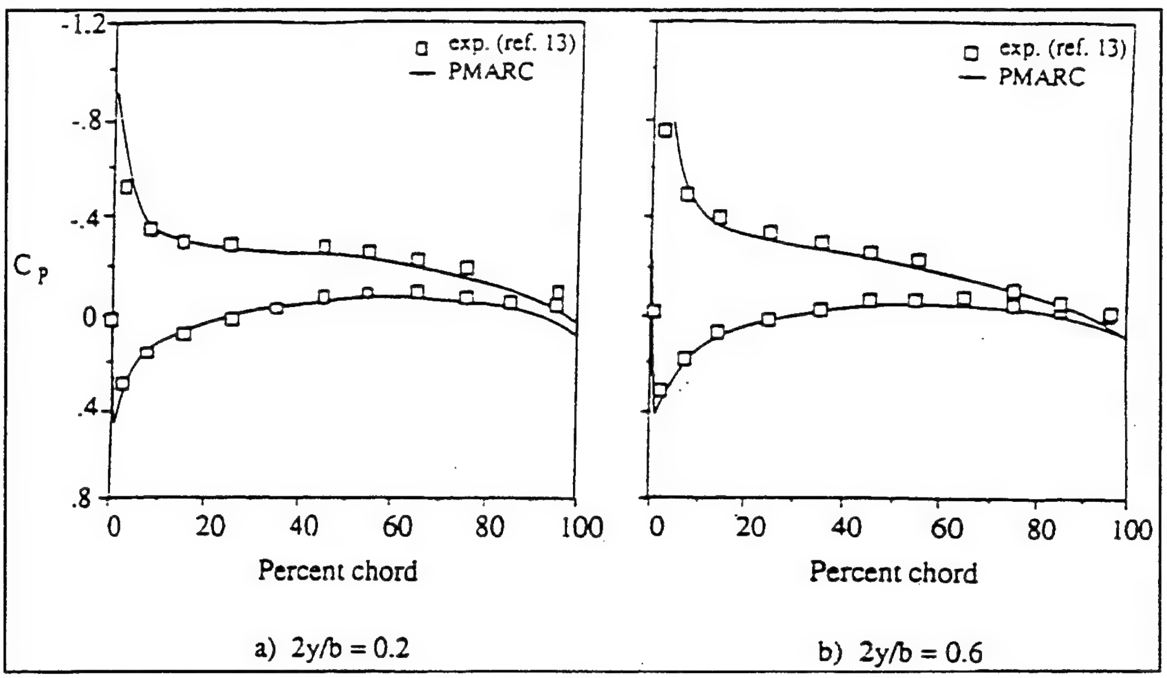

Figure 3.2 Comparison of Experimental Data and PMARC Results for Two Spanwise Stations of the Wing/Body ($\alpha = 4°$), from Ref. [5].

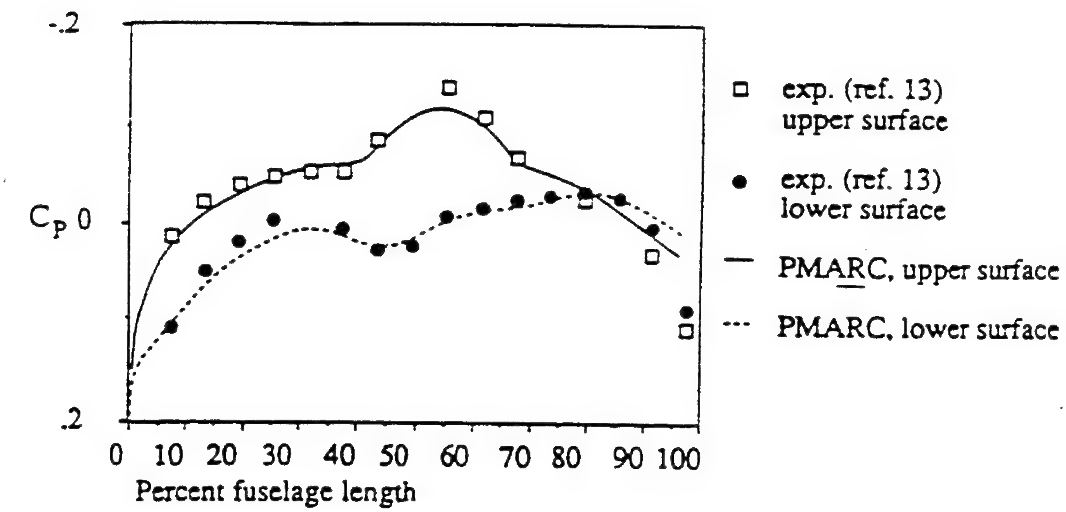

Figure 3.3 Comparison of Experimental Data and PMARC Along the Fuselage Centerline of the Wing/Body Configuration ($\alpha = 4°$), from Ref. [5].

B. CMARC BOUNDARY LAYER ANALYSIS THEORY

CMARC and PMARC use the same two-dimensional integral method to calculate boundary layer characteristics along a surface streamline. A transition model automatically switches from laminar to turbulent calculations. The developers of the PMARC code chose a 2D integral routine over a 3D finite difference grid method due to speed and robustness of the calculations [Ref. 5]. Building a finite difference grid is a difficult and time consuming process requiring the user to develop grids over complex 3D surfaces. In addition, boundary layer calculation times can easily exceed that required for the basic potential flow solution. Reference [9] gives a good outline of three-dimensional finite difference methods.

The CMARC and PMARC User's Guides [Refs. 3 and 5] contain detailed discussions on the development of the CMARC/PMARC boundary layer code starting from the two-dimensional momentum equation:

$$\frac{d\theta}{d\eta} + (2 + H) * \frac{\theta}{U}\frac{dU}{d\eta} = \frac{1}{2}C_f \tag{3.3}$$

The momentum integral equation is numerically integrated along a surface streamline.

The laminar region of the boundary layer is modeled by numerically integrating the following exact differential equation. The equation is solved iteratively through numerical integration along a streamline starting at a stagnation point [Ref. 5]:

$$\theta(\eta)^2 = \frac{0.45\nu}{U(\eta)^6}\int_0^{\eta}\left(1 + 2.222g(K,\mu)\right)U(\eta)^5\,d\eta + \theta(0)^2\left(\frac{U(0)}{U(\mu)}\right)^6 \tag{3.4}$$

where: U - velocity at outer edge of boundary layer

θ - momentum thickness

$K = \frac{\theta^2}{\nu}\frac{dU}{d\eta}$

η - generalized coordinate along a streamline

The value g(K,u) is based on exact solutions for a number of pressure distributions. Initial work was conducted by Thwaites with improvements by Curle [Ref. 10]:

$$g(K,\mu) = F_0(K) - \mu G_0(K) - 0.45 + 6K \tag{3.5}$$

CMARC uses an empirical transition model based on the average pressure gradient, $\overline{K}$, for predicting laminar to turbulent transition. The following relations are used to calculate the transition point [Ref. 5]:

$$\overline{K} = \frac{\int_{\eta_{ins}}^{\eta} K d\eta}{\eta - \eta_{ins}} \qquad 3.6$$

where η_{ins} is the streamline coordinate at instability. And, K is the local pressure gradient at boundary layer instability [Ref. 5]:

$$K = -0.4709 + 0.11066 * \ln(\mathrm{Re}_\theta) + 0.0058591 * \ln^2(\mathrm{Re}_\theta) \qquad (0 \le \mathrm{Re}_\theta \le 650)$$
$$K = 0.69412 - 0.23992 * \ln(\mathrm{Re}_\theta) + 0.0205 * \ln^2(\mathrm{Re}_\theta) \qquad (650 < \mathrm{Re}_\theta \le 10000) \qquad 3.7$$

The local Reynolds number at transition is correlated to $\overline{K}$ with the following expressions [Ref. 5]:

$$\overline{K} = -0.0925 + 0.00007 * \mathrm{Re}_\theta \qquad (0 \le \mathrm{Re}_\theta \le 750)$$
$$\overline{K} = -0.12571 + 0.000114286 * \mathrm{Re}_\theta \qquad (750 < \mathrm{Re}_\theta \le 1100) \qquad 3.8$$
$$\overline{K} = 1.59381 - 0.45543 * \ln(\mathrm{Re}_\theta) + 0.032534 * \ln^2(\mathrm{Re}_\theta) \qquad (1100 < \mathrm{Re}_\theta \le 3000)$$

At transition, the initial turbulent shape factor, H, is given by the following empirical formula that is a fit to data developed by Coles [Ref. 10]:

$$H = \frac{1.4754}{\log_{10}(\mathrm{Re}_\theta)} + 0.9698 \qquad 3.9$$

Provisions are made to check for turbulent reattachment if laminar separation is encountered. At laminar separation, a point calculation is made to determine if the boundary layer will reattach. If reattachment is predicted, the boundary layer code immediately switches to turbulent calculations. No attempt is made to model the laminar separation bubble or provide a transition length. After laminar separation is predicted, the following empirical relations are used to determine if reattachment occurs [Ref. 5]:

$$K = 0.0227 - 0.007575 * \mathrm{Re}_\theta - 0.000001157 * \mathrm{Re}_\theta^{\,2} \qquad (\mathrm{Re}_\theta \ge 125)$$

$$K = -0.09 \qquad (\mathrm{Re}_\theta < 125) \tag{3.10}$$

The boundary layer code in CMARC uses a point transition model. No attempt is made to model a more representative transition length. Turbulent calculations begin at transition using the Nash-Hicks model [Ref. 5]. Calculations continue along the streamline until turbulent separation is predicted or the end of the streamline is reached. No boundary layer data is available after separation.

The authors of PMARC caveat that their boundary layer calculations are quite accurate for predominately 2D flow but break down in regions of large cross flow near separation. This premise was tested in Reference [1] by comparing the predominately 2D flow over the inboard region of a high aspect ratio wing to the finite difference calculations performed by the Naval Postgraduate School Unsteady Potential Flow Code (UPOT). In general, CMARC provided correct trends for both the transition and separation points. However, in all cases, CMARC predicted early transition and late flow separation. As expected, the differences were greatest at lower Reynolds numbers where boundary layer thickness is larger.

Reference [1] also modeled flow over an inclined prolate spheroid. The 6:1 prolate spheroid was chosen because extensive experimental data is available. In addition, the three-dimensional flow around a prolate shperoid is similar to a streamlined slender fuselage. With proper wake placement, CMARC was found to produce accurate normal force and pitching moment coefficients. Over the three-dimensional body, CMARC boundary layer calculations also predicted early transition and late flow separation. Despite inaccuracies, CMARC boundary layer calculations remained useful when used as a design tool for visualizing the trend in transition and separation points with configuration changes.

IV. AERODYNAMIC MODEL OF THE FROG UAV

A. BACKGROUND

The Naval Postgraduate School Aeronautics Department is integrating UAV hardware and software to demonstrate autonomous flight, trajectory tracking and automatic landing. A core requirement for flight control law development is a valid aerodynamic truth model for the UAV airframe. A panel code model of the FROG UAV is one method for estimating many of the stability derivatives required for an aerodynamic truth model. This development effort concentrates on finding the static, rate damping and control power derivatives for both the longitudinal and lateral-directional axes.

Panel code modeling usefulness goes beyond the development of aerodynamic coefficients. Flight control systems require accurate pitot-static and angle-of-attack sensor inputs. CMARC accurately solves on-body static pressure distributions and off-body flow velocities over the predominately attached flow fields of fuselage fore bodies. In this study, correction curves are generated for static source and angle-of-attack probe position errors.

B. FROG UAV DESCRIPTION

The FROG UAV is a small single engine flight test vehicle used for autonomous flight research by the Naval Postgraduate School Aeronautics Department. The aircraft was originally designated the FOG-R by the U. S. Army. It was designed as a small lightweight, battlefield observation platform that could be guided by a fiber optic data link. Table 4.1 presents the basic aircraft specifications.

The aircraft is somewhat unconventional in that the engine is mounted in a nacelle tractor style above the fuselage and wing. The aft fuselage consists of a 1.75 inch diameter aluminum tube which connects the tail surfaces to the main fuselage. Figure 4.1 displays a three view drawing of the FROG UAV.

PARAMETER	MEASUREMENT/UNITS	
Length	8.125 ft	97.5 in
Height	1.75 ft	21 in
Weight	67.7 lbs	
Power Plant	12 Hp / 2 Cycle	
Wing Airfoil	NACA 2415	
Horiz. Stab. Airfoil	NACA 0006 (Approx.)	
$S_w (S_{ref})$	17.57 ft^2	2530 in^2
S_t	3.174 ft^2	457.1 in^2
S_v	0.9818 ft^2	141.4 in^2
c	1.66 ft	20 in
c_t	0.958 ft	11.5 in
b_w	10.54 ft	126.5 in
b_t	3.313 ft	39.75 in
b_v	1.25 ft	15.0 in
l_t	4.44 ft	53.25 in
l_v	4.44 ft	53.25 in
AR_w	6.32	
AR_t	3.46	
AR_v	1.59	
V_H	0.49	
V_v	0.16	

Table 4.1 FROG UAV Characteristics, after Ref. [2].

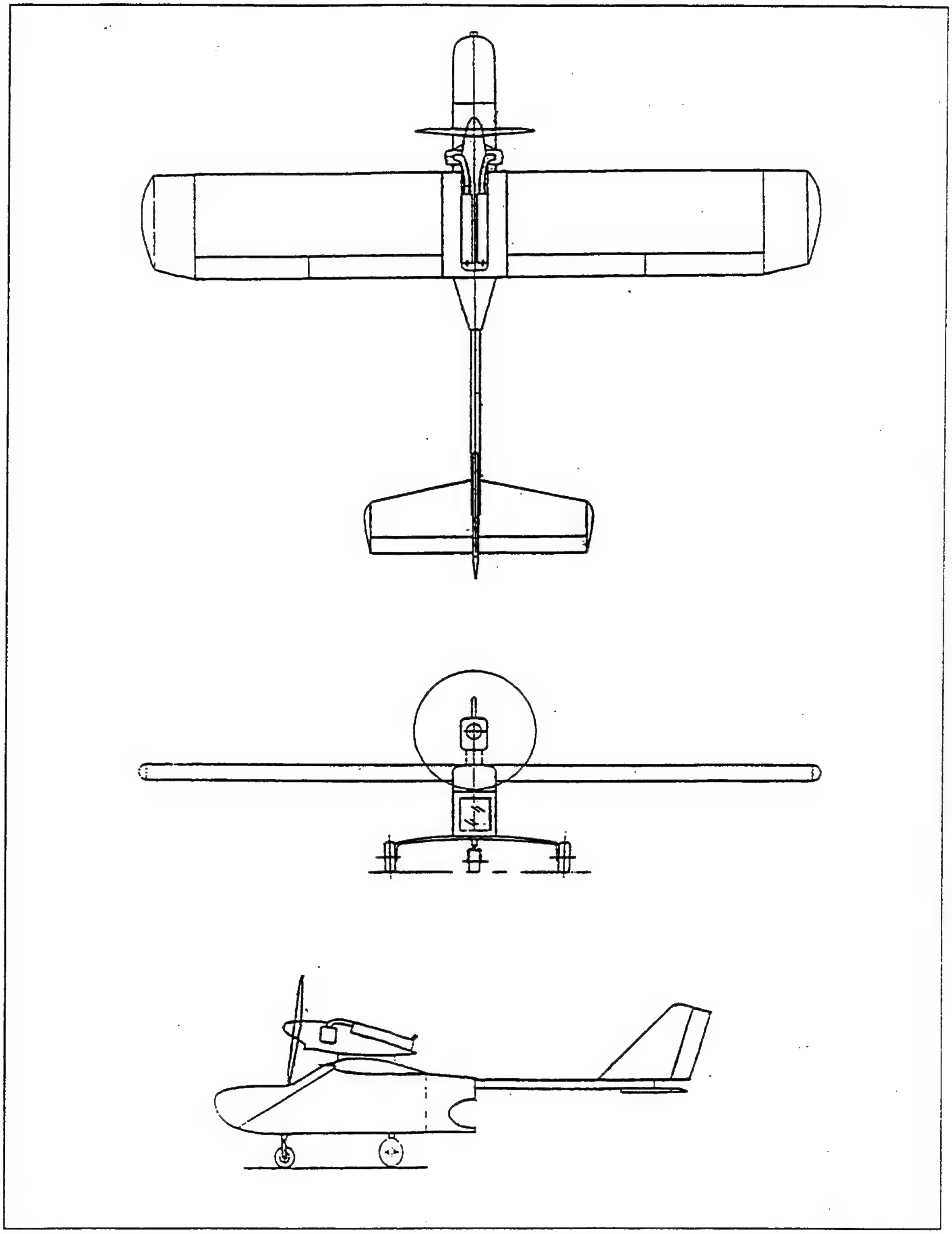

Figure 4.1 FROG UAV Three-View Drawing.

The FROG UAV, as operated by NPS, is equipped with airspeed, angle-of-attack, altitude and control surface sensors. In addition, a miniature Inertial Measurement Unit (IMU) captures aircraft attitude, acceleration and body rates. Data is down linked to a mobile SGI workstation through a spread spectrum modem. Onboard GPS provides differential GPS navigation capability with the ground station used as a reference. The aircraft can be flown by conventional radio control or by up-linking flight control commands from the SGI workstation.

Current flight control development requires a linearized aerodynamic model around the cruise trim point of 60 m.p.h. or 88 ft/s. This flight condition is selected for the development of stability derivative data with CMARC. Table 4.2 lists the aircraft parameters for the trim flight condition.

PARAMETER	MEASUREMENT	UNITS
Weight	67.73	lbs
IXX	12.52	slug-ft^2
IYY	8.43	slug-ft^2
IZZ	18.55	slug-ft^2
Airspeed	60/88	mph and ft/s
Altitude	800	ft MSL
Air Density	0.002327	slug/ft$_3$
Center of Gravity	34.5%	M.A.C
$C_{L\ trim}$	0.4295	n/a
$\alpha_{trim\ (est)}$	-0.04	degrees
δ_{Etrim}	5.1	degrees

Table 4.2 FROG UAV Trim Flight Condition, after Ref.[2].

C. FROG UAV MODELING

1. General

LOFTSMAN is utilized for the creation of all CMARC input file patches except for wing tips. In some cases, CMARC's more efficient built-in capability to model standard NACA 4-digit wing surfaces could be used. However, with the requirement to mesh deflected control surfaces, all patches are created with LOFTSMAN from the start. The complete FROG UAV model with all patches activated is displayed in Figure 4.2.

Appendix A contains detailed descriptions of obtaining stability derivative data in a less formal user guide format.

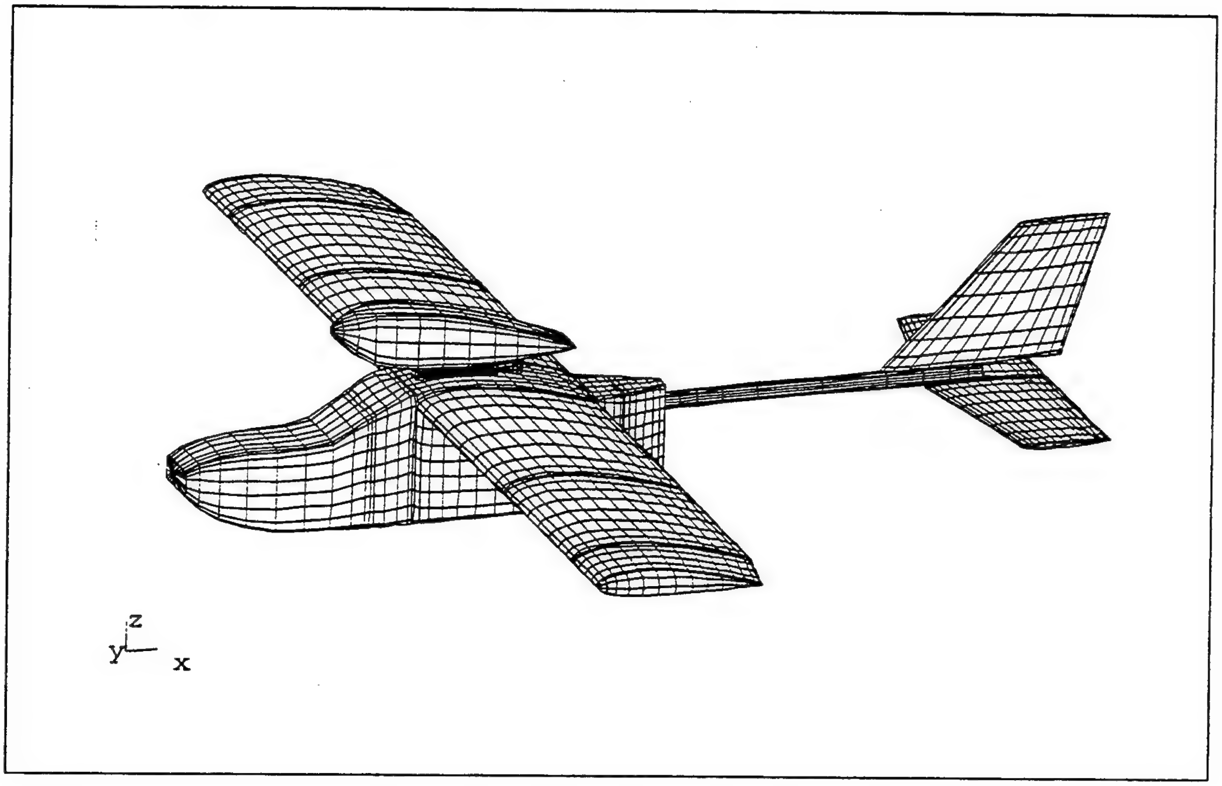

Figure 4.2 FROG UAV Panel Code Model with All Patches Activated.

Some assumptions are made to simplify the modeling process. First, the horizontal and vertical stabilizers are modeled with a NACA 0006 section. The actual surfaces are constructed with a flat section, rounded at the nose and tapered starting at the control surface hinge line to a sharp trailing edge. The NACA 0006 provides a close approximation and allows the use of LOFTMAN's built-in wing lofting capability. For a potential flow solution, this simplification is considered minor.

A second simplification is made regarding the vertical stabilizer's tip rib orientation. The actual rib is canted down 5° with respect to the longitudinal waterline. LOFTSMAN will only model a chord line that is parallel to the waterline (constant BL). Thus, for this study, the vertical tail tip rib is modeled with a constant BL, but the span is adjusted to maintain the same overall surface area.

A third assumption is made regarding aileron control surface hinge lines. The actual FROG UAV ailerons are piano hinged along the upper surface. For simplification of the LOFTSMAN model, all surfaces are hinged at the centerline.

Finally, there is no attempt to model the tricycle landing gear struts or wheel assemblies. The landing gear components do not contribute significantly to the aerodynamic stability derivatives. However, they certainly need to be taken into account when measuring moments of inertia for a dynamic model.

2. Modeling Coordinate System

The model is developed using a coordinate system selected to simplify fuselage measurements. The +x-axis starts even with the nose and runs aft along the bottom of the fuselage, parallel with the tail boom. The bottom of the fuselage is used as the waterline with +z-axis in the up direction. This allows for easy vertical measurements when the aircraft is placed flat on a horizontal surface. The +y-axis runs from centerline outboard parallel to the right wing. Figure 4.3, which displays static-pressure source and alpha vane locations, also shows the location and origin of the modeling coordinate system.

3. LOFTSMAN Patches

LOFTSMAN is used to generate all the model patches except for wing tips. CMARC's built-in capability is used to create wing tip patches. Appendix B contains listings of all the LOFTSMAN input files. Once a surface is meshed, the mesh is saved to a file as a CMARC/PMARC patch. The resulting text file is then opened, and the text is copied and pasted with any text editor into the patch definition section of the CMARC input file. LOFTSMAN patch files are not listed because they are redundant with the patches in the final CMARC input file listed in Appendix C. Multiple patches for the same control surface may be stored in the input file. For instance, two horizontal stabilizer patches with different elevator deflection angles may be kept in the CMARC input file. However, only one may reside in the active patch input section. All other patches for the same aircraft component must reside after the patch with the "last patch" toggle set (TNODS=5).

When saving a patch, LOFTSMAN automatically takes care of all CMARC input formatting. A patch, as formatted by LOFTSMAN, assumes additional patches will follow in the CMARC input file. Therefore, the last segment's TNODS variable is set TNODS=3. When the patch is the last patch in the input file, the TNODS variable must be manually set to TNODS=5. If CMARC hangs up while reading in geometry information, most likely TNODS=5 is missing on the last patch.

a. Fuselage Model

The fuselage is lofted as a B-type body. A B-type body is used when major portions of the fuselage have a circular or oval cross section. The input file is listed in Appendix B. Only the right side is meshed, with a symmetric left side created by toggling the IPATSYM variable to IPATSYM=1. LOFTSMAN assumes that B-type bodies converge to a specific point at the fore and aft ends. The flat aft fuselage face does not provide this single point. A slight modification was made to the aft face to allow automatic meshing as a B-type body. The center of the aft face is extended very slightly, approximately 1/8 inch, to provide a convergence point for the final rear triangular panels. This small deviation is assumed not affect the aerodynamic fidelity of the model for a potential flow solution.

The right side was originally meshed separately from the wing as a 20 x 20 panel patch. This created a low order fit when the wing patch was butted to the side of the fuselage, resulting in overlapping panels. A final mesh was created that flowed around the wing root and fuselage intersection for a high order fit. All the fuselage panels at the wing root join with the adjacent wing panels. This mesh requires that the fuselage be broken up into six separate panels per side. They are the nose patch, the forward transition patch, the top and bottom wing root patches, the aft transition patch and finally the rear fuselage patch. Some manual editing is required to straighten out panels on the upper fuselage patch. When the six patches are added together, the final configuration is modeled with a 44x15 panel patch.

b. Main Wing Patch

The NACA 2415 wing is created with four separate patches to allow the addition of a deflected aileron mesh. CMARC comes with a broad selection of "*.SD" airfoil template files that are automatically loaded during installation. The "NACA2415.SD" file is used for this model. The 10x15 inboard wing patch runs from the wing root, past the flaps, to the start of the aileron. The 10x15 mid-wing patch covers the portion of the wing spanned by the aileron. The tapered outboard wing extension is made with a 6x15 patch. Finally, a 4x15 semi-circular wing tip patch is created using CMARC's built-in wing tip functionality. The wing is set to a 4.5° incidence in the LOFTSMAN input file. Alternatively, the patch could be created with no incidence and then the patch coordinate system could be rotated in the CMARC input file. Together, the three wing patches add to make a 30x15 panel wing model.

The ailerons are meshed at zero degree deflection and five degrees of right rolling moment deflection. For the no deflection case, a single right wing patch is meshed with CMARC's symmetric patch toggle (IPATSYM=1) creating the left patch. For deflected ailerons, separate patches are meshed for each wing. The right wing aileron deflection is five degrees trailing edge up (T.E.U.) and the left wing five degrees trailing edge down (T.E.D.).

c. Horizontal Stabilizer Patch

The horizontal stabilizer and elevator patch is created with a single 10x16 mesh using the "NACA0006.SD" airfoil template. As stated earlier, the actual UAV horizontal stabilizer has flat upper and lower surfaces and a rounded leading edge. The NACA 0006 airfoil is substituted because it provides a close approximation to the leading edged radius and thickness ratio. No other special modifications are required. A tip patch is not added because some of the resulting panels would be too small. In particular, the triangular panels closing out the aft end of the tip are too small in proportion to the other panels, creating singularities due to machine resolution. Initially, an attempt was made to model horizontal and vertical stabilizer wing tips, but the model would not converge with them. Leaving off tip patches does not significantly influence results according to the CMARC User's Guide [Ref. 3].

The elevator spans the entire horizontal stabilizer. Two patches are meshed, one with zero deflection and the second with positive five degrees (+5° T.E.D.) of deflection. The deflected patch is used to obtain the elevator control power derivatives ($C_{L\delta e}$, $C_{M\delta e}$ and $C_{D\delta e}$).

d. Vertical Stabilizer Patch

Two different versions of the vertical stabilizer are used for FROG modeling. An extended vertical stabilizer, which includes the "effective" area of the empennage tail boom, is used to measure the static sideslip and yaw rate damping derivatives. It is a 10x14 panel patch. The second patch models the actual area of the vertical stabilizer. It is a 10x12 patch and is meshed with a five-degree rudder deflection for measuring control power derivatives.

The vertical stabilizer and rudder patches are created with a single mesh using the "NACA0006.SD" airfoil template. As with the horizontal tail stabilizer, the NACA 0006 airfoil closely approximates the vertical surface leading edge radius and thickness ratio. The LOFTSMAN input file is different in that a vertical wing surface

requires a modification to the rib axis. The rib axis must be specified with an x-axis rotation of 90°, a y-axis rotation of 0° and an unspecified (999.0) z-axis rotation. No symmetry is selected for the vertical stabilizer because the patch is already symmetric about the y=0 plane. As with the horizontal stabilizer, a tip patch is not added because some of the resulting panels would be too small.

The rudder spans the entire vertical stabilizer. Two patches are meshed, one with zero deflection and the second with positive five degrees (+5° T.E.L.) of deflection. The deflected patch is used to obtain the elevator control power derivatives ($C_{L\delta e}$, $C_{M\delta e}$ and $C_{D\delta e}$).

e. Tail Boom Patch

The tail boom patch is created as a single 12 x 10 mesh using a B-type body. Again, only the right side is meshed due to symmetry. The LOFTSMAN input file requires modifications at both ends in a similar fashion to the aft fuselage. A single point is added to allow convergence of the triangular panels at either end. With this point, the tail boom has the appearance of being tapered at both ends. The point is then manually edited out in the CMARC input file by replacing the "x" coordinate of the beginning and ending section panels with the correct value. In most cases, the tail boom is left out of solution to aid in convergence. This is due to the small overlapping panels at the fuselage tail boom junction. Being a slender, round tube directly in the fuselage slipstream, the tail boom is assumed to have a small influence on the stability derivatives.

f. Engine Pod Patch

The engine pod patch, or nacelle, is created as a single 15 x 10 mesh using a B-type body. Only the right side is meshed due to symmetry. The prop spinner is an integral part of the patch. No attempt is made to model the prop, engine heads or exhaust system. As with the tail boom, in most cases the engine pod is left off the model used to establish stability derivatives.

g. Engine Pylon Patch

The engine pylon patch is modeled with a single 15 x 10 mesh using an A-type body. A-type bodies are used to model surfaces similar to boat hulls with cornered surfaces or sharp chines. In addition, A-type bodies do not require the body to be completely enclosed. As a result, an A-body was selected to model just the sides of the pylon. Only the right side is meshed due to symmetry. A low order fit is achieved with

the adjacent fuselage and engine pod panels. This results in questionable pressure distributions. As a result, the pylon patch was turned off for most configurations. A future attempt could be made to create a high order fit between the other patches or to model the pylon as a flat surface. This will probably require manual editing of the intersecting patches. Even with a high order fit, a wake cannot be added to the trailing edge of the pylon. It would impact the vertical tail surface

4. Common CMARC Input File Errors

The patches created in LOFTSMAN are assembled into a single CMARC input file with any text editor. The default input file, which comes with CMARC, or any old input file may be modified. There are many errors that will cause CMARC to hang up without an error message. The two most common errors are forgetting to designate the last patch and incorrectly numbering the wake patches.

The last patch must be designated by including a TNODS=5 setting in the last section of the last patch. If it is not included, CMARC hangs up when reading in the geometry. In a similar manner, the last wake must be designated with a NODEW=5 setting. If the last wake is not designated, CMARC hangs up while reading in the wake information. Another common error involves incorrect wake to patch number association. Patch numbering changes whenever patches are disabled or reordered. The KWPACH field for each wake definition must be checked to make sure it reflects the current patch numbering.

D. STATIC-PRESSURE SOURCE AND ALPHA VANE CORRECTIONS THROUGH OFF-BODY FLOW ANALYSIS

CMARC is ideally suited for off-body flow analysis. Off-body streamlines may be placed through a point anywhere in the flow field. CMARC will then follow the streamline up and downstream the distance designated in the input file. This is particularly useful for flow visualization. In addition, CMARC calculates pressure coefficient and velocity at each point along the streamline. For this study, two streamlines are placed through the locations of the static-pressure source and alpha probe locations. Pressure coefficient is used to quantify static source position error and velocity is used to calculate alpha probe position error as a function of FROG UAV angle-of-attack. Both static pressure and AOA are digitized for down link to the ground station allowing the values to be easily corrected. Either a look-up table or curve fit correction can be applied subsequent to being passed to the flight control routines. This analysis

was previously published by the author in Ref. [1], but is included here to provide a single source of UAV modeling conducted to date.

1. Description of the FROG UAV Pitot-Static and AOA Systems

The pitot-static system and angle-of-attack probe share a common flight test boom extending from the nose of the UAV. The boom contains both the total and static pressure ports. Figure 4.3 depicts the general dimensions of the flight test boom installation and the modeling coordinate system.

2. Modeling Off-Body Streamlines

Streamlines are placed at the two locations indicated in Figure 4.3, which correspond to the static source and alpha probe locations. Two off body streamlines were activated in CMARC by setting NSTLIN=2 in the &SLIN1 line. Only a short distance of 2 inches is selected up and downstream in the SU and SD fields to reduce the size of the output file. Figure 4.4 is a POSTMARC rendering of the two off-body streamlines used for sensor corrections. With the model at α_t=0°, notice that the streamline is curving up at the angle-of-attack vane location 6.5 inches in front of the aircraft nose.

3. Analysis of Static Source Position Errors

The position error pressure coefficient, $\Delta C_{P\ pc}$ or $\Delta P_p/q_c$, is a function of free stream Mach number and angle-of-attack provided that the static source is located outside of a thick boundary layer and sideslip is minimized [Ref. 11]. In the case of the FROG UAV with incompressible flow, $\Delta P_p/q_c$ becomes a function of angle-of-attack only. Therefore, corrections can be simply defined as a function of measured angle-of-attack.

A DOS batch file was executed to step the CMARC model through angles-of-attack ranging from -8° to 20°. The batch file incremented the angle-of-attack using CMARC's command line override feature. In addition, a new output file name was designated for each angle-of-attack. Position error pressure coefficient is then read from the off-body streamline listing of the output file at the location corresponding to the static source. Table 4.3 lists the values of $\Delta P_p/q_c$ calculated from CMARC data. Figure 4.5 displays $\Delta C_{P\ pc}$ as a function of indicated angle-of-attack. The second order influence of angle-of-attack is clear with a second order curve fitting tightly through the data points. Of note, the error is relatively constant for a ±8° band around trim angle-of-attack. For incompressible flow, position error pressure coefficient is independent of airspeed and altitude.

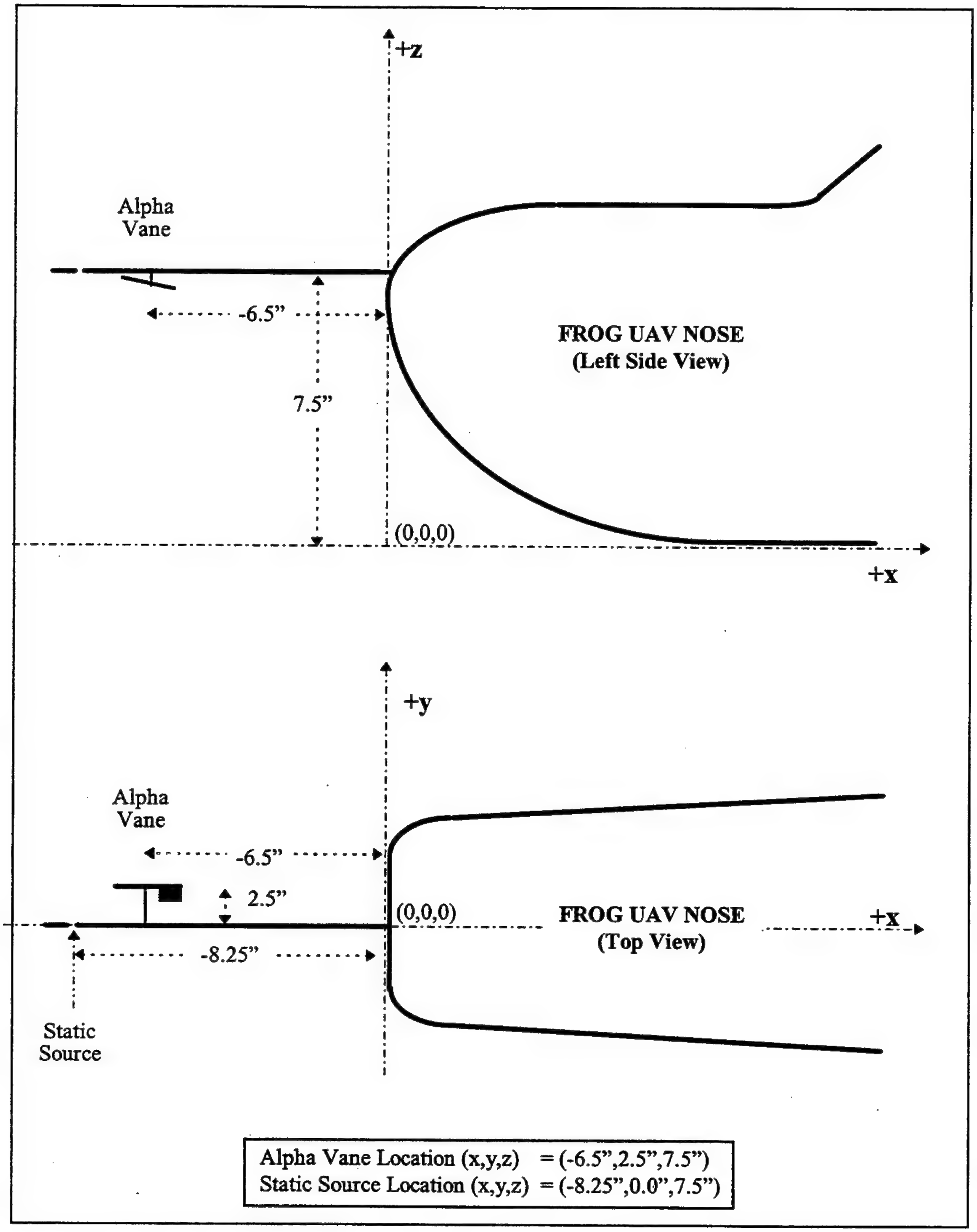

Figure 4.3 Diagram of the FROG UAV Pitot-Static and AOA Systems.

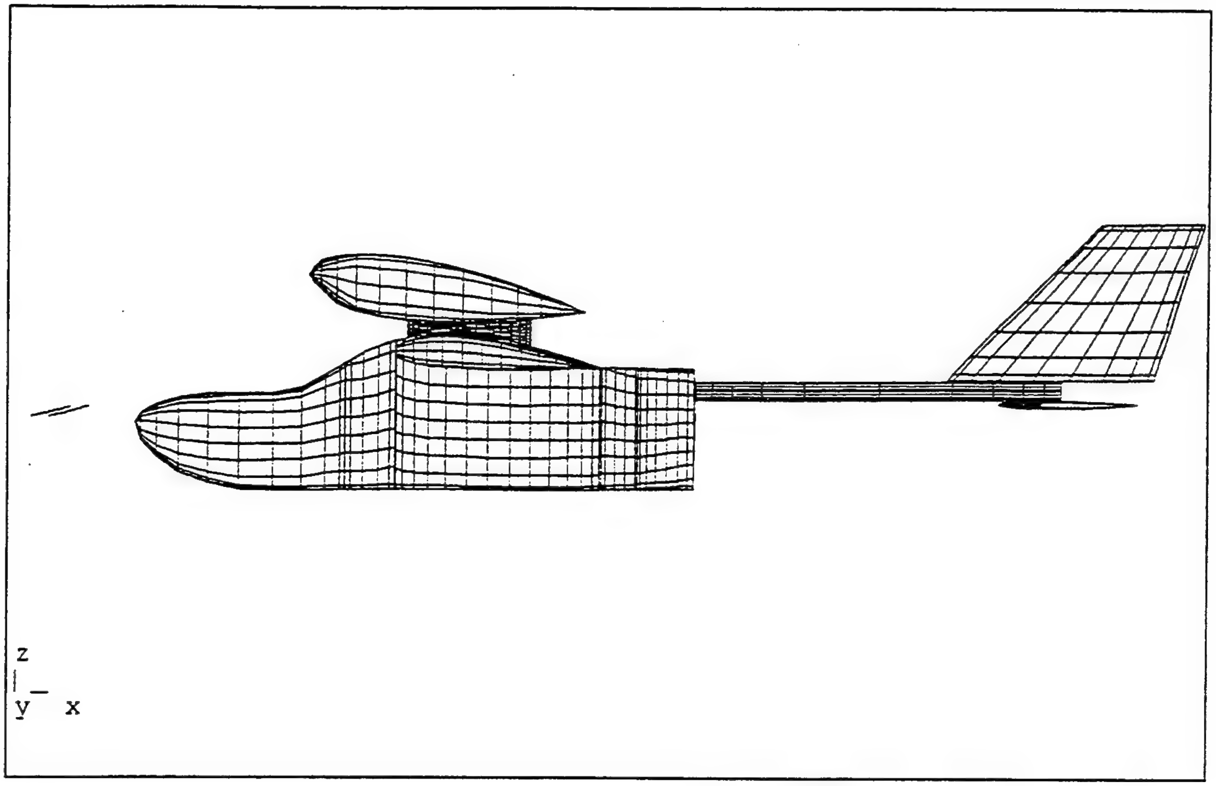

Figure 4.4 FROG Off-Body Streamline Visualization with POSTMARC (α=10°).

Position error pressure coefficient can be turned into position corrections for airspeed and altitude. The following relations were developed which assume small errors and incompressible flow:

$$\Delta V_{pc} = \frac{V_i \Delta C_p}{2} \quad \text{and} \quad \Delta V_{pc} = V_c - V_i \tag{4.1}$$

$$\Delta H_{pc} = \frac{\Delta V_{pc} V_i}{\sigma_{std} g_o} \quad \text{and} \quad \Delta H_{pc} = H_c - H_i \tag{4.2}$$

Where:

ΔH_{pc} is the altitude position correction.

ΔV_{pc} is the velocity position correction.

$\Delta C_p = \frac{\Delta P_p}{q_c}$ or position error pressure coefficient.

σ_{std} is standard day density ratio.

g_o is the gravitational constant.

Table 4.3 displays corrections calculated for both airspeed and altitude at the FROG UAV trim condition of 88 ft/s and 800 ft MSL. The corrections are added to the indicated value to obtain the corrected value. Figures 4.6 and 4.7 display the corrections as a function of indicated angle-of-attack. Again, a second order curve fits nicely through the data points. Equations 4.1 and 4.2 can be used to implement a correction algorithm based on airspeed and altitude.

4. Analysis of Alpha Vane Position Error

Local flow field velocity is extracted from the off-body streamline listing to obtain local angle-of-attack. The alpha vane is assumed to capture the x-z component of the local velocity field and ignore cross flow in the y direction. Flow field velocity is turned into indicated angle-of-attack and angle-of-attack position correction with the following equations:

$$\alpha_i{}^\circ = a\tan\left(\frac{V_z}{V_x}\right) * \frac{180}{\pi} \text{ degrees} \qquad 4.3$$

$$\Delta\alpha^{\circ}_{pc} = \alpha_t - \alpha_i \text{ degrees} \qquad 4.4$$

A DOS batch file is executed to step the CMARC model, with an off-body streamline located at the vane position, through angles-of-attack ranging from -8° to 20°. Local velocity components are then read from the location corresponding to the alpha vane. Table 4.4 lists the values of $\Delta\alpha_{pc}$ calculated from CMARC data. Figure 4.8 displays $\Delta\alpha_{pc}$ as a function of indicated angle-of-attack. Linear and second order curve fit equations are also indicated on Figure 4.8. Angle-of-attack correction is fairly linear through the FROG operating envelope, with approximately -1.25 degrees of position error at the FROG cruise trim condition. The corrections apply at all incompressible airspeeds and all altitudes.

5. Summary of Off-Body Flow Field Analysis

CMARC proved useful for both static-pressure source and alpha vane position corrections. Measured data may be corrected using look-up tables with the values in Table 4.3 and 4.4 or by using the curve fits in Figures 4.5 through 4.8. Flight testing is recommended for validation of sensor corrections obtained from this CMARC off-body flow field analysis.

UAV AOA α_T (deg)	ΔCp_{pc} $\Delta P/q_c$	V Correction $\Delta V_{pc}=V_c-V_i$ (ft/s)	H Correction $\Delta H_{pc}=H_c-H_i$ (ft)
-8	0.1092	4.8	13.5
-6	0.1120	4.9	13.8
-3	0.1141	5.0	14.1
-2	0.1140	5.0	14.1
-1	0.1137	5.0	14.1
0	0.1132	5.0	14.0
1	0.1123	5.0	13.9
2	0.1111	4.9	13.7
3	0.1096	4.8	13.5
4	0.1078	4.8	13.3
5	0.1057	4.7	13.1
6	0.1034	4.6	12.8
8	0.0977	4.3	12.1
10	0.0909	4.0	11.2
12	0.0831	3.7	10.3
14	0.0741	3.3	9.2
16	0.0641	2.8	7.9
18	0.0530	2.3	6.6
20	0.0410	1.8	5.1

Table 4.3 Position Error Corrections for the NPS FROG UAV at V=88 ft/s and H=800 ft MSL. Derived from CMARC Panel Code Off-Body Flow Field Analysis.

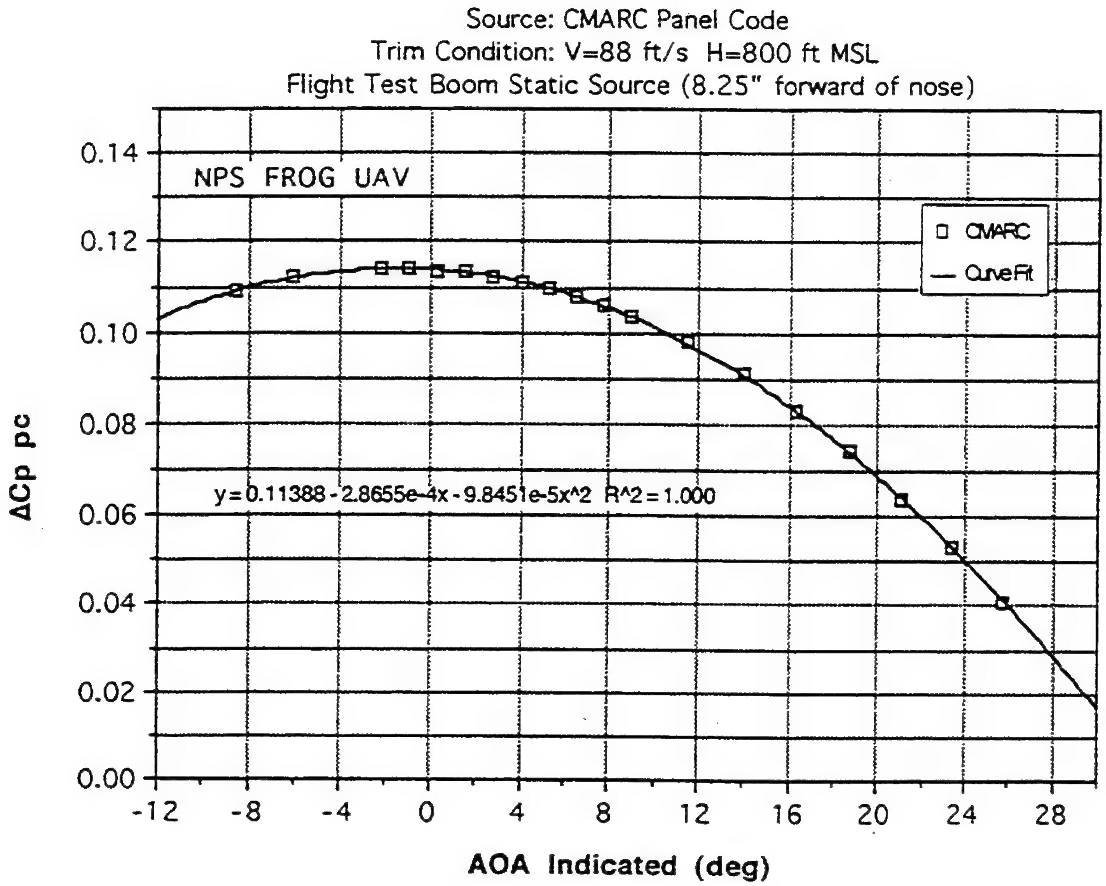

Figure 4.5 **Position Error Pressure Coefficient, $\Delta C_{P\,pc}$, for the NPS FROG UAV. Derived from CMARC Panel Code Off-Body Flow Field Analysis.**

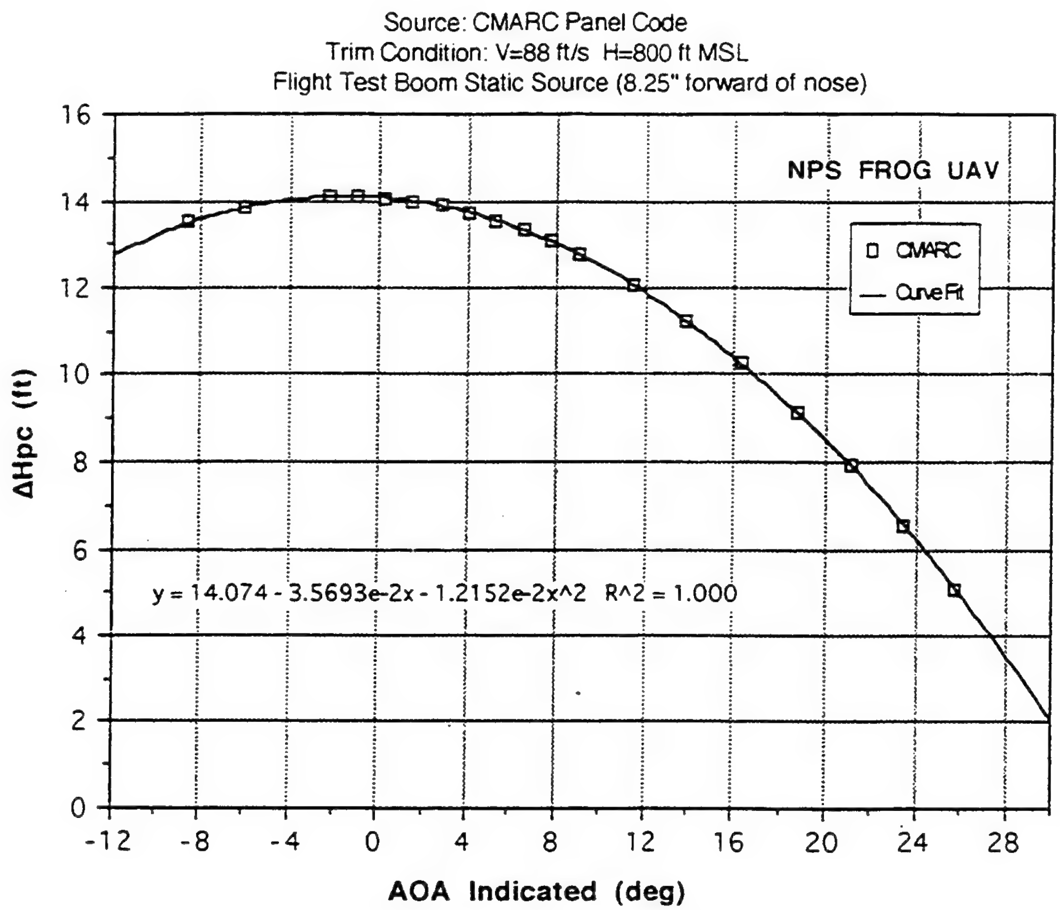

Figure 4.6 Altitude Position Error, ΔH_{pc}, for the NPS FROG UAV at V=88 ft/s and H=800 ft MSL. Derived from CMARC Panel Code Off-Body Flow Field Analysis.

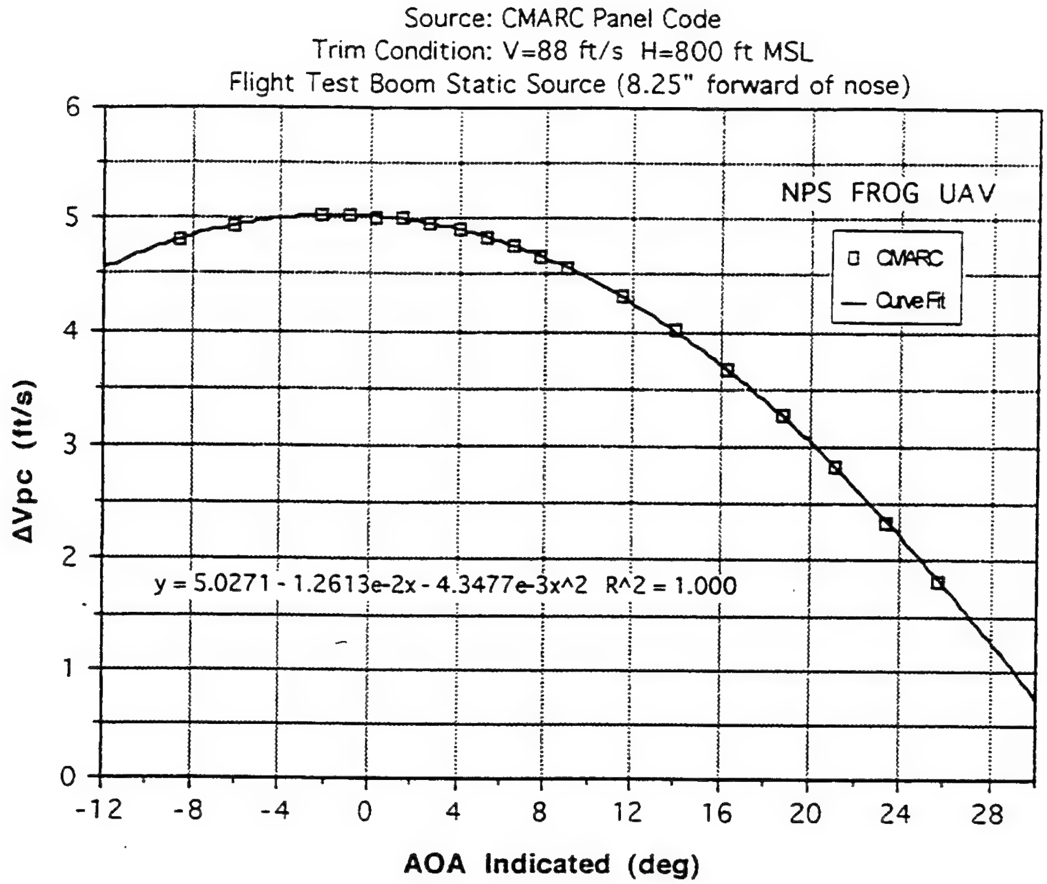

Figure 4.7 Airspeed Position Error, ΔVpc, for the NPS FROG UAV at V=88 ft/s and H=800 ft MSL. Derived from CMARC Panel Code Off-Body Flow Field Analysis.

UAV AOA	Velocity at Alpha Vane			AOA $_{Correction}$	AOA $_{Indicated}$
α_T (deg)	V_x (ft/s)	V_y (ft/s)	V_z (ft/s)	$\Delta\alpha=\alpha_T-\alpha_i$ (deg)	α_i (deg)
-8	80.92	1.66	-12.23	0.60	-8.60
-6	81.27	1.65	-8.65	0.08	-6.08
-3	81.60	1.64	-3.21	-0.75	-2.25
-2	81.67	1.63	-1.47	-0.97	-1.03
-1	81.71	1.63	0.28	-1.20	0.20
0	81.73	1.62	2.13	-1.49	1.49
1	81.73	1.61	3.93	-1.75	2.75
2	81.70	1.60	5.72	-2.00	4.00
3	81.66	1.59	7.51	-2.25	5.25
4	81.58	1.58	9.30	-2.50	6.50
5	81.48	1.57	11.08	-2.75	7.75
6	81.37	1.56	12.88	-2.99	8.99
8	81.07	1.53	16.43	-3.46	11.46
10	80.67	1.51	19.98	-3.91	13.91
12	80.17	1.48	23.50	-4.34	16.34
14	79.61	1.46	26.99	-4.73	18.73
16	78.93	1.43	30.47	-5.11	21.11
18	78.18	1.39	33.90	-5.44	23.44
20	77.34	1.36	37.31	-5.75	25.75

Table 4.4 Angle-of Attack Vane Position Error Corrections for the NPS FROG UAV. Derived from CMARC Panel Code Off-Body Flow Field Analysis.

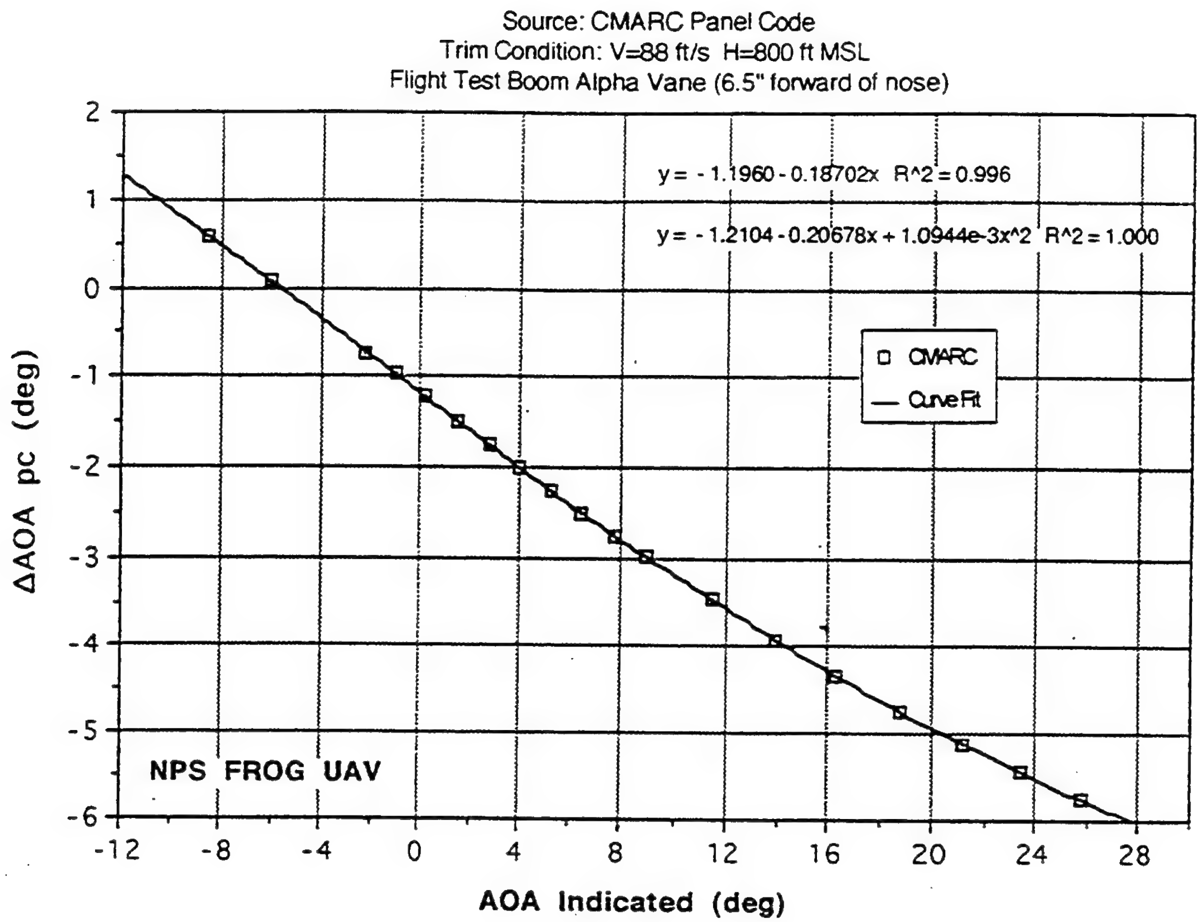

Figure 4.8 **Angle-of-Attack Vane Position Error, $\Delta\alpha_{pc}$, for the NPS FROG UAV. Derived from CMARC Panel Code Off-Body Flow Field Analysis.**

E. DEVELOPMENT OF STABILITY DERIVATIVES

In this section, CMARC is used to develop the longitudinal and lateral-directional stability derivatives for the FROG UAV. The development effort focuses on finding the static, rate-damping and control-power derivatives. The results obtained from CMARC are compared to data sets obtained from empirical estimation techniques and flight-test parameter estimation. In the next section, the stability derivatives are entered into a dynamic model to find modal frequency, damping and response to control deflections.

The potential flow analysis performed by CMARC does not provide accurate viscous drag values. Therefore, total drag is estimated from the flight-test power-off glide ratio and cruise thrust required. The User Guide developed in Appendix A describes in detail how to gather stability derivative data with CMARC. An abbreviated discussion is presented below.

CMARC contains built-in functionality to integrate forces and moments in all axes over the surface of a body. Force and moment coefficients are automatically nondimensionalized based on the mean aerodynamic chord, reference wing area, semi-span and center of gravity location in the CMARC BINP9 input line. Coefficients are presented in both wind and body axes. Of note, CMARC uses the semi-span to nondimensionalize rolling and yawing moment coefficients. Most texts on stability and control, including Roskam [Ref. 12] and Etkin [Ref. 13], nondimensionalize rolling and yawing moments by span. Rolling and yawing moments are nondimensionalized by span in this study. Table 4.5 summarizes the factors for normalizing moments and angular rates. All rolling and yawing moment coefficients presented in this study have been normalized with span by dividing the CMARC output by a factor of two. Table 4.5 also indicates the characteristic time, t*, employed for angle rate data reduction.

In addition to differences in nondimensionalizing moments, CMARC uses the typical CFD axis system shown in Figure 4.9. For this study, all work is performed in the stability axis system. Figure 4.9 also illustrates the standard stability axes implemented in this study. The sign of CMARC roll and yaw moments need to be reversed. The direction for positive control deflections is also shown in Figure 4.9. All control surfaces are patched with positive deflections using the convention in Figure 4.9.

A potential flow solution will not produce satisfactory results for bodies with significant areas of flow separation. Therefore, CMARC models must be analyzed in the linear slope regions for valid results.

MOMENTS	NORMALIZING PARAMETER[1]	RATES	CHARACTERISTIC TIME
$L = C_l \bar{q} S b$	b	$\hat{p} = \dfrac{pb}{2u_o}$	$t^* = b/2u_o$
$M = C_m \bar{q} S \bar{c}$	$\bar{c}$	$\hat{r} = \dfrac{r\bar{c}}{2u_o}$	$t^* = \bar{c}/2u_o$
$N = C_r \bar{q} S b$	b	$\hat{r} = \dfrac{rb}{2u_o}$	$t^* = b/2u_o$

Note: 1) CMARC nondimensionalizes roll and yaw coefficients with b/2.

Table 4.5 Nondimensionalized Moment and Rate Equations.

For the static stability derivatives, the CMARC model is run at two different angles-of-attack and one sideslip angle with zero control surface deflections. The slopes of the force and moment coefficients are then taken to produce the $C_{L\alpha}$ and $C_{m\alpha}$ longitudinal derivatives and the $C_{Y\beta}$, $C_{l\beta}$ and $C_{n\beta}$ lateral-directional derivatives.

For the control-power derivatives, the model is run at the trim condition with successive control deflections. The difference between the results with and without control surface deflections yield the $C_{L\delta e}$, $C_{M\delta e}$ and $C_{D\delta e}$ longitudinal and the $C_{Y\delta r}$, $C_{l\delta r}$, $C_{n\delta r}$, $C_{l\delta a}$ and $C_{n\delta a}$ lateral-directional control-power derivatives.

Development of the damping derivatives is not as straight forward. The static derivatives are obtained with motion disabled. For the longitudinal damping derivatives, the model is run with oscillating vertical plunging motion to obtain the C_L and C_M α-dot terms. The lift and pitching moment coefficients are broken into real (in phase with AOA) and imaginary (out of phase with AOA) components. The imaginary components are due to α-dot effects. Next, the model is run with oscillating pitch motion to obtain the combined α-dot and pitch rate terms. Subtracting the α-dot influence obtained from the plunging motion isolates the pitch rate-damping term from the pitch motion.

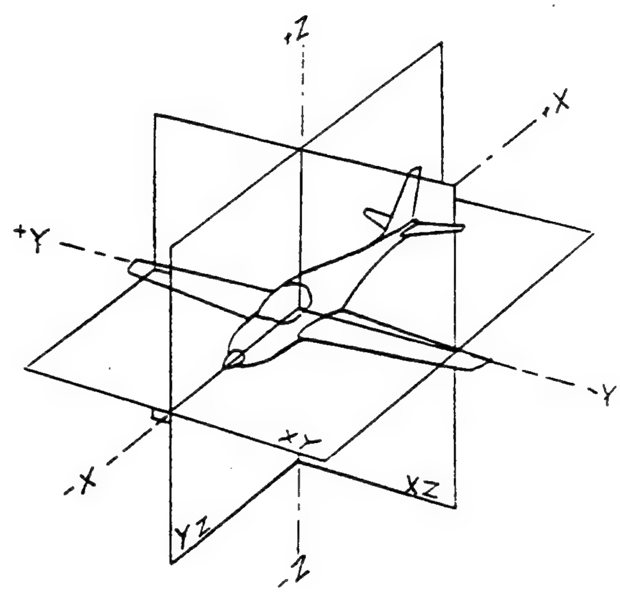

CMARC Axis System

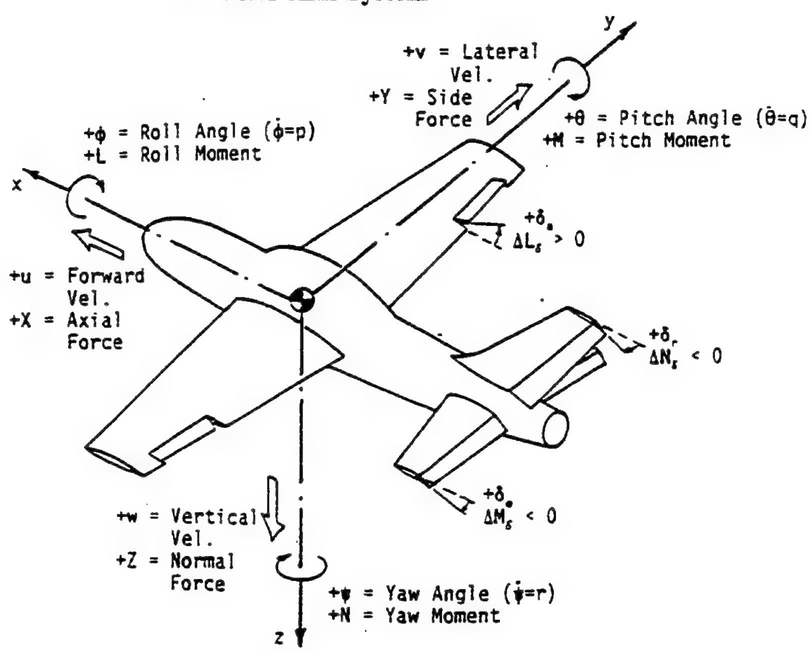

Stability Axis System

Figure 4.9 CMARC CFD Axis System Compared To Stability Axis System. From References [3] and [14] Respectively.

For the lateral-directional analysis, the β-dot terms are assumed to be small. This allows the model to be run with just oscillating roll and yaw motion. As with the longitudinal test case, the imaginary or out of phase component yields the combined β-dot and rate-damping data. With the β–dot terms assumed to be small, the oscillating motion yields the C_Y, C_l, and C_n roll and yaw rate terms directly.

Throughout this chapter, stability derivatives obtained from CMARC are compared to three other data sets. The first comes from classical analysis through the methods presented by Roskam in References [12] and [15]. The second set comes from a classical aerodynamic model developed by Papageorgio [Ref. 2] and further refined through parameter estimation by Engdahl. The resulting parameter estimation model provides a good match to observed flight characteristics and is currently in use by the NPS Department for Aeronautical Engineering for closed-loop flight control development. The third set of data is for the Cessna 172 at the cruise flight condition. The data is only presented for an order of magnitude comparison.

1. Longitudinal Stability Derivatives

a. Static Longitudinal Stability Derivatives

Three basic longitudinal stability derivatives can be measured with just two runs of the CMARC model. The model is first analyzed at an angle-of-attack corresponding to the estimated trim condition. In this case, α_t=0° is selected for the first run. A second CMARC run is conducted with angle-of-attack incremented by one or two degrees. C_L and C_m are then extracted manually from the data files. The slope of C_L and C_m versus angle-of-attack provide the $C_{L\alpha}$ and $C_{m\alpha}$ longitudinal derivatives. For this study, several angles-of-attack were analyzed to check consistency of the slope. In addition, α_{trim} is calculated from the lift curve slope and trim lift coefficient. For the longitudinal analysis, only half the model is analyzed. The symmetric calculation mode is selected by setting both RSYM=0.0 and IPATSYM=0 in the CMARC input file. Equations 4.5 through 4.7 are used for these calculations:

$$C_{L_\alpha} = \frac{\left(C_{L_2} - C_{L_1}\right)}{\left(\alpha_2 - \alpha_1\right)} * \frac{180}{\pi} \text{ per radian} \qquad 4.5$$

$$C_{m_\alpha} = \frac{\left(C_{m_2} - C_{m_1}\right)}{\left(\alpha_2 - \alpha_1\right)} * \frac{180}{\pi} \text{ per radian} \qquad 4.6$$

$$\alpha^\circ{}_{trim} = \alpha^\circ{}_1 + \frac{\left(C_{L_{trim}} - C_{L_1}\right)}{C_{L_\alpha}} * \frac{180}{\pi} \text{ degrees} \qquad 4.7$$

Two FROG UAV model configurations are analyzed in a build-up approach to check results against classical calculations and flight-test data. Figure 4.10 shows the CMARC models. First, just the wing and horizontal tail are considered. The patches for all other surfaces and wakes are turned off and the wing root is extended to centerline. Then, the blended wing/fuselage and horizontal tail are analyzed. Values of $C_{L\alpha}$ and $C_{m\alpha}$ for these two configurations are presented in Table 4.6.

Classical design calculations are also performed to estimate $C_{m\alpha}$ for comparison to CMARC results. Equation 4.8 is used for the calculation of $C_{m\alpha}$:

$$C_{m_\alpha} = a_w\left[\left(h - h_{ac}\right) - V_H \frac{a_t}{a_w}\left(1 - \frac{d\varepsilon}{d\alpha}\right)\right] \qquad 4.8$$

In classical design, the horizontal tail downwash derivative, $d\varepsilon/d\alpha$, is generally selected from empirical data. Using a taper ratio of TR=1:1 and an aspect ratio of AR=6, $d\varepsilon/d\alpha=0.4$ is selected from empirical charts in Ref. [16] for the FROG UAV configuration. Also, calculations for $d\varepsilon/d\alpha=0.25$ are included to illustrate pitching moment sensitivity to the downwash derivative. Table 4.6 lists $C_{m\alpha}$ for each configuration.

The final static longitudinal parameter required is total aircraft drag. Drag coefficient plays an important role in long-period aircraft dynamics. Unfortunately, potential flow panel codes such as CMARC do not provide accurate total drag estimates. They can provide good induced drag predictions. And, if equipped with a boundary layer code like that contained in CMARC, they can provide integrated skin friction results. However, a large total drag contribution in the form of pressure drag due to flow separation is not accounted for. Total drag estimates are made below using the two

simple techniques shown in Equations 4.9 to 4.12. The first method is based on flight-test glide ratio. The second is based on cruise power required and estimated prop efficiency. Note that the selected prop efficiency is relatively low due to the small propeller diameter, high RPM and pusher configuration. The two methods provide drag predictions within 10% of each other. The results are averaged to C_D=0.065 and included in Table 4.6.

Method 1: Lift-to-Drag Ratio (L/D=7 from flight-test)

$$L/D = 7 \quad \Rightarrow \quad D = \frac{L}{7} = \frac{W}{7} = \frac{67.7 \quad lbs}{7} = 9.67 \quad lbs \tag{4.9}$$

$$C_D = \frac{D}{qS} = \frac{9.67 \quad lbs}{0.5 * 0.002327 \quad lb \cdot s^2 / ft^4 * 88^2 \quad ft^2 / s^2 * 17.57 \quad ft^2} = 0.0611 \tag{4.10}$$

Method 2: Cruise Power Setting (HP=5, η_P=0.35)

$$C_D = \frac{D}{qS} = \frac{T_R}{qS} = \frac{HP_R * 550 \quad ftlbs / s / HP * \eta_P / V}{qS} \tag{4.11}$$

$$C_D = \frac{5 \quad HP * 550 \quad ft \cdot lbs / s / HP * 0.35 / 88 \quad ft / s}{0.5 * 0.002327 \quad lb \cdot s^2 / ft^4 * 88^2 \quad ft^2 / s^2 * 17.57 \quad ft^2} = 0.069 \tag{4.12}$$

Average: C_{Dave} =(0.0611+0.069)/2 = 0.065

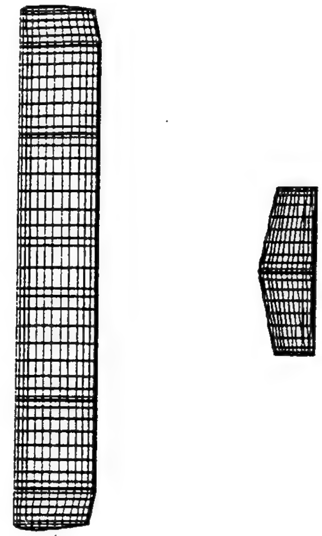

Simplified Wing and Horizontal Tail

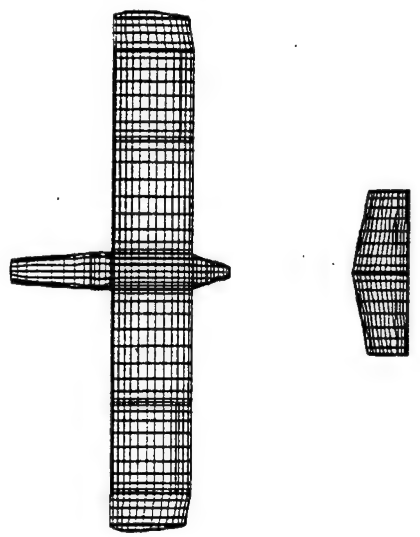

Blended Wing and Fuselage with Horizontal Tail

Figure 4.10 CMARC Models of the FROG UAV for the Determination of Static Longitudinal Stability Derivatives.

Flight-test data for the short-period and phugoid modes were used for longitudinal parameter estimation. Values for $C_{L\alpha}$ and $C_{m\alpha}$ based on preliminary parameter estimation work by Engdahl are presented in Table 4.6.

METHOD	CONFIGURATION[1]	STATIC LONGITUDINAL PARAMETERS				
		α_{trim} [2] (deg)	$C_{L\alpha}$ (per rad)	$C_{m\alpha}$ (per rad)	C_D	$C_{D\alpha}$ (per rad)
CMARC Panel Code	Wing/Horiz Tail	-0.87	4.86	-0.835	n/a	n/a
	Wing/Fuselage/Horiz Tail	-0.01	4.85	-0.413	n/a	0.266
Classical Design[3]	Wing/Horiz Tail - $\delta\varepsilon/\delta\alpha$=0.25	-0.81	4.85	-1.00	n/a	n/a
	Wing/Horiz Tail - $\delta\varepsilon/\delta\alpha$=0.40	-0.82	4.82	-0.70	n/a	0.253
Parameter Estimation[4]	Flying Aircraft	n/a	4.09	-0.42	0.0655	n/a
	C-172[6]	n/a	0.31	-0.89	0.31	0.13

NOTES: 1) CG_x=34.5% M.A.C. / CG_z=8.6" from bottom of fuselage.
2) Zero lift wing incidence is +6.5° from the longitudinal reference line.
3) Classical design after Ref. [12].
4) Parameter estimation from NPS flight test data by Engdahl.
5) Average drag obtained from L/D and cruise power analysis from flight test data.
6) C-172 data from Ref. [12].

Table 4.6 Comparison of FROG UAV Static Longitudinal Stability Derivatives.

Good correlation of lift curve slope ($C_{L\alpha}$) to classical design is demonstrated by the two CMARC configurations in Table 4.6. Both techniques over estimated $C_{L\alpha}$ compared to flight-test data. Neither the classical design technique nor the CMARC model accounts for control surface leakage or separation effects. Modeling actual flight control gap geometry may provide a closer match to experimental data.

Excellent correlation is achieved for $C_{m\alpha}$ between the blended wing/fuselage CMARC model and flight-test results. The low value of $C_{m\alpha}$ implies that $d\varepsilon/d\alpha$ is greater than the 0.4 value selected from empirical charts in Reference [16]. The simplified wing/tail model resulted in a $C_{m\alpha}$ that closely matches classical design predictions with $d\varepsilon/d\alpha$=0.35. Clearly, CMARC modeling provides the value-added capability to capture fuselage influences that are missed with classical design methods.

An investigation was performed to see if improved wake definition could better capture the $d\varepsilon/d\alpha$ downwash derivative. Initially a flexible wake was selected. However, at the cruise angle-of-attack, the flexible wake impacted the horizontal tail causing inaccurate results. A further investigation was made into a streamline based wake definition. A study by Walden et al. [Ref. 17] studied wake turbulence by modeling an aircraft flying in trail of a wake-generating wing. A horizontal tail trailing the main wing is a similar configuration. The study found that a streamline-based wake is the best method for modeling downwash effects. In the study, the model was initially run with a rigid-wake. A streamline was also defined downstream of the main wing trailing edge. After analyzing the first results, the wake was then predefined to follow the streamline. The result was a first iteration on modeling a flexible wake with a predefined rigid-wake. This technique was tried during the course of FROG UAV modeling. However, FROG geometry proved unsuited to this technique. The streamline trailing the wing ended up impacting the horizontal tail. This indicated that a predefined wake would also impact the horizontal tail, resulting in inaccurate result. Figure 4.11 shows the streamline impacting the horizontal tail at cruise angle-of-attack with rigid-wakes selected. With the already close correlation of the rigid-wake results to flight-test data, further efforts to investigate $C_{m\alpha}$ were abandoned.

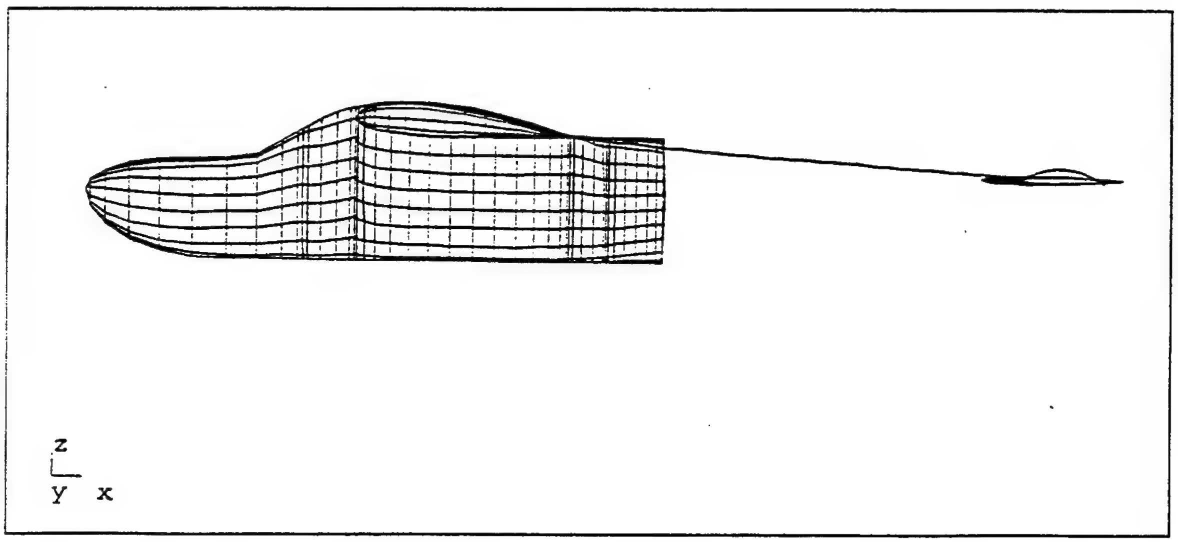

Figure 4.11 Rigid-Wake Streamline for Investigation of Streamline Based Wake Definition.

In summary, for the static longitudinal stability derivatives, CMARC produced accurate values for $C_{m\alpha}$ and a slightly high value of $C_{L\alpha}$. Drag coefficient is obtained by averaging the values from the lift-to-drag ratio and cruise thrust required techniques.

b. Longitudinal Damping Stability Derivatives

The two aircraft motions illustrated in Figure 4.12 are used to develop the longitudinal rate-damping derivatives. A sinusoidal vertical plunging motion isolates the α-dot effects. Oscillatory motion is controlled with the CMARC BINP8A input file line. The oscillating pitch angle captures both the α-dot and pitch rate-damping terms. It is controlled with the CMARC BINP8B input file line. The α-dot influence developed from the plunging motion is subtracted from the pitching motion to isolate the pitch rate effect. All motion is conducted at a frequency of 2π rad/s, which equates to a reduced frequency of k=0.0595 for this configuration and trim airspeed.

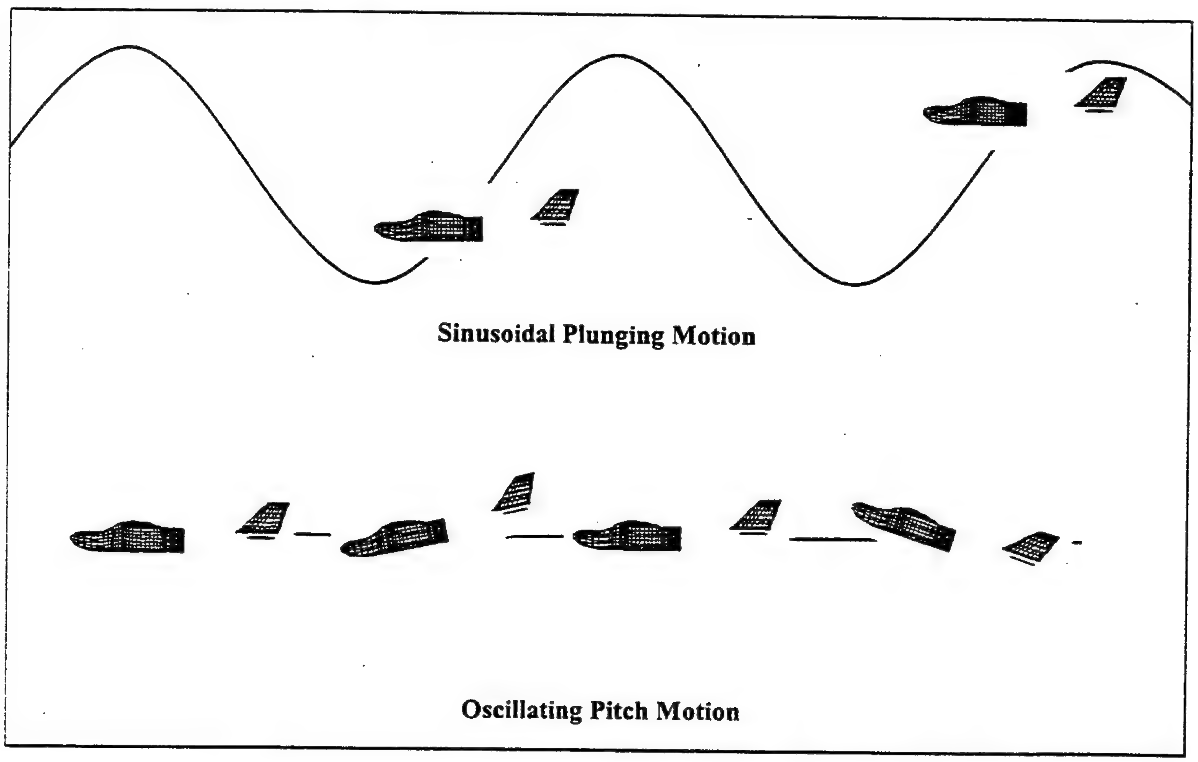

Figure 4.12 Aircraft Motion for the Determination of α-dot and Pitch Rate Damping.

The two models shown in Figure 4.13 are used for the rate-damping investigation. The complete wing/fuselage horizontal tail model is used for both the α-dot and pitch rate-damping terms, while the simplified horizontal tail only model is used to obtain a first approximation of pitch rate-damping. The User Guide in Appendix A provides a more detailed description of the techniques used to gather the dynamic longitudinal stability derivatives.

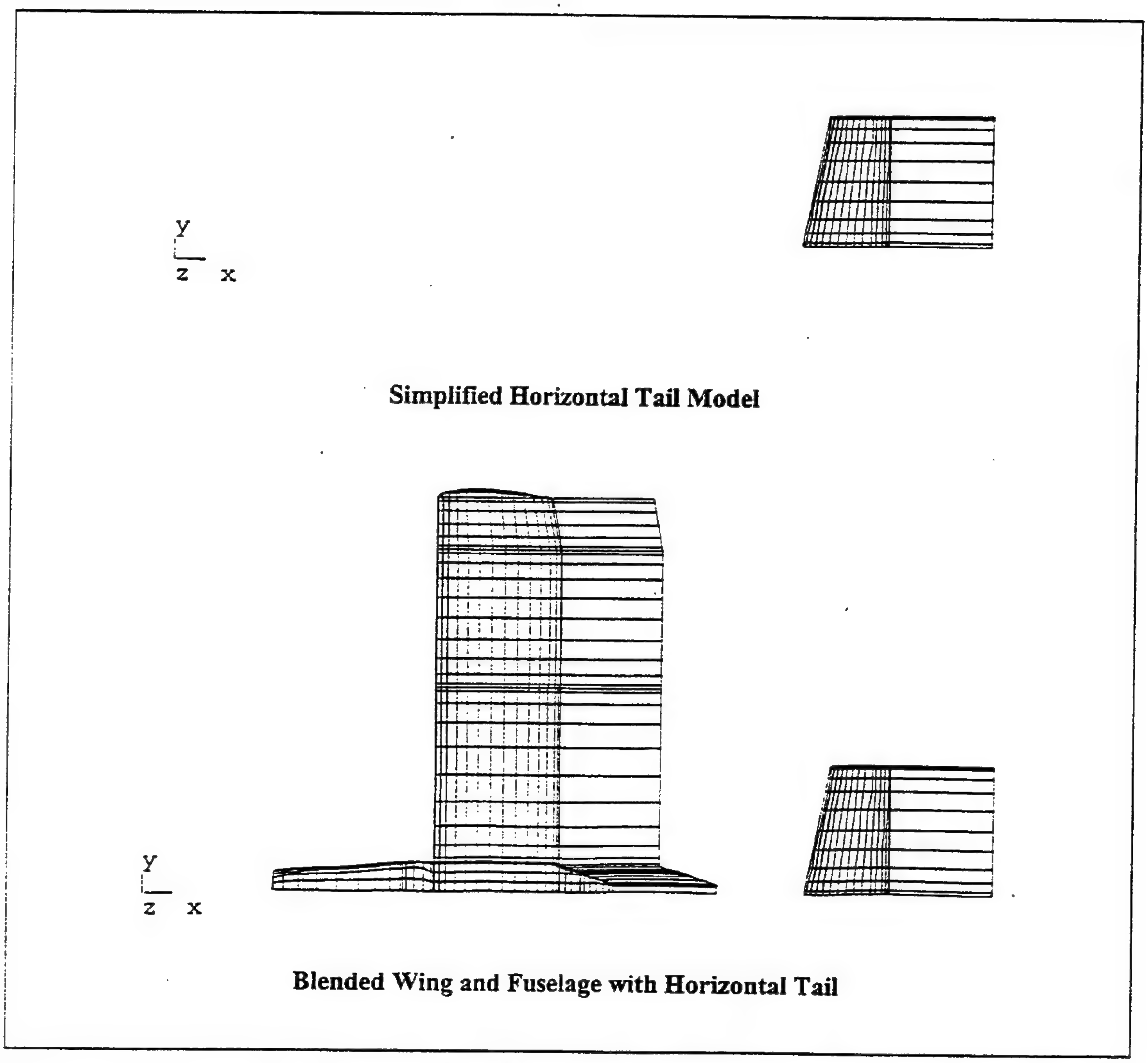

Figure 4.13 CMARC Models of the FROG UAV for the Determination of Longitudinal Rate-Damping.

Traditional design calculations, from Roskam [Ref. 12], are used for comparison to CMARC and flight-test results:

$$C_{L_{\dot{\alpha}}} = 2 * C_{L\alpha_H} * \eta_H * V_H * \frac{\partial \varepsilon}{\partial \alpha} \qquad 4.13$$

$$C_{M_{\dot{\alpha}}} = -2 * C_{L\alpha_H} * \eta_H * V_H \frac{l_t}{\bar{c}} * \frac{\partial \varepsilon}{\partial \alpha} \qquad 4.14$$

$$C_{L_q} = 2 * C_{L\alpha_H} * \eta_H * V_H \qquad 4.15$$

$$C_{M_q} = -2 * C_{L\alpha_H} * \eta_H * V_H \frac{l_t}{\bar{c}} \qquad 4.16$$

where the dynamic pressure ratio at the tail is taken as η_H=1.0

The dynamic longitudinal stability derivatives are presented in Table 4.7. CMARC-obtained values are compared to classical design values and C-172 stability derivatives. Flight-test data is unavailable for the damping derivatives. The aerodynamic model currently in use by the FROG research team implements longitudinal damping coefficients obtained from classical design techniques. The $C_{L\alpha}$-dot and C_{mq} obtained from CMARC for the complete model provided a good match to the classical design data. However, both $C_{L\alpha}$-dot and C_{mq} are over estimated by approximately 50% as compared to classical design values. One possible explanation for the additional damping from CMARC is that the classical approximation only estimates the horizontal tail influence on damping. CMARC also measures wing and fuselage damping influence. The horizontal tail by itself produces values close to the classical calculations. This supports the assertion that CMARC also captures the wing and fuselage influence for the whole model.

METHOD	CONFIGURATION[1]	DYNAMIC LONGITUDINAL PARAMETERS			
		$C_{L\alpha\text{-dot}}$ (deg)	C_{Lq} (per rad)	$C_{m\alpha\text{-dot}}$ (per rad)	C_{mq} (per rad)
Panel Code	Blended Wing-Fuselage/Horiz Tail	1.42	6.82	-6.24	-11.78
	Horizontal Tail only	n/a	4.37	n/a	-11.94
Classical[2]	Wing / Horizontal Tail	1.56	3.89	-4.14	-11.39
Par. Est[3]	Flying Aircraft	n/a	n/a	n/a	n/a
	C-172[4]	1.7	3.9	-5.2	-12.4

NOTES: 1) CG_x=34.5% M.A.C. / CG_z=8.6" from bottom of fuselage.
2) Classical design after Ref. [12].
3) Parameter estimation from flight test data by Engdahl.
4) C-172 data from Ref. [12].

Table 4.7 Comparison of FROG UAV Dynamic Longitudinal Stability Derivatives.

c. *Longitudinal Control-Power Derivatives*

The elevator control-power derivatives are obtained by substituting a 0° deflection horizontal-tail patch for one with +5° trailing edge down deflection. Only one run is required. The difference between the trim condition and the deflected value is divided by the elevator deflection as shown below:

$$C_{L_{\delta e}} = \frac{\left(C_{L_{\delta e_2}} - C_{L_{\delta e_1}}\right)}{\delta e_2 - \delta e_1} * 57.3 \quad per \quad rad \tag{4.17}$$

$$C_{D_{\delta e}} = \frac{\left(C_{D_{\delta e_2}} - C_{D_{\delta e_1}}\right)}{\delta e_2 - \delta e_1} * 57.3 \quad per \quad rad \tag{4.18}$$

$$C_{m_{\delta e}} = \frac{\left(C_{m_{\delta e_2}} - C_{m_{\delta e_1}}\right)}{\delta e_2 - \delta e_1} * 57.3 \quad per \quad rad \tag{4.19}$$

Elevator control-power derivatives are presented in Table 4.8. A classical design estimate of elevator control-power is also shown for comparison. The following relationships from Roskam [Ref. 15] are used for estimating elevator control-power:

$$C_{L_{\delta e}} = C_{L_{\delta F}} * \frac{S_H}{S} \qquad 4.20$$

$$C_{m_{\delta e}} = -C_{L_{\delta e}} * \frac{l_H}{\bar{c}} \quad or \quad C_{m_{\delta e}} = -C_{L_{\delta F}} * V_H \qquad 4.21$$

where $C_{L\delta F}$ is the variation of lift coefficient with elevator deflection found from charts in Roskam [Ref. 15].

In general, the elevator control-power derivatives obtained with CMARC correlate well with classical design techniques. For both $C_{L\delta e}$ and $C_{m\delta e}$, CMARC derived elevator power is approximately 15 percent higher than obtained from classical calculations. However, CMARC significantly under-estimates elevator control-power compared to the parameter estimation model. The most likely explanation for this phenomenon is that the CMARC solution does not model the effects of prop wash. The higher dynamic pressure over the horizontal stabilizer from prop wash increases elevator effectiveness. The parameter estimation model captures this phenomenon. This same trend can be seen in the modeling of rudder control-power. An attempt could be made to model the prop disk effects using CMARC's normal panel velocity definition capability.

METHOD	CONFIGURATION[1]	ELEVATOR CONTROL POWER		
		$C_{L\delta e}$ (per rad)	$C_{D\delta e}$ (per rad)	$C_{m\delta e}$ (per rad)
Panel Code	Blended Wing-Fuselage/Horiz Tail	0.438	0.01	-1.199
Classical[2]	Wing / Horizontal Tail	0.39	n/a	-1.04
Par. Est[3]	Flying Aircraft	1.13	n/a	-1.62
	C-172[4]	0.43	0.06	-1.28

NOTES: 1) CG_x=34.5% M.A.C. / CG_z=8.6" from bottom of fuselage.
2) Classical design after Ref. [12].
3) Parameter estimation from NPS flight test data by Engdahl.
4) C-172 data from Ref. [12]..

Table 4.8 Comparison of FROG UAV Elevator Control-Power Derivatives.

2. Lateral Directional Stability Derivatives

a. Static Lateral-Directional Stability Derivatives

Development of the static lateral-directional stability derivatives is not as straightforward. Both sides of the airframe must be modeled by setting both RSYM=1.0 and IPATSYM=1. This creates symmetric patches around the y=0 plane allowing CMARC to perform asymmetric calculations around the entire body and significantly increases processing times.

Initially, a lateral-directional solution was attempted with a complete airframe model. The longitudinal model was modified by adding the vertical stabilizer. This required what was perceived to be a minor wake modification. Figure 4.14 illustrates the configuration. The wing wake was terminated at the wing root to prevent interference with the vertical stabilizer. This left a wake gap for the vertical stabilizer. The engine nacelle and pylon patches were turned off because the wakes would also impact the vertical stabilizer. This configuration met with mixed success. The values of both C_{yb} and C_{nb} were opposite the expected directions. Under closer inspection, it was determined that the false vortex shed from the wing root caused a destabilizing influence on the vertical stabilizer. Figure 4.15 illustrates the vortex using CMARC's built in off-body streamline capability.

In order to obtain satisfactory results, the model is broken up into two separate groups. The aircraft is modeled with the blended wing and fuselage as one group and the horizontal and vertical stabilizers as another group. Separate solutions are obtained for each group and summed through superposition to obtain the whole aircraft solution. The two separate models are shown in Figure 4.16. This method should be used as a last resort. A complete solution should be used if the airframe geometry allows adequate wake separation from the vertical stabilizer. A complete solution would capture fuselage, wing and vertical stabilizer interactions.

Once the model is defined, it is checked for lateral-directional balance at zero sideslip angle (yaw angle=0°). The side force, rolling and yawing coefficients should be zero when a trial run is performed at zero sideslip. If lateral-directional forces or moments are present, the model and wake geometry should be checked for symmetry.

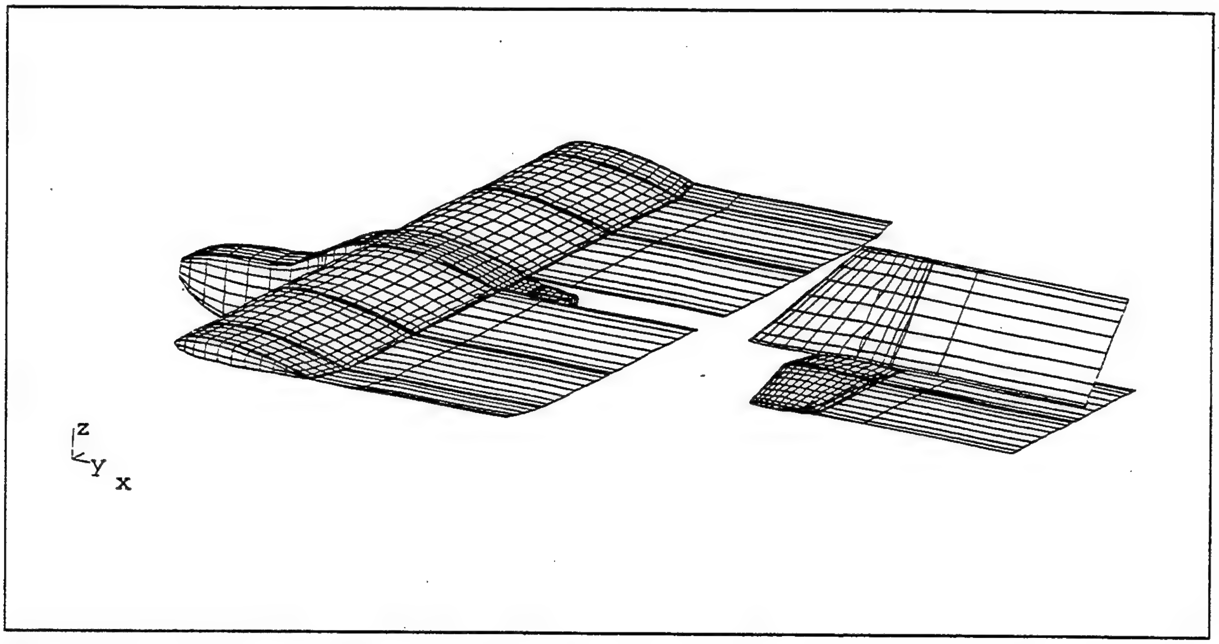

Figure 4.14 Unsuccessful Lateral-Directional Model of the FROG UAV. False Wing Root Vortex Caused Destabilizing Influence on the Vertical Stabilizer.

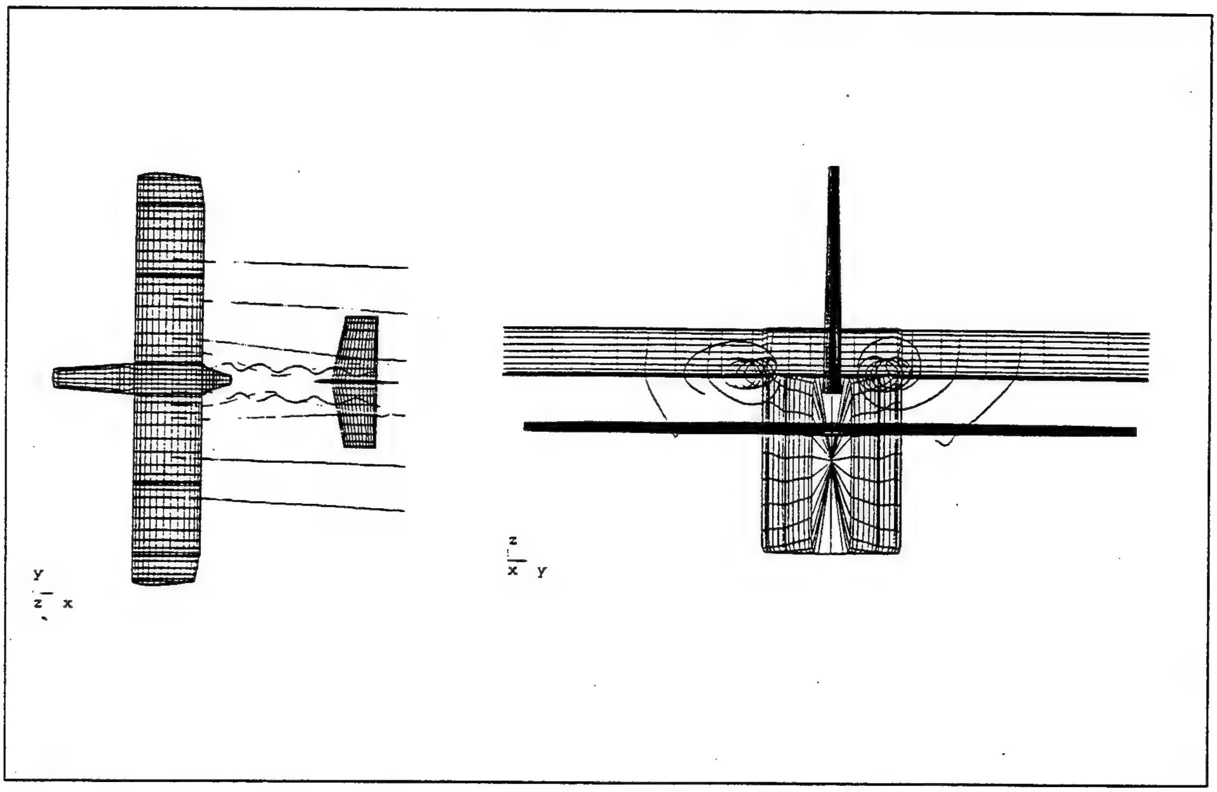

Figure 4.15 Destabilizing Wing Root Vortex Visualized with Off-body Streamlines.

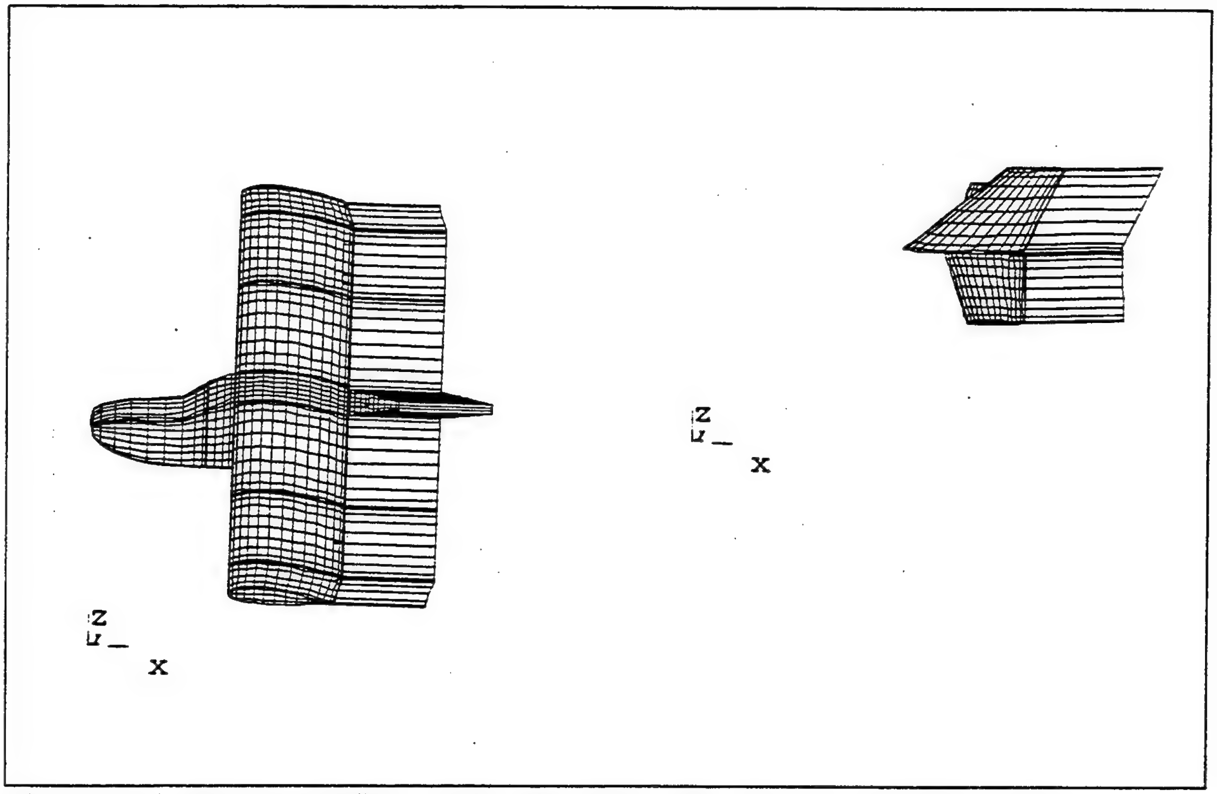

Figure 4.16 Final Simplified Lateral-Directional Models of the FROG UAV. Separate Solutions are Summed to Obtain Complete Airframe Solution.

Next, a single CMARC run is performed with $\alpha = \alpha_{trim}$ and with two degrees of yaw angle. The results from both models are summed. The lateral-directional derivatives, $C_{Y\beta}$, $C_{l\beta}$ and $C_{n\beta}$, are then obtained directly with equations 4.22 through 4.24:

$$C_{Y_\beta} = \frac{C_Y}{\Delta\beta°} * \frac{180}{\pi} \text{ per radian} \tag{4.22}$$

$$C_{l_\beta} = \frac{C_l}{\Delta\beta°} * \frac{180}{\pi} \text{ per radian} \tag{4.23}$$

$$C_{n_\beta} = \frac{C_n}{\Delta\beta°} * \frac{180}{\pi} \text{ per radian} \tag{4.24}$$

It should be noted that the CMARC wind axis is modeled with x-aft and z-up, vice x-forward and z-down for the flight dynamics stability axis. Care must be taken to reverse the signs of the appropriate coefficients to convert from the CMARC wind axis to the flight dynamics stability axis system.

Static lateral-directional stability derivatives obtained from CMARC are presented in Table 4.9. For comparison three other sets of data are also presented. The first comes from classical analysis using methods from Roskam [Ref. 12]. The second set comes from estimates based on data recorded from flight-test sideslip maneuvers, published by Papageorgio in Ref. [2]. The third set comes from parameter estimation, by Engdahl, based on dynamic flight-test maneuvers.

METHOD	CONFIGURATION[1]	STATIC LAT-DIR PARAMETERS		
		$C_{Y\beta}$ (per rad)	$C_{l\beta}$ (per rad)	$C_{n\beta}$ (per rad)
CMARC Panel Code	Wing/Fuselage + Horz/Vert Stabs	-0.249	-0.063	0.063
Classical Design[2]	Wing/Fuselage/Vert Tail	-0.511	-0.055	0.051
Flight Test[3]	Flying Aircraft	-0.700	-0.053	0.057
Parameter Estimation[4]	Flying Aircraft	-0.987	-0.094	0.176
	C-172[5]	-0.310	-0.089	0.065

NOTES: 1) CG_x=34.5% M.A.C. / CG_z=8.6" from bottom of fuselage.
2) Classical design calculations by Roskam's methods, after Ref. [12].
3) Flight test results from steady heading sideslip, from Ref. [2]
4) Parameter estimation from flight test data by Engdahl.
5) C-172 data from Ref. [12].

Table 4.9 Comparison of FROG UAV Static Lateral-Directional Stability Derivatives.

CMARC produced weak results for the $C_{Y\beta}$ side force derivative. A large component of $C_{Y\beta}$, approximately 60%, comes from the fuselage. Side forces are not modeled well by the potential flow solution. In addition, the engine pylon and pod are left off the model due to problems with their wakes impacting the vertical tail. They most likely provide a significant contribution to side force.

CMARC results for weathercock stability, $C_{n\beta}$, and dihedral effect, $C_{l\beta}$, show close correlation to the classical calculations. However, dynamic parameter analysis indicates a considerably higher value for both derivatives. The parameter estimation most likely captures the additional dynamic pressure over the vertical stabilizer from prop wash. As with the longitudinal solutions, an attempt should be made to model the propeller disk with a normal velocity distribution.

b. Lateral-Directional Damping Derivatives

As with the static case, the dynamic solutions are run with separate wing/fuselage and vertical/horizontal stabilizer models. The solutions are summed through superposition. Figure 4.17 shows the two angular motions selected to develop the lateral-directional rate-damping derivatives. The β-dot terms are generally considered to be small. As a result, the sideways plunging motion test case is not run. Yaw rate-damping is obtained directly from the oscillating yawing motion without the requirement to subtract β-dot effects. Yawing motion is conducted at a frequency of 2π rad/s, which equates to a reduced frequency of $k=0.369$ for this configuration and trim airspeed.

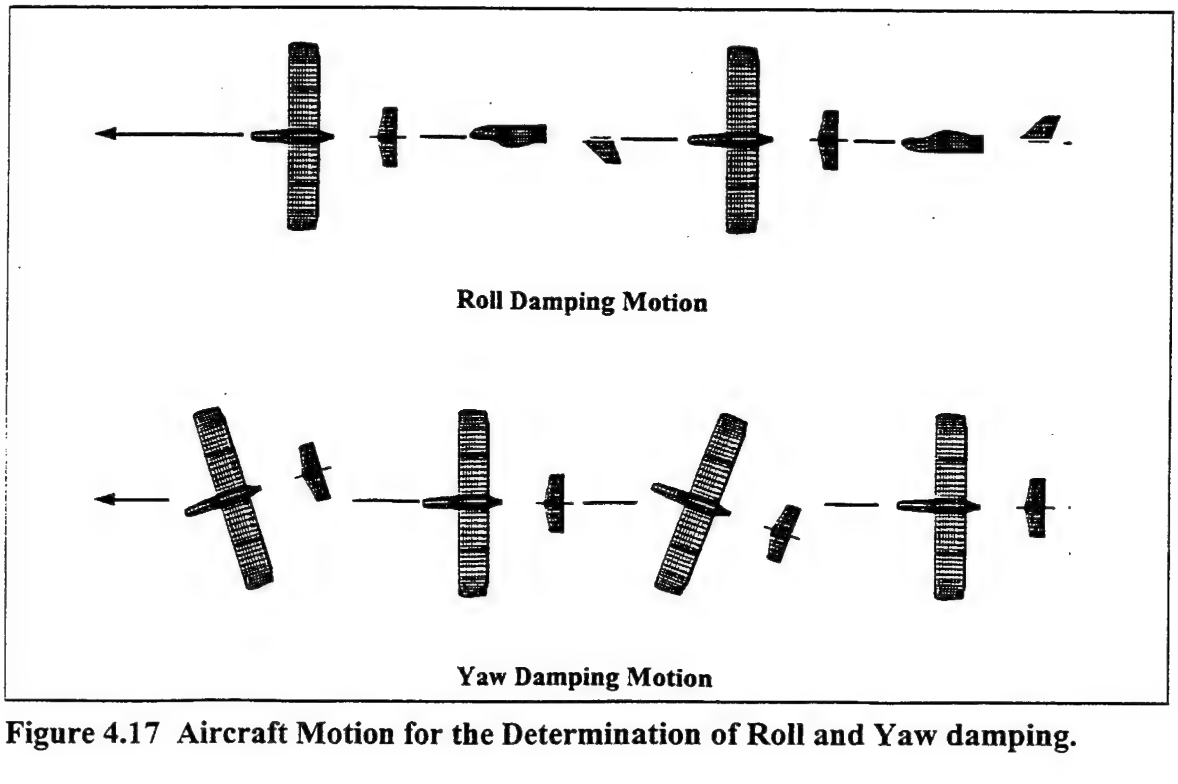

Figure 4.17 Aircraft Motion for the Determination of Roll and Yaw damping.

The roll axis is de-coupled from both angle-of-attack and sideslip. Therefore, roll damping can be obtained directly from a constant rolling motion, as illustrated in Figure 4.17. For the FROG study a roll rate of 20°/sec is selected. Initially a lower roll rate of 5°/sec was used. However, the lower rate produced small values of both side force and yawing moment. A higher roll rate prevented machine resolution from becoming a factor in data reduction. The User Guide in Appendix A provides a more detailed description of the techniques used to gather the dynamic lateral-directional derivatives.

The roll damping stability terms are presented in Table 4.10. Traditional design calculations from Roskam [Ref. 12] were completed for comparison to CMARC and flight-test results. In addition, C-172 data is also presented. CMARC roll damping, C_{lp}, is 50% higher than classical results, but right in line with parameter estimation. CMARC adverse yaw due to roll rate, C_{np}, is approximately one fourth that obtained from either classical calculations or parameter estimation. Of note, CMARC does capture side force due to roll rate. This term is difficult to obtain from classical techniques and is usually assumed to be negligible.

METHOD	CONFIGURATION[1]	ROLL RATE TERMS		
		Cy_p (per rad)	C_{lp} (per rad)	C_{np} (per rad)
CMARC Panel Code	Wing/Fuselage + Horz/Vert Stabs	0.05	-0.452	-0.022
Classical Design[2]	Wing/Fuselage/Vert Tail	0	-0.300	-0.072
Parameter Estimation[3]	Flying Aircraft	0	-0.448	-0.108
	C-172[4]	-0.037	-0.47	-0.03

NOTES: 1) CG_x=34.5% M.A.C. / CG_z=8.6" from bottom of fuselage.
2) Classical design calculations by Roskam's methods, after Ref. [12].
3) Parameter estimation from flight test data by Engdahl.
4) C-172 data from Ref. [12].

Table 4.10 Comparison of FROG UAV Roll Rate Stability Derivatives.

The yaw rate-damping terms are presented in Table 4.11. Traditional design calculations from Roskam [Ref. 12] are presented for comparison to CMARC and flight-test results. C-172 data is also listed. CMARC does an excellent job of predicting yaw damping. Yaw damping, C_{nr}, directly matches the result from parameter estimation. CMARC underestimates roll moment due to yaw rate, C_{lr}, by 25 to 40 percent. And, side force due to yaw rate, C_{Yr}, is overestimated by a factor of three compared to the parameter estimation model. No explanation is readily available to explain these errors.

METHOD	CONFIGURATION[1]	YAW RATE TERMS		
		C_{Yr} (per rad)	C_{lr} (per rad)	C_{nr} (per rad)
CMARC Panel Code	Wing/Fuselage + Horz/Vert Stabs	0.337	0.121	-0.121
Classical Design[2]	Wing/Fuselage/Vert Tail	0.140	0.168	-0.076
Parameter Estimation[3]	Flying Aircraft	0.110	0.208	-0.121
	C-172[4]	0.210	0.096	-0.099

NOTES: 1) CG_x=34.5% M.A.C. / CG_z=8.6" from bottom of fuselage.
2) Classical design calculations by Roskam's methods, after Ref. [12].
3) Parameter estimation from flight test data by Engdahl.
4) C-172 data from Ref [12].

Table 4.11 Comparison of FROG UAV Yaw Rate Stability Derivatives.

c. *Lateral-Directional Control-Power Derivatives*

Aileron and rudder control-power derivatives are presented in Tables 4.12 and 4.13. Classical design calculations are performed using equations 4.25 through 4.30 from Roskam [Ref. 15]:

$$C_{Y_{\delta r}} = \frac{C_{L_{\alpha_v}}}{C_{l_{\alpha_v}}} C_{l_{\delta_r}} K_b \frac{S_v}{S} \qquad 4.25$$

$$C_{l_{\delta r}} = C_{Y_{\delta_r}} \frac{(Z_v \cos\alpha - l_v \sin\alpha)}{b} \tag{4.26}$$

$$C_{n_{\delta r}} = -C_{Y_{\delta_r}} \frac{(l_v \cos\alpha - Z_v \sin\alpha)}{b} \tag{4.27}$$

$$C_{Y_{\delta a}} \approx small \tag{4.28}$$

$$C_{n_{\delta a}} = K * C_L * C_{l_{\delta a}} \tag{4.29}$$

$$C_{l_{\delta a}} = |\alpha_{\delta a}| * \frac{C_{l_\alpha}}{2\pi}\left(\frac{C'_{l_{\delta a}}}{\kappa}\right) \tag{4.30}$$

where $C_{Y\delta F}$, α_δ, κ and $(C'_{l\delta a}/\kappa)$ are empirical values from charts in Roskam [Ref. 15]. Additionally, flight-test parameter analysis and C-172 data are provided for comparison.

METHOD	CONFIGURATION[1]	AILERON CONTROL POWER		
		$C_{Y\delta a}$ (per rad)	$C_{l\delta a}$ (per rad)	$C_{n\delta a}$ (per rad)
CMARC Panel Code	Blended Wing-Fuselage/Horz/Vert Tails	-0.021	0.194	-0.0121
Classical Design[2]	Wing/Fuselage/Vert Tail	0	0.213	-0.0236
Parameter Estimation[3]	Flying Aircraft	0	0.239	-0.0261
	C-172[4]	0	0.178	-0.053

NOTES: 1) CG_x=34.5% M.A.C. / CG_z=8.6" from bottom of fuselage.
2) Classical design calculations by Roskam's methods, after Ref. [12].
3) Parameter estimation from flight test data by Engdahl.
4) C-172 data from Ref. [12].

Table 4.12 Comparison of FROG UAV Aileron Control-Power Derivatives.

In general, CMARC provides aileron control-power estimates in the correct direction and same order of magnitude as both the classical and parameter estimation techniques. Aileron roll control-power shows excellent correlation to both methods. However, CMARC under-estimates adverse yaw due to aileron deflection, $C_{n\delta a}$, by approximately 50%. Yawing moment due to roll rate, C_{np}, is also underestimated by a similar margin. An investigation into the source of CMARC inaccuracies in the modeling of adverse yaw due to aileron deflection and roll rate is warranted.

The rudder control-power derivatives obtained with CMARC show good correlation to classical design techniques. Side force due to rudder deflection, $C_{Y\delta r}$, is 15% greater than classical calculations but closely matches flight-test results. For both $C_{n\delta r}$ and $C_{l\delta r}$, CMARC estimates fall between classical calculations and parameter estimation results. The stronger rudder control-power observed in the parameter estimation model is most likely due to the capturing of prop wash effects.

METHOD	CONFIGURATION[1]	RUDDER CONTROL POWER		
		$C_{Y\delta r}$ (per rad)	$C_{l\delta r}$ (per rad)	$C_{n\delta r}$ (per rad)
CMARC Panel Code	Blended Wing-Fuselage/Horz/Vert Tails	0.0928	0.0040	-0.0453
Classical Design[2]	Wing/Fuselage/Vert Tail	0.081	0.0056	-0.0341
Parameter Estimation[3]	Flying Aircraft	0.093	0.0004	-0.0785
	C-172[4]	0.187	0.015	-0.0657

NOTES: 1) CG_x=34.5% M.A.C. / CG_z=8.6" from bottom of fuselage.
2) Classical design calculations by Roskam's methods, after Ref. [12].
3) Parameter estimation from flight test data by Engdahl.
4) C-172 data from Ref [12].

Table 4.13 Comparison of FROG UAV Rudder Control-Power Derivatives.

3. Summary of CMARC Stability Derivative Analysis

Table 4.14 lists the complete FROG aerodynamic model obtained from CMARC for the trim condition. In summary, CMARC produces reasonably accurate stability derivatives for an initial aerodynamic model. The greatest difficulty is encountered modeling side force due to sideslip and roll rate. The potential flow solution from CMARC fails to adequately capture the side force on the fuselage. Improved fidelity might be obtained by modeling fuselage flow separation with wake separation lines. CMARC also underestimates yawing moment due to roll rate and aileron deflection by large margins.

LONGITUDINAL		LATERAL-DIRECTIONAL	
Derivative	**Value**	**Derivative**	**Value**
C_L	0.4295	$C_{Y\beta}$[1]	-0.2493
C_D	0.065	$C_{l\beta}$	-0.0630
$C_{L\alpha}$	4.845	$C_{n\beta}$	0.6300
$C_{D\alpha}$	0.2664	C_{Yp}	0.0488
$C_{M\alpha}$	-0.4126	C_{lp}	-0.4514
$C_{L\alpha dot}$	1.420	C_{np}	-0.0220
$C_{M\alpha dot}$	-6.264	C_{Yr}	0.3370
C_{Lq}	6.862	C_{lr}	0.1210
C_{Dq}	0	C_{nr}	-0.1210
C_{Mq}	-11.78	$C_{Y\delta r}$	0.0928
$C_{L\delta e}$	0.4378	$C_{l\delta r}$	0.0040
$C_{D\delta e}$	0.0092	$C_{n\delta r}$	-0.0453
$C_{M\delta e}$	-1.199	$C_{Y\delta a}$	-0.0206
		$C_{l\delta a}$	0.1943
		$C_{n\delta a}$	-0.0121

Table 4.14 Summary of CMARC Stability Derivatives for the NPS FROG UAV.

F. COMPARISON OF DYNAMIC AERODYNAMIC MODELS

This section will discuss the dynamic response of the FROG UAV using the CMARC generated aerodynamic model. Specifically, modal frequency and damping are obtained through eigenvalue analysis. Elevator, aileron and rudder control response is found using a linearized state-equation model. Results are compared to the classical design and parameter estimation models.

Dimensional stability derivatives are placed into linearized 4x4 models as outlined by Schmidt in Ref. [14]. The short-period and long-period modes are obtained using the MATLAB eigenvalue decomposition routine. In a similar manner, the lateral-directional plant matrix yields the roll, spiral and Dutch-roll modes. Dynamic response due to step and doublet control inputs is obtained by assembling the complete linear system. This paper uses control deflection sign convention consistent with Figure 4.9 from Ref. [14]. The MATLAB "lsim" command produces the time based output of the linear system. MATLAB is used to plot the dynamic response.

1. Longitudinal Dynamics

a. Longitudinal Dynamic Modes

The longitudinal response of an aircraft can be reduced to a series of four, first-order differential equations. They are typically written in matrix form based on the state variables u/V, α, q and θ. The linearized state-equations, in matrix form as developed by Schmidt in Ref. [14], are listed in equations 4.31 to 4.37:

$$\{\dot{x}\} = [A]\{x\} + \{B\}\delta_e \qquad 4.31$$

$$\{x\} = [u/V \quad \alpha \quad q \quad \theta]^T \qquad 4.32$$

$$[A] = [I_n]^{-1}[A_n] \qquad 4.33$$

$$\{B\}=[I_n]^{-1}\{B_n\} \qquad 4.34$$

$$[A_n]=\begin{vmatrix} VX_u & X_\alpha & 0 & -g\cos\Theta_0 \\ VZ_u & Z_\alpha & (V+Z_q) & -g\sin\Theta_0 \\ VM_u & M_\alpha & M_q & 0 \\ 0 & 0 & 1 & 0 \end{vmatrix} \qquad 4.35$$

$$\{B_n\}=[X_{\delta e} \quad Z_{\delta e} \quad M_{\delta e} \quad 0]^T \qquad 4.36$$

$$[I_n]=\begin{vmatrix} V & 0 & 0 & 0 \\ 0 & (V-Z_{\dot\alpha}) & 0 & 0 \\ 0 & -M_{\dot\alpha} & 1 & 0 \\ 0 & 0 & 0 & 1 \end{vmatrix} = \textit{Inertial} \quad \textit{matrix} \qquad 4.37$$

The non-dimensional stability derivatives generated by CMARC are converted to dimensional derivatives through the transformations listed in Table 4.15. Dimensional derivatives are more convenient because they will lead to time histories being expressed in seconds and frequency in rad/s. The MATLAB script "froguav.m" in Appendix D is used to automate these calculations.

The linearized, longitudinal, state-equation is given by equation 4.31. Note that the plant and control matrices are obtained by pre-multiplying by $[I_n]^{-1}$. The eigenvalues of the plant matrix, [A], yield the longitudinal dynamic modes. The eigenvalues are obtained from the MATLAB script "froguav.m" listed in Appendix D. The results are presented in Table 4.16.

Term	Description	Units
X_u	$-\frac{QS}{mV}(2C_D + M\frac{\partial C_D}{\partial M})$	s^{-1}
X_α	$\frac{QS}{m}(C_L - \frac{\partial C_D}{\partial \alpha})$	$ft\text{-}s^{-2}$
$X_{\dot\alpha}$	$-\frac{QS}{m}\left(\frac{c}{2V}\right)\frac{\partial C_D}{\partial(\dot\alpha c/2V)}$	$ft\text{-}s^{-1}$
X_q	$-\frac{QS}{m}\left(\frac{c}{2V}\right)\frac{\partial C_D}{\partial(qc/2V)}$	$ft\text{-}s^{-1}$
X_δ	$-\frac{QS}{m}\frac{\partial C_D}{\partial \delta}$	$ft\text{-}s^{-2}$
Z_u	$-\frac{QS}{mV}(2C_L + M\frac{\partial C_L}{\partial M})$	s^{-1}
Z_α	$-\frac{QS}{m}(C_D + \frac{\partial C_L}{\partial \alpha})$	$ft\text{-}s^{-2}$
$Z_{\dot\alpha}$	$-\frac{QS}{m}\left(\frac{c}{2V}\right)\frac{\partial C_L}{\partial(\dot\alpha c/2V)}$	$ft\text{-}s^{-1}$
Z_q	$-\frac{QS}{m}\left(\frac{c}{2V}\right)\frac{\partial C_L}{\partial(qc/2V)}$	$ft\text{-}s^{-1}$
Z_δ	$-\frac{QS}{m}\frac{\partial C_L}{\partial \delta}$	$ft\text{-}s^{-2}$
M_u	$\frac{QSc}{I_y V}\frac{\partial C_m}{\partial M}$	$ft\text{-}s^{-1}$
M_α	$\frac{QSc}{I_y}\frac{\partial C_m}{\partial \alpha}$	s^{-2}
$M_{\dot\alpha}$	$\frac{QSC}{I_y}\left(\frac{c}{2V}\right)\frac{\partial C_m}{\partial(\dot\alpha c/2V)}$	s^{-1}
M_q	$\frac{QSC}{I_y}\left(\frac{c}{2V}\right)\frac{\partial C_m}{\partial(qc/2V)}$	s^{-1}
M_δ	$\frac{QSc}{I_y}\frac{\partial C_m}{\partial \delta}$	s^{-2}

Table 4.15 Dimensional Longitudinal Stability Derivatives from Ref. [14].

METHOD	CONFIGURATION[1]	LONGITUDINAL DYNAMIC MODES			
		Short-Period		Phugoid	
		ω_n (rad/s)	ζ	ω_n (rad/s)	ζ
CMARC Panel Code	Wing/Fuselage/Horiz Tail	5.15	0.909	0.358	0.136
Classical Design[2]	Wing/Horiz Tail - $\delta\varepsilon/\delta\alpha$=0.40	5.90	0.734	0.407	0.110
Parameter Estimation[3]	Flying Aircraft	4.67	0.770	0.397	0.101
	C-172	6.027	0.685	0.181	0.116

NOTES: 1) CG_x=34.5% M.A.C. / CG_z=8.6" from bottom of fuselage.

2) Classical design calculations, after Ref. [12].

3) Classical model from Papageorgio [Ref. 2] as modified through parameter estimation from flight test data by Engdahl.

4) C-172 data from Ref. [12].

Table 4.16 Comparison of FROG UAV Dynamic Longitudinal Modes.

Table 4.16 summarizes the longitudinal dynamic modes. The CMARC aerodynamic model provides a better estimate of short-period frequency than the classical design technique. The CMARC short-period frequency is 10% faster than that observed from parameter analysis and damping is 21% higher. The high damping in all three models will produce nearly deadbeat results. The CMARC phugoid, or long period, is 10% slower than observed from flight-test with 40% more damping. Although, it must be pointed out that it is difficult to accurately capture the phugoid mode in flight-test. This is due to difficulty the external pilot has in accurately maintaining wings level trim during the extended period required for capturing phugoid data. Overall, the CMARC aerodynamic model produces satisfactory short-period and phugoid modal data for the development of closed-loop flight controls. Of note, CMARC provides a more accurate prediction of the important short-period natural frequency. The larger error in phugoid frequency is less important to the design of a closed loop controller.

b. Longitudinal Dynamic Response to Control Input

Following dynamic mode analysis, the response to an elevator step-input and a doublet-input is modeled using MATLAB. Dynamic response for the CMARC, classical and parameter analysis models are overlaid for comparison. The linear system is set up using the MATLAB script "froguav.m" in Appendix D. The "lsim" command outputs the time-based response from a time-based control input vector. A -2° (TEU) elevator step-input is selected to keep the response in the linear region. A 5° elevator doublet with a 1.2 second period is used to excite the short-period mode. The selected doublet period closely matches the short-period mode. Dynamic response is displayed in Figures 4.18 and 4.19.

The FROG UAV response to a -2° (TEU) step elevator input is displayed in Figure 4.18. All three aerodynamic models are presented for comparison. The model adjusted by parameter analysis shows a much larger response than either the CMARC or classical design models. The CMARC model produces a final pitch angle change after 4 seconds of 35° versus 45° for the flight-tested model. On closer review, it is noted the $C_{m\delta e}$ =-1.199 from CMARC is considerably less than the $C_{m\delta e}$ = -1.621 from flight-test. It should be noted that the parameter estimation model compensates for real world factors including; air load distortions, sensor measurement errors and prop wash. In other words, the CMARC model assumes uniform displacement and perfect sensors while the flight-test model is empirically fit to a measured response.

The response to a 5° elevator doublet is displayed in Figure 4.19. All three models show a similar frequency and a high degree of damping. As expected, the parameter estimation model produces a larger response. The magnitude of the CMARC response is approximately two thirds of that observed from the flight-test model. Again, this is due to the much larger value of $C_{m\delta e}$ obtained from empirically fitting the parameter estimation model to observed aircraft response. Modeling prop wash with CMARC should produce improved results.

In summary, the CMARC aerodynamic model showed satisfactory longitudinal control response in frequency and damping. It is recommended that $C_{m\delta e}$ be adjusted to increase elevator response.

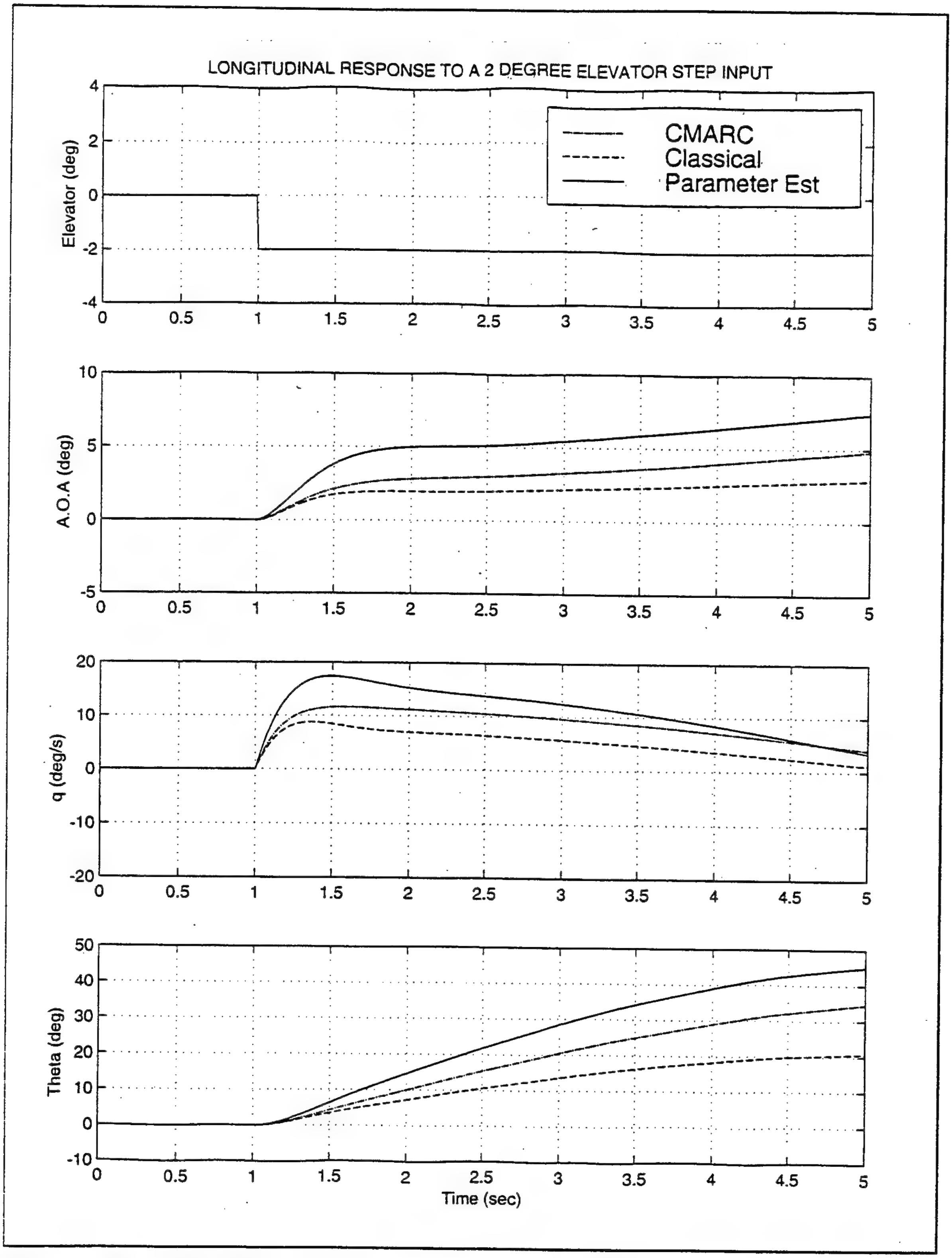

Figure 4.18 FROG UAV Dynamic Response to a -2° (TEU) Elevator Step Input.

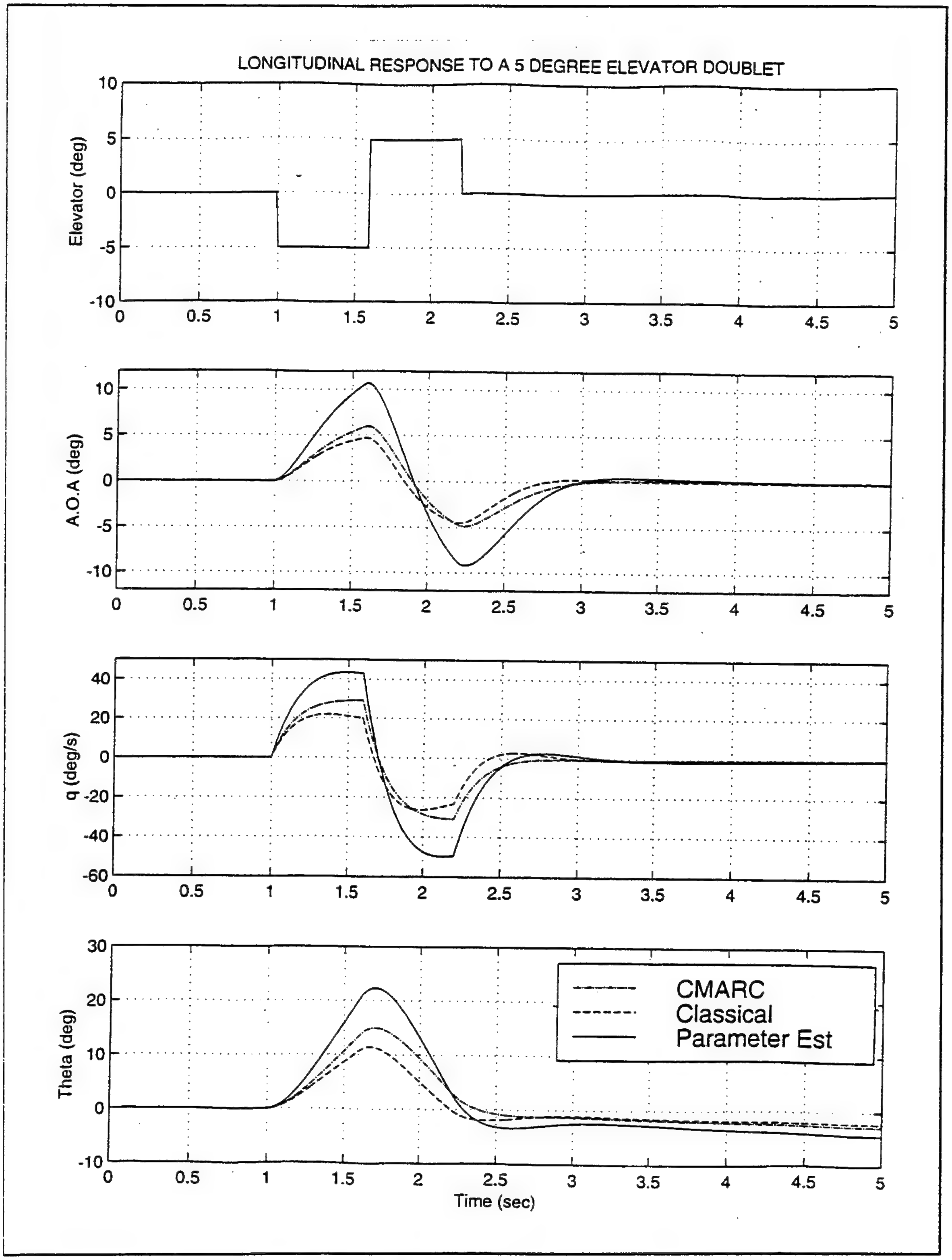

Figure 4.19 FROG UAV Dynamic Response to a 5° Elevator Doublet.

2. Lateral-Directional Dynamics

a. Lateral-Directional Dynamic Modes

The lateral-directional response of an aircraft can also be reduced to a series of four first-order differential equations. They are typically written in matrix form based on the state-variables β, p, φ, and r. The linearized state-equations in matrix form as developed by Schmidt in Ref. [14] are listed in equations 4.38 to 4.44:

$$\{\dot{x}\} = [A]\{x\} + \{B\}\delta_{a/r} \tag{4.38}$$

$$\{x\} = [\beta \quad p \quad \phi \quad r]^T \tag{4.39}$$

$$[A] = [I_n]^{-1}[A_n] \tag{4.40}$$

$$\{B\} = [I_n]^{-1}\{B_n\} \tag{4.41}$$

$$[A_n] = \begin{vmatrix} Y_\beta & Y_p & g\cos\Theta_0 & (Y_r + V) \\ L_\beta & L_p & 0 & L_r \\ 0 & 1 & 0 & 0 \\ N_\beta & N_p & 0 & N_r \end{vmatrix} \tag{4.42}$$

$$\{B_n\} = \left[\frac{Y_{\delta a} \quad L_{\delta a} \quad 0 \quad N_{\delta a}}{Y_{\delta r} \quad L_{\delta r} \quad 0 \quad N_{\delta r}}\right]^T \tag{4.43}$$

$$[I_n] = \begin{vmatrix} V & 0 & 0 & 0 \\ 0 & (V - Z_{\dot\alpha}) & 0 & 0 \\ 0 & -M_{\dot\alpha} & 1 & 0 \\ 0 & 0 & 0 & 1 \end{vmatrix} = \textit{Inertial} \quad \textit{matrix} \tag{4.44}$$

As with the longitudinal axis, the stability derivatives generated by CMARC are dimensionless. However, it is more convenient to use dimensional derivatives. They will lead to time histories being expressed in seconds and frequency in rad/s. The lateral-directional stability derivatives are turned into dimensional derivatives through the transformations listed in Table 4.17 from Ref. [14]. The MATLAB script "froguav.m" in Appendix D is used to automate these calculations.

Term	Description	Units
Y_β	$\frac{QS}{m}\frac{\partial C_y}{\partial \beta}$	ft-s^{-2}
Y_p	$\frac{QS}{m}\left(\frac{b}{2V}\right)\frac{\partial C_y}{\partial(pb/2V)}$	ft-s^{-1}
Y_r	$\frac{QS}{m}\left(\frac{b}{2V}\right)\frac{\partial C_y}{\partial(rb/2V)}$	ft-s^{-1}
Y_δ	$\frac{QS}{m}\frac{\partial C_y}{\partial \delta}$	ft-s^{-2}
L_β	$\frac{QSb}{I_x}\frac{\partial C_\ell}{\partial \beta}$	s^{-2}
L_p	$\frac{QSb}{I_x}\left(\frac{b}{2V}\right)\frac{\partial C_\ell}{\partial(pb/2V)}$	s^{-1}
L_r	$\frac{QSb}{I_x}\left(\frac{b}{2V}\right)\frac{\partial C_\ell}{\partial(rb/2V)}$	s^{-1}
L_δ	$\frac{QSb}{I_x}\frac{\partial C_\ell}{\partial \delta}$	s^{-2}
N_β	$\frac{QSb}{I_z}\frac{\partial C_n}{\partial \beta}$	s^{-2}
N_p	$\frac{QSb}{I_z}\left(\frac{b}{2V}\right)\frac{\partial C_n}{\partial(pb/2V)}$	s^{-1}
N_r	$\frac{QSb}{I_z}\left(\frac{b}{2V}\right)\frac{\partial C_n}{\partial(rb/2V)}$	s^{-1}
N_δ	$\frac{QSb}{I_z}\frac{\partial C_n}{\partial \delta}$	s^{-2}

Table 4.17 Dimensional Lateral-Directional Stability Derivatives from Ref. [14]

The linearized, lateral-directional state-equation is given by equation 4.38. Note that the plant and control matrices are obtained by pre-multiplying by $[I_n]^{-1}$. The dimensional derivatives from Table 4.16 populate the linearized 4x4 plant matrix and control matrices. The plant matrix, [A], is used to obtain the lateral-directional dynamic modes. The eigenvalues are obtained from MATLAB using the "froguav.m" script in Appendix D. The results are presented in Table 4.18.

METHOD	CONFIGURATION[1]	LATERAL-DIRECTIONAL DYNAMIC MODES			
		Dutch-Roll		Roll	Spiral
		ω_n (rad/s)	ζ	ω_n (rad/s)	ω_n (rad/s)
CMARC Panel Code	Wing/Fuselage Group plus Horiz/Vert Stab Group	2.54	0.13	-3.80	0.000
Classical Design[2]	Wing/Fuselage/Horiz Tail	2.48	0.09	-2.83	0.065
Parameter Estimation[3]	Flying Aircraft	4.27	0.14	-3.97	0.090
	C-172[4]	3.38	0.20	12.43	0.01

NOTES: 1) CG_x=34.5% M.A.C. / CG_z=8.6" from bottom of fuselage.
2) Classical design calculations after Ref. [12].
3) Classical model from Papageorgio [Ref. 2] as modified through parameter estimation from flight test data by Engdahl.
4) C172 data from Ref. [12].

Table 4.18 Comparison of FROG UAV Lateral-Directional Dynamic Modes.

The lateral-directional dynamic modes are summarized in Table 4.18. The CMARC aerodynamic model provides significantly better estimates of frequency and damping than the classical design technique for both the Dutch-roll and roll modes. The CMARC Dutch-roll natural frequency, although better than the classical response, is 40% lower than predicted by parameter estimation. Adjustments should be made to the CMARC aerodynamic model to improve Dutch-roll response.

The primary contributor to the Dutch-roll frequency is weathercock stability, $C_{n\beta}$. A review of Table 4.9 shows that $C_{n\beta}$ obtained from CMARC is considerably less than the value obtained through parameter estimation. One potential source of error is the lack of modeling the increased dynamic pressure due to prop wash. The FROG model should be re-worked to include a prop disk to investigate the ability of CMARC to capture prop wash effects.

The CMARC model predicts a neutral spiral mode. This is most likely due to a combination of equal and opposite C_{lr} and C_{nr} ratios. When the C_{lr}/C_{nr} ratio is changed to -2 (approximately that of the analytical and parameter estimation models), the spiral mode comes out close to the analytical model. The weak roll due to yaw-rate, C_{lr}, in the CMARC solution seems to be the main source of error in the spiral mode. The value will need to be modified to produce an acceptable spiral response.

b. Lateral-Directional Dynamic Response to Control Input

Following dynamic-mode analysis, the response to aileron and rudder inputs is modeled using MATLAB. Dynamic response for the CMARC, classical and parameter-analysis models are overlaid for comparison. The linear system is set up using the MATLAB script "froguav.m" in Appendix D. The "lsim" command outputs the time-based response from a time-based input control vector.

The lateral response to a +2° (right wing down) step aileron deflection is shown in Figure 4.20. CMARC steady-state roll-rate is less than that predicted by the other two models. This is expected considering the CMARC model has the lowest ratio of aileron control-power to roll-damping. In addition, the side-force terms, C_{Yp} and $C_{Y\delta a}$, modeled by CMARC both fight roll-rate. They are not included in the other models. Perhaps they should be assumed small and set to zero. CMARC does a significantly better job of modeling the Dutch-roll response. The roll-rate and sideslip traces from the classical design model clearly show excess excitation of the Dutch-roll mode. The CMARC model shows a better correlation to the parameter estimation model for Dutch-roll amplitude and damping. As predicted by the eigenvalues, Dutch-roll frequency is slower than the parameter estimation model.

The lateral-directional response to a 5° aileron doublet is shown in Figure 4.21. The 1.5 second period clearly excites the Dutch-roll mode in all three models. As with the step-input response, the CMARC model provides a significantly better match to

Dutch-roll excitation than the classical design model. Amplitude and damping show a close correlation to the parameter estimation model. A lower Dutch-roll frequency is evident in the CMARC sideslip trace.

The lateral-directional response to a +2° (nose left) rudder deflection is shown in Figure 4.22. The CMARC model demonstrates a close match to the classical design model for Dutch-roll frequency and damping. CMARC shows higher sideslip excitation than the classical design model. A slower Dutch-roll frequency is evident in both the CMARC and classical design models.

The lateral-directional response to a 5° rudder doublet deflection is shown in Figure 4.23. Again, the 1.5 second doublet excites the Dutch-roll mode in all three models. CMARC provides a similar response to the classical design model. As expected, Dutch-roll natural frequency is about 40% slower than the parameter estimation model with similar damping.

In summary, the CMARC lateral-directional model provides FROG dynamics that are similar to the classical design calculations. However, current CMARC lateral-directional dynamics are not adequate for closed-loop controller or autopilot design. Minor adjustments will be required to better match observed flight characteristics. The lateral-directional model should be modified to include a propeller disk. Higher dynamic pressure over the tail surfaces should provide a stronger $C_{n\beta}$ derivative and result in faster Dutch-roll frequency. In addition, the FROG model should be adjusted to provide a higher aileron control-power to roll-damping ratio. This modification will improve roll-rate response.

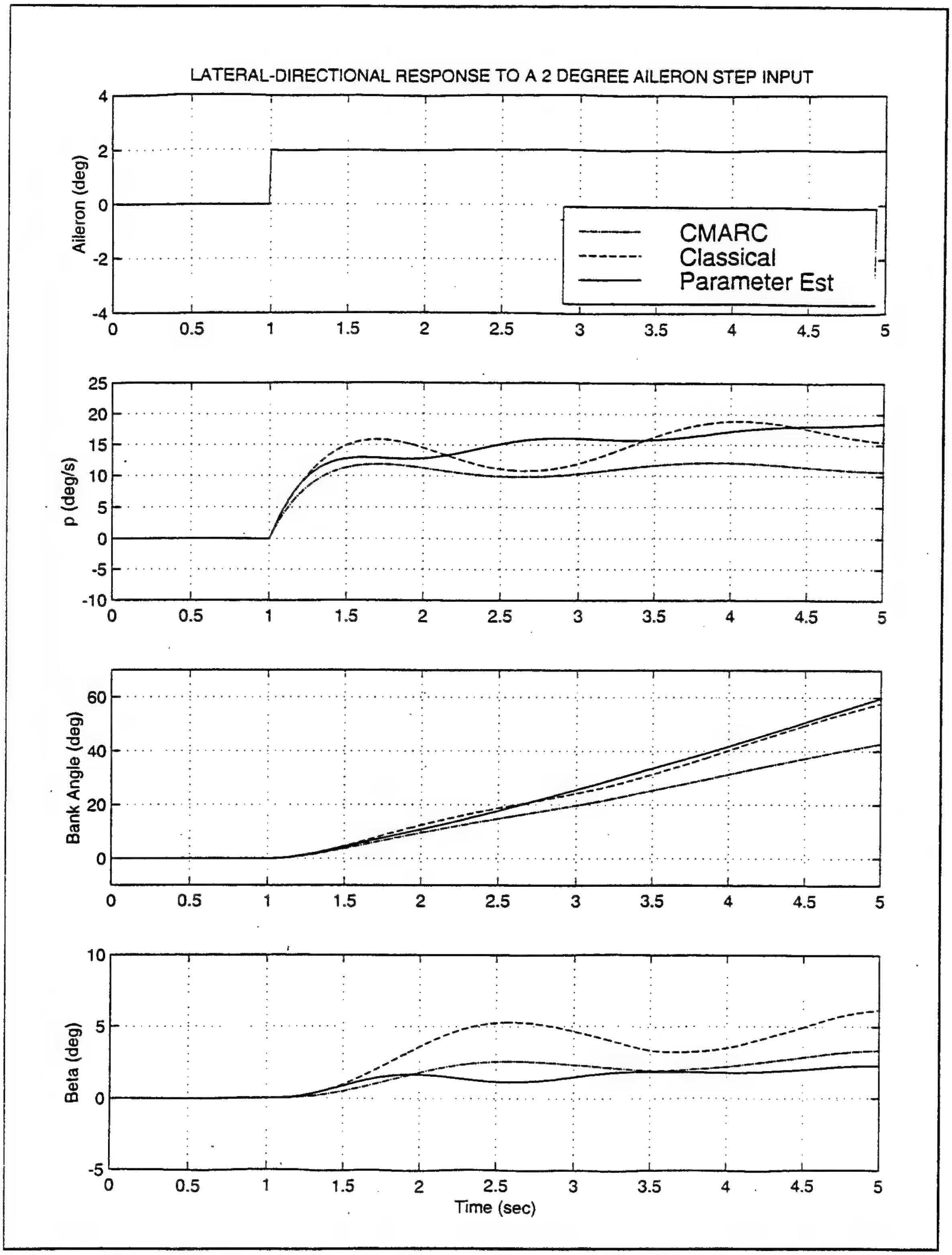

Figure 4.20 FROG UAV Dynamic Response to a +2° (RWD) Aileron Step Input.

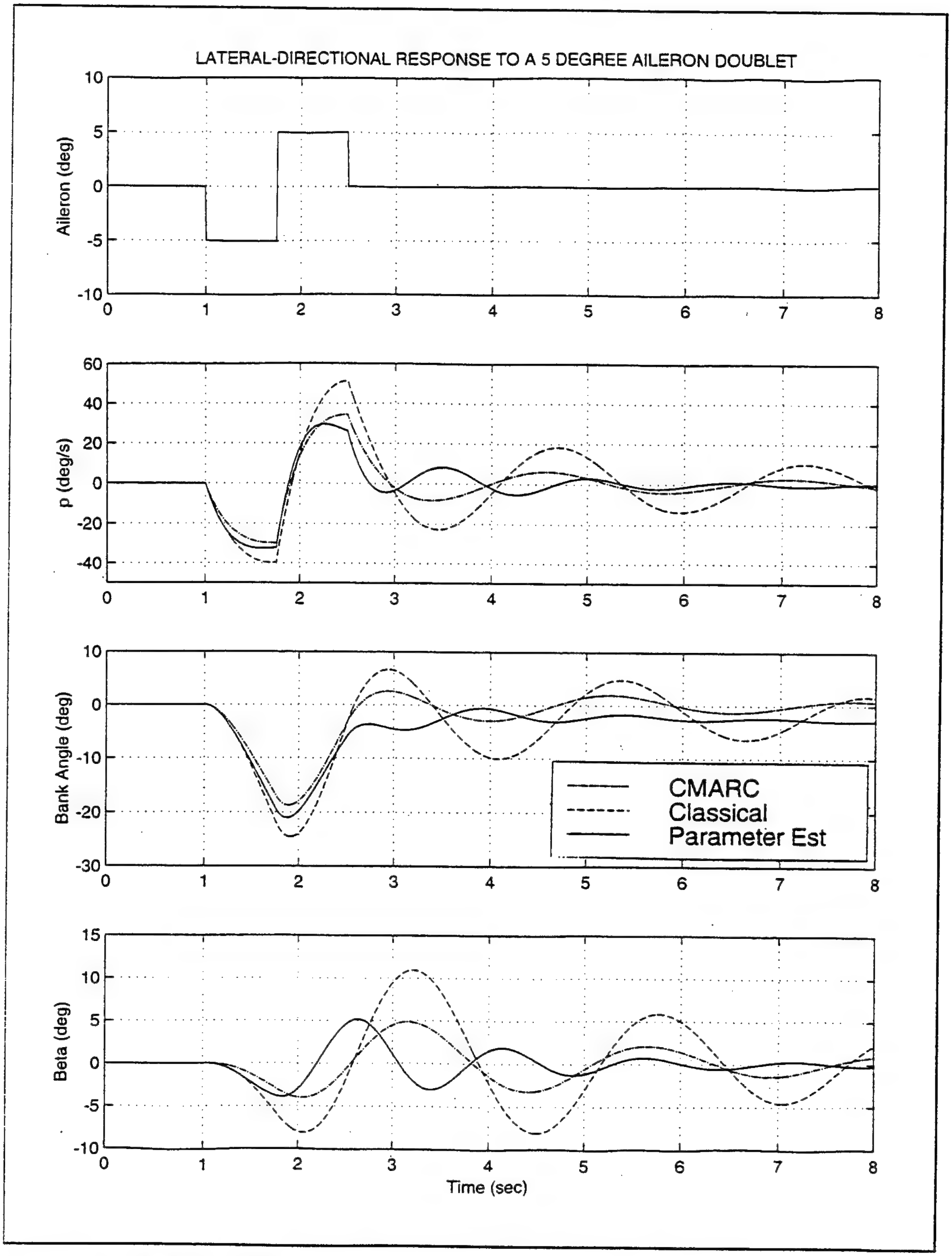

Figure 4.21 FROG UAV Dynamic Response to a 5° Aileron Doublet.

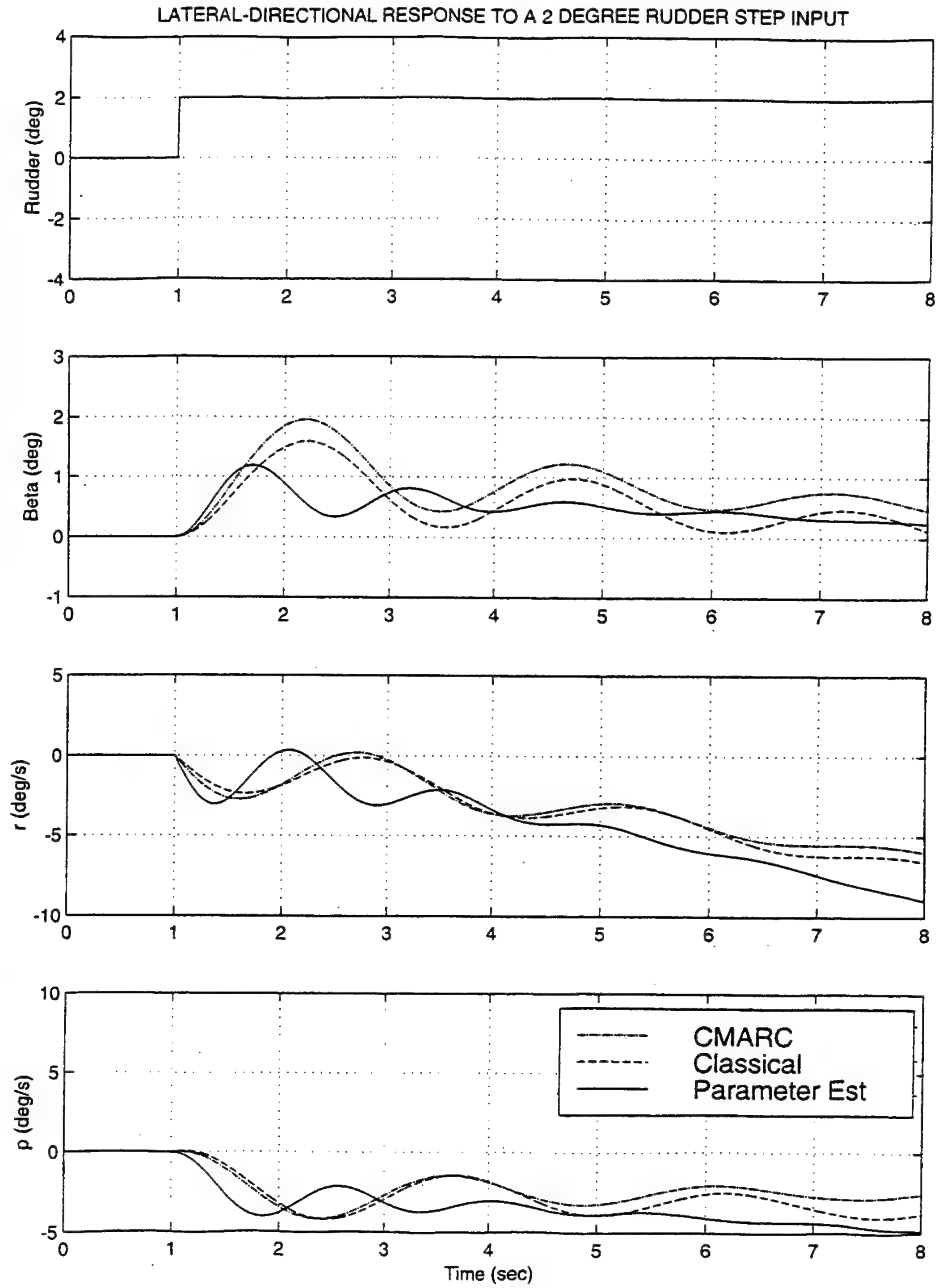

Figure 4.22 FROG UAV Dynamic Response to a +2° (TEL) Rudder Step Input.

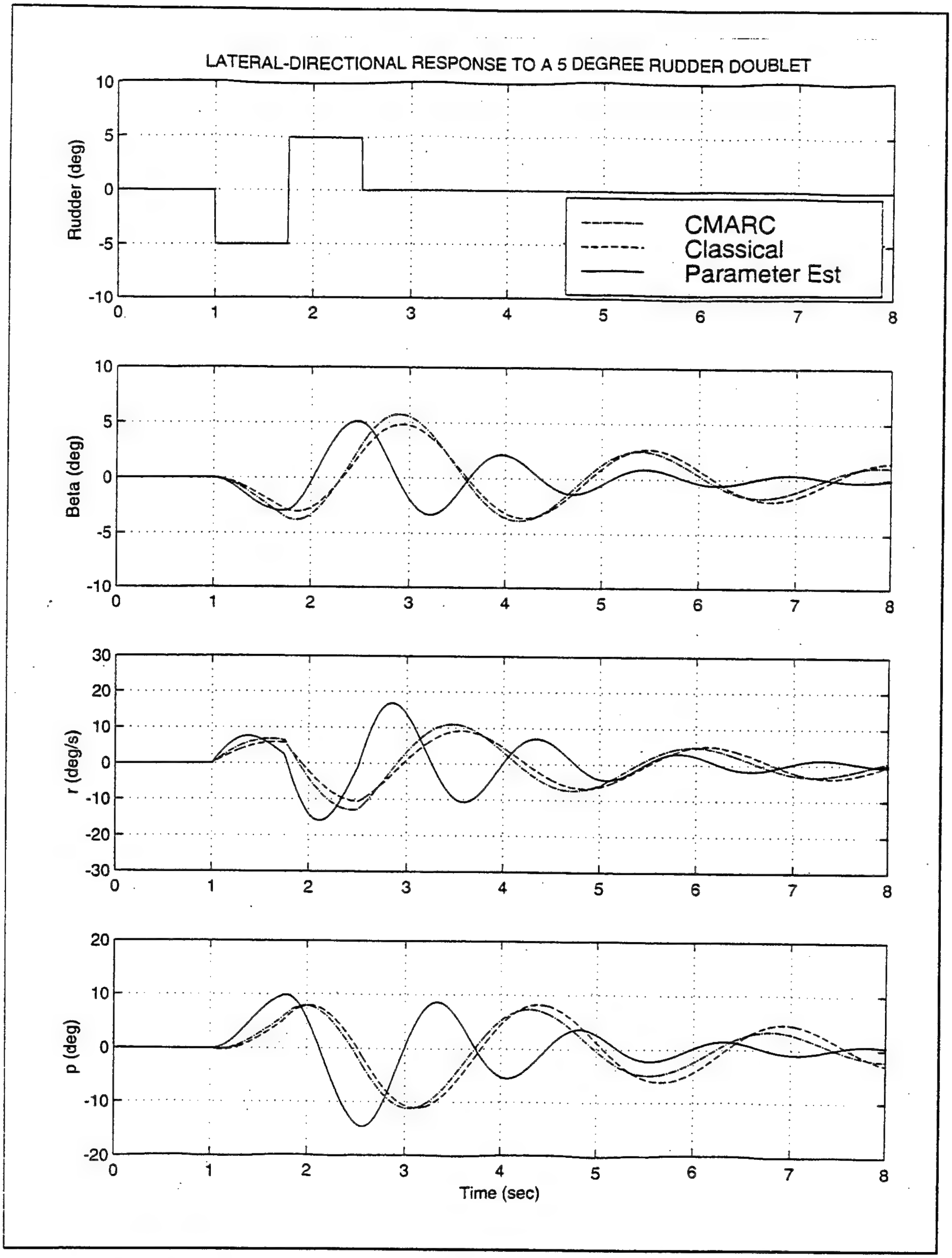

Figure 4.23 FROG UAV Dynamic Response to a 5° Rudder Doublet.

V. CONCLUSIONS AND RECOMMENDATIONS

CMARC is a DOS personal-computer hosted panel-code adopted from the NASA Ames PMARC code. AeroLogic, Inc., created CMARC by converting PMARC FORTRAN 77 source code into the C language. Significant memory management and command-line enhancements were also added. CMARC solves for inviscid, incompressible flow over complex three-dimensional bodies. Emphasis in this study is placed on expanding the use of CMARC to develop a full aerodynamic model of the Naval Postgraduate School FROG UAV. The CMARC stability derivatives are compared to models derived from classical design calculations and parameter estimation. In addition, pitot-static and angle-of-attack sensor position corrections are obtained through CMARC analysis.

The LOFTSMAN and POSTMARC portions of the Personal Simulation Works software suite are used exclusively for the pre-process modeling and post-process visualization of CMARC files. The LOFTSMAN capability to automatically format and generate CMARC input patches is an enhancing characteristic. Functionality should be added to allow the modeling of wing tip ribs that are not parallel to the aircraft centerline.

POSTMARC is an excellent tool for visualizing CMARC output files. The capability to create streamlines and perform boundary-layer calculations external to CMARC is extremely useful. However, much time could be saved if POSTMARC maintained previous settings and selections following translations, rotations and re-scaling. Additionally, a capability to overlay multiple data types is desired.

CMARC off-body flow-field analysis is useful for both static source and angle-of-attack sensor position corrections. In-flight measurements may be corrected using look-up tables or through curve-fits of CMARC-derived data. Flight testing is recommended for validation of sensor corrections obtained from the CMARC off-body analysis.

For the static longitudinal analysis, CMARC produces accurate values for α_{trim} and $C_{M\alpha}$ and a slightly high value of $C_{L\alpha}$. Elevator control-power ($C_{M\delta e}$) from CMARC is considerably weaker than the value obtained from parameter estimation. CMARC-derived pitch-damping is stronger than the pitch-damping from both classical design calculations and parameter estimation.

Longitudinal dynamic-mode analysis shows an acceptable match for short-period and long-period frequency and damping. As expected, a lower dynamic response to

elevator control inputs is observed when compared to the parameter estimation model. However, in all cases, the CMARC aerodynamic model demonstrates better dynamic response than the classical design model. A propeller disk should be added to the CMARC model in an attempt to capture prop-wash effects on the horizontal stabilizer and elevator. Increased elevator control-power would provide a better match with observed flight characteristics.

In general, CMARC provides satisfactory lateral-directional derivatives. Roll-damping closely matches the value obtained through parameter estimation. The greatest difficulty encountered is in modeling side-force due to both sideslip and roll-rate. The potential flow solution from CMARC fails to adequately capture the side force on a slender-body fuselage. Additional wakes, placed along separation lines, may improve fuselage side-force prediction.

Dynamic response to rudder control input shows close correlation in amplitude and damping to the parameter estimation model. However, both the CMARC and classical models of the FROG UAV produced a slower Dutch roll frequency. Steady state roll-rate obtained from the CMARC model is somewhat slower than either the classical design or parameter estimation models.

Overall, the CMARC panel code is found to be suitable for aerodynamic modeling of the Naval Postgraduate School FROG UAV. CMARC-derived stability derivatives are sufficiently accurate for incorporation into an initial aerodynamic model. The CMARC aerodynamic model demonstrated better longitudinal dynamic response than the classical design model. Lateral-directional response is similar to that obtained from classical design techniques. Adjustment through comparison with flight-test data is still required to optimize the CMARC model. Future studies should concentrate on improving CMARC modeling of fuselage side force through the addition of separation wake lines. Additionally, the propeller disk should be modeled in an attempt to capture the effects of increased dynamic pressure over the horizontal and vertical tail surfaces.

APPENDIX A

CMARC STABILITY DERIVATIVE USER GUIDE

CMARC USER GUIDE

FOR

OBTAINING STABILITY DERIVATIVE DATA

by

CDR Steve Pollard
September 1998

Naval Postgraduate School
Department of Aeronautics and Astronautics

APPENDIX A

TABLE OF CONTENTS

A. INTRODUCTION

1. CMARC Panel Code and Limitations

CMARC is a PC hosted panel code. The code is useful for gathering aircraft stability data subject to the limitation of inviscid, potential flow solutions. Panel codes assume fully attached flow. Therefore, care must be taken to gather stability data in the linear region of the lift curve slope where separation effects are minimized. The results obtained from CMARC should always be spot checked with classical design calculations.

CMARC and PMARC have been shown to produce functionally equivalent results. The guide describes the use of DOS batch files for automating CMARC data runs on a PC. PMARC, hosted on an SGI machine, will require the use of UNIX batch commands.

2. Overview of Obtaining Stability Derivatives with CMARC

An overview of the methods to obtain stability derivatives follows. The detailed description and data reduction methods can be found in the appropriate section of the user guide.

For the static stability derivatives, the CMARC model is run at two different angles-of-attack and one sideslip angle. The static solutions are obtained without control surface deflections. The slopes of the force and moment coefficients are then taken to produce the $C_{L\alpha}$ and $C_{m\alpha}$ longitudinal derivatives and the $C_{Y\beta}$, $C_{l\beta}$ and $C_{n\beta}$ lateral-directional derivatives.

For the control power derivatives, the model is run at the trim condition with successive elevator, aileron and rudder control deflections. The difference between the results with and without control surface deflections yield the $C_{L\delta e}$, $C_{M\delta e}$ and $C_{D\delta e}$ longitudinal and the $C_{Y\delta r}$, $C_{l\delta r}$, $C_{n\delta r}$, $C_{l\delta a}$ and $C_{n\delta a}$ lateral-directional control power derivatives.

Development of the damping derivatives is not as straight forward. For the dynamic derivatives, motion is enabled around the center of gravity. With motion turned on, it is extremely important to ensure that the global origin and C.G. are co-located. If they are not, a rotation around a specific axis will also create a translation at the C.G.

For the longitudinal damping derivatives, the model is run with oscillating vertical plunging motion to obtain the C_L and C_M α-dot terms. The lift and pitching moment coefficients are broken into real (in phase with AOA) and imaginary (out of phase with AOA) components. The imaginary components are due to α-dot effects. Next, the model is run with oscillating pitch motion to obtain the combined α-dot and pitch rate terms. Subtracting the α-dot influence obtained from the plunging motion isolates the pitch rate damping term from the pitch motion.

For the lateral-directional analysis, the β-dot terms are generally negligible. This allows the model to be run with just oscillating roll and yaw motion. As with the longitudinal test case, the imaginary or out of phase component yields the combined β-dot and rate damping data. With the β–dot terms assumed negligible, the oscillating motion yields the C_Y, C_l, and C_n roll and yaw rate terms directly.

3. Coefficient Normalization and Stability Axis System

CMARC contains built-in functionality to integrate forces and moments over the surface of a body. Forces and moments are automatically normalized into non-dimensional coefficients based on the mean aerodynamic chord, reference wing area, semi-span and center of gravity location in the CMARC BINP9 input line. CMARC outputs coefficients in both the wind and body axes. Of note, CMARC uses the semi-span to normalize rolling and yawing moment coefficients. Most texts on stability and control, including Roskam's "Aircraft Flight Dynamics" and Etkin's "Dynamics of Flight," normalize rolling and yawing moments by span. This user guide will normalize roll and yaw moments by span. Table A.1 summarizes the factors for normalizing moments and angular rates. All rolling and yawing moment coefficients presented in this guide have been normalized with span by dividing the CMARC output by a factor of two. Table A.1 also indicates the characteristic time, t*, employed for angle rate data reduction.

In addition to differences in normalizing moments, CMARC uses the typical CFD axes system shown in Figure A.1. This user guide will perform all calculations in the stability axes system as illustrated in Figure A.1. The sign of CMARC roll and yaw moments need to be reversed. The direction for positive control deflections is also shown in Figure A.1. All control surfaces are patched with positive deflections using the convention in Figure A.1.

MOMENTS	NORMALIZING PARAMETER[1]	RATES	CHARACTERISTIC TIME
$L = C_l \bar{q} S b$	b	$\hat{p} = \frac{pb}{2u_o}$	$t^* = b/2u_o$
$M = C_m \bar{q} S \bar{c}$	$\bar{c}$	$\hat{r} = \frac{r\bar{c}}{2u_o}$	$t^* = \bar{c}/2u_o$
$N = C_r \bar{q} S b$	b	$\hat{r} = \frac{rb}{2u_o}$	$t^* = b/2u_o$

Note: 1) CMARC normalizes roll and yaw coefficients with b/2.

Table A.1 Normalized Moment and Rate Equations.

B. MODEL VALIDATION

1. Initial Solution at the Trim Condition

Once a CMARC model is built up, a reference solution is obtained at the desired trim condition. Initial hand calculations or flight test data can be used to select the estimated cruise angle-of-attack. Use POSTMARC to visualize the reference solution. Check to make sure the pressure distribution is consistent with expected results. Stagnation zones (Cp=1) should be evident on the leading and trailing edges of the flight surfaces and aerodynamic bodies. Lower pressure should be observed on the top of lifting surfaces and tip loss should be observed near the wing tips. Wakes should trail from the expected surfaces.

If abnormal pressure distribution is observed, check for inverted panel orientation. This is accomplished by changing the color for positive and negative panel orientations using the "View >> Color" pull-down menu. The default color is white for both orientations. Change the inside to a contrasting color such as red. All panels should face in the positive out direction. If a patch has panels oriented inward, change the orientation of the patch with the "IREV" term in the initial patch definition.

Check that the model is symmetric around the lateral and directional axes with sideslip set to zero. Residual rolling or yawing moment without a control deflection is an indication of an asymmetric model.

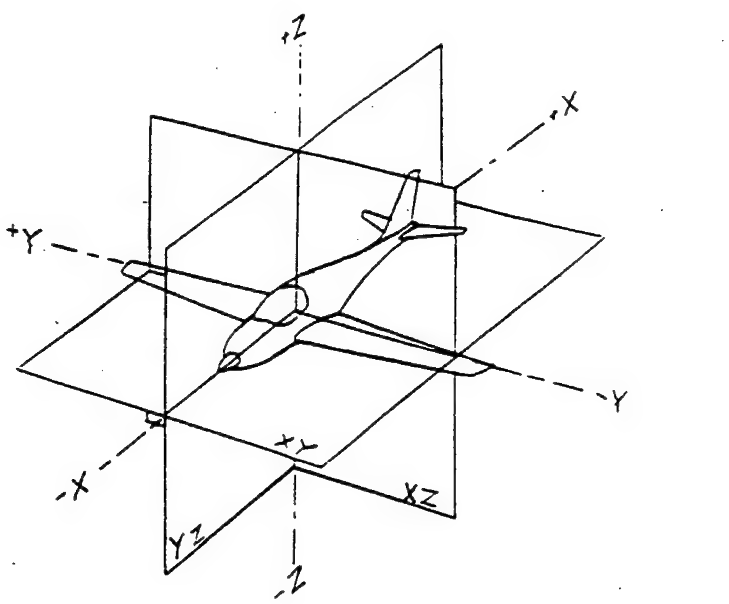

CMARC Axis System

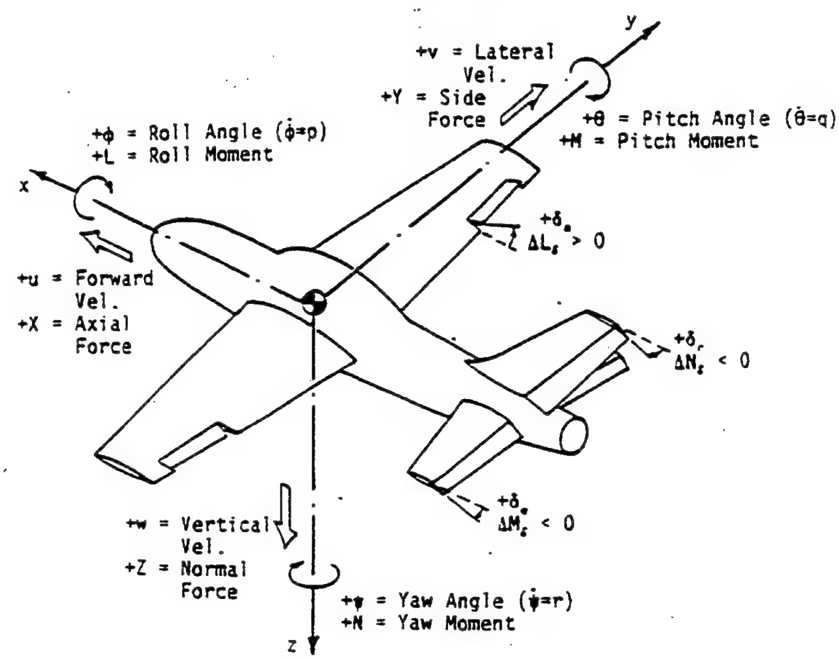

Stability Axis System

Figure A.1 CMARC CFD Axis System Compared To Stability Axis System. From References [3] and [14] Respectively.

Pitching moment should be checked for a reasonable value. Don't forget to verify that the origin of the global coordinate system is set to the center-of-gravity (C.G.). It is important to remember that the damping derivatives will be obtained by inducing motion around the center-of-gravity. If the C.G. and origin are not collocated, angular motion will generate undesired translation at the C.G.

Next, the lift coefficient from the initial solution is checked to make sure it is in the "ballpark." If a major discrepancy is noted, the input file will have to be checked closely for error. Be sure to check the normalizing factors such as wing area, reference chord and semi-span. If every thing looks good, try increasing or decreasing the angle-of-attack to see if a slight adjustment will bring the lift coefficient in line with the hand calculation. Once the model exhibits symmetry with a reasonable lift distribution, you're ready to start gathering data.

C. LONGITUDINAL STABILITY DERIVATIVES

This section will describe CMARC methods for the development of longitudinal stability derivatives to include the static, rate damping and control power derivatives. As stated earlier, the results obtained from CMARC should be checked against classical design calculations. The potential flow analysis performed by CMARC does not provide accurate viscous drag values. Total drag can be estimated from the flight test power-off glide ratio or cruise thrust required. If this data is unavailable, then empirical data from publications such as Hoerner's "Fluid Dynamic Drag" can be used to estimate total drag.

For the longitudinal analysis, only half the model is analyzed. This cuts the model size in half, resulting in much quicker solutions. The symmetric calculation mode is selected by setting both RSYM=0.0 and IPATSYM=0 in the CMARC input file. Remove the vertical tail patch if it interferes with wing or fuselage wakes. Figure A.2 shows the FROG model configuration used to find the longitudinal derivatives. A rigid wake is selected that is continuous from wingtip to wingtip. As will be seen in a later section, the vertical tail is added for the lateral-directional solutions. This requires the use of a modified wing wake to avoid the vertical tail.

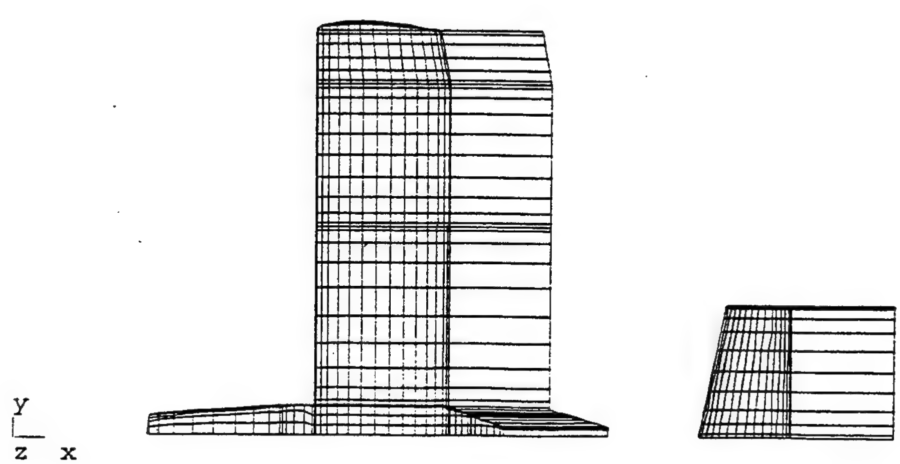

Blended Wing and Fuselage with Horizontal Tail

Figure A.2 FROG UAV Model for Obtaining Longitudinal Stability Derivatives.

1. Static Longitudinal Stability Derivatives

a. Static Longitudinal Stability Equations

Three basic longitudinal stability derivatives can be measured with just two runs of the CMARC model. The model is first analyzed at an angle-of-attack corresponding to the estimated trim condition. For the FROG case, α_t=0° is selected for the first run based on hand calculations. A second CMARC run is conducted with angle-of-attack incremented by one or two degrees. C_L, C_D and C_m are then extracted manually from the data files. The slope of C_L, C_D and C_m versus angle-of-attack provides the $C_{L\alpha}$, $C_{D\alpha}$ and $C_{m\alpha}$ longitudinal derivatives. Additional solutions should be obtained to check for lift slope linearity. In addition, α_{trim} is calculated from the lift curve slope and trim lift coefficient. Equations A.1 through A.4 are used for these calculations.

$$C_{L_\alpha} = \frac{(C_{L_2} - C_{L_1})}{(\alpha_2 - \alpha_1)} * \frac{180}{\pi} \text{ per radian} \qquad \text{A.1}$$

$$C_{D_\alpha} = \frac{(C_{D_2} - C_{D_1})}{(\alpha_2 - \alpha_1)} * \frac{180}{\pi} \text{ per radian} \qquad \text{A.2}$$

$$C_{m_\alpha} = \frac{(C_{m_2} - C_{m_1})}{(\alpha_2 - \alpha_1)} * \frac{180}{\pi} \text{ per radian} \qquad \text{A.3}$$

$$\alpha^\circ_{trim} = \alpha^\circ_1 + \frac{(C_{L_{trim}} - C_{L_1})}{C_{L_\alpha}} * \frac{180}{\pi} \text{ degrees} \qquad \text{A.4}$$

b. Sample Static Longitudinal Stability Data Reduction

Table A.2 presents CMARC solutions for the FROG UAV at two angles-of-attack. Sample calculations for obtaining the static derivatives are demonstrated below. The calculations are easily implemented in a spreadsheet or with a MATLAB script.

RUN #	AOA	CL	CD	CY	C_m	C_n	C_l
1	0°	0.4300	0.0277	0.0000	0.0444	0.0000	0.0000
2	2°	0.5991	0.0370	0.0000	0.0300	0.0000	0.0000

Table A.2 FROG UAV Static Longitudinal Stability Data.

Sample Calculations:

$$C_{L_\alpha} = \frac{(0.5991 - 0.4300)}{(2-0)} * \frac{180}{\pi} = 4.8444 \text{ per radian} \qquad \text{A.5}$$

$$C_{D_\alpha} = \frac{(0.0370 - 0.0277)}{(2-0)} * \frac{180}{\pi} = 0.2664 \text{ per radian} \qquad \text{A.6}$$

$$C_{m_\alpha} = \frac{(0.0300 - 0.0444)}{(2-0)} * \frac{180}{\pi} = -0.4125 \text{ per radian} \qquad \text{A.7}$$

$$\alpha°_{trim} = 0° + \frac{(0.4295 - 0.4300)}{4.8444} * \frac{180}{\pi} = -0.0059° \approx 0° \qquad \text{A.8}$$

c. *Sample Total Drag Coefficient Calculation*

The final static longitudinal parameter required is total aircraft drag. C_D plays an important role in long period aircraft dynamics. Unfortunately, potential flow panel codes such as CMARC do not provide accurate total drag estimates. They can provide good induced drag predictions. In addition, if equipped with a boundary layer code like that contained in CMARC, they can provide integrated skin friction results. However, a large total drag contribution in the form of separation drag is not accounted for. Total drag estimates are made below using the two simple techniques shown in Equations A.9 to A.12. The first method is based on the flight-tested glide ratio. The second is based on cruise power required and estimated prop efficiency. Note that the selected prop efficiency is relatively low due to the FROG UAV small propeller diameter,

high RPM and pusher configuration. The two methods provide drag predictions within 10% of each other. The results are averaged to C_D=0.065.

Method 1: Lift-to-Drag Ratio (L/D=7 from flight test)

$$L/D = 7 \quad \Rightarrow \quad D = \frac{L}{7} = \frac{W}{7} = \frac{67.7 \quad lbs}{7} = 9.67 \quad lbs \qquad \text{A.9}$$

$$C_D = \frac{D}{qS} = \frac{9.67 \quad lbs}{0.5 * 0.002327 \quad lb \cdot s^2 / ft^4 * 88^2 \quad ft^2 / s^2 * 17.57 \quad ft^2} = 0.0611 \qquad \text{A.10}$$

Method 2: Cruise Power Setting (HP=5, η_P=0.35)

$$C_D = \frac{D}{qS} = \frac{T_R}{qS} = \frac{HP_R * 550 \quad ftlbs / s / HP * \eta_P / V}{qS} \qquad \text{A.11}$$

$$C_D = \frac{5 \quad HP * 550 \quad ft \cdot lbs / s / HP * 0.35 / 88 \quad ft / s}{0.5 * 0.002327 \quad lb \cdot s^2 / ft^4 * 88^2 \quad ft^2 / s^2 * 17.57 \quad ft^2} = 0.069 \qquad \text{A.12}$$

2. Longitudinal Control Power Stability Derivatives

a. Longitudinal Control Power Equations

The elevator control power derivatives are obtained by substituting a 0° deflection horizontal tail patch for one with positive elevator deflection. Only one run is required. For the FROG UAV study, +5° (TED) deflection is used. The difference between the trim condition and the deflected value is divided by the elevator deflection as shown below. Note that $C_{D\delta e}$ from CMARC only includes induced drag due to elevator deflection:

$$C_{L\delta e} = \frac{\left(C_{L\delta e_2} - C_{L\delta e_1}\right)}{\delta e_2 - \delta e_1} * \frac{180}{\pi} \quad per \quad rad \qquad \text{A.13}$$

$$C_{D\delta e} = \frac{\left(C_{D\delta e_2} - C_{D\delta e_1}\right)}{\delta e_2 - \delta e_1} * \frac{180}{\pi} \quad per \quad rad \qquad \text{A.14}$$

$$C_{m_{\delta e}} = \frac{\left(C_{m_{\delta e_2}} - C_{m_{\delta e_1}}\right)}{\delta e_2 - \delta e_1} * \frac{180}{\pi} \quad per \quad rad \tag{A.15}$$

$$\delta e^{\circ}{}_{trim} = \frac{\left(C_{m @ trim(\delta e = 0)}\right)}{C_{m_{\delta e}}} * \frac{180}{\pi} \quad \deg \tag{A.16}$$

b. Sample Longitudinal Control Power Data Reduction

Table A.3 presents CMARC solutions for two elevator deflections. Sample calculations for obtaining elevator control power are demonstrated below. The calculations are easily implemented in a spreadsheet or with a MATLAB script.

$$C_{L_{\delta e}} = \frac{(0.4641 - 0.4259)}{(5 - 0)} * \frac{180}{\pi} = 0.4378 \text{ per radian} \tag{A.17}$$

$$C_{D_{\delta e}} = \frac{(0.0178 - 0.0170)}{(5 - 0)} * \frac{180}{\pi} = 0.0092 \text{ per radian} \tag{A.18}$$

$$C_{m_{\delta e}} = \frac{(-0.0942 - 0.0104)}{(5 - 0)} * \frac{180}{\pi} = -1.199 \text{ per radian} \tag{A.19}$$

$$\delta e^{\circ}{}_{trim} = \frac{(0.0104)}{-1.199} * \frac{180}{\pi} = -0.50^{\circ} \tag{A.20}$$

RUN #	δ_e	CL	CD	CY	C_m	C_n	C_l
1	0°	0.4259	0.0170	0.0000	0.0104	0.0000	0.0001
2	5°	0.4641	0.0178	0.0000	-0.0942	0.0000	0.0001

Table A.3 FROG UAV Elevator Control Power Data.

3. Longitudinal *α-dot* Damping Derivatives

a. Longitudinal α-dot Derivative Methods and Equations

Two motions selected are to develop the longitudinal rate damping derivatives. A sinusoidal plunging motion in the z-axis is used to extract the α-dot terms. Then an oscillatory pitching motion is used to obtain the combined α-dot and pitch rate terms. The α-dot are then subtracted to yield the pitch rate damping. All motion for FROG data gathering is conducted at a frequency of 2π rad/s, which equates to a reduced frequency of k=0.0595 for this configuration and trim airspeed.

The sinusoidal plunging motion illustrated in Figure A.3 is used to isolate the α-dot derivatives. Z-axis plunging motion is controlled with the CMARC BINP8B input file line. A frequency of 2π rad/s and an amplitude of C/2=10 inches are selected for the FROG study. Greater amplitude was initially selected, but the induced angle of attack caused the rigid wake to impact the horizontal tail. An example BINP8B input line is shown below:

```
&BINP8B   DXMAX=0.0,    DYMAX=0.0,    DZMAX=10.0
          WTX=0.0,      WTY=0.0,      WTZ=6.283,     &END
```

The number of time steps and time step interval is chosen to create a nice sinusoidal output through at least two cycles of motion. In the FROG study, a plunging motion frequency of ω=2π rad/s or one cycle/sec is utilized. Fifty time steps are chosen with an interval of 0.05 seconds, which creates 2.5 cycles of plunging motion. After the solution is obtained, the "total coefficient" data is extracted for plotting. The data can be picked out manually, or a data retrieval program can be created for the task. For the FROG study, the data is extracted manually and pasted into an "Excel" spreadsheet for plotting. In addition to the CMARC output, plunging motion phase angle and induced angle-of-attack are calculated using Equations A.21 and A.22. Induced angle-of-attack is used to find the phase angle of the response with respect to angle-of-attack. Table A.4 shows representative FROG data for 20 time steps.

$$\phi_{plunge} = \#_{timestep} * dt * \varpi_{plunge} * \frac{180}{\pi} \text{ degrees} \quad \text{A.21}$$

$$\alpha_{induced} = \cos(\phi_{plunge}) \frac{A_{plunge}}{U_o} * \varpi_{plunge} * \frac{180}{\pi} \text{ degrees} \quad \text{A.22}$$

Where:
- ϕ_{plunge} - plunging motion phase angle
- $\alpha_{induced}$ - induced angle-of-attack from the plunging motion
- $\#_{timestep}$ - time step
- dt - time step interval
- ω_{plunge} - plunging frequency
- A_{plunge} - plunging amplitude
- U_o - reference free stream velocity

Step	ϕ (deg)	$\alpha_{induced}$	CL	CD	CY	C_m	C_n	C_l
0	0	-3.41	0.0001	0.0327	0.0000	0.0173	0.0000	0.0000
1	18	-3.24	0.1318	0.0300	0.0000	0.0744	0.0000	0.0000
2	36	-2.76	0.1928	0.0299	0.0000	0.0485	0.0000	0.0000
3	54	-2.00	0.2631	0.0316	0.0000	0.0294	0.0000	0.0000
4	72	-1.05	0.3451	0.0318	0.0000	0.0218	0.0000	0.0000
5	90	0.00	0.4336	0.0297	0.0000	0.0169	0.0000	0.0000
6	108	1.05	0.5216	0.0252	0.0000	0.0126	0.0000	0.0000
7	126	2.00	0.6009	0.0189	0.0000	0.0087	0.0000	0.0000
8	144	2.76	0.6636	0.0123	0.0000	0.0067	0.0000	0.0000
9	162	3.24	0.7029	0.0069	0.0000	0.0089	0.0000	0.0000
10	180	3.41	0.7160	0.0042	0.0000	0.0139	0.0000	0.0000
11	198	3.24	0.7009	0.0048	0.0000	0.0232	0.0000	0.0000
12	216	2.76	0.6594	0.0085	0.0000	0.0344	0.0000	0.0000
13	234	2.00	0.5952	0.0142	0.0000	0.0474	0.0000	0.0000
14	252	1.05	0.5141	0.0204	0.0000	0.0596	0.0000	0.0000
15	270	0.00	0.4254	0.0255	0.0000	0.0704	0.0000	0.0000
16	288	-1.05	0.3370	0.0286	0.0000	0.0762	0.0000	0.0000
17	306	-2.00	0.2582	0.0297	0.0000	0.0776	0.0000	0.0000
18	324	-2.76	0.1964	0.0292	0.0000	0.0734	0.0000	0.0000
19	342	-3.24	0.1561	0.0283	0.0000	0.0713	0.0000	0.0000
20	360	-3.41	0.1398	0.0277	0.0000	0.0727	0.0000	0.0000

Table A.4 Sample Plunging Motion Data for 20 Time Steps

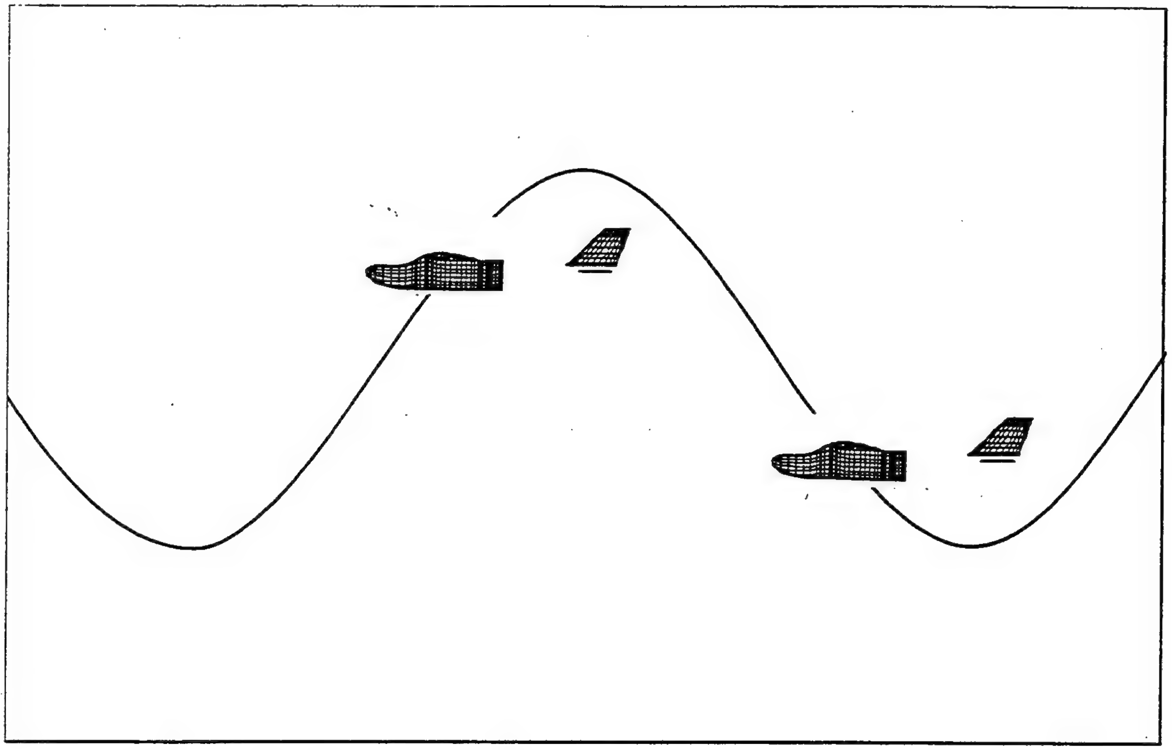

Figure A.3 Vertical Plunging Motion for Obtaining the α-dot Derivatives.

The α-dot stability derivatives are extracted using the methods outlined in Etkin [Ref. 13]. First, the C_L and C_m responses are plotted as a function of plunging phase angle. Induced angle-of-attack is also plotted on the right hand vertical axis. Figure A.4 is a representative plot of CMARC data for the FROG UAV study. The response to plunging motion can be broken up into real and imaginary components. Figure A.5 is a graphical representation of the real and imaginary components. The out-of-phase (imaginary) portion of C_L or C_m is the α-dot contribution. It is normalized by dividing by the amplitude of $\alpha_{induced}$ and the reduced frequency. The phase angle is measured between the lift or pitching moment response and the induced angle-of-attack. Equations A.23 through A.27 are used to solve for $C_{L\alpha dot}$ and $C_{m\alpha dot}$.

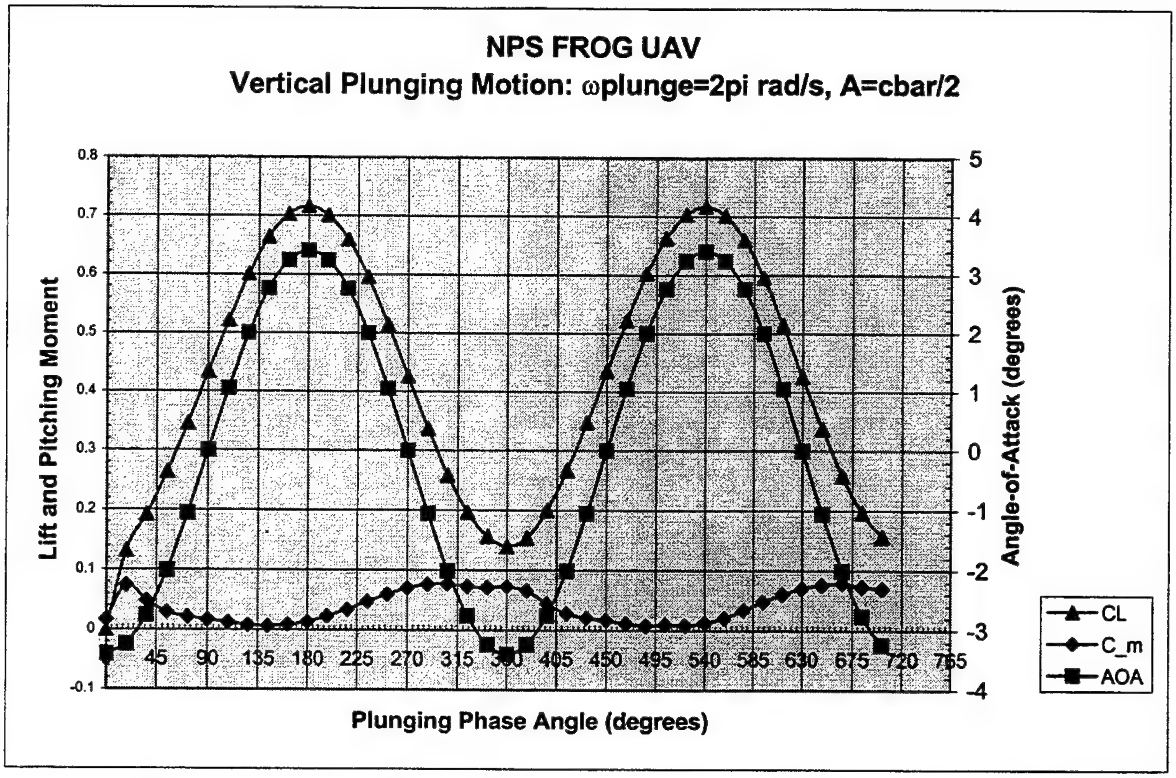

Figure A.4 Representative Vertical Plunging Motion Data for the FROG UAV.

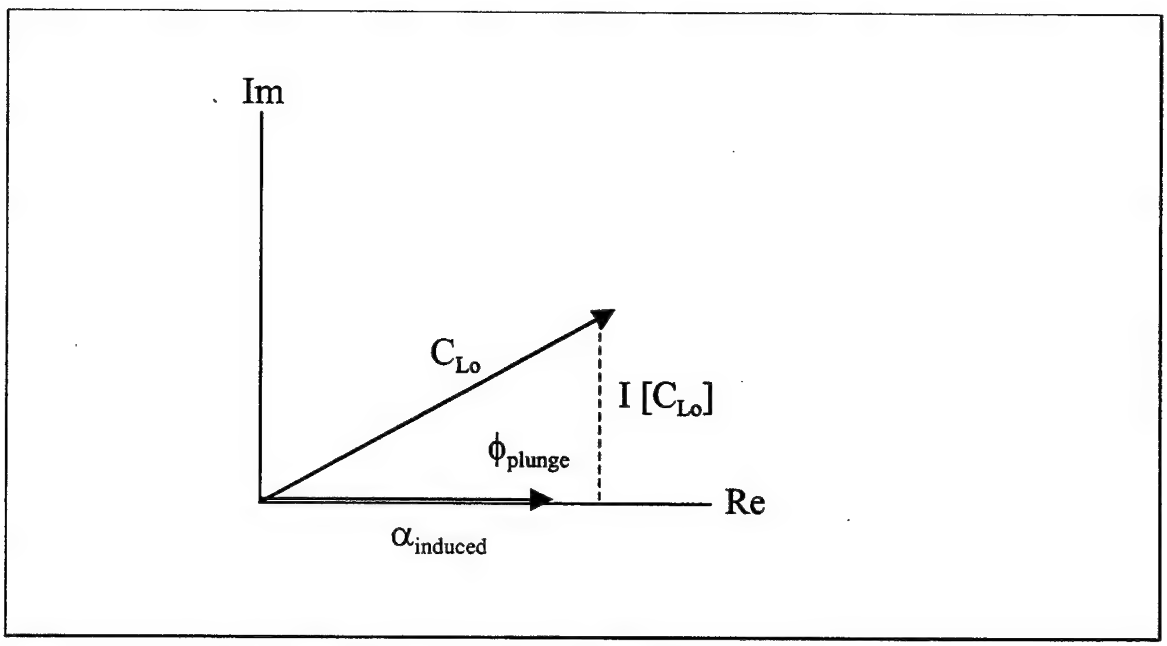

Figure A.5 Complex Response to Vertical Plunging Motion.

The phase angle between the C_L (or C_m) response and the induced angle-of-attack is measured graphically or through numerical curve fit techniques. If the graphical method is used, the graph scales may be narrowed around the area of interest to facilitate the phase angle measurement. For instance, Figure A.4 shows that lift coefficient and angle-of attack are nearly in-phase. When the x-axis scale is zoomed into the peak of the curves, one can see that lift coefficient leads angle-of-attack by one degree. Alternatively, the phase angle may be measured from where the parameter crosses the trim value.

$$C_{L_{\dot{\alpha}}} = \frac{I\lfloor C_{L_o} \rfloor}{\alpha_o k} \qquad \text{A.23}$$

$$C_{m_{\dot{\alpha}}} = \frac{I\lfloor C_{m_o} \rfloor}{\alpha_o k} \qquad \text{A.24}$$

$$\alpha_o = \frac{A}{U_o}\omega_{plunge} \qquad \text{A.25}$$

$$I\left[C_{L_o}\right] = C_{L_o}\sin(\phi) \quad and \quad I\left[C_{m_o}\right] = C_{m_o}\sin(\phi) \qquad \text{A.26}$$

$$k = \frac{\bar{c}/2}{U_o}\varpi_{plunge} \qquad \text{A.27}$$

Where:

ϕ	- Phase angle between C_L (or C_m) response and $\alpha_{induced}$
$\alpha_{induced}$	- Induced angle-of-attack from the plunging motion
C_{Lo}	- Amplitude of lift coefficient response
C_{mo}	- Amplitude of pitching moment coefficient response
α_o	- Amplitude of the induced angle-of-attack
k	- Reduced frequency
U_o	- Reference free stream velocity

b. Sample Longitudinal α-dot Data Reduction

Sample data reduction is presented below in Equations A.28 through A.32. The phase angle between the response and the induced angle-of-attack was measured graphically by zooming the graph axes to expand the area of interest.

$$k = \frac{\bar{c}/2}{U_o} \varpi_{plunge} = \frac{20\ in/2}{1056\ \ in/s} * 2\pi rad/s = 0.0595 \qquad \text{A.28}$$

$$I[C_{L_o}] = C_{L_o} \sin(\phi) = \frac{(0.7160 - 0.1398)}{2} * \sin(1°) = 0.005028$$

A.29

$$I[C_{m_o}] = C_{m_o} \sin(\phi) = (0.0776 - 0.0087) * \sin(-140°) = -0.0222$$

$$\alpha_o = \frac{A}{U_o} \omega_{plunge} = \frac{20 in/2}{1056 in/s} * 2\pi = 0.0595 \quad rad * \frac{180}{\pi} = 3.41° \qquad \text{A.30}$$

$$C_{L_{\dot{\alpha}}} = \frac{I[C_{L_o}]}{\alpha_o k} = \frac{0.005028}{0.0595 * 0.0595} = 1.420 \qquad \text{A.31}$$

$$C_{m_{\dot{\alpha}}} = \frac{I[C_{m_o}]}{\alpha_o k} = \frac{-0.0222}{0.0595 * 00595} = -6.264 \qquad \text{A.32}$$

4. Longitudinal Pitch Rate Damping Derivatives

a. Longitudinal Pitch Rate Damping Methods and Equations

A sinusoidal plunging motion in the z-axis was used to extract the α-dot terms. Now, an oscillatory pitching motion is used to obtain the combined α-dot and pitch rate terms. The α-dot influence is then subtracted to yield pitch rate damping. All motion for FROG data gathering is conducted at a frequency of 2π rad/s, which equates to a reduced frequency of k=0.0595 for this configuration and trim airspeed.

The sinusoidal pitch rate motion illustrated in Figure A.6 is used to isolate the combined α-dot and pitch rate influence. Oscillating pitch motion is controlled with the CMARC BINP8A input file line. A frequency of 2π rad/s and an amplitude of $\pm 1.5°$ are selected for the FROG study. Any larger pitch amplitude would cause the wake to impact the horizontal tail. An example BINP8A input line is shown below. Note that pitch amplitude is in degrees and frequency is in rad/sec:

```
&BINP8A    PHIMAX=0.0,    THEMAX=1.5,    PSIMAX=0.0
           WTX=0.0,       WTY=6.283,     WTZ=0.0,       &END
```

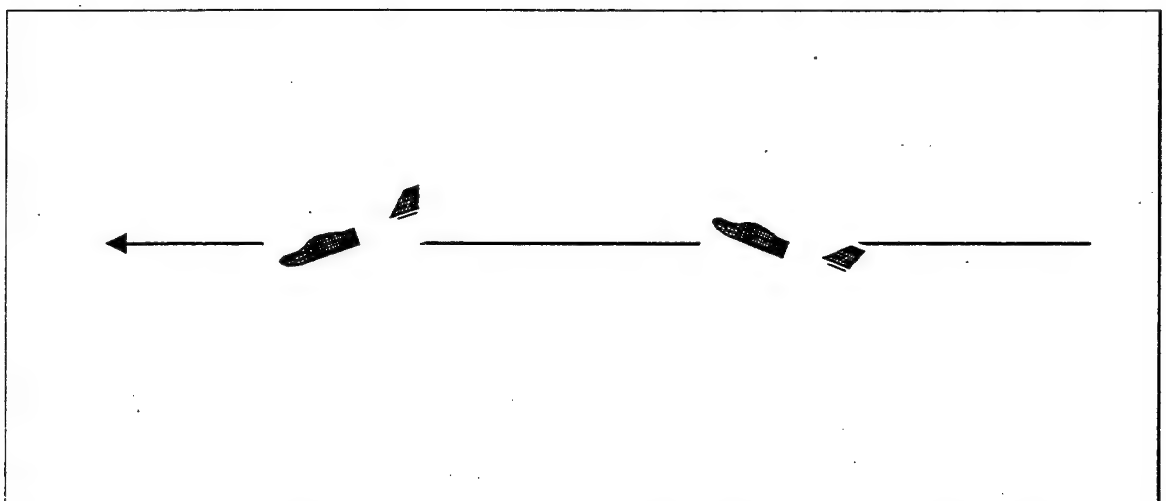

Figure A.6 Pitching Motion for Obtaining the Pitch Rate Damping Derivatives.

The number of time steps and time step interval is chosen to create a nice sinusoidal output through at least two cycles of motion. In the FROG study, a pitching

motion frequency of $\omega=2\pi$ rad/s or one cycle/sec is utilized. Fifty time steps are chosen with an interval of 0.05 seconds. This combination yields 2.5 cycles of pitching motion. After the solution is obtained, the "total coefficient" data is extracted for plotting. The data can be picked out manually, or a data retrieval program can be created for the task. For the FROG study, the data is extracted manually and pasted into an "Excel" spreadsheet for plotting. In addition to the CMARC output, pitch motion phase angle and angle-of-attack are calculated using Equations A.33 and A.34. Lift and pitching moment phase angle is obtained with respect to angle-of-attack. Usually, the second motion cycle is used to ensure that all start up transients have subsided. Table A.5 shows representative FROG data for 20 time steps.

$$\phi_{pitch} = \#_{timestep} * dt * \varpi_{pitch} * \frac{180}{\pi} \text{ degrees} \qquad \text{A.33}$$

$$\alpha = \theta = \sin(\phi_{pitch}) A_{pitch} \text{ degrees} \qquad \text{A.34}$$

Where:

ϕ_{pitch} - pitching motion phase angle
α - Angle-of-attack from the pitching motion
$\#_{timestep}$ - time step
dt - time step interval
ω_{pitch} - pitching frequency
A_{pitch} - pitch amplitude

Step	ϕ (deg)	α	CL	CD	CY	C_m	C_n	C_l
0	0	0.00	0.0540	0.0273	0.0000	0.0828	0.0000	0.0000
1	18	0.46	0.4545	0.0364	0.0000	-0.0462	0.0000	0.0000
2	36	0.88	0.4961	0.0344	0.0000	0.0303	0.0000	0.0000
3	54	1.21	0.5312	0.0347	0.0000	0.0226	0.0000	0.0000
4	72	1.43	0.5491	0.0351	0.0000	0.0270	0.0000	0.0000
5	90	1.50	0.5541	0.0348	0.0000	0.0310	0.0000	0.0000
6	108	1.43	0.5435	0.0338	0.0000	0.0447	0.0000	0.0000
7	126	1.21	0.5227	0.0321	0.0000	0.0535	0.0000	0.0000
8	144	0.88	0.4925	0.0302	0.0000	0.0618	0.0000	0.0000
9	162	0.46	0.4557	0.0281	0.0000	0.0692	0.0000	0.0000
10	180	0.00	0.4167	0.0262	0.0000	0.0727	0.0000	0.0000
11	198	-0.46	0.3787	0.0247	0.0000	0.0741	0.0000	0.0000
12	216	-0.88	0.3457	0.0236	0.0000	0.0720	0.0000	0.0000
13	234	-1.21	0.3218	0.0230	0.0000	0.0648	0.0000	0.0000
14	252	-1.43	0.3075	0.0227	0.0000	0.0585	0.0000	0.0000
15	270	-1.50	0.3055	0.0228	0.0000	0.0499	0.0000	0.0000
16	288	-1.43	0.3158	0.0233	0.0000	0.0402	0.0000	0.0000
17	306	-1.21	0.3369	0.0241	0.0000	0.0323	0.0000	0.0000
18	324	-0.88	0.3674	0.0254	0.0000	0.0246	0.0000	0.0000
19	342	-0.46	0.4039	0.0271	0.0000	0.0191	0.0000	0.0000
20	360	0.00	0.4429	0.0290	0.0000	0.0153	0.0000	0.0000

Table A.5 Sample Pitch Motion Data for 20 Time Steps

The C_L and C_m responses are plotted as a function of pitch motion phase angle. Angle-of-attack is also plotted on the right hand vertical axis. Figure A.7 is a representative plot of CMARC data for the FROG UAV study. The out-of-phase (imaginary) portion of C_L or C_m is the combined α-dot and pitch damping contribution. As seen in Equations A.35 and A.36, the α-dot contribution is subtracted from the total to yield the pitch damping influence. The pitch rate contribution is normalized by pitch rate and t^*. The phase angle is measured between the lift or pitching moment response and angle-of-attack. Equations A.35 through A.44 are used to solve for C_{Lq} and C_{mq}. Equations A.35 and A.36 assume that the α-dot and pitch rate contributions are in phase with each other. The α-dot contribution is small, so there isn't harm done if the two contributions are somewhat out-of-phase. Consequently, the α-dot contribution is calculated based on the maximum α-dot rate observed.

$$I\left[C_{L_{\dot{\alpha}+q}}\right]=I\left[C_{L_{\dot{\alpha}}}\right]+I\left[C_{L_q}\right] \tag{A.35}$$

$$I\left[C_{m_{\dot{\alpha}+q}}\right]=I\left[C_{m_{\dot{\alpha}}}\right]+I\left[C_{m_q}\right] \tag{A.36}$$

$$I\left[C_{L_{\dot{\alpha}+q}}\right] = \sin(\phi)\left[C_{L_{\dot{\alpha}+q}}\right] \qquad \text{A.37}$$

$$I\left[C_{L_{\dot{\alpha}+q}}\right] = \sin(\phi)\left[C_{L_{\dot{\alpha}+q}}\right] \qquad \text{A.38}$$

$$I\left[C_{L_{\dot{\alpha}}}\right] = C_{L_{\dot{\alpha}}} * \dot{\alpha}_{\max} * t^* \qquad \text{A.39}$$

$$I\left[C_{m_{\dot{\alpha}}}\right] = C_{m_{\dot{\alpha}}} * \dot{\alpha}_{\max} * t^* \qquad \text{A.40}$$

$$I\left[C_{L_q}\right] = C_{L_q} * q_{\max} * t^* \qquad \text{A.41}$$

$$I\left[C_{m_q}\right] = C_{m_q} * q_{\max} * t^* \qquad \text{A.42}$$

$$q_{\max} = \dot{\alpha}_{\max} = \frac{A_{\theta_{\deg}}}{57.3 \, {}^{\deg}\!/_{rad}} * \omega_{pitch} \quad \text{rad/s} \qquad \text{A.43}$$

$$t^* = \frac{\overline{c}}{2} U_0 \qquad \text{A.44}$$

Where:

$[C_{L\,\alpha\text{-dot}+q}]$	- Amplitude of C_L response from pitching motion
$[C_{m\,\alpha\text{-dot}+q}]$	- Amplitude of C_m response from pitching motion
$I[C_{L\,\alpha\text{-dot}+q}]$	- Out-of-phase C_L due to α-dot and pitch rate damping
$I[C_{m\,\alpha\text{-dot}+q}]$	- Out-of-phase C_m due to α-dot and pitch rate damping
$I[C_{L\,q}]$	- C_L coefficient contribution from pitch rate damping
$I[C_{m\,q}]$	- C_m coefficient contribution from pitch rate damping
$I[C_{L\,\alpha\text{-dot}}]$	- C_L coefficient contribution from α-dot damping
$I[C_{m\,\alpha\text{-dot}}]$	- C_m coefficient contribution from α-dot damping
t^*	- Characteristic time

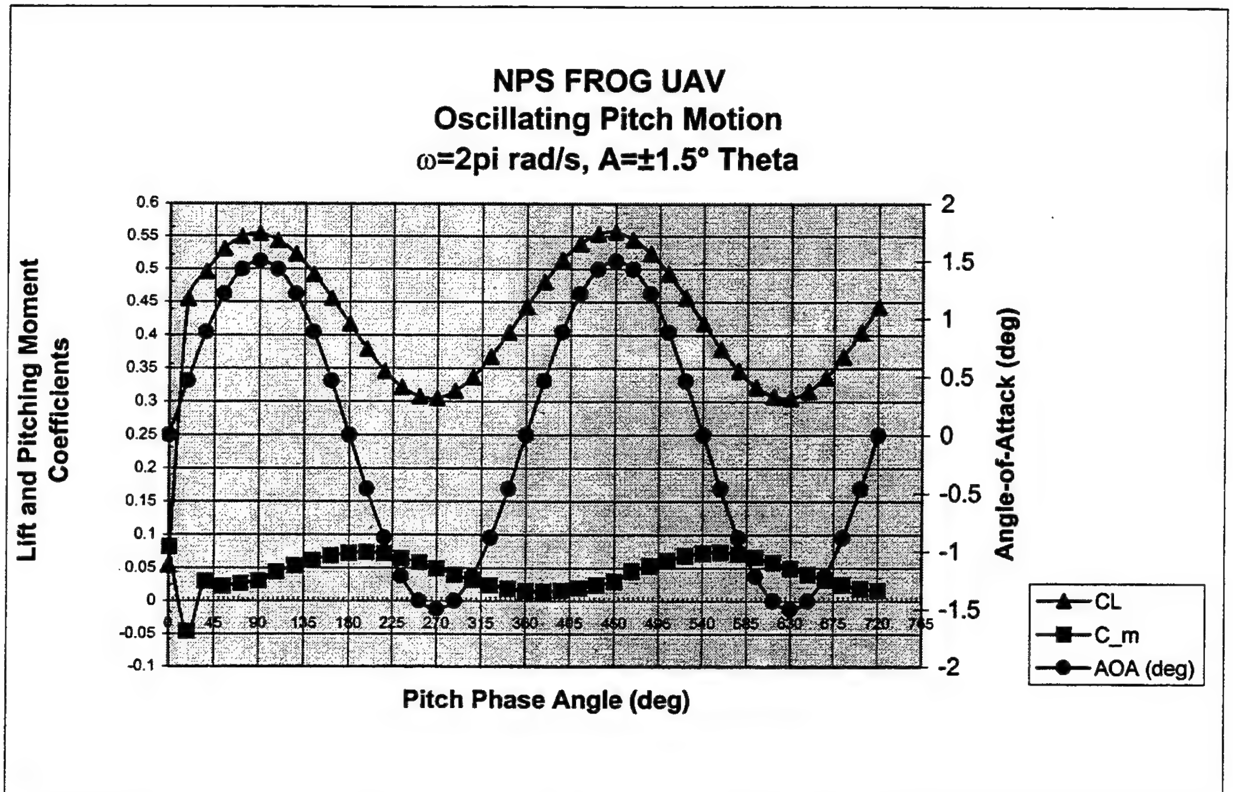

Figure A.7 Representative Pitch Motion Data for the FROG UAV.

b. Sample Pitch Rate Damping Data Reduction

Sample pitch rate damping data reduction is presented below in Equations A.45 through A.54. The phase angle between angle-of-attack and the C_L or C_m response was measured graphically by zooming the graph axes to expand the area of interest.

$$t^* = \frac{\bar{c}/2}{U_0} = \frac{20in/2}{1056\frac{in}{\sec}} = 0.009470\sec \qquad \text{A.45}$$

$$q_{\max} = \dot{\alpha}_{\max} = \frac{A_{\theta_{\deg}}}{57.3\,{}^{\deg}/_{rad}} * \omega_{pitch} = \frac{1.5°}{57.3°/_{rad}} * 2\pi \quad rad/s = 0.1645\,\text{rad/s} \qquad \text{A.46}$$

$$I\left[C_{L_{\dot{\alpha}}}\right] = C_{L_{\dot{\alpha}}} * \dot{\alpha}_{\max} * t^* = 1.420 * 0.1645 * 0.009470 = 0.002212 \qquad \text{A.47}$$

$$I\left[C_{m_{\dot{\alpha}}}\right]=C_{m_{\dot{\alpha}}}*\dot{\alpha}_{\max}*t^{*}=-6.264*0.1645*0.009470=-0.009758 \qquad \text{A.48}$$

$$I\left[C_{L_{\dot{\alpha}+q}}\right]=\sin(\phi)\left[C_{L_{\dot{\alpha}+q}}\right]=\sin(6°)*[0.1234]=0.0129 \qquad \text{A.49}$$

$$I\left[C_{m_{\dot{\alpha}+q}}\right]=\sin(\phi)\left[C_{m_{\dot{\alpha}+q}}\right]=\sin(-100°)*[0.02853]=-0.02810 \qquad \text{A.50}$$

$$I\left[C_{L_q}\right]=I\left[C_{L_{\dot{\alpha}+q}}\right]-I\left[C_{L_{\dot{\alpha}}}\right]=0.0129-0.002212=0.01069 \qquad \text{A.51}$$

$$I\left[C_{m_q}\right]=I\left[C_{m_{\dot{\alpha}+q}}\right]-I\left[C_{m_{\dot{\alpha}}}\right]=-0.02810-(-0.009758)=-0.01834 \qquad \text{A.52}$$

$$C_{L_q}=\frac{I\left[C_{L_q}\right]}{q_{\max}*t^{*}}=\frac{0.01069}{0.1645*0.009470}=6.862 \qquad \text{A.53}$$

$$C_{m_q}=\frac{I\left[C_{m_q}\right]}{q_{\max}*t^{*}}=\frac{-0.01834}{0.1645*0.009470}=-11.78 \qquad \text{A.54}$$

C. LATERAL-DIRECTIONAL STABILITY DERIVATIVES

This section will describe CMARC methods for the development of lateral-directional stability derivatives to include the static, rate damping and control power derivatives. The results obtained from CMARC should be spot checked against classical design calculations.

Of note, CMARC uses the semi-span to normalize rolling and yawing moment coefficients. Most texts on stability and control, including Roskam [Ref. 12] and Etkin [Ref. 13], normalize rolling and yawing moments by span. This study will normalize roll and yaw moments by span. Table A.1 summarizes the factors for normalizing moments and angular rates. All rolling and yawing moment coefficients presented in this study have been normalized with span by dividing the CMARC output by a factor of two. Table A.1 also indicates the characteristic time, t*, employed for angle rate data reduction.

For the lateral-directional analysis, both sides of the body must be modeled. The easiest way to do this is to activate the symmetric patch toggle for each patch (IPATSYM=1). Then, turn off symmetric calculations (RSYM=1.0). This creates symmetric patches around the y=0 plane, allowing CMARC to perform asymmetric calculations around the entire body. Processing times are significantly increased compared to the symmetric case. Wakes must be defined for each side of the model based on the new patch numbers. In addition, don't forget to update the adjacent patch numbers of the wingtips.

The vertical tail is activated for the lateral-directional study. This requires that the wing and fuselage group be run separately from the horizontal and vertical stabilizer group. This de-coupling is required to keep the wing wake from hitting the vertical stabilizer. The two sets of results are summed to get the total response. Typically, the sidewash derivative, $d\varepsilon/d\beta$ is small, making separate solutions feasible. The main draw back is that separate solutions will not capture the finer interactions that a complete model would capture. However, many aircraft configurations will not require the de-coupling of the empennage surfaces. If the configuration permits, run the lateral-directional test cases as a complete airframe model. Figure A.8 shows the FROG model configurations used to find the lateral-directional derivatives.

It should be noted that the CMARC wind axes are modeled with X-aft/Z-up, vice X-forward/Z-down for the typical stability axes system. Positive yaw angle in CMARC creates positive sideslip in the stability axes system. Care must be taken to reverse the signs of the appropriate coefficients to convert from the CMARC wind axes to the stability axis system shown in Figure A.1.

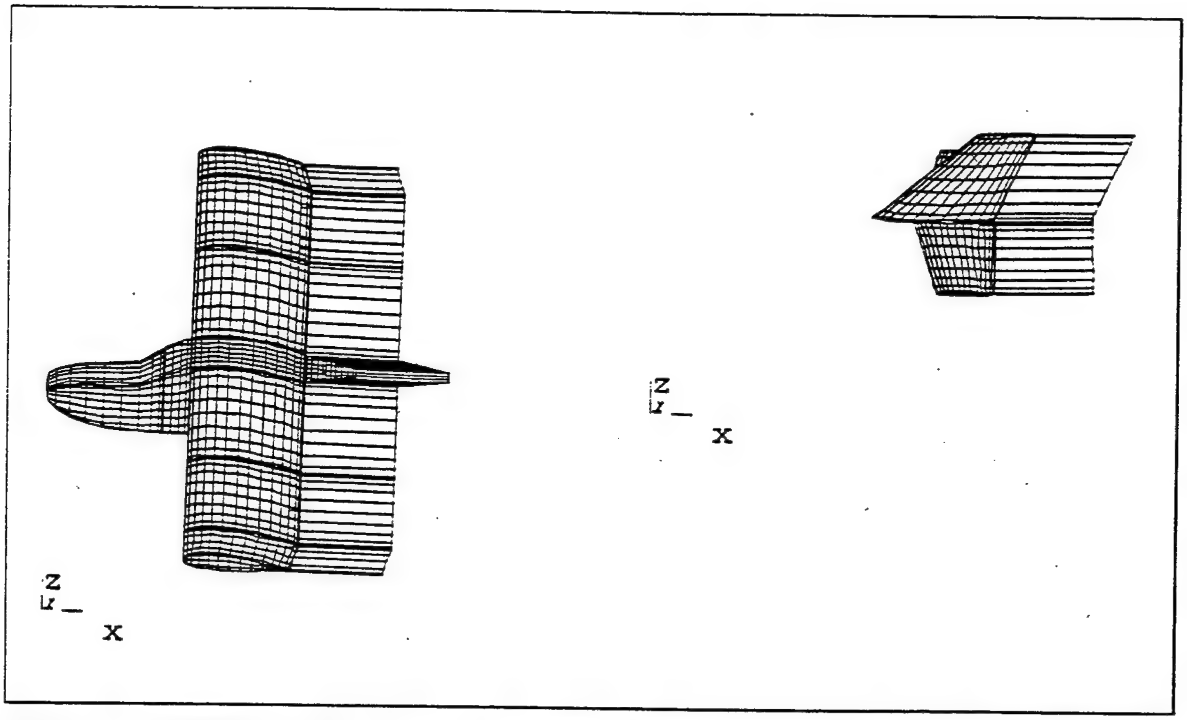

Figure A.7 FROG UAV Lateral-Directional Models.

1. Static Lateral Directional Stability Derivatives

a. Static Lateral-Directional Stability Equations

Three lateral-directional stability derivatives are measured with the first two runs of the CMARC model. The model is first analyzed at the estimated trim condition with zero sideslip. The baseline solution should be compared to the longitudinal baseline. If the lift coefficient differs significantly, the wake modification assumptions may need to be revisited. The model is then checked for lateral-directional

balance at zero sideslip angle (yaw angle =0). The side force, rolling and yawing coefficients should be zero when a trial run is performed at zero sideslip. If lateral-directional forces or moments are present, the model and wake geometry should be checked for symmetry. Visualization with LOFTSMAN will assist in spotting the problem.

For the FROG case, α_{trim}=0° and β=0° is selected for the baseline. A second CMARC run is then conducted with yaw angle incremented by one or two degrees. C_Y, C_l and C_n are then extracted manually from the data files. The slope of C_Y, C_l and C_n versus sideslip provides the $C_{Y\beta}$, $C_{l\beta}$ and $C_{n\beta}$ longitudinal derivatives. Additional solutions can be obtained to check for slope linearity. Equations A.55 through A.57 are used for these calculations:

$$C_{Y_\beta} = \frac{C_Y}{\Delta\beta^\circ} * \frac{180}{\pi} \text{ per radian} \qquad \text{A.55}$$

$$C_{l_\beta} = \frac{C_l}{\Delta\beta^\circ} * \frac{180}{\pi} \text{ per radian} \qquad \text{A.56}$$

$$C_{n_\beta} = \frac{C_n}{\Delta\beta^\circ} * \frac{180}{\pi} \text{ per radian} \qquad \text{A.57}$$

b. Sample Static Lateral-Directional Data Reduction

Table A.6 presents CMARC solutions for the FROG UAV at two angles-of-attack. Data is for the summed contribution of the wing/fuselage and tail group models. Roll and yaw moments are already divided by a factor of two. This normalizes by span to compensate for the CMARC output, which is normalized by semi-span. Sample calculations for obtaining the static derivatives are demonstrated below. The calculations are easily implemented in a spreadsheet or with a MATLAB script.

RUN #	β	CL	CD	CY	C_m	C_n	C_l
1	0°	0.4432	0.0145	0.0000	0.0048	0.0000	0.0000
2	2°	0.4452	0.0148	-0.0087	0.0038	0.0022	-0.0022

Table A.6 FROG UAV Static Lateral-Directional Stability Data at α_{trim}=0°.

Sample Calculations:

$$C_{Y_\beta} = \frac{C_Y}{\Delta\beta^\circ} * \frac{180}{\pi} = \frac{-0.0087}{2^\circ} * \frac{180}{\pi}\frac{deg}{rad} = -0.2493 \text{ per radian} \qquad \text{A.55}$$

$$C_{l_\beta} = \frac{C_l}{\Delta\beta^\circ} * \frac{180}{\pi} = \frac{-0.0022}{2^\circ} * \frac{180}{\pi}\frac{deg}{rad} = 0.0630 \text{ per radian}$$

A.56

$$C_{n_\beta} = \frac{C_n}{\Delta\beta^\circ} * \frac{180}{\pi} = \frac{0.0022}{2^\circ} * \frac{180}{\pi}\frac{deg}{rad} = 0.0630 \text{ per radian} \qquad \text{A.57}$$

3. Lateral-Directional Control Power Stability Derivatives

a. Lateral-Directional Control Power Equations

The rudder control power derivatives are obtained by substituting a 0° deflection vertical stabilizer patch for one with positive rudder deflection. Only one run is required. For the FROG UAV study, +5° (TEL) deflection is used. The difference between the trim condition and the deflected value is divided by the rudder deflection as shown below:

$$C_{Y_{\delta a}} = \frac{\left(C_{Y_{\delta a_2}} - C_{Y_{\delta a_1}}\right)}{\delta a_2 - \delta a_1} * \frac{180}{\pi} \quad per \quad rad \qquad \text{A.58}$$

$$C_{l_{\delta a}} = \frac{\left(C_{l_{\delta a_2}} - C_{l_{\delta a_1}}\right)}{\delta a_2 - \delta a_1} * \frac{180}{\pi} \quad per \quad rad \qquad \text{A.59}$$

$$C_{n_{\delta a}} = \frac{\left(C_{n_{\delta a_2}} - C_{n_{\delta a_1}}\right)}{\delta a_2 - \delta a_1} * \frac{180}{\pi} \quad per \quad rad \qquad \text{A.60}$$

$$C_{Y_{\delta r}} = \frac{\left(C_{Y_{\delta r_2}} - C_{Y_{\delta r_1}}\right)}{\delta r_2 - \delta r_1} * \frac{180}{\pi} \quad per \quad rad \qquad \text{A.61}$$

$$C_{l_{\delta r}} = \frac{\left(C_{l_{\delta r_2}} - C_{l_{\delta r_1}}\right)}{\delta r_2 - \delta r_1} * \frac{180}{\pi} \quad per \quad rad \tag{A.62}$$

$$C_{n_{\delta r}} = \frac{\left(C_{n_{\delta r_2}} - C_{n_{\delta r_1}}\right)}{\delta r_2 - \delta r_1} * \frac{180}{\pi} \quad per \quad rad \tag{A.63}$$

b. *Sample Lateral-Directional Control Power Data Reduction*

Tables A.7 and A.8 present CMARC solutions for aileron and rudder deflections. Sample calculations for obtaining aileron and rudder control power are demonstrated below. The calculations are easily implemented in a spreadsheet or with a MATLAB script.

$$C_{Y_{\delta a}} = \frac{\left(C_{Y_{\delta a_2}} - C_{Y_{\delta a_1}}\right)}{\delta a_2 - \delta a_1} * \frac{180}{\pi} = \frac{(-0.0018 - 0)}{(5-0)} * \frac{180}{\pi} = -0.0103 \tag{A.64}$$

$$C_{l_{\delta a}} = \frac{\left(C_{l_{\delta a_2}} - C_{l_{\delta a_1}}\right)}{\delta a_2 - \delta a_1} * \frac{180}{\pi} = \frac{(0.01695 - 0)}{(5-0)} * \frac{180}{\pi} = 0.1943 \tag{A.65}$$

$$C_{n_{\delta a}} = \frac{\left(C_{n_{\delta a_2}} - C_{n_{\delta a_1}}\right)}{\delta a_2 - \delta a_1} * \frac{180}{\pi} = \frac{(-0.00105 - 0)}{(5-0)} * \frac{180}{\pi} = -0.0120 \tag{A.66}$$

$$C_{Y_{\delta r}} = \frac{\left(C_{Y_{\delta r_2}} - C_{Y_{\delta r_1}}\right)}{\delta r_2 - \delta r_1} * \frac{180}{\pi} = \frac{(0.0081 - 0)}{(5-0)} * \frac{180}{\pi} = 0.0928 \tag{A.67}$$

$$C_{l_{\delta r}} = \frac{\left(C_{l_{\delta r_2}} - C_{l_{\delta r_1}}\right)}{\delta r_2 - \delta r_1} * \frac{180}{\pi} = \frac{(0.00035 - 0)}{(5-0)} * \frac{180}{\pi} = 0.0040 \tag{A.68}$$

$$C_{n_{\delta r}} = \frac{\left(C_{n_{\delta r_2}} - C_{n_{\delta r_1}}\right)}{\delta r_2 - \delta r_1} * \frac{180}{\pi} = \frac{(-0.00395 - 0)}{(5-0)} * \frac{180}{\pi} = -0.0453 \tag{A.69}$$

RUN #	δa	CL	CD	CY	C_m	C_n	C_l
1	0°	0.4259	0.0170	0.0000	0.0104	0.0000	0.0000
2	5°	0.4005	0.0173	-0.0018	0.0199	-0.00105	0.01695

Table A.7 FROG UAV Aileron Control Power Data at α_{trim}=0°.

RUN #	δr	CL	CD	CY	C_m	C_n	C_l
1	0°	0.4259	0.0170	0.0000	0.0104	0.0000	0.0000
2	5°	0.4258	0.0170	0.0081	0.0107	-0.00395	0.00035

Table A.8 FROG UAV Rudder Control Power Data at α_{trim}=0°.

3. Yaw Rate Damping Derivatives

a. Yaw Rate Derivative Methods and Equations

Only one motion is required for the yaw rate terms. The β-dot terms are generally considered negligible. Therefore, a sideways plunging motion is not required. The yaw rate terms are yielded directly from an oscillating yawing motion as depicted in Figure A.8. Yawing motion data for the FROG is gathered at a frequency of 2π rad/s, which equates to a reduced frequency of k=0.369 for this configuration and trim airspeed. Oscillating yaw motion is controlled with the CMARC BINP8A input file line. An amplitude of ±2° is selected for the FROG study. An example BINP8A input line is shown below. Note that yaw amplitude is in degrees and frequency is in rad/sec:

```
&BINP8A   PHIMAX=0.0,   THEMAX=1.5,   PSIMAX=0.0
          WTX=0.0,      WTY=6.283,    WTZ=0.0,      &END
```

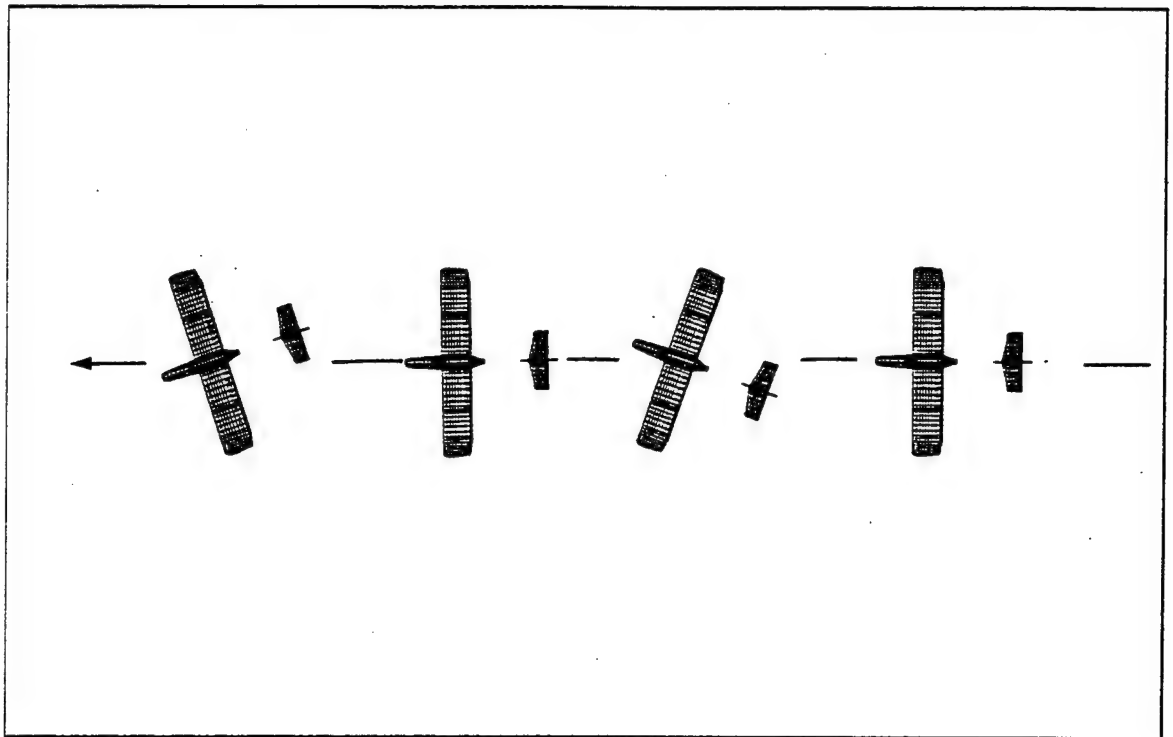

Figure A.8 Yawing Motion for Obtaining the Yaw Rate Derivatives.

The number of time steps and time step interval is chosen to create a nice sinusoidal output through at least two cycles of motion. In the FROG study, a yawing motion frequency of ω=2π rad/s or one cycle/sec is utilized. Fifty time steps are chosen with an interval of 0.05 seconds, which creates 2.5 cycles of yawing motion. After the solution is obtained, the "total coefficient" data is extracted for plotting. The data can be picked out manually, or a data retrieval program can be created for the task. For the FROG study, the data is extracted manually and pasted into an "Excel" spreadsheet for plotting. As discussed earlier, the FROG model was split into wing/fuselage and tail groups for the lateral-directional study. Both sets of data are pasted into the Excel spreadsheet and summed. The total value is then plotted. In addition, yawing motion phase and sideslip angles are also calculated using Equations A.70 and A.71. Yawing motion phase angle is plotted on the x-axis and sideslip is plotted on the right hand axis. Table A.9 shows representative FROG yaw rate data for 20 time steps.

$$\phi_{yaw} = \#_{timestep} * dt * \varpi_{yaw} * \frac{180}{\pi} \text{ degrees} \qquad \text{A.70}$$

$$\beta = \sin(\phi_{yaw}) * A_{yaw} \text{ degrees} \tag{A.71}$$

Where:

- ϕ_{yaw} - yawing motion phase angle
- β - Sideslip angle from yawing motion
- $\#_{timestep}$ - time step
- dt - time step interval
- ω_{yaw} - Yawing frequency
- A_{yaw} - Yaw angle amplitude

Step	φ (deg)	β	CL	CD	CY	C_m	C_n	C_l
0	0	0.00	0.0534	0.0111	-0.0005	0.085	0.0003	-0.0002
1	18	0.62	0.4004	0.0195	-0.007	-0.0107	0.0023	-0.0023
2	36	1.18	0.4329	0.0161	-0.0087	-0.0009	0.0026	-0.0026
3	54	1.62	0.4388	0.0152	-0.0098	0.0019	0.0027	-0.0027
4	72	1.90	0.4416	0.0149	-0.0098	0.0027	0.0026	-0.0026
5	90	2.00	0.4428	0.0149	-0.0089	0.0033	0.0022	-0.0022
6	108	1.90	0.4435	0.0147	-0.0071	0.0039	0.0016	-0.0016
7	126	1.62	0.444	0.0146	-0.0046	0.0044	0.0008	-0.0008
8	144	1.18	0.4444	0.0146	-0.0017	0.0049	0.0000	0.0000
9	162	0.62	0.4447	0.0144	0.0014	0.0051	-0.0009	0.0009
10	180	0.00	0.445	0.0144	0.0043	0.0048	-0.0016	0.0016
11	198	-0.62	0.4452	0.0145	0.0069	0.0044	-0.0022	0.0022
12	216	-1.18	0.4453	0.0146	0.0087	0.004	-0.0026	0.0026
13	234	-1.62	0.4452	0.0147	0.0098	0.0035	-0.0027	0.0027
14	252	-1.90	0.4451	0.0147	0.0098	0.0034	-0.0026	0.0025
15	270	-2.00	0.4449	0.0148	0.0089	0.0036	-0.0022	0.0021
16	288	-1.90	0.4448	0.0146	0.0071	0.0041	-0.0016	0.0015
17	306	-1.62	0.4449	0.0146	0.0046	0.0045	-0.0008	0.0008
18	324	-1.17	0.445	0.0145	0.0017	0.005	0.0000	-0.0001
19	342	-0.62	0.4452	0.0144	-0.0014	0.0051	0.0009	-0.0009
20	360	0.00	0.4454	0.0144	-0.0044	0.0049	0.0016	-0.0016

Table A.9 Sample FROG UAV Yawing Motion Data for 20 Time Steps

The C_Y, C_l and C_m responses are plotted as a function of yawing phase angle. Sideslip is also plotted on the right hand vertical axis. Figure A.9 is a representative plot of CMARC data for the FROG UAV study. The out-of-phase (imaginary) portion of C_Y, C_l or C_m is due to the yaw rate damping contribution. The β-dot contribution is considered small and is ignored. The phase angle is measured between the coefficient response and sideslip angle. In this case, the zero crossing

method of measuring phase angle proves to the easiest and most accurate. The phase angle is simply measured from the parameter to sideslip angle where they cross the x-axis in the same direction. The yaw rate damping contribution is normalized by maximum yaw rate and t^*. Equations A.72 through A.76 are used to solve for C_{Yr}, C_{lr} and C_{nr}.

$$C_{Y_r} = \frac{I[C_Y]}{r_{\max} * t^*}, \quad where \quad I[C_Y] = \sin(\phi_{yaw})[C_Y] \qquad \text{A.72}$$

$$C_{l_r} = \frac{I[C_l]}{r_{\max} * t^*}, \quad where \quad I[C_l] = \sin(\phi_{yaw})[C_l] \qquad \text{A.73}$$

$$C_{n_r} = \frac{I[C_n]}{r_{\max} * t^*}, \quad where \quad I[C_n] = \sin(\phi_{yaw})[C_n] \qquad \text{A.74}$$

$$r_{\max} = \frac{A_{\varphi\deg}}{57.3 \, {}^{\deg}\!/_{rad}} * \omega_{yaw} \quad \text{rad/s} \qquad \text{A.75}$$

$$t^* = \frac{{}^{b}\!/_{2}}{U_0} \quad \text{sec} \qquad \text{A.76}$$

Where:

$[C_Y]$	- Amplitude of C_Y response from yawing motion
$[C_l]$	- Amplitude of C_l response from yawing motion
$[C_n]$	- Amplitude of C_n response from yawing motion
$I[C_Y]$	- C_Y coefficient contribution from yaw rate damping
$I[C_l]$	- C_l coefficient contribution from yaw rate damping
$I[C_n]$	- C_n coefficient contribution from yaw rate damping
t^*	- Characteristic time

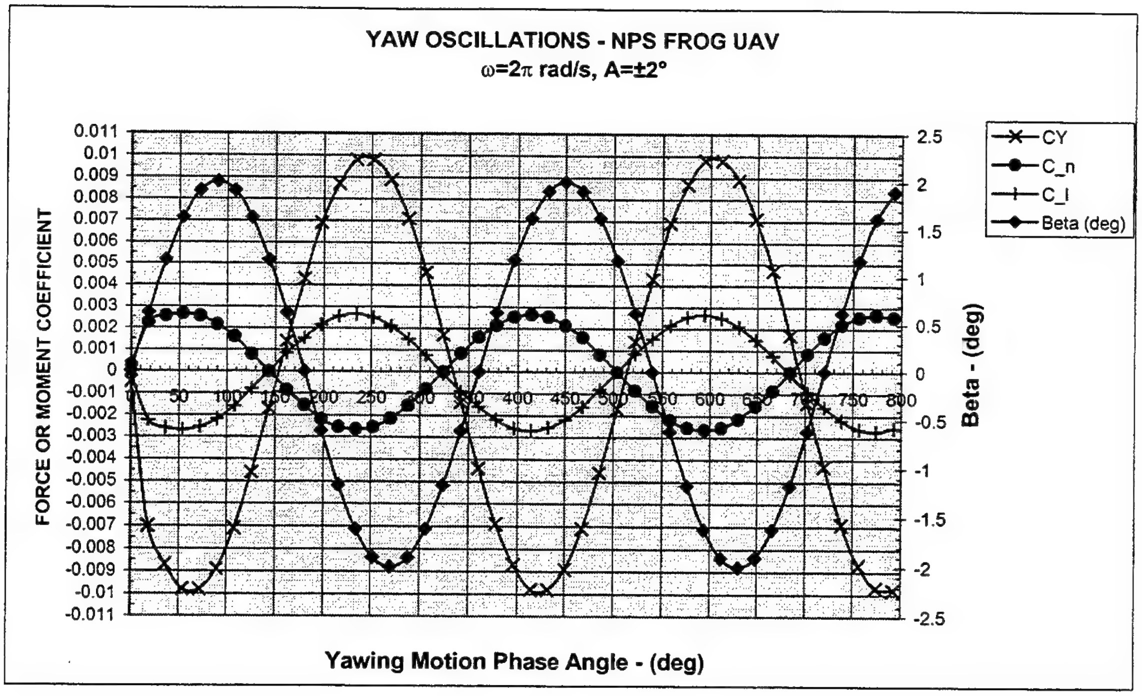

Figure A.9 Representative Yawing Motion Plot for the FROG UAV.

b. Sample Yaw Rate Damping Data Reduction

Sample data reduction is presented below in Equations A.28 through A.32. The phase angle between the response and the sideslip angle is measured graphically by zooming in on the x-axis zero crossing.

$$t^* = \frac{b/2}{U_0} = \frac{124in/2}{1056\,in/s} = 0.0587 \quad \text{sec} \qquad \text{A.77}$$

$$r_{\max} = \frac{A_{\varphi\deg}}{57.3\,{}^\circ/rad} * \omega_{yaw} = \frac{2^\circ}{57.3\,{}^\circ/rad} * 2\pi\, rad/\sec = 0.2193 \quad \text{rad/s} \qquad \text{A.78}$$

$$C_{Y_r} = \frac{I[C_Y]}{r_{\max} * t^*} = \frac{\sin(\phi_{yaw})[C_Y]}{r_{\max} * t^*} = \frac{\sin(154°)[0.0099]}{0.2193 * 0.0587} = 0.3371 \qquad \text{A.79}$$

$$C_{l_r} = \frac{I[C_l]}{r_{\max} * t^*} = \frac{\sin(\phi_{yaw})[C_l]}{r_{\max} * t^*} = \frac{\sin(144°)[0.00265]}{0.2193 * 0.0587} = 0.1210 \qquad \text{A.80}$$

$$C_{n_r} = \frac{I[C_n]}{r_{\max} * t^*} = \frac{\sin(\phi_{yaw})[C_n]}{r_{\max} * t^*} = \frac{\sin(-36°)[0.00265]}{0.2193 * 0.0587} = -0.1210 \qquad \text{A.81}$$

4. Roll Rate Damping Derivatives

a. Roll Rate Derivative Methods and Equations

Gathering roll damping data is straightforward. Unlike the pitch or yaw rate terms, there is no change in angle-of-attack or sideslip with the rolling motion. Therefore, roll damping effects can be measured with pure rolling motion around the x-axis. As with the yaw damping case, the wing/fuselage and tail models are run separately. The results are then summed. A rigid wake seems to work well, which provides a solution after just a few time steps.

Roll damping data for the FROG is gathered at a 20 deg/sec roll rate. Initially, a 5 deg/sec roll rate was selected, but the yawing moment coefficient was low enough that numerical resolution would effect the results. The higher rate provided a sufficiently large response for all terms. Pure rolling motion is controlled by the PHIDOT term in the CMARC BINP8 input file line. An example BINP8 input line is shown below. Note that roll rate is in deg/sec:

```
&BINP8    ALDEG=0.0,      YAWDEG=0.0,     PHIDOT=20.0
          THEDOT=0.0,     PSIDOT=0.0,     &END
```

The roll rate damping terms are obtained by normalizing the CMARC output by roll rate, p, and characteristic time, t*. Equations A.82 through A.85 are used for these calculations.

$$C_{Y_p} = \frac{C_Y}{p * t^*} \qquad \text{A.82}$$

$$C_{l_p} = \frac{C_l}{p * t^*} \qquad \text{A.83}$$

$$C_{n_p} = \frac{C_n}{p * t^*} \qquad \text{A.84}$$

$$t^* = \frac{b/2}{U_0} \text{ sec} \qquad \text{A.85}$$

Where:

$[C_Y]$	- Amplitude of C_Y response from roll rate
$[C_l]$	- Amplitude of C_l response from roll rate
$[C_n]$	- Amplitude of C_n response from roll rate
p	- Roll rate
t^*	- Characteristic time

d. *Sample Roll Rate Damping Data Reduction*

Tables A.10 presents the CMARC roll damping solution for the FROG UAV. The data is the summed contributions from the wing/fuselage and tail surface models. Sample roll damping calculations presented below in Equations A.86 through A.89. The calculations are easily implemented in a spreadsheet or with a MATLAB script.

$$t^* = \frac{b/2}{U_0} = \frac{62in}{1056\,in/s} = 0.0587 \text{ sec} \qquad \text{A.86}$$

$$C_{Y_p} = \frac{C_Y}{p * t^*} = \frac{0.0010}{20\frac{\deg}{\sec} * \frac{\pi}{180}\frac{\deg}{rad} * 0.0587\sec} = 0.0488 \qquad \text{A.87}$$

$$C_{l_p} = \frac{C_l}{p * t^*} = \frac{-0.00925}{20\frac{\deg}{\sec} * \frac{\pi}{180}\frac{\deg}{rad} * 0.0587\sec} = 0.4514 \qquad \text{A.88}$$

$$C_{n_p} = \frac{C_n}{p * t^*} = \frac{-0.00045}{20\frac{\deg}{\sec} * \frac{\pi}{180}\frac{\deg}{rad} * 0.0587\sec} = -0.0220 \qquad \text{A.89}$$

RUN #	p	CL	CD	CY	C_m	C_n	C_l
1	0 deg/s	0.4432	0.0145	0.0000	0.0048	0.0000	0.0000
2	20 deg/s	0.4435	0.0143	0.0010	0.0047	-0.00045	-0.00925

Table A.10 FROG UAV Roll Damping Data at α_{trim}=0° and β=0°.

APPENDIX B

LOFTSMAN INPUT FILES FOR FROG UAV MODELING

```
FROG UAV Fuselage Moldlines

File name: fogfusa
Last revision:  4/12/97

-------------------------------------------------------------------

BOTTOM WATERLINE

Segments: 3

Fore end        0,6.5
Aft end         12,0    53.0,0  53.5,5.75
Corner          0,0     S       53.5,0
Curvature       .69             0.95
-------------------------------------------------------------------

WAIST WATERLINE

Segments: 1

Fore end        0,6.5
Aft end         53.5,6.5
Corner          S
Curvature
-------------------------------------------------------------------

TOP WATERLINE

Segments: 7

Fore end        0,6.5
Aft end         8,9.3   15.2,9.3   21.6,13.0   29.0,14.6   44.6,11.6
53.0,11.5   53.5,6.5
Corner          0,9.3      S          S        24.3,14.6   35.4,14.6
S      53.5,11.5
Curvature       0.7                               0.71        0.81
.95
-------------------------------------------------------------------

MAXIMUM BUTTLINE DISTANCE FROM PLANE OF SYMMETRY

Segments: 6

Fore end        0,0
Aft end         1,3     1,3     22,4.5    43.6,4.5   53.1,1.3    53.5,0

Corner          0,2.9   S        S         S          S
53.5,1.3
Curvature       .9                                   0.8         0.95
-------------------------------------------------------------------
```

```
BOTTOM K FACTOR

Segments: 3

Fore end        0,0.93
Aft end         12.0,0.98      43.6,0.98      53.5,0.95
Corner          S              S              S
Curvature
-------------------------------------------------------------------
TOP K FACTOR

Segments: 4

Fore end        0,0.90
Aft end         15.20,0.95      24,1.0        44.65,1.0      53.5,0.95

Corner          S               S             S              S
Curvature
-------------------------------------------------------------------
BUTTLINE AT PLANE OF SYMMETRY

Segments: 0
```

```
NPS FROG UAV Right Wing - Loftsman Input File

Date: 3/30/98

Breaks: 5

Break 1

Axis: 24.65,0,13.1
Axis/chord: 0
Chord: 20.0
Incidence: 4.5
Cant: 0
Section file: N2415
T/C ratio: 0.1500
Spars: 0
Panel rib angles: 0,999.0000,0.0000

Break 2

Axis: 24.65,6,13.1
Axis/chord: 0
Chord: 20.0
Incidence: 4.5
Cant: 0
Section file: N2415
T/C ratio: 0.1500
Spars: 0
Panel rib angles: 0,999.0000,0.0000

Break 3

Axis: 24.65,31.5,13.1
Axis/chord: 0
Chord: 20.0
Incidence: 4.5
Cant: 0
Section file: N2415
T/C ratio: 0.1500
Spars: 0
Panel rib angles: 0,999.0000,0.0000

Break 4

Axis: 24.65,53.0,13.1
Axis/chord: 0
Chord: 20.0
Incidence: 4.5
Cant: 0
Section file: N2415
T/C ratio: 0.1500
Spars: 0
Panel rib angles: 0,999.0000,0.0000

Break 5

Axis: 24.65,61.0,13.1
Axis/chord: 0
Chord: 18.5
Incidence: 4.5
Cant: 0
Section file: N2415
T/C ratio: 0.1500
Spars: 0
```

```
NPS FROG UAV Left Wing - Loftsman Input File

Date: 3/30/98

Breaks: 5

Break 1

Axis: 24.65,0,13.1
Axis/chord: 0
Chord: 20.0
Incidence: 4.5
Cant: 0
Section file: N2415
T/C ratio: 0.1500
Spars: 0
Panel rib angles: 0,999.0000,0.0000

Break 2

Axis: 24.65,-6,13.1
Axis/chord: 0
Chord: 20.0
Incidence: 4.5
Cant: 0
Section file: N2415
T/C ratio: 0.1500
Spars: 0
Panel rib angles: 0,999.0000,0.0000

Break 3

Axis: 24.65,-31.5,13.1
Axis/chord: 0
Chord: 20.0
Incidence: 4.5
Cant: 0
Section file: N2415
T/C ratio: 0.1500
Spars: 0
Panel rib angles: 0,999.0000,0.0000

Break 4

Axis: 24.65,-53.0,13.1
Axis/chord: 0
Chord: 20.0
Incidence: 4.5
Cant: 0
Section file: N2415
T/C ratio: 0.1500
Spars: 0
Panel rib angles: 0,999.0000,0.0000

Break 5

Axis: 24.65,-61.0,13.1
Axis/chord: 0
Chord: 18.5
Incidence: 4.5
Cant: 0
Section file: N2415
T/C ratio: 0.1500
Spars: 0
```

```
FROG Horizontal Tail

Date: 4/14/97

Breaks: 2

Break 1

Axis: 82.5,0,8.09
Axis/chord: 0
Chord: 13.5
Incidence: 0
Cant: 0
Section file: N0006
T/C ratio: 0.06
Spars: 0
Panel rib angles: 0,999.0000,0.0000

Break 2

Axis: 86.5,19.875,8.09
Axis/chord: 0
Chord: 9.55
Incidence: 0
Cant: 0
Section file: N0006
T/C ratio: 0.06
Spars: 0
Panel rib angles: 0,999.0000,0.0000
```

```
FROG UAV Vertical Tail - LOFTSMAN input file

Date: 4/14/97

Breaks: 2

Break 1

Axis: 77.5,0,10.4
Axis/chord: 0
Chord: 20
Incidence: 0
Cant: 90
Section file: N0006
T/C ratio: 0.06
Spars: 0
Panel rib angles: 90,0,999

Break 2

Axis: 92.35,0,25.15
Axis/chord: 0
Chord: 10
Incidence: 0
Cant: 90
Section file: N0006
T/C ratio: 0.06
Spars: 0
Panel rib angles: 90,0,999
```

```
FROG UAV Vertical Tail - LOFTSMAN input file

Date: 4/14/97 Mod; 8/5/98 to include projected area of vstab
through tail boom.

Breaks: 2

Break 1

Axis: 75.6,0,8.5
Axis/chord: 0
Chord: 20
Incidence: 0
Cant: 90
Section file: N0006
T/C ratio: 0.06
Spars: 0
Panel rib angles: 90,0,999

Break 2

Axis: 92.35,0,25.15
Axis/chord: 0
Chord: 10
Incidence: 0
Cant: 90
Section file: N0006
T/C ratio: 0.06
Spars: 0
Panel rib angles: 90,0,999
```

```
FROG UAV Tail Boom

File name: frogboom
Last revision:  4/28/97

4/28:  added rounded start and finish to close ends
------------------------------------------------------------------
BOTTOM WATERLINE

Segments: 3

Fore end        53.5,9.375
Aft end             54,8.5                         88,8.5
88.5,9.375
Corner          53.5,8.5                  S
88.5,8.5
Curvature       0.707
0.707
------------------------------------------------------------------
WAIST WATERLINE

Segments: 1

Fore end        53.5,9.375
Aft end             88.5, 9.375
Corner          S
Curvature
------------------------------------------------------------------
TOP WATERLINE

Segments: 3

Fore end        53.5,9.375
Aft end             54.0,10.25                       88,10.25
88.5,9.375
Corner          53.5,10.25                    S
88.5,10.25
Curvature           0.707
0.707
------------------------------------------------------------------
MAXIMUM BUTTLINE DISTANCE FROM PLANE OF SYMMETRY

Segments: 3

Fore end        53.5,0
Aft end             54,0.875                           88,0.875
88.5,0
Corner          53.5,0.875                         S
88.5,0.875
Curvature       0.707
0.707
------------------------------------------------------------------
BOTTOM K FACTOR

Segments: 1

Fore end        53.5,0.707
Aft end             88.5, 0.707
Corner          S
Curvature
------------------------------------------------------------------
TOP K FACTOR

Segments: 1

Fore end        53.5,0.707
Aft end             88.5, 0.707
Corner          S
Curvature
------------------------------------------------------------------
BUTTLINE AT PLANE OF SYMMETRY
Segments: 0
```

```
FROG UAV ENGINE NACELLE

File name: fogenpod
Last revision:  4/13/97
------------------------------------------------------------------
BOTTOM WATERLINE

Segments: 4

Fore end     16.5,20.4
Aft end      18.2,18.6   21.0,16.8    31.0,15.75   43.0, 16.8

Corner       16.6,19.6   19.15,17.35  23.8,15.9    35.6,15.65
Curvature    0.79         0.83        0.72          0.73
------------------------------------------------------------------
WAIST WATERLINE

Segments: 1

Fore end     16.5,20.4
Aft end      43.0,16.8
Corner       S
Curvature
------------------------------------------------------------------
TOP WATERLINE

Segments: 4

Fore end     16.3,20.4
Aft end      18.45,22.1  27.0,21.75    35.0,19.8    43.0,16.8

Corner       16.75,21.3  21.4,22.5     30.4,21.3    38.3,18.75
Curvature    0.79             0.80          0.70          0.75
------------------------------------------------------------------
MAXIMUM BUTTLINE DISTANCE FROM PLANE OF SYMMETRY

Segments: 4

Fore end     16.5,0
Aft end      18.2,1.6    23.0,2.3    40.8,2.3     43.0,0

Corner       16.5,0.70   20.1,2.25   S            43.0,2.3
Curvature    0.72             0.75                     0.90
------------------------------------------------------------------
BOTTOM K FACTOR

Segments: 4

Fore end     16.5,0.707
Aft end      18.2,0.707   24.0,0.93     42.0,0.93    43.0,0.75
Corner       S             20,0.93             S            S
Curvature                  0.9
------------------------------------------------------------------
TOP K FACTOR

Segments: 4

Fore end     16.5,0.707
Aft end      18.45,0.707    24.5,0.93    42.0,0.93
43.0,0.75
Corner       S              20.3,0.93         S            S
Curvature                   0.9
------------------------------------------------------------------
BUTTLINE AT PLANE OF SYMMETRY
Segments: 0
```

```
FOG UAV ENGINE PYLON (Lofted as A-Body Type)

File name: FOGPYLON
Last revision: 4/13/97

Strips: 3
Sym: Y

M1B

Segments: 1

  Fore end       25.8,0
   Aft end       37.7,0
    Corner       S
  K factor       S

M1W

Segments: 1

  Fore end    25.8,14.15
   Aft end    37.7,13.65
    Corner    29.4,15.45
  K factor    0.72

C1B

Segments: S

C1W

Segments: S

K1

Segments: S

M2B

Segments: 1
 Fore end     25.8,0
   Aft end    37.7,0
    Corner    25.8,3.8
  K factor    0.71

M2W

Segments: =M1W

C2B

Segments: S

C2W

Segments: S

K2

Segments: S

M3B

Segments: =M2B

M3W

Segments: 1

 Fore end    25.8,16.1
   Aft end    37.7,16.1
    Corner    33.65,15.35
  K factor    0.65

C3B

Segments: S

C3W

Segments: S

K3

Segments: S

M4B

Segments: =M1B

M4W

Segments: =M3W
```

APPENDIX C

FROG UAV CMARC INPUT FILE

```
FROGUAV.in:   - Final CAMRC input file which includes all patch and wake definitions.
              - Off body streamlines for pitot-static analysis

NPS FROG UAV CMARC/PMARCPANEL MODEL - Units = inches

 Created by:  Steve Pollard  4/2/98

 Revised:  9/6/98 - Modified to be final baseline for report.  Currently set-up
                    with full span wing/fuselage wake for lateral-directional
                    analysis of wing/fuselage group. Wakes and patches
                    can be activated to produce the desired configurations.

 &BINP2   LSTINP=2,    LSTOUT=0,    LSTFRQ=0,    LENRUN=0,    LPLTYP=1,          &END
 &BINP3   LSTGEO=0,    LSTNAB=0,    LSTWAK=0,    LSTCPV=0,                       &END
 &BINP4   MAXIT=400,    SOLRES=0.001,                                            &END
 &BINP5   NTSTPS= 50,  DTSTEP=0.05,                                              &END
 &BINP6   RSYM=1.0,    RGPR=0.0,    RFF=5.0,  RCORES=0.0080, RCOREW=0.0080,      &END
 &BINP7   VINF=1056.00,  VSOUND=13392.0,                                         &END
 &BINP8   ALDEG= 0.00, YAWDEG=0.0,  PHIDOT=0.0,  THEDOT=0.0,   PSIDOT=0.0,       &END
 &BINP8A  PHIMAX= 0.0, THEMAX= 0.0, PSIMAX=2.0,
             WRX=0.0,     WRY=0.0,     WRZ=6.283,                                &END
 &BINP8B  DXMAX=0.0,   DYMAX=0.0,   DZMAX=0.0,
             WTX=0.0,     WTY=0.0,     WTZ=0.0,                                  &END
 &BINP9   CBAR=20,   SREF=2530.0, SSPAN= 62,
             RMPX=0.00,   RMPY=0.00,   RMPZ=0.00,                                &END
 &BINP10  NORSET=0,    NBCHGE=0,    NCZONE=0,
             NCZPCH=0,    CZDUB=0.0,   VREF=0.0,                                 &END
 &BINP11  NORPCH=0,    NORF=0,      NORL=0,
             NOCF=0,      NOCL=0,      VNORM=0.0,                                &END
 &BINP12  KPAN=0,      KSIDE=0,     NEWNAB=0,    NEWSID=0,                       &END
 &BINP13  NBLIT=0,                                                               &END


 &ASEM1   ASEMX=-31.55,      ASEMY=0.00,       ASEMZ=-8.5700,
             ASCAL=1.00,        ATHET=0.00,       NODEA=5,                       &END
 &ASEM2   APXX=0.00,        APYY=0.00,        APZZ=0.00,
             AHXX=0.00,         AHYY=1.00,        AHZZ=0.00,                     &END


 &COMP1   COMPX= 0.0000,     COMPY= 0.0000,     COMPZ= 0.0000,
             CSCAL=  1.000,     CTHET=    0.0,      NODEC= 5,                    &END
 &COMP2   CPXX= 0.0000,      CPYY= 0.0000,      CPZZ= 0.0000,
             CHXX= 0.0000,       CHYY=  1.000,       CHZZ= 0.0000,               &END

 &PATCH1 IREV=0, IDPAT=2, MAKE=0, KCOMP=1, KASS=1, IPATSYM=1, IPATCOP=0,         &END
   FUSELAGE_NOSE
 &SECT1 STX=0.0, STY=0.0, STZ=0.0, SCALE=1.0, ALF=0.0, THETA=0.0, INMODE=4,
  TNODS=0, TNPS=0, TINTS=0, &END
    0.0000    0.0000    6.5000
    0.0000    0.0000    6.5000
    0.0000    0.0000    6.5000
    0.0000    0.0000    6.5000
    0.0000    0.0000    6.5000
    0.0000    0.0000    6.5000
    0.0000    0.0000    6.5000
    0.0000    0.0000    6.5000
    0.0000    0.0000    6.5000
    0.0000    0.0000    6.5000
    0.0000    0.0000    6.5000
    0.0000    0.0000    6.5000
    0.0000    0.0000    6.5000
    0.0000    0.0000    6.5000
    0.0000    0.0000    6.5000
    0.0000    0.0000    6.5000
 &BPNODE TNODE=3, TNPC=0, TINTC=0, &END
 &SECT1 STX=0.0, STY=0.0, STZ=0.0, SCALE=1.0, ALF=0.0, THETA=0.0, INMODE=4,
  TNODS=0, TNPS=0, TINTS=0, &END
    0.4894    0.0000    4.8456
    0.4894    0.9694    4.8472
    0.4894    1.8700    4.8569
    0.4894    2.4101    4.8828
    0.4894    2.6949    4.9422
    0.4894    2.8308    5.0656
    0.4894    2.8941    5.3171
    0.4894    2.9200    5.7981
    0.4894    2.9252    6.5846
    0.4894    2.9005    6.9893
    0.4894    2.8237    7.2119
    0.4894    2.6669    7.3254
    0.4894    2.3672    7.3842
    0.4894    1.8372    7.4126
    0.4894    0.9694    7.4244
    0.4894    0.0000    7.4266
 &BPNODE TNODE=3, TNPC=0, TINTC=0, &END
 &SECT1 STX=0.0, STY=0.0, STZ=0.0, SCALE=1.0, ALF=0.0, THETA=0.0, INMODE=4,
  TNODS=0, TNPS=0, TINTS=0, &END
    1.9098    0.0000    3.2261
    1.9098    1.2120    3.2304
    1.9098    2.1514    3.2527
    1.9098    2.6464    3.3105
    1.9098    2.8844    3.4400
    1.9098    2.9946    3.7159
    1.9098    3.0431    4.2715
    1.9098    3.0617    5.2972
    1.9098    3.0650    6.5092
    1.9098    3.0481    7.3382
    1.9098    2.9862    7.8079
    1.9098    2.8504    8.0540
    1.9098    2.5827    8.1796
    1.9098    2.0806    8.2410
    1.9098    1.1960    8.2673
    1.9098    0.0000    8.2731
 &BPNODE TNODE=3, TNPC=0, TINTC=0, &END
 &SECT1 STX=0.0, STY=0.0, STZ=0.0, SCALE=1.0, ALF=0.0, THETA=0.0, INMODE=4,
  TNODS=0, TNPS=0, TINTS=0, &END
    4.1221    0.0000    1.8058
    4.1221    1.3792    1.8110
    4.1221    2.3922    1.8401
    4.1221    2.8791    1.9216
    4.1221    3.0873    2.1152
    4.1221    3.1756    2.5617
    4.1221    3.2104    3.4985
    4.1221    3.2210    4.8740
    4.1221    3.2230    6.2532
    4.1221    3.2129    7.5020
    4.1221    3.1635    8.2308
    4.1221    3.0419    8.6115
    4.1221    2.7927    8.7934
    4.1221    2.2900    8.8805
    4.1221    1.3537    8.9164
    4.1221    0.0000    8.9243
 &BPNODE TNODE=3, TNPC=0, TINTC=0, &END
 &SECT1 STX=0.0, STY=0.0, STZ=0.0, SCALE=1.0, ALF=0.0, THETA=0.0, INMODE=4,
  TNODS=0, TNPS=0, TINTS=0, &END
    6.9098    0.0000    0.7304
    6.9098    1.4829    0.7343
    6.9098    2.6474    0.7608
    6.9098    3.1478    0.8479
    6.9098    3.3299    1.0887
    6.9098    3.3948    1.7151
    6.9098    3.4159    3.0358
    6.9098    3.4209    4.5188
    6.9098    3.4221    6.0017
    6.9098    3.4168    7.4676
    6.9098    3.3779    8.4328
    6.9098    3.2701    8.9147
    6.9098    3.0302    9.1303
    6.9098    2.5077    9.2266
    6.9098    1.4679    9.2637
```

```
  6.9098    0.0000    9.2711
&BPNODE TNODE=3, TNPC=0, TINTC=0, &END
&SECT1 STX=0.0, STY=0.0, STZ=0.0, SCALE=1.0, ALF=0.0, THETA=0.0, INMODE=4,
 TNODS=0, TNPS=0, TINTS=0, &END
 10.0000    0.0000    0.1152
 10.0000    1.5156    0.1169
 10.0000    2.8805    0.1323
 10.0000    3.4347    0.2022
 10.0000    3.5900    0.4599
 10.0000    3.6311    1.2905
 10.0000    3.6402    2.7963
 10.0000    3.6423    4.3120
 10.0000    3.6428    5.8276
 10.0000    3.6400    7.3433
 10.0000    3.6087    8.4519
 10.0000    3.5110    8.9679
 10.0000    3.2695    9.1801
 10.0000    2.7005    9.2654
 10.0000    1.5113    9.2951
 10.0000    0.0000    9.3000
&BPNODE TNODE=3, TNPC=0, TINTC=0, &END
&SECT1 STX=0.0, STY=0.0, STZ=0.0, SCALE=1.0, ALF=0.0, THETA=0.0, INMODE=4,
 TNODS=0, TNPS=0, TINTS=0, &END
 13.0902    0.0000    0.0000
 13.0902    1.5138    0.0007
 13.0902    3.0061    0.0077
 13.0902    3.6868    0.0552
 13.0902    3.8313    0.3019
 13.0902    3.8583    1.3036
 13.0902    3.8623    2.8174
 13.0902    3.8633    4.3312
 13.0902    3.8636    5.8451
 13.0902    3.8614    7.3589
 13.0902    3.8344    8.5203
 13.0902    3.7416    9.0232
 13.0902    3.4903    9.2092
 13.0902    2.8478    9.2766
 13.0902    1.5130    9.2971
 13.0902    0.0000    9.3000
&BPNODE TNODE=3, TNPC=0, TINTC=0, &END
&SECT1 STX=0.0, STY=0.0, STZ=0.0, SCALE=1.0, ALF=0.0, THETA=0.0, INMODE=4,
 TNODS=0, TNPS=0, TINTS=0, &END
 15.8779    0.0000    0.0000
 15.8779    1.5558    0.0007
 15.8779    3.1041    0.0070
 15.8779    3.8653    0.0517
 15.8779    4.0270    0.2880
 15.8779    4.0569    1.2775
 15.8779    4.0614    2.8332
 15.8779    4.0624    4.3890
 15.8779    4.0627    5.9448
 15.8779    4.0612    7.5006
 15.8779    4.0415    8.8474
 15.8779    3.9629    9.4248
 15.8779    3.7146    9.6156
 15.8779    3.0056    9.6748
 15.8779    1.5544    9.6899
 15.8779    0.0000    9.6919
&BPNODE TNODE=3, TNPC=0, TINTC=0, &END
&SECT1 STX=0.0, STY=0.0, STZ=0.0, SCALE=1.0, ALF=0.0, THETA=0.0, INMODE=4,
 TNODS=0, TNPS=0, TINTS=0, &END
 18.0902    0.0000    0.0000
 18.0902    1.6509    0.0007
 18.0902    3.2889    0.0077
 18.0902    4.0453    0.0611
 18.0902    4.1913    0.3563
 18.0902    4.2164    1.5673
 18.0902    4.2198    3.2182
 18.0902    4.2206    4.8691
 18.0902    4.2207    6.5200
 18.0902    4.2195    8.1710
 18.0902    4.2094    9.8015
 18.0902    4.1567   10.6520
 18.0902    3.9490   10.8950
 18.0902    3.2238   10.9567
 18.0902    1.6504   10.9694
 18.0902    0.0000   10.9709
&BPNODE TNODE=3, TNPC=0, TINTC=0, &END
&SECT1 STX=0.0, STY=0.0, STZ=0.0, SCALE=1.0, ALF=0.0, THETA=0.0, INMODE=4,
 TNODS=0, TNPS=0, TINTS=0, &END
 19.5106    0.0000    0.0000
 19.5106    1.7043    0.0007
 19.5106    3.3938    0.0081
 19.5106    4.1553    0.0661
 19.5106    4.2955    0.3979
 19.5106    4.3184    1.7232
 19.5106    4.3214    3.4275
 19.5106    4.3221    5.1318
 19.5106    4.3222    6.8361
 19.5106    4.3214    8.5405
 19.5106    4.3169   10.2448
 19.5106    4.2840   11.4245
 19.5106    4.1133   11.7224
 19.5106    3.3665   11.7816
 19.5106    1.7041   11.7911
 19.5106    0.0000   11.7920
&BPNODE TNODE=3, TNPC=0, TINTC=0, &END
&SECT1 STX=0.0, STY=0.0, STZ=0.0, SCALE=1.0, ALF=0.0, THETA=0.0, INMODE=4,
 TNODS=3, TNPS=0, TINTS=0, &END
 20.0000    0.0000    0.0000
 20.0000    1.7202    0.0007
 20.0000    3.4256    0.0081
 20.0000    4.1917    0.0673
 20.0000    4.3314    0.4135
 20.0000    4.3535    1.7754
 20.0000    4.3564    3.4956
 20.0000    4.3571    5.2158
 20.0000    4.3571    6.9360
 20.0000    4.3565    8.6562
 20.0000    4.3532   10.3763
 20.0000    4.3272   11.6828
 20.0000    4.1713   12.0088
 20.0000    3.4117   12.0661
 20.0000    1.7202   12.0742
 20.0000    0.0000   12.0750
&BPNODE TNODE=3, TNPC=0, TINTC=0, &END

&PATCH1 IREV=0, IDPAT=2, MAKE=0, KCOMP=1, KASS=1, IPATSYM=1, IPATCOP=0, &END
  ROOT TRANSITION FORE STARBOARD
&SECT1 STX=0.0, STY=0.0, STZ=0.0, SCALE=1.0, ALF=0.0, THETA=0.0, INMODE=4,
 TNODS=0, TNPS=0, TINTS=0, &END
 20.0000    0.0000    0.0000
 20.0000    1.7202    0.0007
 20.0000    3.4256    0.0081
 20.0000    4.1917    0.0673
 20.0000    4.3314    0.4135
 20.0000    4.3535    1.7754
 20.0000    4.3564    3.4956
 20.0000    4.3571    5.2158
 20.0000    4.3571    6.9360
 20.0000    4.3565    8.6562
 20.0000    4.3532   10.3763
 20.0000    4.3272   11.6828
 20.0000    4.1713   12.0088
 20.0000    3.4117   12.0661
 20.0000    1.7202   12.0742
 20.0000    0.0000   12.0750
&BPNODE TNODE=3, TNPC=0, TINTC=0, &END
&SECT1 STX=0.0, STY=0.0, STZ=0.0, SCALE=1.0, ALF=0.0, THETA=0.0, INMODE=4,
 TNODS=0, TNPS=0, TINTS=0, &END
```

```
  20.4440     0.0000     0.0000
  20.4440     1.7171     0.0007
  20.4440     3.4241     0.0078
  20.4440     4.2151     0.0644
  20.4440     4.3616     0.3949
  20.4440     4.3850     1.7224
  20.4440     4.3881     3.4395
  20.4440     4.3888     5.1566
  20.4440     4.3889     6.8736
  20.4440     4.3885     8.5907
  20.4440     4.3865    10.3078
  20.4440     4.3707    11.8182
  20.4440     4.2485    12.2579
  20.4440     3.5302    12.3232
  20.4440     1.7837    12.3310
  20.4440     0.0000    12.3317
&BPNODE TNODE=3, TNPC=0, TINTC=0, &END
&SECT1 STX=0.0, STY=0.0, STZ=0.0, SCALE=1.0, ALF=0.0, THETA=0.0, INMODE=4,
 TNODS=0, TNPS=0, TINTS=0, &END
  21.6065     0.0000     0.0000
  21.6065     1.7392     0.0007
  21.6065     3.4719     0.0076
  21.6065     4.2930     0.0637
  21.6065     4.4441     0.3949
  21.6065     4.4680     1.7396
  21.6065     4.4711     3.4788
  21.6065     4.4718     5.2180
  21.6065     4.4719     6.9572
  21.6065     4.4717     8.6964
  21.6065     4.4711    10.4355
  21.6065     4.4667    12.1724
  21.6065     4.3976    12.9316
  21.6065     3.6877    12.9989
  21.6065     1.8477    13.0035
  21.6065     0.0000    13.0039
&BPNODE TNODE=3, TNPC=0, TINTC=0, &END
&SECT1 STX=0.0, STY=0.0, STZ=0.0, SCALE=1.0, ALF=0.0, THETA=0.0, INMODE=4,
 TNODS=0, TNPS=0, TINTS=0, &END
  23.0435     0.0000     0.0000
  23.0435     1.7813     0.0007
  23.0435     3.5493     0.0083
  23.0435     4.3384     0.0714
  23.0435     4.4761     0.4540
  23.0435     4.4967     1.9224
  23.0435     4.4994     3.7037
  23.0435     4.4999     5.4850
  23.0435     4.5000     7.2664
  23.0435     4.5000     9.0477
  23.0435     4.4999    10.8290
  23.0435     4.4993    12.6104
  23.0435     4.4647    13.6074
  23.0435     3.4428    13.6337
  23.0435     1.7214    13.6342
  23.0435     0.0000    13.6343
&BPNODE TNODE=3, TNPC=0, TINTC=0, &END
&SECT1 STX=0.0, STY=0.0, STZ=0.0, SCALE=1.0, ALF=0.0, THETA=0.0, INMODE=4,
 TNODS=0, TNPS=0, TINTS=0, &END
  24.2060     0.0000     0.0000
  24.2060     1.8135     0.0008
  24.2060     3.6032     0.0090
  24.2060     4.3543     0.0795
  24.2060     4.4793     0.5138
  24.2060     4.4972     2.0834
  24.2060     4.4995     3.8970
  24.2060     4.5000     5.7105
  24.2060     4.5000     7.5240
  24.2060     4.5000     9.3376
  24.2060     4.5000    11.1511
  24.2060     4.5000    12.9647
  24.2060     4.2423    13.9775
  24.2060     2.8282    13.9775
  24.2060     1.4141    13.9775
  24.2060     0.0000    13.9775
&BPNODE TNODE=3, TNPC=0, TINTC=0, &END
&SECT1 STX=0.0, STY=0.0, STZ=0.0, SCALE=1.0, ALF=0.0, THETA=0.0, INMODE=4,
 TNODS=3, TNPS=0, TINTS=0, &END
  24.6500     0.0000     0.0000
  24.6500     1.8258     0.0008
  24.6500     3.6231     0.0094
  24.6500     4.3600     0.0829
  24.6500     4.4804     0.5384
  24.6500     4.4973     2.1449
  24.6500     4.4995     3.9708
  24.6500     4.5000     5.7966
  24.6500     4.5000     7.6225
  24.6500     4.5000     9.4483
  24.6500     4.5000    11.2742
  24.6500     4.5000    13.1000
  24.6500     4.2213    14.0848
  24.6500     2.8142    14.0848
  24.6500     1.4071    14.0848
  24.6500     0.0000    14.0848
&BPNODE TNODE=3, TNPC=0, TINTC=0, &END

&PATCH1 IREV=0, IDPAT=2, MAKE=0, KCOMP=1, KASS=1, IPATSYM=1, IPATCOP=0, &END
  ROOT LOWER STARBOARD
&SECT1 STX=0.0, STY=0.0, STZ=0.0, SCALE=1.0, ALF=0.0, THETA=0.0, INMODE=4,
 TNODS=0, TNPS=0, TINTS=0, &END
  24.6500     0.0000     0.0000
  24.6500     1.8258     0.0008
  24.6500     3.6231     0.0094
  24.6500     4.3600     0.0829
  24.6500     4.4804     0.5384
  24.6500     4.4973     2.1449
  24.6500     4.4995     3.9708
  24.6500     4.5000     5.7966
  24.6500     4.5000     7.6225
  24.6500     4.5000     9.4483
  24.6500     4.5000    11.2742
  24.6500     4.5000    13.1000
&BPNODE TNODE=3, TNPC=0, TINTC=0, &END
&SECT1 STX=0.0, STY=0.0, STZ=0.0, SCALE=1.0, ALF=0.0, THETA=0.0, INMODE=4,
 TNODS=0, TNPS=0, TINTS=0, &END
  24.8679     0.0000     0.0000
  24.8679     1.7867     0.0007
  24.8679     3.5584     0.0084
  24.8679     4.3412     0.0727
  24.8679     4.4766     0.4634
  24.8679     4.4968     1.9491
  24.8679     4.4994     3.7357
  24.8679     4.4999     5.5224
  24.8679     4.5000     7.3091
  24.8679     4.5000     9.0958
  24.8679     4.5000    10.8824
  24.8679     4.5000    12.6691
&BPNODE TNODE=3, TNPC=0, TINTC=0, &END
&SECT1 STX=0.0, STY=0.0, STZ=0.0, SCALE=1.0, ALF=0.0, THETA=0.0, INMODE=4,
 TNODS=0, TNPS=0, TINTS=0, &END
  25.5119     0.0000     0.0000
  25.5119     1.7519     0.0007
  25.5119     3.4973     0.0076
  25.5119     4.3223     0.0646
  25.5119     4.4728     0.4048
  25.5119     4.4962     1.7750
  25.5119     4.4992     3.5269
  25.5119     4.4999     5.2788
  25.5119     4.5000     7.0306
  25.5119     4.5000     8.7825
  25.5119     4.5000    10.5344
  25.5119     4.5000    12.2862
```

```
&BPNODE TNODE=3, TNPC=0, TINTC=0, &END
&SECT1 STX=0.0, STY=0.0, STZ=0.0, SCALE=1.0, ALF=0.0, THETA=0.0, INMODE=4,
 TNODS=0, TNPS=0, TINTS=0, &END
  26.5541    0.0000    0.0000
  26.5541    1.7230    0.0007
  26.5541    3.4441    0.0070
  26.5541    4.3050    0.0585
  26.5541    4.4691    0.3614
  26.5541    4.4956    1.6308
  26.5541    4.4991    3.3539
  26.5541    4.4999    5.0769
  26.5541    4.5000    6.7999
  26.5541    4.5000    8.5229
  26.5541    4.5000   10.2460
  26.5541    4.5000   11.9690
&BPNODE TNODE=3, TNPC=0, TINTC=0, &END
&SECT1 STX=0.0, STY=0.0, STZ=0.0, SCALE=1.0, ALF=0.0, THETA=0.0, INMODE=4,
 TNODS=0, TNPS=0, TINTS=0, &END
  27.9487    0.0000    0.0000
  27.9487    1.7011    0.0006
  27.9487    3.4020    0.0066
  27.9487    4.2909    0.0542
  27.9487    4.4660    0.3314
  27.9487    4.4951    1.5215
  27.9487    4.4990    3.2226
  27.9487    4.4998    4.9237
  27.9487    4.5000    6.6249
  27.9487    4.5000    8.3260
  27.9487    4.5000   10.0272
  27.9487    4.5000   11.7283
&BPNODE TNODE=3, TNPC=0, TINTC=0, &END
&SECT1 STX=0.0, STY=0.0, STZ=0.0, SCALE=1.0, ALF=0.0, THETA=0.0, INMODE=4,
 TNODS=0, TNPS=0, TINTS=0, &END
  29.6349    0.0000    0.0000
  29.6349    1.6863    0.0006
  29.6349    3.3725    0.0063
  29.6349    4.2808    0.0515
  29.6349    4.4638    0.3122
  29.6349    4.4947    1.4471
  29.6349    4.4989    3.1333
  29.6349    4.4998    4.8196
  29.6349    4.5000    6.5059
  29.6349    4.5000    8.1922
  29.6349    4.5000    9.8784
  29.6349    4.5000   11.5647
&BPNODE TNODE=3, TNPC=0, TINTC=0, &END
&SECT1 STX=0.0, STY=0.0, STZ=0.0, SCALE=1.0, ALF=0.0, THETA=0.0, INMODE=4,
 TNODS=0, TNPS=0, TINTS=0, &END
  31.5390    0.0000    0.0000
  31.5390    1.6769    0.0006
  31.5390    3.3538    0.0061
  31.5390    4.2741    0.0499
  31.5390    4.4623    0.3007
  31.5390    4.4944    1.4001
  31.5390    4.4989    3.0770
  31.5390    4.4998    4.7539
  31.5390    4.5000    6.4308
  31.5390    4.5000    8.1077
  31.5390    4.5000    9.7845
  31.5390    4.5000   11.4614
&BPNODE TNODE=3, TNPC=0, TINTC=0, &END
&SECT1 STX=0.0, STY=0.0, STZ=0.0, SCALE=1.0, ALF=0.0, THETA=0.0, INMODE=4,
 TNODS=0, TNPS=0, TINTS=0, &END
  33.5777    0.0000    0.0000
  33.5777    1.6712    0.0006
  33.5777    3.3424    0.0060
  33.5777    4.2700    0.0489
  33.5777    4.4613    0.2939
  33.5777    4.4943    1.3718
  33.5777    4.4988    3.0430
  33.5777    4.4998    4.7142
  33.5777    4.5000    6.3855
  33.5777    4.5000    8.0567
  33.5777    4.5000    9.7279
  33.5777    4.5000   11.3991
&BPNODE TNODE=3, TNPC=0, TINTC=0, &END
&SECT1 STX=0.0, STY=0.0, STZ=0.0, SCALE=1.0, ALF=0.0, THETA=0.0, INMODE=4,
 TNODS=0, TNPS=0, TINTS=0, &END
  35.6619    0.0000    0.0000
  35.6619    1.6694    0.0006
  35.6619    3.3388    0.0060
  35.6619    4.2687    0.0486
  35.6619    4.4610    0.2918
  35.6619    4.4942    1.3627
  35.6619    4.4988    3.0321
  35.6619    4.4998    4.7015
  35.6619    4.5000    6.3708
  35.6619    4.5000    8.0402
  35.6619    4.5000    9.7096
  35.6619    4.5000   11.3790
&BPNODE TNODE=3, TNPC=0, TINTC=0, &END
&SECT1 STX=0.0, STY=0.0, STZ=0.0, SCALE=1.0, ALF=0.0, THETA=0.0, INMODE=4,
 TNODS=0, TNPS=0, TINTS=0, &END
  37.7006    0.0000    0.0000
  37.7006    1.6701    0.0006
  37.7006    3.3402    0.0060
  37.7006    4.2692    0.0487
  37.7006    4.4611    0.2926
  37.7006    4.4942    1.3663
  37.7006    4.4988    3.0365
  37.7006    4.4998    4.7066
  37.7006    4.5000    6.3767
  37.7006    4.5000    8.0468
  37.7006    4.5000    9.7170
  37.7006    4.5000   11.3871
&BPNODE TNODE=3, TNPC=0, TINTC=0, &END
&SECT1 STX=0.0, STY=0.0, STZ=0.0, SCALE=1.0, ALF=0.0, THETA=0.0, INMODE=4,
 TNODS=0, TNPS=0, TINTS=0, &END
  39.6047    0.0000    0.0000
  39.6047    1.6716    0.0006
  39.6047    3.3432    0.0060
  39.6047    4.2703    0.0490
  39.6047    4.4614    0.2944
  39.6047    4.4943    1.3737
  39.6047    4.4988    3.0452
  39.6047    4.4998    4.7168
  39.6047    4.5000    6.3884
  39.6047    4.5000    8.0600
  39.6047    4.5000    9.7316
  39.6047    4.5000   11.4032
&BPNODE TNODE=3, TNPC=0, TINTC=0, &END
&SECT1 STX=0.0, STY=0.0, STZ=0.0, SCALE=1.0, ALF=0.0, THETA=0.0, INMODE=4,
 TNODS=0, TNPS=0, TINTS=0, &END
  41.2909    0.0000    0.0000
  41.2909    1.6739    0.0006
  41.2909    3.3479    0.0061
  41.2909    4.2720    0.0494
  41.2909    4.4618    0.2971
  41.2909    4.4943    1.3854
  41.2909    4.4988    3.0593
  41.2909    4.4998    4.7332
  41.2909    4.5000    6.4072
  41.2909    4.5000    8.0811
  41.2909    4.5000    9.7550
  41.2909    4.5000   11.4290
&BPNODE TNODE=3, TNPC=0, TINTC=0, &END
&SECT1 STX=0.0, STY=0.0, STZ=0.0, SCALE=1.0, ALF=0.0, THETA=0.0, INMODE=4,
 TNODS=0, TNPS=0, TINTS=0, &END
  42.6855    0.0000    0.0000
  42.6855    1.6764    0.0006
```

```
   42.6855    3.3529    0.0061
   42.6855    4.2738    0.0498
   42.6855    4.4622    0.3001
   42.6855    4.4944    1.3979
   42.6855    4.4989    3.0743
   42.6855    4.4998    4.7507
   42.6855    4.5000    6.4272
   42.6855    4.5000    8.1036
   42.6855    4.5000    9.7800
   42.6855    4.5000   11.4565
 &BPNODE TNODE=3, TNPC=0, TINTC=0, &END
 &SECT1 STX=0.0, STY=0.0, STZ=0.0, SCALE=1.0, ALF=0.0, THETA=0.0, INMODE=4,
  TNODS=0, TNPS=0, TINTS=0, &END
   43.7277    0.0000    0.0000
   43.7277    1.6766    0.0007
   43.7277    3.3528    0.0067
   43.7277    4.2374    0.0530
   43.7277    4.4194    0.3099
   43.7277    4.4514    1.4174
   43.7277    4.4558    3.0940
   43.7277    4.4568    4.7706
   43.7277    4.4570    6.4472
   43.7277    4.4570    8.1238
   43.7277    4.4570    9.8004
   43.7277    4.4570   11.4770
 &BPNODE TNODE=3, TNPC=0, TINTC=0, &END
 &SECT1 STX=0.0, STY=0.0, STZ=0.0, SCALE=1.0, ALF=0.0, THETA=0.0, INMODE=4,
  TNODS=0, TNPS=0, TINTS=0, &END
   44.3717    0.0000    0.0000
   44.3717    1.6650    0.0009
   44.3717    3.3021    0.0097
   44.3717    4.0431    0.0680
   44.3717    4.2033    0.3596
   44.3717    4.2341    1.5030
   44.3717    4.2388    3.1680
   44.3717    4.2398    4.8331
   44.3717    4.2400    6.4981
   44.3717    4.2400    8.1631
   44.3717    4.2400    9.8282
   44.3717    4.2400   11.4932
 &BPNODE TNODE=3, TNPC=0, TINTC=0, &END
 &SECT1 STX=0.0, STY=0.0, STZ=0.0, SCALE=1.0, ALF=0.0, THETA=0.0, INMODE=4,
  TNODS=3, TNPS=0, TINTS=0, &END
   44.5909    0.0000    0.0000
   44.5909    1.6672    0.0010
   44.5909    3.2859    0.0111
   44.5909    3.9797    0.0752
   44.5909    4.1306    0.3843
   44.5909    4.1604    1.5597
   44.5909    4.1650    3.2268
   44.5909    4.1660    4.8940
   44.5909    4.1662    6.5612
   44.5909    4.1662    8.2284
   44.5909    4.1662    9.8955
   44.5909    4.1662   11.5627
 &BPNODE TNODE=3, TNPC=0, TINTC=0, &END

 &PATCH1 IREV=0, IDPAT=2, MAKE=0, KCOMP=1, KASS=1, IPATSYM=1, IPATCOP=0, &END
   ROOT UPPER STARBOARD
 &SECT1 STX=0.0, STY=0.0, STZ=0.0, SCALE=1.0, ALF=0.0, THETA=0.0, INMODE=4,
  TNODS=0, TNPS=0, TINTS=0, &END
   24.6500    4.5000   13.1000
   24.6500    4.2213   14.0848
   24.6500    2.8142   14.0848
   24.6500    1.4071   14.0848
   24.6500    0.0000   14.0848
 &BPNODE TNODE=3, TNPC=0, TINTC=0, &END
 &SECT1 STX=0.0, STY=0.0, STZ=0.0, SCALE=1.0, ALF=0.0, THETA=0.0, INMODE=4,
  TNODS=0, TNPS=0, TINTS=0, &END
   24.8679    4.5000   13.5517
   24.8679    4.2213   14.1334
   24.8679    2.8142   14.1334
   24.8679    1.4071   14.1334
   24.8679    0.0000   14.1334
 &BPNODE TNODE=3, TNPC=0, TINTC=0, &END
 &SECT1 STX=0.0, STY=0.0, STZ=0.0, SCALE=1.0, ALF=0.0, THETA=0.0, INMODE=4,
  TNODS=0, TNPS=0, TINTS=0, &END
   25.5119    4.5000   13.9485
   25.5119    4.2213   14.2622
   25.5119    2.8142   14.2622
   25.5119    1.4071   14.2622
   25.5119    0.0000   14.2622
 &BPNODE TNODE=3, TNPC=0, TINTC=0, &END
 &SECT1 STX=0.0, STY=0.0, STZ=0.0, SCALE=1.0, ALF=0.0, THETA=0.0, INMODE=4,
  TNODS=0, TNPS=0, TINTS=0, &END
   26.5541    4.5000   14.2646
   26.5541    4.2213   14.4272
   26.5541    2.8142   14.4272
   26.5541    1.4071   14.4272
   26.5541    0.0000   14.4272
 &BPNODE TNODE=3, TNPC=0, TINTC=0, &END
 &SECT1 STX=0.0, STY=0.0, STZ=0.0, SCALE=1.0, ALF=0.0, THETA=0.0, INMODE=4,
  TNODS=0, TNPS=0, TINTS=0, &END
   27.9487    4.5000   14.4706
   27.9487    4.2213   14.5653
   27.9487    2.8142   14.5653
   27.9487    1.4071   14.5653
   27.9487    0.0000   14.5653
 &BPNODE TNODE=3, TNPC=0, TINTC=0, &END
 &SECT1 STX=0.0, STY=0.0, STZ=0.0, SCALE=1.0, ALF=0.0, THETA=0.0, INMODE=4,
  TNODS=0, TNPS=0, TINTS=0, &END
   29.6349    4.5000   14.5367
   29.6349    4.2213   14.5971
   29.6349    2.8142   14.5971
   29.6349    1.4071   14.5971
   29.6349    0.0000   14.5971
 &BPNODE TNODE=3, TNPC=0, TINTC=0, &END
 &SECT1 STX=0.0, STY=0.0, STZ=0.0, SCALE=1.0, ALF=0.0, THETA=0.0, INMODE=4,
  TNODS=0, TNPS=0, TINTS=0, &END
   31.5390    4.5000   14.4449
   31.5390    4.2213   14.5447
   31.5390    2.8142   14.5447
   31.5390    1.4071   14.5447
   31.5390    0.0000   14.5447
 &BPNODE TNODE=3, TNPC=0, TINTC=0, &END
 &SECT1 STX=0.0, STY=0.0, STZ=0.0, SCALE=1.0, ALF=0.0, THETA=0.0, INMODE=4,
  TNODS=0, TNPS=0, TINTS=0, &END
   33.5777    4.5000   14.2088
   33.5777    4.2213   14.3864
   33.5777    2.8142   14.3864
   33.5777    1.4071   14.3864
   33.5777    0.0000   14.3864
 &BPNODE TNODE=3, TNPC=0, TINTC=0, &END
 &SECT1 STX=0.0, STY=0.0, STZ=0.0, SCALE=1.0, ALF=0.0, THETA=0.0, INMODE=4,
  TNODS=0, TNPS=0, TINTS=0, &END
   35.6619    4.5000   13.8627
   35.6619    4.2213   14.0807
   35.6619    2.8142   14.0807
   35.6619    1.4071   14.0807
   35.6619    0.0000   14.0807
 &BPNODE TNODE=3, TNPC=0, TINTC=0, &END
 &SECT1 STX=0.0, STY=0.0, STZ=0.0, SCALE=1.0, ALF=0.0, THETA=0.0, INMODE=4,
  TNODS=0, TNPS=0, TINTS=0, &END
   37.7006    4.5000   13.4473
   37.7006    4.2213   13.6423
   37.7006    2.8142   13.6423
   37.7006    1.4071   13.6423
   37.7006    0.0000   13.6423
 &BPNODE TNODE=3, TNPC=0, TINTC=0, &END
 &SECT1 STX=0.0, STY=0.0, STZ=0.0, SCALE=1.0, ALF=0.0, THETA=0.0, INMODE=4,
```

```
TNODS=0, TNPS=0, TINTS=0, &END
 39.6047    4.5000   12.9980
 39.6047    4.2213   13.1398
 39.6047    2.8142   13.1398
 39.6047    1.4071   13.1398
 39.6047    0.0000   13.1398
&BPNODE TNODE=3, TNPC=0, TINTC=0, &END
&SECT1 STX=0.0, STY=0.0, STZ=0.0, SCALE=1.0, ALF=0.0, THETA=0.0, INMODE=4,
 TNODS=0, TNPS=0, TINTS=0, &END
 41.2909    4.5000   12.5573
 41.2909    4.2213   12.6458
 41.2909    2.8142   12.6458
 41.2909    1.4071   12.6458
 41.2909    0.0000   12.6458
&BPNODE TNODE=3, TNPC=0, TINTC=0, &END
&SECT1 STX=0.0, STY=0.0, STZ=0.0, SCALE=1.0, ALF=0.0, THETA=0.0, INMODE=4,
 TNODS=0, TNPS=0, TINTS=0, &END
 42.6855    4.5000   12.1606
 42.6855    4.2213   12.2144
 42.6855    2.8142   12.2144
 42.6855    1.4071   12.2144
 42.6855    0.0000   12.2144
&BPNODE TNODE=3, TNPC=0, TINTC=0, &END
&SECT1 STX=0.0, STY=0.0, STZ=0.0, SCALE=1.0, ALF=0.0, THETA=0.0, INMODE=4,
 TNODS=0, TNPS=0, TINTS=0, &END
 43.7277    4.4570   11.8400
 43.7277    4.1900   11.8826
 43.7277    2.8142   11.8826
 43.7277    1.4071   11.8826
 43.7277    0.0000   11.8826
&BPNODE TNODE=3, TNPC=0, TINTC=0, &END
&SECT1 STX=0.0, STY=0.0, STZ=0.0, SCALE=1.0, ALF=0.0, THETA=0.0, INMODE=4,
 TNODS=0, TNPS=0, TINTS=0, &END
 44.3717    4.2400   11.6336
 44.3717    3.9900   11.6743
 44.3717    2.8142   11.6743
 44.3717    1.4071   11.6743
 44.3717    0.0000   11.6743
&BPNODE TNODE=3, TNPC=0, TINTC=0, &END
&SECT1 STX=0.0, STY=0.0, STZ=0.0, SCALE=1.0, ALF=0.0, THETA=0.0, INMODE=4,
 TNODS=3, TNPS=0, TINTS=0, &END
 44.5909    4.1662   11.5627
 44.5909    3.9300   11.6030
 44.5909    2.8142   11.6030
 44.5909    1.4071    11.6030
 44.5909    0.0000   11.6030
&BPNODE TNODE=3, TNPC=0, TINTC=0, &END

&PATCH1 IREV=0, IDPAT=2, MAKE=0, KCOMP=1, KASS=1, IPATSYM=1, IPATCOP=0, &END
 ROOT TRANSITION AFT STARBOARD
&SECT1 STX=0.0, STY=0.0, STZ=0.0, SCALE=1.0, ALF=0.0, THETA=0.0, INMODE=4,
 TNODS=0, TNPS=0, TINTS=0, &END
 44.5909    0.0000    0.0000
 44.5909    1.6672    0.0010
 44.5909    3.2859    0.0111
 44.5909    3.9797    0.0752
 44.5909    4.1306    0.3843
 44.5909    4.1604    1.5597
 44.5909    4.1650    3.2268
 44.5909    4.1660    4.8940
 44.5909    4.1662    6.5612
 44.5909    4.1662    8.2284
 44.5909    4.1662    9.8955
 44.5909    4.1662   11.5627
 44.5909    3.9300   11.6030
 44.5909    2.8142   11.6030
 44.5909    1.4071    11.6030
 44.5909    0.0000   11.6030
&BPNODE TNODE=3, TNPC=0, TINTC=0, &END
&SECT1 STX=0.0, STY=0.0, STZ=0.0, SCALE=1.0, ALF=0.0, THETA=0.0, INMODE=4,
 TNODS=0, TNPS=0, TINTS=0, &END
 44.9164    0.0000    0.0000
 44.9164    1.6527    0.0012
 44.9164    3.2292    0.0128
 44.9164    3.8750    0.0819
 44.9164    4.0206    0.4023
 44.9164    4.0505    1.5694
 44.9164    4.0553    3.2220
 44.9164    4.0564    4.8747
 44.9164    4.0566    6.5274
 44.9164    4.0566    8.1800
 44.9164    4.0566    9.8327
 44.9164    4.0562   11.4773
 44.9164    3.8438   11.5962
 44.9164    2.8142   11.5962
 44.9164    1.4071   11.5962
 44.9164    0.0000   11.5962
&BPNODE TNODE=3, TNPC=0, TINTC=0, &END
&SECT1 STX=0.0, STY=0.0, STZ=0.0, SCALE=1.0, ALF=0.0, THETA=0.0, INMODE=4,
 TNODS=0, TNPS=0, TINTS=0, &END
 45.7687    0.0000    0.0000
 45.7687    1.6149    0.0016
 45.7687    3.0609    0.0178
 45.7687    3.6006    0.1009
 45.7687    3.7321    0.4387
 45.7687    3.7625    1.5799
 45.7687    3.7679    3.1948
 45.7687    3.7692    4.8097
 45.7687    3.7695    6.4245
 45.7687    3.7695    8.0394
 45.7687    3.7693    9.6543
 45.7687    3.7674   11.2536
 45.7687    3.5600   11.5767
 45.7687    2.8142   11.5857
 45.7687    1.4071   11.5860
 45.7687    0.0000   11.5861
&BPNODE TNODE=3, TNPC=0, TINTC=0, &END
&SECT1 STX=0.0, STY=0.0, STZ=0.0, SCALE=1.0, ALF=0.0, THETA=0.0, INMODE=4,
 TNODS=0, TNPS=0, TINTS=0, &END
 46.8222    0.0000    0.0000
 46.8222    1.5638    0.0025
 46.8222    2.8199    0.0253
 46.8222    3.2590    0.1249
 46.8222    3.3765    0.4866
 46.8222    3.4068    1.5991
 46.8222    3.4128    3.1628
 46.8222    3.4143    4.7266
 46.8222    3.4146    6.2903
 46.8222    3.4146    7.8541
 46.8222    3.4142    9.4178
 46.8222    3.4111   10.9772
 46.8222    3.3229   11.5231
 46.8222    2.8650   11.5700
 46.8222    1.4071   11.5733
 46.8222    0.0000   11.5735
&BPNODE TNODE=3, TNPC=0, TINTC=0, &END
&SECT1 STX=0.0, STY=0.0, STZ=0.0, SCALE=1.0, ALF=0.0, THETA=0.0, INMODE=4,
 TNODS=0, TNPS=0, TINTS=0, &END
 47.6745    0.0000    0.0000
 47.6745    1.5223    0.0036
 47.6745    2.6098    0.0323
 47.6745    2.9827    0.1456
 47.6745    3.0895    0.5253
 47.6745    3.1192    1.6204
 47.6745    3.1255    3.1427
 47.6745    3.1271    4.6650
 47.6745    3.1275    6.1873
 47.6745    3.1275    7.7096
 47.6745    3.1269    9.2319
 47.6745    3.1232   10.7536
```

```
   47.6745     3.0838    11.4579
   47.6745     2.7717    11.5525
   47.6745     1.4071    11.5627
   47.6745     0.0000    11.5634
 &BPNODE TNODE=3, TNPC=0, TINTC=0, &END
 &SECT1 STX=0.0, STY=0.0, STZ=0.0, SCALE=1.0, ALF=0.0, THETA=0.0, INMODE=4,
  TNODS=3, TNPS=0, TINTS=0, &END
   48.0000     0.0000     0.0000
   48.0000     1.5058     0.0041
   48.0000     2.5263     0.0352
   48.0000     2.8769     0.1533
   48.0000     2.9802     0.5421
   48.0000     3.0094     1.6335
   48.0000     3.0158     3.1393
   48.0000     3.0175     4.6450
   48.0000     3.0179     6.1508
   48.0000     3.0178     7.6566
   48.0000     3.0172     9.1624
   48.0000     3.0134    10.6681
   48.0000     2.9761    11.4292
   48.0000     2.7054    11.5444
   48.0000     1.4071    11.5586
   48.0000     0.0000    11.5595
 &BPNODE TNODE=3, TNPC=0, TINTC=0, &END

 &PATCH1 IREV=0, IDPAT=2, MAKE=0, KCOMP=1, KASS=1, IPATSYM=1, IPATCOP=0,
&END
   FUSELAGE_AFT
 &SECT1 STX=0.0, STY=0.0, STZ=0.0, SCALE=1.0, ALF=0.0, THETA=0.0, INMODE=4,
  TNODS=0, TNPS=0, TINTS=0, &END
   48.0000     0.0000     0.0000
   48.0000     1.5058     0.0041
   48.0000     2.5263     0.0352
   48.0000     2.8769     0.1533
   48.0000     2.9802     0.5421
   48.0000     3.0094     1.6335
   48.0000     3.0158     3.1393
   48.0000     3.0175     4.6450
   48.0000     3.0179     6.1508
   48.0000     3.0178     7.6566
   48.0000     3.0172     9.1624
   48.0000     3.0134    10.6681
   48.0000     2.9761    11.4292
   48.0000     2.7054    11.5444
   48.0000     1.5058    11.5586
   48.0000     0.0000    11.5595
 &BPNODE TNODE=3, TNPC=0, TINTC=0, &END
 &SECT1 STX=0.0, STY=0.0, STZ=0.0, SCALE=1.0, ALF=0.0, THETA=0.0, INMODE=4,
  TNODS=0, TNPS=0, TINTS=0, &END
   48.2093     0.0000     0.0000
   48.2093     1.5001     0.0045
   48.2093     2.4757     0.0375
   48.2093     2.8105     0.1604
   48.2093     2.9106     0.5614
   48.2093     2.9390     1.6667
   48.2093     2.9453     3.1668
   48.2093     2.9469     4.6669
   48.2093     2.9474     6.1670
   48.2093     2.9473     7.6670
   48.2093     2.9466     9.1671
   48.2093     2.9424    10.6669
   48.2093     2.9044    11.4175
   48.2093     2.6462    11.5397
   48.2093     1.4996    11.5559
   48.2093     0.0000    11.5570
 &BPNODE TNODE=3, TNPC=0, TINTC=0, &END
 &SECT1 STX=0.0, STY=0.0, STZ=0.0, SCALE=1.0, ALF=0.0, THETA=0.0, INMODE=4,
  TNODS=0, TNPS=0, TINTS=0, &END
   48.8055     0.0000     0.0000
   48.8055     1.4733     0.0060
   48.8055     2.3269     0.0446
   48.8055     2.6221     0.1829
   48.8055     2.7120     0.6123
   48.8055     2.7385     1.7484
   48.8055     2.7445     3.2309
   48.8055     2.7462     4.7134
   48.8055     2.7466     6.1959
   48.8055     2.7465     7.6784
   48.8055     2.7456     9.1609
   48.8055     2.7404    10.6408
   48.8055     2.7016    11.3810
   48.8055     2.4736    11.5252
   48.8055     1.4808    11.5480
   48.8055     0.0000    11.5499
 &BPNODE TNODE=3, TNPC=0, TINTC=0, &END
 &SECT1 STX=0.0, STY=0.0, STZ=0.0, SCALE=1.0, ALF=0.0, THETA=0.0, INMODE=4,
  TNODS=0, TNPS=0, TINTS=0, &END
   49.6976     0.0000     0.0000
   49.6976     1.3923     0.0085
   49.6976     2.0943     0.0564
   49.6976     2.3385     0.2185
   49.6976     2.4154     0.6980
   49.6976     2.4387     1.8818
   49.6976     2.4441     3.3356
   49.6976     2.4457     4.7894
   49.6976     2.4461     6.2432
   49.6976     2.4459     7.6970
   49.6976     2.4448     9.1508
   49.6976     2.4382    10.5961
   49.6976     2.3990    11.3282
   49.6976     2.2089    11.5012
   49.6976     1.4448    11.5354
   49.6976     0.0000    11.5393
 &BPNODE TNODE=3, TNPC=0, TINTC=0, &END
 &SECT1 STX=0.0, STY=0.0, STZ=0.0, SCALE=1.0, ALF=0.0, THETA=0.0, INMODE=4,
  TNODS=0, TNPS=0, TINTS=0, &END
   50.7500     0.0000     0.0000
   50.7500     1.2503     0.0119
   50.7500     1.8087     0.0723
   50.7500     2.0016     0.2624
   50.7500     2.0654     0.8001
   50.7500     2.0851     2.0280
   50.7500     2.0898     3.4449
   50.7500     2.0912     4.8618
   50.7500     2.0916     6.2787
   50.7500     2.0914     7.6956
   50.7500     2.0900     9.1125
   50.7500     2.0826    10.5181
   50.7500     2.0449    11.2629
   50.7500     1.8881    11.4705
   50.7500     1.3215    11.5194
   50.7500     0.0000    11.5268
 &BPNODE TNODE=3, TNPC=0, TINTC=0, &END
 &SECT1 STX=0.0, STY=0.0, STZ=0.0, SCALE=1.0, ALF=0.0, THETA=0.0, INMODE=4,
  TNODS=0, TNPS=0, TINTS=0, &END
   51.8024     0.0000     0.0000
   51.8024     1.0710     0.0155
   51.8024     1.5126     0.0897
   51.8024     1.6649     0.3144
   51.8024     1.7158     0.9210
   51.8024     1.7316     2.1843
   51.8024     1.7355     3.5578
   51.8024     1.7368     4.9313
   51.8024     1.7371     6.3049
   51.8024     1.7369     7.6784
   51.8024     1.7353     9.0519
   51.8024     1.7278    10.4187
   51.8024     1.6936    11.1932
   51.8024     1.5648    11.4376
   51.8024     1.1343    11.5024
```

```
 51.8024    0.0000   11.5143
&BPNODE TNODE=3, TNPC=0, TINTC=0, &END
&SECT1 STX=0.0, STY=0.0, STZ=0.0, SCALE=1.0, ALF=0.0, THETA=0.0, INMODE=4,
 TNODS=0, TNPS=0, TINTS=0, &END
  52.6945    0.0000    0.0000
  52.6945    0.8991    0.0186
  52.6945    1.2562    0.1053
  52.6945    1.3782    0.3607
  52.6945    1.4194    1.0318
  52.6945    1.4320    2.3099
  52.6945    1.4352    3.6427
  52.6945    1.4363    4.9756
  52.6945    1.4366    6.3084
  52.6945    1.4363    7.6413
  52.6945    1.4348    8.9741
  52.6945    1.4280   10.3058
  52.6945    1.3981   11.1267
  52.6945    1.2909   11.4083
  52.6945    0.9497   11.4877
  52.6945    0.0000   11.5036
&BPNODE TNODE=3, TNPC=0, TINTC=0, &END
&SECT1 STX=0.0, STY=0.0, STZ=0.0, SCALE=1.0, ALF=0.0, THETA=0.0, INMODE=4,
 TNODS=0, TNPS=0, TINTS=0, &END
  53.2907    0.0000    0.0142
  53.2907    0.7868    0.0350
  53.2907    1.0933    0.1303
  53.2907    1.1979    0.4106
  53.2907    1.2330    1.1338
  53.2907    1.2435    2.4132
  53.2907    1.2463    3.7174
  53.2907    1.2472    5.0216
  53.2907    1.2475    6.3259
  53.2907    1.2472    7.6301
  53.2907    1.2458    8.9343
  53.2907    1.2394   10.2385
  53.2907    1.2120   11.0812
  53.2907    1.1171   11.3809
  53.2907    0.8219   11.4693
  53.2907    0.0000   11.4876
&BPNODE TNODE=3, TNPC=0, TINTC=0, &END
&SECT1 STX=0.0, STY=0.0, STZ=0.0, SCALE=1.0, ALF=0.0, THETA=0.0, INMODE=4,
 TNODS=3, TNPS=0, TINTS=0, &END
  53.5000    0.0000    5.7500
  53.5000    0.0000    5.7539
  53.5000    0.0000    5.7578
  53.5000    0.0000    5.7852
  53.5000    0.0000    5.8447
  53.5000    0.0000    5.9043
  53.5000    0.0000    5.9639
  53.5000    0.0000    6.0234
  53.5000    0.0000    6.0830
  53.5000    0.0000    6.1426
  53.5000    0.0000    6.2021
  53.5000    0.0000    6.2617
  53.5000    0.0000    6.3213
  53.5000    0.0000    6.3809
  53.5000    0.0000    6.4404
  53.5000    0.0000    6.5000
&BPNODE TNODE=3, TNPC=0, TINTC=0, &END

&PATCH1 IREV=0, IDPAT=1, MAKE=0, KCOMP=1, KASS=1, IPATSYM=1, IPATCOP=0, &END
 INBOARD WING - 10X15
&SECT1 STX=0.0, STY=0.0, STZ=0.0, SCALE=1.0, ALF=0.0, THETA=0.0, INMODE=4,
 TNODS=0, TNPS=0, TINTS=0, &END
  44.5909    4.1662   11.5627
  44.3717    4.2400   11.4932
  43.7277    4.4570   11.4770
  42.6855    4.5000   11.4565
  41.2909    4.5000   11.4290
  39.6047    4.5000   11.4032
  37.7006    4.5000   11.3871
  35.6619    4.5000   11.3790
  33.5777    4.5000   11.3991
  31.5390    4.5000   11.4614
  29.6349    4.5000   11.5647
  27.9487    4.5000   11.7283
  26.5541    4.5000   11.9690
  25.5119    4.5000   12.2862
  24.8679    4.5000   12.6691
  24.6500    4.5000   13.1000
&BPNODE TNODE=1, TNPC=0, TINTC=0, &END
  24.8679    4.5000   13.5517
  25.5119    4.5000   13.9485
  26.5541    4.5000   14.2646
  27.9487    4.5000   14.4706
  29.6349    4.5000   14.5367
  31.5390    4.5000   14.4449
  33.5777    4.5000   14.2088
  35.6619    4.5000   13.8627
  37.7006    4.5000   13.4473
  39.6047    4.5000   12.9980
  41.2909    4.5000   12.5573
  42.6855    4.5000   12.1606
  43.7277    4.4570   11.8400
  44.3717    4.2400   11.6336
  44.5909    4.1662   11.5627
&BPNODE TNODE=3, TNPC=0, TINTC=0, &END
&SECT1 STX=0.0, STY=0.0, STZ=0.0, SCALE=1.0, ALF=0.0, THETA=0.0, INMODE=4,
 TNODS=0, TNPS=0, TINTS=0, &END
  44.5896    5.1607   11.5308
  44.3717    5.1607   11.4914
  43.7277    5.1607   11.4763
  42.6855    5.1607   11.4563
  41.2909    5.1607   11.4289
  39.6047    5.1607   11.4032
  37.7006    5.1607   11.3871
  35.6619    5.1607   11.3790
  33.5777    5.1607   11.3991
  31.5390    5.1607   11.4614
  29.6349    5.1607   11.5647
  27.9487    5.1607   11.7283
  26.5541    5.1607   11.9690
  25.5119    5.1607   12.2862
  24.8679    5.1607   12.6691
  24.6500    5.1607   13.1000
&BPNODE TNODE=1, TNPC=0, TINTC=0, &END
  24.8679    5.1607   13.5517
  25.5119    5.1607   13.9485
  26.5541    5.1607   14.2646
  27.9487    5.1607   14.4706
  29.6349    5.1607   14.5367
  31.5390    5.1607   14.4449
  33.5777    5.1607   14.2088
  35.6619    5.1607   13.8627
  37.7006    5.1607   13.4473
  39.6047    5.1607   12.9980
  41.2909    5.1607   12.5573
  42.6855    5.1607   12.1607
  43.7277    5.1607   11.8407
  44.3717    5.1607   11.6352
  44.5896    5.1607   11.5308
&BPNODE TNODE=3, TNPC=0, TINTC=0, &END
&SECT1 STX=0.0, STY=0.0, STZ=0.0, SCALE=1.0, ALF=0.0, THETA=0.0, INMODE=4,
 TNODS=0, TNPS=0, TINTS=0, &END
  44.5896    7.0783   11.5308
  44.3717    7.0783   11.4914
  43.7277    7.0783   11.4763
  42.6855    7.0783   11.4563
  41.2909    7.0783   11.4289
  39.6047    7.0783   11.4032
```

```
   37.7006    7.0783    11.3871
   35.6619    7.0783    11.3790
   33.5777    7.0783    11.3991
   31.5390    7.0783    11.4614
   29.6349    7.0783    11.5647
   27.9487    7.0783    11.7283
   26.5541    7.0783    11.9690
   25.5119    7.0783    12.2862
   24.8679    7.0783    12.6691
   24.6500    7.0783    13.1000
&BPNODE TNODE=1, TNPC=0, TINTC=0, &END
   24.8679    7.0783    13.5517
   25.5119    7.0783    13.9485
   26.5541    7.0783    14.2646
   27.9487    7.0783    14.4706
   29.6349    7.0783    14.5367
   31.5390    7.0783    14.4449
   33.5777    7.0783    14.2088
   35.6619    7.0783    13.8627
   37.7006    7.0783    13.4473
   39.6047    7.0783    12.9980
   41.2909    7.0783    12.5573
   42.6855    7.0783    12.1607
   43.7277    7.0783    11.8407
   44.3717    7.0783    11.6352
   44.5896    7.0783    11.5308
&BPNODE TNODE=3, TNPC=0, TINTC=0, &END
&SECT1 STX=0.0, STY=0.0, STZ=0.0, SCALE=1.0, ALF=0.0, THETA=0.0, INMODE=4,
 TNODS=0, TNPS=0, TINTS=0, &END
   44.5896   10.0649    11.5308
   44.3717   10.0649    11.4914
   43.7277   10.0649    11.4763
   42.6855   10.0649    11.4563
   41.2909   10.0649    11.4289
   39.6047   10.0649    11.4032
   37.7006   10.0649    11.3871
   35.6619   10.0649    11.3790
   33.5777   10.0649    11.3991
   31.5390   10.0649    11.4614
   29.6349   10.0649    11.5647
   27.9487   10.0649    11.7283
   26.5541   10.0649    11.9690
   25.5119   10.0649    12.2862
   24.8679   10.0649    12.6691
   24.6500   10.0649    13.1000
&BPNODE TNODE=1, TNPC=0, TINTC=0, &END
   24.8679   10.0649    13.5517
   25.5119   10.0649    13.9485
   26.5541   10.0649    14.2646
   27.9487   10.0649    14.4706
   29.6349   10.0649    14.5367
   31.5390   10.0649    14.4449
   33.5777   10.0649    14.2088
   35.6619   10.0649    13.8627
   37.7006   10.0649    13.4473
   39.6047   10.0649    12.9980
   41.2909   10.0649    12.5573
   42.6855   10.0649    12.1607
   43.7277   10.0649    11.8407
   44.3717   10.0649    11.6352
   44.5896   10.0649    11.5308
&BPNODE TNODE=3, TNPC=0, TINTC=0, &END
&SECT1 STX=0.0, STY=0.0, STZ=0.0, SCALE=1.0, ALF=0.0, THETA=0.0, INMODE=4,
 TNODS=0, TNPS=0, TINTS=0, &END
   44.5896   13.8283    11.5308
   44.3717   13.8283    11.4914
   43.7277   13.8283    11.4763
   42.6855   13.8283    11.4563
   41.2909   13.8283    11.4289
   39.6047   13.8283    11.4032
```

```
   37.7006   13.8283    11.3871
   35.6619   13.8283    11.3790
   33.5777   13.8283    11.3991
   31.5390   13.8283    11.4614
   29.6349   13.8283    11.5647
   27.9487   13.8283    11.7283
   26.5541   13.8283    11.9690
   25.5119   13.8283    12.2862
   24.8679   13.8283    12.6691
   24.6500   13.8283    13.1000
&BPNODE TNODE=1, TNPC=0, TINTC=0, &END
   24.8679   13.8283    13.5517
   25.5119   13.8283    13.9485
   26.5541   13.8283    14.2646
   27.9487   13.8283    14.4706
   29.6349   13.8283    14.5367
   31.5390   13.8283    14.4449
   33.5777   13.8283    14.2088
   35.6619   13.8283    13.8627
   37.7006   13.8283    13.4473
   39.6047   13.8283    12.9980
   41.2909   13.8283    12.5573
   42.6855   13.8283    12.1607
   43.7277   13.8283    11.8407
   44.3717   13.8283    11.6352
   44.5896   13.8283    11.5308
&BPNODE TNODE=3, TNPC=0, TINTC=0, &END
&SECT1 STX=0.0, STY=0.0, STZ=0.0, SCALE=1.0, ALF=0.0, THETA=0.0, INMODE=4,
 TNODS=0, TNPS=0, TINTS=0, &END
   44.5896   18.0000    11.5308
   44.3717   18.0000    11.4914
   43.7277   18.0000    11.4763
   42.6855   18.0000    11.4563
   41.2909   18.0000    11.4289
   39.6047   18.0000    11.4032
   37.7006   18.0000    11.3871
   35.6619   18.0000    11.3790
   33.5777   18.0000    11.3991
   31.5390   18.0000    11.4614
   29.6349   18.0000    11.5647
   27.9487   18.0000    11.7283
   26.5541   18.0000    11.9690
   25.5119   18.0000    12.2862
   24.8679   18.0000    12.6691
   24.6500   18.0000    13.1000
&BPNODE TNODE=1, TNPC=0, TINTC=0, &END
   24.8679   18.0000    13.5517
   25.5119   18.0000    13.9485
   26.5541   18.0000    14.2646
   27.9487   18.0000    14.4706
   29.6349   18.0000    14.5367
   31.5390   18.0000    14.4449
   33.5777   18.0000    14.2088
   35.6619   18.0000    13.8627
   37.7006   18.0000    13.4473
   39.6047   18.0000    12.9980
   41.2909   18.0000    12.5573
   42.6855   18.0000    12.1607
   43.7277   18.0000    11.8407
   44.3717   18.0000    11.6352
   44.5896   18.0000    11.5308
&BPNODE TNODE=3, TNPC=0, TINTC=0, &END
&SECT1 STX=0.0, STY=0.0, STZ=0.0, SCALE=1.0, ALF=0.0, THETA=0.0, INMODE=4,
 TNODS=0, TNPS=0, TINTS=0, &END
   44.5896   22.1717    11.5308
   44.3717   22.1717    11.4914
   43.7277   22.1717    11.4763
   42.6855   22.1717    11.4563
   41.2909   22.1717    11.4289
   39.6047   22.1717    11.4032
```

```
 37.7006   22.1717   11.3871
 35.6619   22.1717   11.3790
 33.5777   22.1717   11.3991
 31.5390   22.1717   11.4614
 29.6349   22.1717   11.5647
 27.9487   22.1717   11.7283
 26.5541   22.1717   11.9690
 25.5119   22.1717   12.2862
 24.8679   22.1717   12.6691
 24.6500   22.1717   13.1000
&BPNODE TNODE=1, TNPC=0, TINTC=0, &END
 24.8679   22.1717   13.5517
 25.5119   22.1717   13.9485
 26.5541   22.1717   14.2646
 27.9487   22.1717   14.4706
 29.6349   22.1717   14.5367
 31.5390   22.1717   14.4449
 33.5777   22.1717   14.2088
 35.6619   22.1717   13.8627
 37.7006   22.1717   13.4473
 39.6047   22.1717   12.9980
 41.2909   22.1717   12.5573
 42.6855   22.1717   12.1607
 43.7277   22.1717   11.8407
 44.3717   22.1717   11.6352
 44.5896   22.1717   11.5308
&BPNODE TNODE=3, TNPC=0, TINTC=0, &END
&SECT1 STX=0.0, STY=0.0, STZ=0.0, SCALE=1.0, ALF=0.0, THETA=0.0, INMODE=4,
 TNODS=0, TNPS=0, TINTS=0, &END
 44.5896   25.9351   11.5308
 44.3717   25.9351   11.4914
 43.7277   25.9351   11.4763
 42.6855   25.9351   11.4563
 41.2909   25.9351   11.4289
 39.6047   25.9351   11.4032
 37.7006   25.9351   11.3871
 35.6619   25.9351   11.3790
 33.5777   25.9351   11.3991
 31.5390   25.9351   11.4614
 29.6349   25.9351   11.5647
 27.9487   25.9351   11.7283
 26.5541   25.9351   11.9690
 25.5119   25.9351   12.2862
 24.8679   25.9351   12.6691
 24.6500   25.9351   13.1000
&BPNODE TNODE=1, TNPC=0, TINTC=0, &END
 24.8679   25.9351   13.5517
 25.5119   25.9351   13.9485
 26.5541   25.9351   14.2646
 27.9487   25.9351   14.4706
 29.6349   25.9351   14.5367
 31.5390   25.9351   14.4449
 33.5777   25.9351   14.2088
 35.6619   25.9351   13.8627
 37.7006   25.9351   13.4473
 39.6047   25.9351   12.9980
 41.2909   25.9351   12.5573
 42.6855   25.9351   12.1607
 43.7277   25.9351   11.8407
 44.3717   25.9351   11.6352
 44.5896   25.9351   11.5308
&BPNODE TNODE=3, TNPC=0, TINTC=0, &END
&SECT1 STX=0.0, STY=0.0, STZ=0.0, SCALE=1.0, ALF=0.0, THETA=0.0, INMODE=4,
 TNODS=0, TNPS=0, TINTS=0, &END
 44.5896   28.9217   11.5308
 44.3717   28.9217   11.4914
 43.7277   28.9217   11.4763
 42.6855   28.9217   11.4563
 41.2909   28.9217   11.4289
 39.6047   28.9217   11.4032
```

```
 37.7006   28.9217   11.3871
 35.6619   28.9217   11.3790
 33.5777   28.9217   11.3991
 31.5390   28.9217   11.4614
 29.6349   28.9217   11.5647
 27.9487   28.9217   11.7283
 26.5541   28.9217   11.9690
 25.5119   28.9217   12.2862
 24.8679   28.9217   12.6691
 24.6500   28.9217   13.1000
&BPNODE TNODE=1, TNPC=0, TINTC=0, &END
 24.8679   28.9217   13.5517
 25.5119   28.9217   13.9485
 26.5541   28.9217   14.2646
 27.9487   28.9217   14.4706
 29.6349   28.9217   14.5367
 31.5390   28.9217   14.4449
 33.5777   28.9217   14.2088
 35.6619   28.9217   13.8627
 37.7006   28.9217   13.4473
 39.6047   28.9217   12.9980
 41.2909   28.9217   12.5573
 42.6855   28.9217   12.1607
 43.7277   28.9217   11.8407
 44.3717   28.9217   11.6352
 44.5896   28.9217   11.5308
&BPNODE TNODE=3, TNPC=0, TINTC=0, &END
&SECT1 STX=0.0, STY=0.0, STZ=0.0, SCALE=1.0, ALF=0.0, THETA=0.0, INMODE=4,
 TNODS=0, TNPS=0, TINTS=0, &END
 44.5896   30.8393   11.5308
 44.3717   30.8393   11.4914
 43.7277   30.8393   11.4763
 42.6855   30.8393   11.4563
 41.2909   30.8393   11.4289
 39.6047   30.8393   11.4032
 37.7006   30.8393   11.3871
 35.6619   30.8393   11.3790
 33.5777   30.8393   11.3991
 31.5390   30.8393   11.4614
 29.6349   30.8393   11.5647
 27.9487   30.8393   11.7283
 26.5541   30.8393   11.9690
 25.5119   30.8393   12.2862
 24.8679   30.8393   12.6691
 24.6500   30.8393   13.1000
&BPNODE TNODE=1, TNPC=0, TINTC=0, &END
 24.8679   30.8393   13.5517
 25.5119   30.8393   13.9485
 26.5541   30.8393   14.2646
 27.9487   30.8393   14.4706
 29.6349   30.8393   14.5367
 31.5390   30.8393   14.4449
 33.5777   30.8393   14.2088
 35.6619   30.8393   13.8627
 37.7006   30.8393   13.4473
 39.6047   30.8393   12.9980
 41.2909   30.8393   12.5573
 42.6855   30.8393   12.1607
 43.7277   30.8393   11.8407
 44.3717   30.8393   11.6352
 44.5896   30.8393   11.5308
&BPNODE TNODE=3, TNPC=0, TINTC=0, &END
&SECT1 STX=0.0, STY=0.0, STZ=0.0, SCALE=1.0, ALF=0.0, THETA=0.0, INMODE=4,
 TNODS=3, TNPS=0, TINTS=0, &END
 44.5896   31.5000   11.5308
 44.3717   31.5000   11.4914
 43.7277   31.5000   11.4763
 42.6855   31.5000   11.4563
 41.2909   31.5000   11.4289
 39.6047   31.5000   11.4032
```

```
  37.7006    31.5000    11.3871
  35.6619    31.5000    11.3790
  33.5777    31.5000    11.3991
  31.5390    31.5000    11.4614
  29.6349    31.5000    11.5647
  27.9487    31.5000    11.7283
  26.5541    31.5000    11.9690
  25.5119    31.5000    12.2862
  24.8679    31.5000    12.6691
  24.6500    31.5000    13.1000
&BPNODE TNODE=1, TNPC=0, TINTC=0, &END
  24.8679    31.5000    13.5517
  25.5119    31.5000    13.9485
  26.5541    31.5000    14.2646
  27.9487    31.5000    14.4706
  29.6349    31.5000    14.5367
  31.5390    31.5000    14.4449
  33.5777    31.5000    14.2088
  35.6619    31.5000    13.8627
  37.7006    31.5000    13.4473
  39.6047    31.5000    12.9980
  41.2909    31.5000    12.5573
  42.6855    31.5000    12.1607
  43.7277    31.5000    11.8407
  44.3717    31.5000    11.6352
  44.5896    31.5000    11.5308
&BPNODE TNODE=3, TNPC=0, TINTC=0, &END

&PATCH1 IREV=0, IDPAT=1, MAKE=0, KCOMP=1, KASS=1, IPATSYM=0, IPATCOP=0, &END
  RT AIL- NO DEFLECTION (10X15)
&SECT1 STX=0.0, STY=0.0, STZ=0.0, SCALE=1.0, ALF=0.0, THETA=0.0, INMODE=4,
 TNODS=0, TNPS=0, TINTS=0, &END
  44.5896    31.5000    11.5308
  44.3717    31.5000    11.4932
  43.7277    31.5000    11.4770
  42.6855    31.5000    11.4565
  41.2909    31.5000    11.4290
  39.6047    31.5000    11.4032
  37.7006    31.5000    11.3871
  35.6619    31.5000    11.3790
  33.5777    31.5000    11.3991
  31.5390    31.5000    11.4614
  29.6349    31.5000    11.5647
  27.9487    31.5000    11.7283
  26.5541    31.5000    11.9690
  25.5119    31.5000    12.2862
  24.8679    31.5000    12.6691
  24.6500    31.5000    13.1000
&BPNODE TNODE=1, TNPC=0, TINTC=0, &END
  24.8679    31.5000    13.5517
  25.5119    31.5000    13.9485
  26.5541    31.5000    14.2646
  27.9487    31.5000    14.4706
  29.6349    31.5000    14.5367
  31.5390    31.5000    14.4449
  33.5777    31.5000    14.2088
  35.6619    31.5000    13.8627
  37.7006    31.5000    13.4473
  39.6047    31.5000    12.9980
  41.2909    31.5000    12.5573
  42.6855    31.5000    12.1606
  43.7277    31.5000    11.8400
  44.3717    31.5000    11.6336
  44.5896    31.5000    11.5308
&BPNODE TNODE=3, TNPC=0, TINTC=0, &END
&SECT1 STX=0.0, STY=0.0, STZ=0.0, SCALE=1.0, ALF=0.0, THETA=0.0, INMODE=4,
 TNODS=0, TNPS=0, TINTS=0, &END
  44.5896    32.0261    11.5308
  44.4315    32.0261    11.4948
  43.7855    32.0261    11.4783
  42.7402    32.0261    11.4575
  41.1500    32.0261    11.4266
  39.6500    32.0261    11.4037
  37.7402    32.0261    11.3873
  35.6953    32.0261    11.3790
  33.6047    32.0261    11.3986
  31.5598    32.0261    11.4606
  29.6500    32.0261    11.5637
  27.9587    32.0261    11.7270
  26.5598    32.0261    11.9677
  25.5145    32.0261    12.2851
  24.8685    32.0261    12.6685
  24.6500    32.0261    13.1000
&BPNODE TNODE=1, TNPC=0, TINTC=0, &END
  24.8685    32.0261    13.5524
  25.5145    32.0261    13.9496
  26.5598    32.0261    14.2658
  27.9587    32.0261    14.4714
  29.6500    32.0261    14.5366
  31.5598    32.0261    14.4431
  33.6047    32.0261    14.2049
  35.6953    32.0261    13.8565
  37.7402    32.0261    13.4385
  39.6500    32.0261    12.9867
  41.3413    32.0261    12.5435
  42.7402    32.0261    12.1443
  43.7855    32.0261    11.8217
  44.4315    32.0261    11.6143
  44.5896    32.0261    11.5308
&BPNODE TNODE=3, TNPC=0, TINTC=0, &END
&SECT1 STX=0.0, STY=0.0, STZ=0.0, SCALE=1.0, ALF=0.0, THETA=0.0, INMODE=4,
 TNODS=0, TNPS=0, TINTS=0, &END
  44.5896    33.5531    11.5308
  44.4315    33.5531    11.4948
  43.7855    33.5531    11.4783
  42.7402    33.5531    11.4575
  41.1500    33.5531    11.4266
  39.6500    33.5531    11.4037
  37.7402    33.5531    11.3873
  35.6953    33.5531    11.3790
  33.6047    33.5531    11.3986
  31.5598    33.5531    11.4606
  29.6500    33.5531    11.5637
  27.9587    33.5531    11.7270
  26.5598    33.5531    11.9677
  25.5145    33.5531    12.2851
  24.8685    33.5531    12.6685
  24.6500    33.5531    13.1000
&BPNODE TNODE=1, TNPC=0, TINTC=0, &END
  24.8685    33.5531    13.5524
  25.5145    33.5531    13.9496
  26.5598    33.5531    14.2658
  27.9587    33.5531    14.4714
  29.6500    33.5531    14.5366
  31.5598    33.5531    14.4431
  33.6047    33.5531    14.2049
  35.6953    33.5531    13.8565
  37.7402    33.5531    13.4385
  39.6500    33.5531    12.9867
  41.3413    33.5531    12.5435
  42.7402    33.5531    12.1443
  43.7855    33.5531    11.8217
  44.4315    33.5531    11.6143
  44.5896    33.5531    11.5308
&BPNODE TNODE=3, TNPC=0, TINTC=0, &END
&SECT1 STX=0.0, STY=0.0, STZ=0.0, SCALE=1.0, ALF=0.0, THETA=0.0, INMODE=4,
 TNODS=0, TNPS=0, TINTS=0, &END
  44.5896    35.9313    11.5308
  44.4315    35.9313    11.4948
  43.7855    35.9313    11.4783
```

```
 42.7402   35.9313   11.4575
 41.1500   35.9313   11.4266
 39.6500   35.9313   11.4037
 37.7402   35.9313   11.3873
 35.6953   35.9313   11.3790
 33.6047   35.9313   11.3986
 31.5598   35.9313   11.4606
 29.6500   35.9313   11.5637
 27.9587   35.9313   11.7270
 26.5598   35.9313   11.9677
 25.5145   35.9313   12.2851
 24.8685   35.9313   12.6685
 24.6500   35.9313   13.1000
&BPNODE TNODE=1, TNPC=0, TINTC=0, &END
 24.8685   35.9313   13.5524
 25.5145   35.9313   13.9496
 26.5598   35.9313   14.2658
 27.9587   35.9313   14.4714
 29.6500   35.9313   14.5366
 31.5598   35.9313   14.4431
 33.6047   35.9313   14.2049
 35.6953   35.9313   13.8565
 37.7402   35.9313   13.4385
 39.6500   35.9313   12.9867
 41.3413   35.9313   12.5435
 42.7402   35.9313   12.1443
 43.7855   35.9313   11.8217
 44.4315   35.9313   11.6143
 44.5896   35.9313   11.5308
&BPNODE TNODE=3, TNPC=0, TINTC=0, &END
&SECT1 STX=0.0, STY=0.0, STZ=0.0, SCALE=1.0, ALF=0.0, THETA=0.0, INMODE=4,
 TNODS=0, TNPS=0, TINTS=0, &END
 44.5896   38.9281   11.5308
 44.4315   38.9281   11.4948
 43.7855   38.9281   11.4783
 42.7402   38.9281   11.4575
 41.1500   38.9281   11.4266
 39.6500   38.9281   11.4037
 37.7402   38.9281   11.3873
 35.6953   38.9281   11.3790
 33.6047   38.9281   11.3986
 31.5598   38.9281   11.4606
 29.6500   38.9281   11.5637
 27.9587   38.9281   11.7270
 26.5598   38.9281   11.9677
 25.5145   38.9281   12.2851
 24.8685   38.9281   12.6685
 24.6500   38.9281   13.1000
&BPNODE TNODE=1, TNPC=0, TINTC=0, &END
 24.8685   38.9281   13.5524
 25.5145   38.9281   13.9496
 26.5598   38.9281   14.2658
 27.9587   38.9281   14.4714
 29.6500   38.9281   14.5366
 31.5598   38.9281   14.4431
 33.6047   38.9281   14.2049
 35.6953   38.9281   13.8565
 37.7402   38.9281   13.4385
 39.6500   38.9281   12.9867
 41.3413   38.9281   12.5435
 42.7402   38.9281   12.1443
 43.7855   38.9281   11.8217
 44.4315   38.9281   11.6143
 44.5896   38.9281   11.5308
&BPNODE TNODE=3, TNPC=0, TINTC=0, &END
&SECT1 STX=0.0, STY=0.0, STZ=0.0, SCALE=1.0, ALF=0.0, THETA=0.0, INMODE=4,
 TNODS=0, TNPS=0, TINTS=0, &END
 44.5896   42.2500   11.5308
 44.4315   42.2500   11.4948
 43.7855   42.2500   11.4783
```

```
 42.7402   42.2500   11.4575
 41.1500   42.2500   11.4266
 39.6500   42.2500   11.4037
 37.7402   42.2500   11.3873
 35.6953   42.2500   11.3790
 33.6047   42.2500   11.3986
 31.5598   42.2500   11.4606
 29.6500   42.2500   11.5637
 27.9587   42.2500   11.7270
 26.5598   42.2500   11.9677
 25.5145   42.2500   12.2851
 24.8685   42.2500   12.6685
 24.6500   42.2500   13.1000
&BPNODE TNODE=1, TNPC=0, TINTC=0, &END
 24.8685   42.2500   13.5524
 25.5145   42.2500   13.9496
 26.5598   42.2500   14.2658
 27.9587   42.2500   14.4714
 29.6500   42.2500   14.5366
 31.5598   42.2500   14.4431
 33.6047   42.2500   14.2049
 35.6953   42.2500   13.8565
 37.7402   42.2500   13.4385
 39.6500   42.2500   12.9867
 41.3413   42.2500   12.5435
 42.7402   42.2500   12.1443
 43.7855   42.2500   11.8217
 44.4315   42.2500   11.6143
 44.5896   42.2500   11.5308
&BPNODE TNODE=3, TNPC=0, TINTC=0, &END
&SECT1 STX=0.0, STY=0.0, STZ=0.0, SCALE=1.0, ALF=0.0, THETA=0.0, INMODE=4,
 TNODS=0, TNPS=0, TINTS=0, &END
 44.5896   45.5719   11.5308
 44.4315   45.5719   11.4948
 43.7855   45.5719   11.4783
 42.7402   45.5719   11.4575
 41.1500   45.5719   11.4266
 39.6500   45.5719   11.4037
 37.7402   45.5719   11.3873
 35.6953   45.5719   11.3790
 33.6047   45.5719   11.3986
 31.5598   45.5719   11.4606
 29.6500   45.5719   11.5637
 27.9587   45.5719   11.7270
 26.5598   45.5719   11.9677
 25.5145   45.5719   12.2851
 24.8685   45.5719   12.6685
 24.6500   45.5719   13.1000
&BPNODE TNODE=1, TNPC=0, TINTC=0, &END
 24.8685   45.5719   13.5524
 25.5145   45.5719   13.9496
 26.5598   45.5719   14.2658
 27.9587   45.5719   14.4714
 29.6500   45.5719   14.5366
 31.5598   45.5719   14.4431
 33.6047   45.5719   14.2049
 35.6953   45.5719   13.8565
 37.7402   45.5719   13.4385
 39.6500   45.5719   12.9867
 41.3413   45.5719   12.5435
 42.7402   45.5719   12.1443
 43.7855   45.5719   11.8217
 44.4315   45.5719   11.6143
 44.5896   45.5719   11.5308
&BPNODE TNODE=3, TNPC=0, TINTC=0, &END
&SECT1 STX=0.0, STY=0.0, STZ=0.0, SCALE=1.0, ALF=0.0, THETA=0.0, INMODE=4,
 TNODS=0, TNPS=0, TINTS=0, &END
 44.5896   48.5687   11.5308
 44.4315   48.5687   11.4948
 43.7855   48.5687   11.4783
```

```
  42.7402   48.5687   11.4575
  41.1500   48.5687   11.4266
  39.6500   48.5687   11.4037
  37.7402   48.5687   11.3873
  35.6953   48.5687   11.3790
  33.6047   48.5687   11.3986
  31.5598   48.5687   11.4606
  29.6500   48.5687   11.5637
  27.9587   48.5687   11.7270
  26.5598   48.5687   11.9677
  25.5145   48.5687   12.2851
  24.8685   48.5687   12.6685
  24.6500   48.5687   13.1000
&BPNODE TNODE=1, TNPC=0, TINTC=0, &END
  24.8685   48.5687   13.5524
  25.5145   48.5687   13.9496
  26.5598   48.5687   14.2658
  27.9587   48.5687   14.4714
  29.6500   48.5687   14.5366
  31.5598   48.5687   14.4431
  33.6047   48.5687   14.2049
  35.6953   48.5687   13.8565
  37.7402   48.5687   13.4385
  39.6500   48.5687   12.9867
  41.3413   48.5687   12.5435
  42.7402   48.5687   12.1443
  43.7855   48.5687   11.8217
  44.4315   48.5687   11.6143
  44.5896   48.5687   11.5308
&BPNODE TNODE=3, TNPC=0, TINTC=0, &END
&SECT1 STX=0.0, STY=0.0, STZ=0.0, SCALE=1.0, ALF=0.0, THETA=0.0, INMODE=4,
 TNODS=0, TNPS=0, TINTS=0, &END
  44.5896   50.9469   11.5308
  44.4315   50.9469   11.4948
  43.7855   50.9469   11.4783
  42.7402   50.9469   11.4575
  41.1500   50.9469   11.4266
  39.6500   50.9469   11.4037
  37.7402   50.9469   11.3873
  35.6953   50.9469   11.3790
  33.6047   50.9469   11.3986
  31.5598   50.9469   11.4606
  29.6500   50.9469   11.5637
  27.9587   50.9469   11.7270
  26.5598   50.9469   11.9677
  25.5145   50.9469   12.2851
  24.8685   50.9469   12.6685
  24.6500   50.9469   13.1000
&BPNODE TNODE=1, TNPC=0, TINTC=0, &END
  24.8685   50.9469   13.5524
  25.5145   50.9469   13.9496
  26.5598   50.9469   14.2658
  27.9587   50.9469   14.4714
  29.6500   50.9469   14.5366
  31.5598   50.9469   14.4431
  33.6047   50.9469   14.2049
  35.6953   50.9469   13.8565
  37.7402   50.9469   13.4385
  39.6500   50.9469   12.9867
  41.3413   50.9469   12.5435
  42.7402   50.9469   12.1443
  43.7855   50.9469   11.8217
  44.4315   50.9469   11.6143
  44.5896   50.9469   11.5308
&BPNODE TNODE=3, TNPC=0, TINTC=0, &END
&SECT1 STX=0.0, STY=0.0, STZ=0.0, SCALE=1.0, ALF=0.0, THETA=0.0, INMODE=4,
 TNODS=0, TNPS=0, TINTS=0, &END
  44.5896   52.4739   11.5308
  44.4315   52.4739   11.4948
  43.7855   52.4739   11.4783
```

```
  42.7402   52.4739   11.4575
  41.1500   52.4739   11.4266
  39.6500   52.4739   11.4037
  37.7402   52.4739   11.3873
  35.6953   52.4739   11.3790
  33.6047   52.4739   11.3986
  31.5598   52.4739   11.4606
  29.6500   52.4739   11.5637
  27.9587   52.4739   11.7270
  26.5598   52.4739   11.9677
  25.5145   52.4739   12.2851
  24.8685   52.4739   12.6685
  24.6500   52.4739   13.1000
&BPNODE TNODE=1, TNPC=0, TINTC=0, &END
  24.8685   52.4739   13.5524
  25.5145   52.4739   13.9496
  26.5598   52.4739   14.2658
  27.9587   52.4739   14.4714
  29.6500   52.4739   14.5366
  31.5598   52.4739   14.4431
  33.6047   52.4739   14.2049
  35.6953   52.4739   13.8565
  37.7402   52.4739   13.4385
  39.6500   52.4739   12.9867
  41.3413   52.4739   12.5435
  42.7402   52.4739   12.1443
  43.7855   52.4739   11.8217
  44.4315   52.4739   11.6143
  44.5896   52.4739   11.5308
&BPNODE TNODE=3, TNPC=0, TINTC=0, &END
&SECT1 STX=0.0, STY=0.0, STZ=0.0, SCALE=1.0, ALF=0.0, THETA=0.0, INMODE=4,
 TNODS=3, TNPS=0, TINTS=0, &END
  44.5896   53.0000   11.5308
  44.3717   53.0000   11.4932
  43.7277   53.0000   11.4770
  42.6855   53.0000   11.4565
  41.2909   53.0000   11.4290
  39.6047   53.0000   11.4032
  37.7006   53.0000   11.3871
  35.6619   53.0000   11.3790
  33.5777   53.0000   11.3991
  31.5390   53.0000   11.4614
  29.6349   53.0000   11.5647
  27.9487   53.0000   11.7283
  26.5541   53.0000   11.9690
  25.5119   53.0000   12.2862
  24.8679   53.0000   12.6691
  24.6500   53.0000   13.1000
&BPNODE TNODE=1, TNPC=0, TINTC=0, &END
  24.8679   53.0000   13.5517
  25.5119   53.0000   13.9485
  26.5541   53.0000   14.2646
  27.9487   53.0000   14.4706
  29.6349   53.0000   14.5367
  31.5390   53.0000   14.4449
  33.5777   53.0000   14.2088
  35.6619   53.0000   13.8627
  37.7006   53.0000   13.4473
  39.6047   53.0000   12.9980
  41.2909   53.0000   12.5573
  42.6855   53.0000   12.1606
  43.7277   53.0000   11.8400
  44.3717   53.0000   11.6336
  44.5896   53.0000   11.5308
&BPNODE TNODE=3, TNPC=0, TINTC=0, &END

&PATCH1 IREV=-1, IDPAT=1, MAKE=0, KCOMP=1, KASS=1, IPATSYM=0, IPATCOP=0, &END
  LEFT AIL NO DEFLECTION 10X15
&SECT1 STX=0.0, STY=0.0, STZ=0.0, SCALE=1.0, ALF=0.0, THETA=0.0, INMODE=4,
 TNODS=0, TNPS=0, TINTS=0, &END
```

```
  44.5896  -31.5000   11.5308
  44.3717  -31.5000   11.4932
  43.7277  -31.5000   11.4770
  42.6855  -31.5000   11.4565
  41.2909  -31.5000   11.4290
  39.6047  -31.5000   11.4032
  37.7006  -31.5000   11.3871
  35.6619  -31.5000   11.3790
  33.5777  -31.5000   11.3991
  31.5390  -31.5000   11.4614
  29.6349  -31.5000   11.5647
  27.9487  -31.5000   11.7283
  26.5541  -31.5000   11.9690
  25.5119  -31.5000   12.2862
  24.8679  -31.5000   12.6691
  24.6500  -31.5000   13.1000
&BPNODE TNODE=1, TNPC=0, TINTC=0, &END
  24.8679  -31.5000   13.5517
  25.5119  -31.5000   13.9485
  26.5541  -31.5000   14.2646
  27.9487  -31.5000   14.4706
  29.6349  -31.5000   14.5367
  31.5390  -31.5000   14.4449
  33.5777  -31.5000   14.2088
  35.6619  -31.5000   13.8627
  37.7006  -31.5000   13.4473
  39.6047  -31.5000   12.9980
  41.2909  -31.5000   12.5573
  42.6855  -31.5000   12.1606
  43.7277  -31.5000   11.8400
  44.3717  -31.5000   11.6336
  44.5896  -31.5000   11.5308
&BPNODE TNODE=3, TNPC=0, TINTC=0, &END
&SECT1 STX=0.0, STY=0.0, STZ=0.0, SCALE=1.0, ALF=0.0, THETA=0.0, INMODE=4,
 TNODS=0, TNPS=0, TINTS=0, &END
  44.5896  -32.0261   11.5308
  44.4315  -32.0261   11.4948
  43.7855  -32.0261   11.4783
  42.7402  -32.0261   11.4575
  40.9000  -32.0261   11.4223
  39.6500  -32.0261   11.4037
  37.7402  -32.0261   11.3873
  35.6953  -32.0261   11.3790
  33.6047  -32.0261   11.3986
  31.5598  -32.0261   11.4606
  29.6500  -32.0261   11.5637
  27.9587  -32.0261   11.7270
  26.5598  -32.0261   11.9677
  25.5145  -32.0261   12.2851
  24.8685  -32.0261   12.6685
  24.6500  -32.0261   13.1000
&BPNODE TNODE=1, TNPC=0, TINTC=0, &END
  24.8685  -32.0261   13.5524
  25.5145  -32.0261   13.9496
  26.5598  -32.0261   14.2658
  27.9587  -32.0261   14.4714
  29.6500  -32.0261   14.5366
  31.5598  -32.0261   14.4431
  33.6047  -32.0261   14.2049
  35.6953  -32.0261   13.8565
  37.7402  -32.0261   13.4385
  39.6500  -32.0261   12.9867
  41.3413  -32.0261   12.5435
  42.7402  -32.0261   12.1443
  43.7855  -32.0261   11.8217
  44.4315  -32.0261   11.6143
  44.5896  -32.0261   11.5308
&BPNODE TNODE=3, TNPC=0, TINTC=0, &END
&SECT1 STX=0.0, STY=0.0, STZ=0.0, SCALE=1.0, ALF=0.0, THETA=0.0, INMODE=4,
 TNODS=0, TNPS=0, TINTS=0, &END
```

```
  44.5896  -33.5531   11.5308
  44.4315  -33.5531   11.4948
  43.7855  -33.5531   11.4783
  42.7402  -33.5531   11.4575
  40.9000  -33.5531   11.4223
  39.6500  -33.5531   11.4037
  37.7402  -33.5531   11.3873
  35.6953  -33.5531   11.3790
  33.6047  -33.5531   11.3986
  31.5598  -33.5531   11.4606
  29.6500  -33.5531   11.5637
  27.9587  -33.5531   11.7270
  26.5598  -33.5531   11.9677
  25.5145  -33.5531   12.2851
  24.8685  -33.5531   12.6685
  24.6500  -33.5531   13.1000
&BPNODE TNODE=1, TNPC=0, TINTC=0, &END
  24.8685  -33.5531   13.5524
  25.5145  -33.5531   13.9496
  26.5598  -33.5531   14.2658
  27.9587  -33.5531   14.4714
  29.6500  -33.5531   14.5366
  31.5598  -33.5531   14.4431
  33.6047  -33.5531   14.2049
  35.6953  -33.5531   13.8565
  37.7402  -33.5531   13.4385
  39.6500  -33.5531   12.9867
  41.3413  -33.5531   12.5435
  42.7402  -33.5531   12.1443
  43.7855  -33.5531   11.8217
  44.4315  -33.5531   11.6143
  44.5896  -33.5531   11.5308
&BPNODE TNODE=3, TNPC=0, TINTC=0, &END
&SECT1 STX=0.0, STY=0.0, STZ=0.0, SCALE=1.0, ALF=0.0, THETA=0.0, INMODE=4,
 TNODS=0, TNPS=0, TINTS=0, &END
  44.5896  -35.9313   11.5308
  44.4315  -35.9313   11.4948
  43.7855  -35.9313   11.4783
  42.7402  -35.9313   11.4575
  40.9000  -35.9313   11.4223
  39.6500  -35.9313   11.4037
  37.7402  -35.9313   11.3873
  35.6953  -35.9313   11.3790
  33.6047  -35.9313   11.3986
  31.5598  -35.9313   11.4606
  29.6500  -35.9313   11.5637
  27.9587  -35.9313   11.7270
  26.5598  -35.9313   11.9677
  25.5145  -35.9313   12.2851
  24.8685  -35.9313   12.6685
  24.6500  -35.9313   13.1000
&BPNODE TNODE=1, TNPC=0, TINTC=0, &END
  24.8685  -35.9313   13.5524
  25.5145  -35.9313   13.9496
  26.5598  -35.9313   14.2658
  27.9587  -35.9313   14.4714
  29.6500  -35.9313   14.5366
  31.5598  -35.9313   14.4431
  33.6047  -35.9313   14.2049
  35.6953  -35.9313   13.8565
  37.7402  -35.9313   13.4385
  39.6500  -35.9313   12.9867
  41.3413  -35.9313   12.5435
  42.7402  -35.9313   12.1443
  43.7855  -35.9313   11.8217
  44.4315  -35.9313   11.6143
  44.5896  -35.9313   11.5308
&BPNODE TNODE=3, TNPC=0, TINTC=0, &END
&SECT1 STX=0.0, STY=0.0, STZ=0.0, SCALE=1.0, ALF=0.0, THETA=0.0, INMODE=4,
 TNODS=0, TNPS=0, TINTS=0, &END
```

```
  44.5896  -38.9281   11.5308
  44.4315  -38.9281   11.4948
  43.7855  -38.9281   11.4783
  42.7402  -38.9281   11.4575
  40.9000  -38.9281   11.4223
  39.6500  -38.9281   11.4037
  37.7402  -38.9281   11.3873
  35.6953  -38.9281   11.3790
  33.6047  -38.9281   11.3986
  31.5598  -38.9281   11.4606
  29.6500  -38.9281   11.5637
  27.9587  -38.9281   11.7270
  26.5598  -38.9281   11.9677
  25.5145  -38.9281   12.2851
  24.8685  -38.9281   12.6685
  24.6500  -38.9281   13.1000
&BPNODE TNODE=1, TNPC=0, TINTC=0, &END
  24.8685  -38.9281   13.5524
  25.5145  -38.9281   13.9496
  26.5598  -38.9281   14.2658
  27.9587  -38.9281   14.4714
  29.6500  -38.9281   14.5366
  31.5598  -38.9281   14.4431
  33.6047  -38.9281   14.2049
  35.6953  -38.9281   13.8565
  37.7402  -38.9281   13.4385
  39.6500  -38.9281   12.9867
  41.3413  -38.9281   12.5435
  42.7402  -38.9281   12.1443
  43.7855  -38.9281   11.8217
  44.4315  -38.9281   11.6143
  44.5896  -38.9281   11.5308
&BPNODE TNODE=3, TNPC=0, TINTC=0, &END
&SECT1 STX=0.0, STY=0.0, STZ=0.0, SCALE=1.0, ALF=0.0, THETA=0.0, INMODE=4,
 TNODS=0, TNPS=0, TINTS=0, &END
  44.5896  -42.2500   11.5308
  44.4315  -42.2500   11.4948
  43.7855  -42.2500   11.4783
  42.7402  -42.2500   11.4575
  40.9000  -42.2500   11.4223
  39.6500  -42.2500   11.4037
  37.7402  -42.2500   11.3873
  35.6953  -42.2500   11.3790
  33.6047  -42.2500   11.3986
  31.5598  -42.2500   11.4606
  29.6500  -42.2500   11.5637
  27.9587  -42.2500   11.7270
  26.5598  -42.2500   11.9677
  25.5145  -42.2500   12.2851
  24.8685  -42.2500   12.6685
  24.6500  -42.2500   13.1000
&BPNODE TNODE=1, TNPC=0, TINTC=0, &END
  24.8685  -42.2500   13.5524
  25.5145  -42.2500   13.9496
  26.5598  -42.2500   14.2658
  27.9587  -42.2500   14.4714
  29.6500  -42.2500   14.5366
  31.5598  -42.2500   14.4431
  33.6047  -42.2500   14.2049
  35.6953  -42.2500   13.8565
  37.7402  -42.2500   13.4385
  39.6500  -42.2500   12.9867
  41.3413  -42.2500   12.5435
  42.7402  -42.2500   12.1443
  43.7855  -42.2500   11.8217
  44.4315  -42.2500   11.6143
  44.5896  -42.2500   11.5308
&BPNODE TNODE=3, TNPC=0, TINTC=0, &END
&SECT1 STX=0.0, STY=0.0, STZ=0.0, SCALE=1.0, ALF=0.0, THETA=0.0, INMODE=4,
 TNODS=0, TNPS=0, TINTS=0, &END
```

```
  44.5896  -45.5719   11.5308
  44.4315  -45.5719   11.4948
  43.7855  -45.5719   11.4783
  42.7402  -45.5719   11.4575
  40.9000  -45.5719   11.4223
  39.6500  -45.5719   11.4037
  37.7402  -45.5719   11.3873
  35.6953  -45.5719   11.3790
  33.6047  -45.5719   11.3986
  31.5598  -45.5719   11.4606
  29.6500  -45.5719   11.5637
  27.9587  -45.5719   11.7270
  26.5598  -45.5719   11.9677
  25.5145  -45.5719   12.2851
  24.8685  -45.5719   12.6685
  24.6500  -45.5719   13.1000
&BPNODE TNODE=1, TNPC=0, TINTC=0, &END
  24.8685  -45.5719   13.5524
  25.5145  -45.5719   13.9496
  26.5598  -45.5719   14.2658
  27.9587  -45.5719   14.4714
  29.6500  -45.5719   14.5366
  31.5598  -45.5719   14.4431
  33.6047  -45.5719   14.2049
  35.6953  -45.5719   13.8565
  37.7402  -45.5719   13.4385
  39.6500  -45.5719   12.9867
  41.3413  -45.5719   12.5435
  42.7402  -45.5719   12.1443
  43.7855  -45.5719   11.8217
  44.4315  -45.5719   11.6143
  44.5896  -45.5719   11.5308
&BPNODE TNODE=3, TNPC=0, TINTC=0, &END
&SECT1 STX=0.0, STY=0.0, STZ=0.0, SCALE=1.0, ALF=0.0, THETA=0.0, INMODE=4,
 TNODS=0, TNPS=0, TINTS=0, &END
  44.5896  -48.5687   11.5308
  44.4315  -48.5687   11.4948
  43.7855  -48.5687   11.4783
  42.7402  -48.5687   11.4575
  40.9000  -48.5687   11.4223
  39.6500  -48.5687   11.4037
  37.7402  -48.5687   11.3873
  35.6953  -48.5687   11.3790
  33.6047  -48.5687   11.3986
  31.5598  -48.5687   11.4606
  29.6500  -48.5687   11.5637
  27.9587  -48.5687   11.7270
  26.5598  -48.5687   11.9677
  25.5145  -48.5687   12.2851
  24.8685  -48.5687   12.6685
  24.6500  -48.5687   13.1000
&BPNODE TNODE=1, TNPC=0, TINTC=0, &END
  24.8685  -48.5687   13.5524
  25.5145  -48.5687   13.9496
  26.5598  -48.5687   14.2658
  27.9587  -48.5687   14.4714
  29.6500  -48.5687   14.5366
  31.5598  -48.5687   14.4431
  33.6047  -48.5687   14.2049
  35.6953  -48.5687   13.8565
  37.7402  -48.5687   13.4385
  39.6500  -48.5687   12.9867
  41.3413  -48.5687   12.5435
  42.7402  -48.5687   12.1443
  43.7855  -48.5687   11.8217
  44.4315  -48.5687   11.6143
  44.5896  -48.5687   11.5308
&BPNODE TNODE=3, TNPC=0, TINTC=0, &END
&SECT1 STX=0.0, STY=0.0, STZ=0.0, SCALE=1.0, ALF=0.0, THETA=0.0, INMODE=4,
 TNODS=0, TNPS=0, TINTS=0, &END
```

```
 44.5896  -50.9469   11.5308
 44.4315  -50.9469   11.4948
 43.7855  -50.9469   11.4783
 42.7402  -50.9469   11.4575
 40.9000  -50.9469   11.4223
 39.6500  -50.9469   11.4037
 37.7402  -50.9469   11.3873
 35.6953  -50.9469   11.3790
 33.6047  -50.9469   11.3986
 31.5598  -50.9469   11.4606
 29.6500  -50.9469   11.5637
 27.9587  -50.9469   11.7270
 26.5598  -50.9469   11.9677
 25.5145  -50.9469   12.2851
 24.8685  -50.9469   12.6685
 24.6500  -50.9469   13.1000
&BPNODE TNODE=1, TNPC=0, TINTC=0, &END
 24.8685  -50.9469   13.5524
 25.5145  -50.9469   13.9496
 26.5598  -50.9469   14.2658
 27.9587  -50.9469   14.4714
 29.6500  -50.9469   14.5366
 31.5598  -50.9469   14.4431
 33.6047  -50.9469   14.2049
 35.6953  -50.9469   13.8565
 37.7402  -50.9469   13.4385
 39.6500  -50.9469   12.9867
 41.3413  -50.9469   12.5435
 42.7402  -50.9469   12.1443
 43.7855  -50.9469   11.8217
 44.4315  -50.9469   11.6143
 44.5896  -50.9469   11.5308
&BPNODE TNODE=3, TNPC=0, TINTC=0, &END
&SECT1 STX=0.0, STY=0.0, STZ=0.0, SCALE=1.0, ALF=0.0, THETA=0.0, INMODE=4,
 TNODS=0, TNPS=0, TINTS=0, &END
 44.5896  -52.4739   11.5308
 44.4315  -52.4739   11.4948
 43.7855  -52.4739   11.4783
 42.7402  -52.4739   11.4575
 40.9000  -52.4739   11.4223
 39.6500  -52.4739   11.4037
 37.7402  -52.4739   11.3873
 35.6953  -52.4739   11.3790
 33.6047  -52.4739   11.3986
 31.5598  -52.4739   11.4606
 29.6500  -52.4739   11.5637
 27.9587  -52.4739   11.7270
 26.5598  -52.4739   11.9677
 25.5145  -52.4739   12.2851
 24.8685  -52.4739   12.6685
 24.6500  -52.4739   13.1000
&BPNODE TNODE=1, TNPC=0, TINTC=0, &END
 24.8685  -52.4739   13.5524
 25.5145  -52.4739   13.9496
 26.5598  -52.4739   14.2658
 27.9587  -52.4739   14.4714
 29.6500  -52.4739   14.5366
 31.5598  -52.4739   14.4431
 33.6047  -52.4739   14.2049
 35.6953  -52.4739   13.8565
 37.7402  -52.4739   13.4385
 39.6500  -52.4739   12.9867
 41.3413  -52.4739   12.5435
 42.7402  -52.4739   12.1443
 43.7855  -52.4739   11.8217
 44.4315  -52.4739   11.6143
 44.5896  -52.4739   11.5308
&BPNODE TNODE=3, TNPC=0, TINTC=0, &END
&SECT1 STX=0.0, STY=0.0, STZ=0.0, SCALE=1.0, ALF=0.0, THETA=0.0, INMODE=4,
 TNODS=3, TNPS=0, TINTS=0, &END
 44.5896  -53.0000   11.5308
 44.3717  -53.0000   11.4932
 43.7277  -53.0000   11.4770
 42.6855  -53.0000   11.4565
 41.2909  -53.0000   11.4290
 39.6047  -53.0000   11.4032
 37.7006  -53.0000   11.3871
 35.6619  -53.0000   11.3790
 33.5777  -53.0000   11.3991
 31.5390  -53.0000   11.4614
 29.6349  -53.0000   11.5647
 27.9487  -53.0000   11.7283
 26.5541  -53.0000   11.9690
 25.5119  -53.0000   12.2862
 24.8679  -53.0000   12.6691
 24.6500  -53.0000   13.1000
&BPNODE TNODE=1, TNPC=0, TINTC=0, &END
 24.8679  -53.0000   13.5517
 25.5119  -53.0000   13.9485
 26.5541  -53.0000   14.2646
 27.9487  -53.0000   14.4706
 29.6349  -53.0000   14.5367
 31.5390  -53.0000   14.4449
 33.5777  -53.0000   14.2088
 35.6619  -53.0000   13.8627
 37.7006  -53.0000   13.4473
 39.6047  -53.0000   12.9980
 41.2909  -53.0000   12.5573
 42.6855  -53.0000   12.1606
 43.7277  -53.0000   11.8400
 44.3717  -53.0000   11.6336
 44.5896  -53.0000   11.5308
&BPNODE TNODE=3, TNPC=0, TINTC=0, &END

&PATCH1 IREV=0, IDPAT=1, MAKE=0, KCOMP=1, KASS=1, IPATSYM=1, IPATCOP=0, &END
 WING OUTBOARD TAPERED- 6X15
&SECT1 STX=0.0, STY=0.0, STZ=0.0, SCALE=1.0, ALF=0.0, THETA=0.0, INMODE=4,
 TNODS=0, TNPS=0, TINTS=0, &END
 44.5896   53.0000   11.5308
 44.3717   53.0000   11.4914
 43.7277   53.0000   11.4763
 42.6855   53.0000   11.4563
 41.2909   53.0000   11.4289
 39.6047   53.0000   11.4032
 37.7006   53.0000   11.3871
 35.6619   53.0000   11.3790
 33.5777   53.0000   11.3991
 31.5390   53.0000   11.4614
 29.6349   53.0000   11.5647
 27.9487   53.0000   11.7283
 26.5541   53.0000   11.9690
 25.5119   53.0000   12.2862
 24.8679   53.0000   12.6691
 24.6500   53.0000   13.1000
&BPNODE TNODE=1, TNPC=0, TINTC=0, &END
 24.8679   53.0000   13.5517
 25.5119   53.0000   13.9485
 26.5541   53.0000   14.2646
 27.9487   53.0000   14.4706
 29.6349   53.0000   14.5367
 31.5390   53.0000   14.4449
 33.5777   53.0000   14.2088
 35.6619   53.0000   13.8627
 37.7006   53.0000   13.4473
 39.6047   53.0000   12.9980
 41.2909   53.0000   12.5573
 42.6855   53.0000   12.1607
 43.7277   53.0000   11.8407
 44.3717   53.0000   11.6352
 44.5896   53.0000   11.5308
```

```
&BPNODE TNODE=3, TNPC=0, TINTC=0, &END
&SECT1 STX=0.0, STY=0.0, STZ=0.0, SCALE=1.0, ALF=0.0, THETA=0.0, INMODE=4,
 TNODS=0, TNPS=0, TINTS=0, &END
  44.4894   53.5359   11.5387
  44.2727   53.5359   11.4994
  43.6318   53.5359   11.4845
  42.5949   53.5359   11.4646
  41.2073   53.5359   11.4373
  39.5296   53.5359   11.4117
  37.6351   53.5359   11.3957
  35.6066   53.5359   11.3877
  33.5328   53.5359   11.4077
  31.5044   53.5359   11.4697
  29.6099   53.5359   11.5724
  27.9321   53.5359   11.7352
  26.5445   53.5359   11.9747
  25.5076   53.5359   12.2903
  24.8668   53.5359   12.6713
  24.6500   53.5359   13.1000
&BPNODE TNODE=1, TNPC=0, TINTC=0, &END
  24.8668   53.5359   13.5495
  25.5076   53.5359   13.9442
  26.5445   53.5359   14.2588
  27.9321   53.5359   14.4637
  29.6099   53.5359   14.5294
  31.5044   53.5359   14.4381
  33.5328   53.5359   14.2033
  35.6066   53.5359   13.8589
  37.6351   53.5359   13.4455
  39.5296   53.5359   12.9985
  41.2073   53.5359   12.5600
  42.5949   53.5359   12.1654
  43.6318   53.5359   11.8470
  44.2727   53.5359   11.6426
  44.4894   53.5359   11.5387
&BPNODE TNODE=3, TNPC=0, TINTC=0, &END
&SECT1 STX=0.0, STY=0.0, STZ=0.0, SCALE=1.0, ALF=0.0, THETA=0.0, INMODE=4,
 TNODS=0, TNPS=0, TINTS=0, &END
  44.2157   55.0000   11.5602
  44.0020   55.0000   11.5215
  43.3700   55.0000   11.5068
  42.3474   55.0000   11.4872
  40.9789   55.0000   11.4603
  39.3243   55.0000   11.4350
  37.4559   55.0000   11.4192
  35.4555   55.0000   11.4113
  33.4103   55.0000   11.4310
  31.4098   55.0000   11.4922
  29.5414   55.0000   11.5935
  27.8869   55.0000   11.7540
  26.5184   55.0000   11.9902
  25.4958   55.0000   12.3015
  24.8638   55.0000   12.6772
  24.6500   55.0000   13.1000
&BPNODE TNODE=1, TNPC=0, TINTC=0, &END
  24.8638   55.0000   13.5433
  25.4958   55.0000   13.9326
  26.5184   55.0000   14.2428
  27.8869   55.0000   14.4449
  29.5414   55.0000   14.5097
  31.4098   55.0000   14.4196
  33.4103   55.0000   14.1881
  35.4555   55.0000   13.8484
  37.4559   55.0000   13.4407
  39.3243   55.0000   12.9999
  40.9789   55.0000   12.5675
  42.3474   55.0000   12.1783
  43.3700   55.0000   11.8643
  44.0020   55.0000   11.6627
  44.2157   55.0000   11.5602
```

```
&BPNODE TNODE=3, TNPC=0, TINTC=0, &END
&SECT1 STX=0.0, STY=0.0, STZ=0.0, SCALE=1.0, ALF=0.0, THETA=0.0, INMODE=4,
 TNODS=0, TNPS=0, TINTS=0, &END
  43.8419   57.0000   11.5897
  43.6322   57.0000   11.5517
  43.0123   57.0000   11.5372
  42.0092   57.0000   11.5180
  40.6669   57.0000   11.4916
  39.0439   57.0000   11.4668
  37.2112   57.0000   11.4513
  35.2490   57.0000   11.4436
  33.2429   57.0000   11.4629
  31.2806   57.0000   11.5229
  29.4480   57.0000   11.6223
  27.8250   57.0000   11.7798
  26.4827   57.0000   12.0114
  25.4796   57.0000   12.3168
  24.8597   57.0000   12.6853
  24.6500   57.0000   13.1000
&BPNODE TNODE=1, TNPC=0, TINTC=0, &END
  24.8597   57.0000   13.5348
  25.4796   57.0000   13.9167
  26.4827   57.0000   14.2209
  27.8250   57.0000   14.4192
  29.4480   57.0000   14.4828
  31.2806   57.0000   14.3944
  33.2429   57.0000   14.1673
  35.2490   57.0000   13.8341
  37.2112   57.0000   13.4342
  39.0439   57.0000   13.0018
  40.6669   57.0000   12.5777
  42.0092   57.0000   12.1959
  43.0123   57.0000   11.8879
  43.6322   57.0000   11.6901
  43.8419   57.0000   11.5897
&BPNODE TNODE=3, TNPC=0, TINTC=0, &END
&SECT1 STX=0.0, STY=0.0, STZ=0.0, SCALE=1.0, ALF=0.0, THETA=0.0, INMODE=4,
 TNODS=0, TNPS=0, TINTS=0, &END
  43.4680   59.0000   11.6191
  43.2624   59.0000   11.5819
  42.6545   59.0000   11.5676
  41.6710   59.0000   11.5488
  40.3548   59.0000   11.5229
  38.7635   59.0000   11.4986
  36.9665   59.0000   11.4834
  35.0425   59.0000   11.4758
  33.0755   59.0000   11.4948
  31.1515   59.0000   11.5536
  29.3545   59.0000   11.6511
  27.7632   59.0000   11.8055
  26.4470   59.0000   12.0326
  25.4635   59.0000   12.3320
  24.8556   59.0000   12.6933
  24.6500   59.0000   13.1000
&BPNODE TNODE=1, TNPC=0, TINTC=0, &END
  24.8556   59.0000   13.5263
  25.4635   59.0000   13.9007
  26.4470   59.0000   14.1991
  27.7632   59.0000   14.3935
  29.3545   59.0000   14.4559
  31.1515   59.0000   14.3692
  33.0755   59.0000   14.1465
  35.0425   59.0000   13.8198
  36.9665   59.0000   13.4277
  38.7635   59.0000   13.0037
  40.3548   59.0000   12.5878
  41.6710   59.0000   12.2135
  42.6545   59.0000   11.9115
  43.2624   59.0000   11.7176
  43.4680   59.0000   11.6191
```

```
&BPNODE TNODE=3, TNPC=0, TINTC=0, &END
&SECT1 STX=0.0, STY=0.0, STZ=0.0, SCALE=1.0, ALF=0.0, THETA=0.0, INMODE=4,
 TNODS=0, TNPS=0, TINTS=0, &END
  43.1943   60.4641   11.6406
  42.9917   60.4641   11.6039
  42.3927   60.4641   11.5899
  41.4235   60.4641   11.5714
  40.1264   60.4641   11.5459
  38.5582   60.4641   11.5219
  36.7874   60.4641   11.5069
  34.8914   60.4641   11.4995
  32.9530   60.4641   11.5181
  31.0569   60.4641   11.5761
  29.2861   60.4641   11.6721
  27.7179   60.4641   11.8243
  26.4208   60.4641   12.0481
  25.4516   60.4641   12.3432
  24.8526   60.4641   12.6993
  24.6500   60.4641   13.1000
&BPNODE TNODE=1, TNPC=0, TINTC=0, &END
  24.8526   60.4641   13.5201
  25.4516   60.4641   13.8891
  26.4208   60.4641   14.1831
  27.7179   60.4641   14.3747
  29.2861   60.4641   14.4361
  31.0569   60.4641   14.3507
  32.9530   60.4641   14.1313
  34.8914   60.4641   13.8093
  36.7874   60.4641   13.4230
  38.5582   60.4641   13.0051
  40.1264   60.4641   12.5953
  41.4235   60.4641   12.2264
  42.3927   60.4641   11.9288
  42.9917   60.4641   11.7377
  43.1943   60.4641   11.6406
&BPNODE TNODE=3, TNPC=0, TINTC=0, &END
&SECT1 STX=0.0, STY=0.0, STZ=0.0, SCALE=1.0, ALF=0.0, THETA=0.0, INMODE=4,
 TNODS=3, TNPS=0, TINTS=0, &END
  43.0941   61.0000   11.6485
  42.8926   61.0000   11.6120
  42.2968   61.0000   11.5981
  41.3329   61.0000   11.5796
  40.0428   61.0000   11.5543
  38.4831   61.0000   11.5304
  36.7218   61.0000   11.5156
  34.8360   61.0000   11.5081
  32.9081   61.0000   11.5267
  31.0223   61.0000   11.5843
  29.2610   61.0000   11.6799
  27.7013   61.0000   11.8312
  26.4113   61.0000   12.0538
  25.4473   61.0000   12.3473
  24.8515   61.0000   12.7014
  24.6500   61.0000   13.1000
&BPNODE TNODE=1, TNPC=0, TINTC=0, &END
  24.8515   61.0000   13.5178
  25.4473   61.0000   13.8848
  26.4113   61.0000   14.1773
  27.7013   61.0000   14.3678
  29.2610   61.0000   14.4289
  31.0223   61.0000   14.3440
  32.9081   61.0000   14.1257
  34.8360   61.0000   13.8055
  36.7218   61.0000   13.4212
  38.4831   61.0000   13.0057
  40.0428   61.0000   12.5980
  41.3329   61.0000   12.2311
  42.2968   61.0000   11.9351
  42.8926   61.0000   11.7451
  43.0941   61.0000   11.6485
```

```
&BPNODE TNODE=3, TNPC=0, TINTC=0, &END

&PATCH1  IREV=  0, IDPAT= 1, MAKE=   17, KCOMP= 1, KASS= 1, IPATSYM=1,
            IPATCOP=0,                                                    &END
WING_TIP_Half_Round
&PATCH2  ITYP=  2,    TNODS= 5,    TNPS=   4,    TINTS= 3,      &END


&PATCH1 IREV=0, IDPAT=1, MAKE=0, KCOMP=1, KASS=1, IPATSYM=1, IPATCOP=0, &END
  HORIZ STAB 0 deg 10X16
&SECT1 STX=0.0, STY=0.0, STZ=0.0, SCALE=1.0, ALF=0.0, THETA=0.0, INMODE=4,
 TNODS=0, TNPS=0, TINTS=0, &END
  96.0000    0.0000    8.090
  95.8703    0.0000    8.0726
  95.4862    0.0000    8.0464
  94.8624    0.0000    8.0056
  94.0230    0.0000    7.9542
  93.0001    0.0000    7.8965
  91.8331    0.0000    7.8370
  90.5669    0.0000    7.7806
  89.2500    0.0000    7.7327
  87.9331    0.0000    7.6989
  86.6669    0.0000    7.6850
  85.4999    0.0000    7.6952
  84.4770    0.0000    7.7316
  83.6376    0.0000    7.7933
  83.0138    0.0000    7.8771
  82.6297    0.0000    7.9775
  82.5000    0.0000    8.0900
&BPNODE TNODE=1, TNPC=0, TINTC=0, &END
  82.6297    0.0000    8.2025
  83.0138    0.0000    8.3029
  83.6376    0.0000    8.3867
  84.4770    0.0000    8.4484
  85.4999    0.0000    8.4848
  86.6669    0.0000    8.4950
  87.9331    0.0000    8.4811
  89.2500    0.0000    8.4473
  90.5669    0.0000    8.3994
  91.8331    0.0000    8.3430
  93.0001    0.0000    8.2835
  94.0230    0.0000    8.2258
  94.8624    0.0000    8.1744
  95.4862    0.0000    8.1336
  95.8703    0.0000    8.1074
  96.0000    0.0000    8.090
&BPNODE TNODE=3, TNPC=0, TINTC=0, &END
&SECT1 STX=0.0, STY=0.0, STZ=0.0, SCALE=1.0, ALF=0.0, THETA=0.0, INMODE=4,
 TNODS=0, TNPS=0, TINTS=0, &END
  96.0012    0.4864    8.090
  95.8725    0.4864    8.0727
  95.4911    0.4864    8.0467
  94.8718    0.4864    8.0062
  94.0384    0.4864    7.9552
  93.2391    0.4864    7.9097
  91.8642    0.4864    7.8388
  90.6070    0.4864    7.7828
  89.2996    0.4864    7.7352
  87.9921    0.4864    7.7017
  86.7349    0.4864    7.6879
  85.5763    0.4864    7.6980
  84.5608    0.4864    7.7342
  83.7273    0.4864    7.7954
  83.1080    0.4864    7.8787
  82.7267    0.4864    7.9783
  82.5979    0.4864    8.0900
&BPNODE TNODE=1, TNPC=0, TINTC=0, &END
```

```
 82.7267    0.4864    8.2017
 83.1080    0.4864    8.3013
 83.7273    0.4864    8.3846
 84.5608    0.4864    8.4458
 85.5763    0.4864    8.4820
 86.7349    0.4864    8.4921
 87.9921    0.4864    8.4783
 89.2996    0.4864    8.4448
 90.6070    0.4864    8.3972
 91.8642    0.4864    8.3412
 93.2391    0.4864    8.2703
 94.0384    0.4864    8.2248
 94.8718    0.4864    8.1738
 95.4911    0.4864    8.1333
 95.8725    0.4864    8.1073
 96.0012    0.4864    8.090
&BPNODE TNODE=3, TNPC=0, TINTC=0, &END
&SECT1 STX=0.0, STY=0.0, STZ=0.0, SCALE=1.0, ALF=0.0, THETA=0.0, INMODE=4,
 TNODS=0, TNPS=0, TINTS=0, &END
 96.0048    1.8979    8.090
 95.8787    1.8979    8.0731
 95.5053    1.8979    8.0476
 94.8990    1.8979    8.0080
 94.0830    1.8979    7.9580
 93.2212    1.8979    7.9091
 91.9543    1.8979    7.8441
 90.7234    1.8979    7.7892
 89.4434    1.8979    7.7426
 88.1633    1.8979    7.7098
 86.9324    1.8979    7.6963
 85.7980    1.8979    7.7062
 84.8038    1.8979    7.7416
 83.9878    1.8979    7.8015
 83.3814    1.8979    7.8831
 83.0080    1.8979    7.9806
 82.8820    1.8979    8.0900
&BPNODE TNODE=1, TNPC=0, TINTC=0, &END
 83.0080    1.8979    8.1994
 83.3814    1.8979    8.2969
 83.9878    1.8979    8.3785
 84.8038    1.8979    8.4384
 85.7980    1.8979    8.4738
 86.9324    1.8979    8.4837
 88.1633    1.8979    8.4702
 89.4434    1.8979    8.4374
 90.7234    1.8979    8.3908
 91.9543    1.8979    8.3359
 93.2212    1.8979    8.2709
 94.0830    1.8979    8.2220
 94.8990    1.8979    8.1720
 95.5053    1.8979    8.1324
 95.8787    1.8979    8.1069
 96.0048    1.8979    8.090
&BPNODE TNODE=3, TNPC=0, TINTC=0, &END
&SECT1 STX=0.0, STY=0.0, STZ=0.0, SCALE=1.0, ALF=0.0, THETA=0.0, INMODE=4,
 TNODS=0, TNPS=0, TINTS=0, &END
 96.0103    4.0964    8.090
 95.8884    4.0964    8.0736
 95.5275    4.0964    8.0490
 94.9413    4.0964    8.0107
 94.1525    4.0964    7.9624
 93.2001    4.0964    7.9086
 92.0947    4.0964    7.8523
 90.9048    4.0964    7.7992
 89.6674    4.0964    7.7542
 88.4299    4.0964    7.7224
 87.2400    4.0964    7.7094
 86.1434    4.0964    7.7190
 85.1822    4.0964    7.7532
 84.3934    4.0964    7.8111
 83.8073    4.0964    7.8900
 83.4463    4.0964    7.9843
 83.3244    4.0964    8.0900
&BPNODE TNODE=1, TNPC=0, TINTC=0, &END
 83.4463    4.0964    8.1957
 83.8073    4.0964    8.2900
 84.3934    4.0964    8.3689
 85.1822    4.0964    8.4268
 86.1434    4.0964    8.4610
 87.2400    4.0964    8.4706
 88.4299    4.0964    8.4576
 89.6674    4.0964    8.4258
 90.9048    4.0964    8.3808
 92.0947    4.0964    8.3277
 93.2001    4.0964    8.2714
 94.1525    4.0964    8.2176
 94.9413    4.0964    8.1693
 95.5275    4.0964    8.1310
 95.8884    4.0964    8.1064
 96.0103    4.0964    8.090
&BPNODE TNODE=3, TNPC=0, TINTC=0, &END
&SECT1 STX=0.0, STY=0.0, STZ=0.0, SCALE=1.0, ALF=0.0, THETA=0.0, INMODE=4,
 TNODS=0, TNPS=0, TINTS=0, &END
 96.0173    6.8666    8.090
 95.9007    6.8666    8.0743
 95.5554    6.8666    8.0508
 94.9947    6.8666    8.0141
 94.2401    6.8666    7.9680
 93.1853    6.8666    7.9088
 92.2716    6.8666    7.8626
 91.1334    6.8666    7.8119
 89.9496    6.8666    7.7688
 88.7659    6.8666    7.7384
 87.6276    6.8666    7.7259
 86.5786    6.8666    7.7351
 85.6591    6.8666    7.7678
 84.9046    6.8666    7.8233
 84.3438    6.8666    7.8987
 83.9986    6.8666    7.9889
 83.8820    6.8666    8.0900
&BPNODE TNODE=1, TNPC=0, TINTC=0, &END
 83.9986    6.8666    8.1911
 84.3438    6.8666    8.2813
 84.9046    6.8666    8.3567
 85.6591    6.8666    8.4122
 86.5786    6.8666    8.4449
 87.6276    6.8666    8.4541
 88.7659    6.8666    8.4416
 89.9496    6.8666    8.4112
 91.1334    6.8666    8.3681
 92.2716    6.8666    8.3174
 93.3206    6.8666    8.2639
 94.2401    6.8666    8.2120
 94.9947    6.8666    8.1659
 95.5554    6.8666    8.1292
 95.9007    6.8666    8.1057
 96.0173    6.8666    8.090
&BPNODE TNODE=3, TNPC=0, TINTC=0, &END
&SECT1 STX=0.0, STY=0.0, STZ=0.0, SCALE=1.0, ALF=0.0, THETA=0.0, INMODE=4,
 TNODS=0, TNPS=0, TINTS=0, &END
 96.0250    9.9375    8.090
 95.9143    9.9375    8.0751
 95.5864    9.9375    8.0528
 95.0538    9.9375    8.0180
 94.3372    9.9375    7.9741
 93.1841    9.9375    7.9099
 92.4677    9.9375    7.8740
 91.3867    9.9375    7.8258
 90.2625    9.9375    7.7849
 89.1383    9.9375    7.7561
```

```
 88.0573    9.9375    7.7442
 87.0610    9.9375    7.7530
 86.1878    9.9375    7.7840
 85.4712    9.9375    7.8367
 84.9386    9.9375    7.9083
 84.6107    9.9375    7.9939
 84.5000    9.9375    8.0900
&BPNODE TNODE=1, TNPC=0, TINTC=0, &END
 84.6107    9.9375    8.1861
 84.9386    9.9375    8.2717
 85.4712    9.9375    8.3433
 86.1878    9.9375    8.3960
 87.0610    9.9375    8.4270
 88.0573    9.9375    8.4358
 89.1383    9.9375    8.4239
 90.2625    9.9375    8.3951
 91.3867    9.9375    8.3542
 92.4677    9.9375    8.3060
 93.4640    9.9375    8.2552
 94.3372    9.9375    8.2059
 95.0538    9.9375    8.1620
 95.5864    9.9375    8.1272
 95.9143    9.9375    8.1049
 96.0250    9.9375    8.090
&BPNODE TNODE=3, TNPC=0, TINTC=0, &END
&SECT1 STX=0.0, STY=0.0, STZ=0.0, SCALE=1.0, ALF=0.0, THETA=0.0, INMODE=4,
 TNODS=0, TNPS=0, TINTS=0, &END
 96.0327   13.0084    8.090
 95.9279   13.0084    8.0759
 95.6173   13.0084    8.0547
 95.1130   13.0084    8.0218
 94.4343   13.0084    7.9802
 93.1989   13.0084    7.9121
 92.6638   13.0084    7.8855
 91.6401   13.0084    7.8398
 90.5754   13.0084    7.8011
 89.5107   13.0084    7.7738
 88.4869   13.0084    7.7626
 87.5434   13.0084    7.7708
 86.7165   13.0084    7.8002
 86.0378   13.0084    7.8501
 85.5334   13.0084    7.9179

 85.2229   13.0084    7.9990
 85.1180   13.0084    8.0900
&BPNODE TNODE=1, TNPC=0, TINTC=0, &END
 85.2229   13.0084    8.1810
 85.5334   13.0084    8.2621
 86.0378   13.0084    8.3299
 86.7165   13.0084    8.3798
 87.5434   13.0084    8.4092
 88.4869   13.0084    8.4174
 89.5107   13.0084    8.4062
 90.5754   13.0084    8.3789
 91.6401   13.0084    8.3402
 92.6638   13.0084    8.2945
 93.6073   13.0084    8.2464
 94.4343   13.0084    8.1998
 95.1130   13.0084    8.1582
 95.6173   13.0084    8.1253
 95.9279   13.0084    8.1041
 96.0327   13.0084    8.090
&BPNODE TNODE=3, TNPC=0, TINTC=0, &END
&SECT1 STX=0.0, STY=0.0, STZ=0.0, SCALE=1.0, ALF=0.0, THETA=0.0, INMODE=4,
 TNODS=0, TNPS=0, TINTS=0, &END
 96.0397   15.7786    8.090
 95.9401   15.7786    8.0766
 95.6452   15.7786    8.0565
 95.1664   15.7786    8.0252
 94.5219   15.7786    7.9858
 93.7366   15.7786    7.9414
 93.2260   15.7786    7.9148
 91.8686   15.7786    7.8524
 90.8576   15.7786    7.8157
 89.8467   15.7786    7.7897
 88.8745   15.7786    7.7791
 87.9786   15.7786    7.7869
 87.1934   15.7786    7.8148
 86.5489   15.7786    7.8622
 86.0700   15.7786    7.9266
 85.7751   15.7786    8.0036
 85.6756   15.7786    8.0900
&BPNODE TNODE=1, TNPC=0, TINTC=0, &END
 85.7751   15.7786    8.1764
 86.0700   15.7786    8.2534
 86.5489   15.7786    8.3178
 87.1934   15.7786    8.3652
 87.9786   15.7786    8.3931
 88.8745   15.7786    8.4009
 89.8467   15.7786    8.3903
 90.8576   15.7786    8.3643
 91.8686   15.7786    8.3276
 93.2260   15.7786    8.2652
 93.7366   15.7786    8.2386
 94.5219   15.7786    8.1942
 95.1664   15.7786    8.1548
 95.6452   15.7786    8.1235
 95.9401   15.7786    8.1034
 96.0397   15.7786    8.090
&BPNODE TNODE=3, TNPC=0, TINTC=0, &END
&SECT1 STX=0.0, STY=0.0, STZ=0.0, SCALE=1.0, ALF=0.0, THETA=0.0, INMODE=4,
 TNODS=0, TNPS=0, TINTS=0, &END
 96.0452   17.9771    8.090
 95.9499   17.9771    8.0772
 95.6674   17.9771    8.0579
 95.2087   17.9771    8.0279
 94.5914   17.9771    7.9902
 93.8393   17.9771    7.9477
 93.2568   17.9771    7.9175
 92.0500   17.9771    7.8625
 91.0816   17.9771    7.8272
 90.1133   17.9771    7.8024
 89.1821   17.9771    7.7922
 88.3240   17.9771    7.7997
 87.5718   17.9771    7.8264
 86.9546   17.9771    7.8718
 86.4959   17.9771    7.9335
 86.2134   17.9771    8.0073
 86.1180   17.9771    8.0900
&BPNODE TNODE=1, TNPC=0, TINTC=0, &END
 86.2134   17.9771    8.1727
 86.4959   17.9771    8.2465
 86.9546   17.9771    8.3082
 87.5718   17.9771    8.3536
 88.3240   17.9771    8.3803
 89.1821   17.9771    8.3878
 90.1133   17.9771    8.3776
 91.0816   17.9771    8.3528
 92.0500   17.9771    8.3175
 93.2568   17.9771    8.2625
 93.8393   17.9771    8.2323
 94.5914   17.9771    8.1898
 95.2087   17.9771    8.1521
 95.6674   17.9771    8.1221
 95.9499   17.9771    8.1028
 96.0452   17.9771    8.090
&BPNODE TNODE=3, TNPC=0, TINTC=0, &END
&SECT1 STX=0.0, STY=0.0, STZ=0.0, SCALE=1.0, ALF=0.0, THETA=0.0, INMODE=4,
 TNODS=0, TNPS=0, TINTS=0, &END
 96.0488   19.3886    8.090
```

```
   95.9561    19.3886     8.0775
   95.6816    19.3886     8.0588
   95.2359    19.3886     8.0297
   94.6361    19.3886     7.9930
   93.9051    19.3886     7.9517
   93.2810    19.3886     7.9195
   92.1664    19.3886     7.8689
   91.2254    19.3886     7.8347
   90.2845    19.3886     7.8105
   89.3796    19.3886     7.8006
   88.5457    19.3886     7.8079
   87.8148    19.3886     7.8339
   87.2150    19.3886     7.8780
   86.7693    19.3886     7.9379
   86.4948    19.3886     8.0096
   86.4021    19.3886     8.0900
&BPNODE TNODE=1, TNPC=0, TINTC=0, &END
   86.4948    19.3886     8.1704
   86.7693    19.3886     8.2421
   87.2150    19.3886     8.3020
   87.8148    19.3886     8.3461
   88.5457    19.3886     8.3721
   89.3796    19.3886     8.3794
   90.2845    19.3886     8.3695
   91.2254    19.3886     8.3453
   92.1664    19.3886     8.3111
   93.2810    19.3886     8.2605
   93.9051    19.3886     8.2283
   94.6361    19.3886     8.1870
   95.2359    19.3886     8.1503
   95.6816    19.3886     8.1212
   95.9561    19.3886     8.1025
   96.0488    19.3886     8.090
&BPNODE TNODE=3, TNPC=0, TINTC=0, &END
&SECT1 STX=0.0, STY=0.0, STZ=0.0, SCALE=1.0, ALF=0.0, THETA=0.0, INMODE=4,
 TNODS=3, TNPS=0, TINTS=0, &END
   96.0500    19.8750     8.090
   95.9582    19.8750     8.0777
   95.6865    19.8750     8.0591
   95.2453    19.8750     8.0303
   94.6514    19.8750     7.9940
   93.9278    19.8750     7.9531
   93.1023    19.8750     7.9111
   92.2066    19.8750     7.8711
   91.2750    19.8750     7.8372
   90.3434    19.8750     7.8133
   89.4477    19.8750     7.8035
   88.6222    19.8750     7.8107
   87.8986    19.8750     7.8365
   87.3047    19.8750     7.8801
   86.8635    19.8750     7.9394
   86.5918    19.8750     8.0104
   86.5000    19.8750     8.0900
&BPNODE TNODE=1, TNPC=0, TINTC=0, &END
   86.5918    19.8750     8.1696
   86.8635    19.8750     8.2406
   87.3047    19.8750     8.2999
   87.8986    19.8750     8.3435
   88.6222    19.8750     8.3693
   89.4477    19.8750     8.3765
   90.3434    19.8750     8.3667
   91.2750    19.8750     8.3428
   92.2066    19.8750     8.3089
   93.1023    19.8750     8.2689
   93.9278    19.8750     8.2269
   94.6514    19.8750     8.1860
   95.2453    19.8750     8.1497
   95.6865    19.8750     8.1209
   95.9582    19.8750     8.1023
   96.0500    19.8750     8.090
&BPNODE TNODE=3, TNPC=0, TINTC=0, &END

&PATCH1 IREV=0, IDPAT=1, MAKE=0, KCOMP=1, KASS=1, IPATSYM=0, IPATCOP=0, &END
  14X10_VERT_STAB_PROJECTED_Area_of_Tailboom
&SECT1 STX=0.0, STY=0.0, STZ=0.0, SCALE=1.0, ALF=0.0, THETA=0.0, INMODE=4,
 TNODS=0, TNPS=0, TINTS=0, &END
   95.6000     0.0000     8.5000
   95.3094     0.0306     8.5000
   94.4546     0.0898     8.5000
   93.0851     0.1764     8.5000
   91.2806     0.2799     8.5000
   89.1460     0.3881     8.5000
   86.8054     0.4877     8.5000
   84.3946     0.5633     8.5000
   82.0540     0.5990     8.5000
   79.9194     0.5821     8.5000
   78.1149     0.5065     8.5000
   76.7454     0.3761     8.5000
   75.8906     0.2025     8.5000
   75.6000     0.0000     8.5000
   75.8906    -0.2025     8.5000
   76.7454    -0.3761     8.5000
   78.1149    -0.5065     8.5000
   79.9194    -0.5821     8.5000
   82.0540    -0.5990     8.5000
   84.3946    -0.5633     8.5000
   86.8054    -0.4877     8.5000
   89.1460    -0.3881     8.5000
   91.2806    -0.2799     8.5000
   93.0851    -0.1764     8.5000
   94.4546    -0.0898     8.5000
   95.3094    -0.0306     8.5000
   95.6000     0.0000     8.5000
&BPNODE TNODE=3, TNPC=0, TINTC=0, &END
&SECT1 STX=0.0, STY=0.0, STZ=0.0, SCALE=1.0, ALF=0.0, THETA=0.0, INMODE=4,
 TNODS=0, TNPS=0, TINTS=0, &END
   95.7652     0.0000     8.9075
   95.4782     0.0303     8.9075
   94.6338     0.0887     8.9075
   93.2811     0.1742     8.9075
   91.4987     0.2765     8.9075
   89.3902     0.3834     8.9075
   87.0782     0.4817     8.9075
   84.6969     0.5564     8.9075
   82.3849     0.5917     8.9075
   80.2764     0.5750     8.9075
   78.4940     0.5003     8.9075
   77.1413     0.3715     8.9075
   76.2969     0.2001     8.9075
   76.0099     0.0000     8.9075
   76.2969    -0.2001     8.9075
   77.1413    -0.3715     8.9075
   78.4940    -0.5003     8.9075
   80.2764    -0.5750     8.9075
   82.3849    -0.5917     8.9075
   84.6969    -0.5564     8.9075
   87.0782    -0.4817     8.9075
   89.3902    -0.3834     8.9075
   91.4987    -0.2765     8.9075
   93.2811    -0.1742     8.9075
   94.6338    -0.0887     8.9075
   95.4782    -0.0303     8.9075
   95.7652     0.0000     8.9075
&BPNODE TNODE=3, TNPC=0, TINTC=0, &END
&SECT1 STX=0.0, STY=0.0, STZ=0.0, SCALE=1.0, ALF=0.0, THETA=0.0, INMODE=4,
 TNODS=0, TNPS=0, TINTS=0, &END
   96.2446     0.0000    10.0899
   95.9679     0.0292    10.0899
   95.1538     0.0855    10.0899
```

```
  93.8498    0.1679   10.0899
  92.1314    0.2665   10.0899
  90.0988    0.3696   10.0899
  87.8698    0.4644   10.0899
  85.5742    0.5364   10.0899
  83.3453    0.5704   10.0899
  81.3126    0.5543   10.0899
  79.5943    0.4824   10.0899
  78.2902    0.3581   10.0899
  77.4762    0.1929   10.0899
  77.1995    0.0000   10.0899
  77.4762   -0.1929   10.0899
  78.2902   -0.3581   10.0899
  79.5943   -0.4824   10.0899
  81.3126   -0.5543   10.0899
  83.3453   -0.5704   10.0899
  85.5742   -0.5364   10.0899
  87.8698   -0.4644   10.0899
  90.0988   -0.3696   10.0899
  92.1314   -0.2665   10.0899
  93.8498   -0.1679   10.0899
  95.1538   -0.0855   10.0899
  95.9679   -0.0292   10.0899
  96.2446    0.0000   10.0899
&BPNODE TNODE=3, TNPC=0, TINTC=0, &END
&SECT1 STX=0.0, STY=0.0, STZ=0.0, SCALE=1.0, ALF=0.0, THETA=0.0, INMODE=4,
 TNODS=0, TNPS=0, TINTS=0, &END
  96.9912    0.0000   11.9317
  96.7306    0.0275   11.9317
  95.9638    0.0806   11.9317
  94.7355    0.1582   11.9317
  93.1170    0.2511   11.9317
  91.2024    0.3481   11.9317
  89.1029    0.4374   11.9317
  86.9406    0.5052   11.9317
  84.8411    0.5373   11.9317
  82.9265    0.5221   11.9317
  81.3080    0.4543   11.9317
  80.0797    0.3373   11.9317
  79.3129    0.1817   11.9317
  79.0523    0.0000   11.9317
  79.3129   -0.1817   11.9317
  80.0797   -0.3373   11.9317
  81.3080   -0.4543   11.9317
  82.9265   -0.5221   11.9317
  84.8411   -0.5373   11.9317
  86.9406   -0.5052   11.9317
  89.1029   -0.4374   11.9317
  91.2024   -0.3481   11.9317
  93.1170   -0.2511   11.9317
  94.7355   -0.1582   11.9317
  95.9638   -0.0806   11.9317
  96.7306   -0.0275   11.9317
  96.9912    0.0000   11.9317
&BPNODE TNODE=3, TNPC=0, TINTC=0, &END
&SECT1 STX=0.0, STY=0.0, STZ=0.0, SCALE=1.0, ALF=0.0, THETA=0.0, INMODE=4,
 TNODS=0, TNPS=0, TINTS=0, &END
  97.9321    0.0000   14.2524
  97.6917    0.0253   14.2524
  96.9845    0.0743   14.2524
  95.8516    0.1459   14.2524
  94.3589    0.2316   14.2524
  92.5930    0.3211   14.2524
  90.6567    0.4034   14.2524
  88.6624    0.4660   14.2524
  86.7260    0.4956   14.2524
  84.9602    0.4815   14.2524
  83.4674    0.4190   14.2524
  82.3346    0.3111   14.2524
  81.6274    0.1676   14.2524
  81.3870    0.0000   14.2524
  81.6274   -0.1676   14.2524
  82.3346   -0.3111   14.2524
  83.4674   -0.4190   14.2524
  84.9602   -0.4815   14.2524
  86.7260   -0.4956   14.2524
  88.6624   -0.4660   14.2524
  90.6567   -0.4034   14.2524
  92.5930   -0.3211   14.2524
  94.3589   -0.2316   14.2524
  95.8516   -0.1459   14.2524
  96.9845   -0.0743   14.2524
  97.6917   -0.0253   14.2524
  97.9321    0.0000   14.2524
&BPNODE TNODE=3, TNPC=0, TINTC=0, &END
&SECT1 STX=0.0, STY=0.0, STZ=0.0, SCALE=1.0, ALF=0.0, THETA=0.0, INMODE=4,
 TNODS=0, TNPS=0, TINTS=0, &END
  98.9750    0.0000   16.8250
  98.7571    0.0230   16.8250
  98.1159    0.0674   16.8250
  97.0888    0.1323   16.8250
  95.7355    0.2099   16.8250
  94.1345    0.2911   16.8250
  92.3790    0.3657   16.8250
  90.5710    0.4224   16.8250
  88.8155    0.4493   16.8250
  87.2145    0.4366   16.8250
  85.8612    0.3799   16.8250
  84.8341    0.2821   16.8250
  84.1929    0.1519   16.8250
  83.9750    0.0000   16.8250
  84.1929   -0.1519   16.8250
  84.8341   -0.2821   16.8250
  85.8612   -0.3799   16.8250
  87.2145   -0.4366   16.8250
  88.8155   -0.4493   16.8250
  90.5710   -0.4224   16.8250
  92.3790   -0.3657   16.8250
  94.1345   -0.2911   16.8250
  95.7355   -0.2099   16.8250
  97.0888   -0.1323   16.8250
  98.1159   -0.0674   16.8250
  98.7571   -0.0230   16.8250
  98.9750    0.0000   16.8250
&BPNODE TNODE=3, TNPC=0, TINTC=0, &END
&SECT1 STX=0.0, STY=0.0, STZ=0.0, SCALE=1.0, ALF=0.0, THETA=0.0, INMODE=4,
 TNODS=0, TNPS=0, TINTS=0, &END
 100.0179    0.0000   19.3976
  99.8224    0.0206   19.3976
  99.2473    0.0604   19.3976
  98.3260    0.1186   19.3976
  97.1121    0.1883   19.3976
  95.6761    0.2611   19.3976
  94.1014    0.3281   19.3976
  92.4796    0.3789   19.3976
  90.9049    0.4030   19.3976
  89.4688    0.3916   19.3976
  88.2549    0.3408   19.3976
  87.3336    0.2530   19.3976
  86.7585    0.1363   19.3976
  86.5630    0.0000   19.3976
  86.7585   -0.1363   19.3976
  87.3336   -0.2530   19.3976
  88.2549   -0.3408   19.3976
  89.4688   -0.3916   19.3976
  90.9049   -0.4030   19.3976
  92.4796   -0.3789   19.3976
  94.1014   -0.3281   19.3976
  95.6761   -0.2611   19.3976
  97.1121   -0.1883   19.3976
```

```
  98.3260   -0.1186   19.3976
  99.2473   -0.0604   19.3976
  99.8224   -0.0206   19.3976
 100.0179    0.0000   19.3976
&BPNODE TNODE=3, TNPC=0, TINTC=0, &END
&SECT1 STX=0.0, STY=0.0, STZ=0.0, SCALE=1.0, ALF=0.0, THETA=0.0, INMODE=4,
 TNODS=0, TNPS=0, TINTS=0, &END
 100.9588    0.0000   21.7183
 100.7835    0.0185   21.7183
 100.2680    0.0542   21.7183
  99.4422    0.1064   21.7183
  98.3540    0.1688   21.7183
  97.0667    0.2341   21.7183
  95.6551    0.2941   21.7183
  94.2013    0.3397   21.7183
  92.7898    0.3613   21.7183
  91.5025    0.3510   21.7183
  90.4143    0.3055   21.7183
  89.5885    0.2268   21.7183
  89.0729    0.1221   21.7183
  88.8977    0.0000   21.7183
  89.0729   -0.1221   21.7183
  89.5885   -0.2268   21.7183
  90.4143   -0.3055   21.7183
  91.5025   -0.3510   21.7183
  92.7898   -0.3613   21.7183
  94.2013   -0.3397   21.7183
  95.6551   -0.2941   21.7183
  97.0667   -0.2341   21.7183
  98.3540   -0.1688   21.7183
  99.4422   -0.1064   21.7183
 100.2680   -0.0542   21.7183
 100.7835   -0.0185   21.7183
 100.9588    0.0000   21.7183
&BPNODE TNODE=3, TNPC=0, TINTC=0, &END
&SECT1 STX=0.0, STY=0.0, STZ=0.0, SCALE=1.0, ALF=0.0, THETA=0.0, INMODE=4,
 TNODS=0, TNPS=0, TINTS=0, &END
 101.7054    0.0000   23.5601
 101.5463    0.0168   23.5601
 101.0780    0.0492   23.5601
 100.3279    0.0966   23.5601
  99.3395    0.1533   23.5601
  98.1703    0.2126   23.5601
  96.8882    0.2671   23.5601
  95.5677    0.3085   23.5601
  94.2856    0.3281   23.5601
  93.1164    0.3188   23.5601
  92.1280    0.2775   23.5601
  91.3779    0.2060   23.5601
  90.9097    0.1109   23.5601
  90.7505    0.0000   23.5601
  90.9097   -0.1109   23.5601
  91.3779   -0.2060   23.5601
  92.1280   -0.2775   23.5601
  93.1164   -0.3188   23.5601
  94.2856   -0.3281   23.5601
  95.5677   -0.3085   23.5601
  96.8882   -0.2671   23.5601
  98.1703   -0.2126   23.5601
  99.3395   -0.1533   23.5601
 100.3279   -0.0966   23.5601
 101.0780   -0.0492   23.5601
 101.5463   -0.0168   23.5601
 101.7054    0.0000   23.5601
&BPNODE TNODE=3, TNPC=0, TINTC=0, &END
&SECT1 STX=0.0, STY=0.0, STZ=0.0, SCALE=1.0, ALF=0.0, THETA=0.0, INMODE=4,
 TNODS=0, TNPS=0, TINTS=0, &END
 102.1848    0.0000   24.7425
 102.0360    0.0157   24.7425
 101.5981    0.0460   24.7425
 100.8966    0.0903   24.7425
  99.9723    0.1434   24.7425
  98.8789    0.1988   24.7425
  97.6799    0.2498   24.7425
  96.4450    0.2885   24.7425
  95.2460    0.3069   24.7425
  94.1526    0.2982   24.7425
  93.2283    0.2595   24.7425
  92.5268    0.1926   24.7425
  92.0889    0.1038   24.7425
  91.9401    0.0000   24.7425
  92.0889   -0.1038   24.7425
  92.5268   -0.1926   24.7425
  93.2283   -0.2595   24.7425
  94.1526   -0.2982   24.7425
  95.2460   -0.3069   24.7425
  96.4450   -0.2885   24.7425
  97.6799   -0.2498   24.7425
  98.8789   -0.1988   24.7425
  99.9723   -0.1434   24.7425
 100.8966   -0.0903   24.7425
 101.5981   -0.0460   24.7425
 102.0360   -0.0157   24.7425
 102.1848    0.0000   24.7425
&BPNODE TNODE=3, TNPC=0, TINTC=0, &END
&SECT1 STX=0.0, STY=0.0, STZ=0.0, SCALE=1.0, ALF=0.0, THETA=0.0, INMODE=4,
 TNODS=5, TNPS=0, TINTS=0, &END
 102.3500    0.0000   25.1500
 102.2047    0.0153   25.1500
 101.7773    0.0449   25.1500
 101.0926    0.0882   25.1500
 100.1903    0.1400   25.1500
  99.1230    0.1941   25.1500
  97.9527    0.2438   25.1500
  96.7473    0.2816   25.1500
  95.5770    0.2995   25.1500
  94.5097    0.2911   25.1500
  93.6074    0.2533   25.1500
  92.9227    0.1880   25.1500
  92.4953    0.1013   25.1500
  92.3500    0.0000   25.1500
  92.4953   -0.1013   25.1500
  92.9227   -0.1880   25.1500
  93.6074   -0.2533   25.1500
  94.5097   -0.2911   25.1500
  95.5770   -0.2995   25.1500
  96.7473   -0.2816   25.1500
  97.9527   -0.2438   25.1500
  99.1230   -0.1941   25.1500
 100.1903   -0.1400   25.1500
 101.0926   -0.0882   25.1500
 101.7773   -0.0449   25.1500
 102.2047   -0.0153   25.1500
 102.3500    0.0000   25.1500
&BPNODE TNODE=3, TNPC=0, TINTC=0, &END


&PATCH1 IREV=0, IDPAT=2, MAKE=0, KCOMP=1, KASS=1, IPATSYM=1, IPATCOP=0, &END
   FOG_PYLON
&SECT1 STX=0.0, STY=0.0, STZ=0.0, SCALE=1.0, ALF=0.0, THETA=0.0, INMODE=4,
 TNODS=0, TNPS=0, TINTS=0, &END
  25.8000    0.0000   14.3100
  25.8000    0.0000   14.3516
  25.8000    0.0000   14.5358
  25.8000    0.0000   14.7201
  25.8000    0.0000   14.9044
  25.8000    0.0000   15.0886
  25.8000    0.0000   15.2729
  25.8000    0.0000   15.4572
  25.8000    0.0000   15.6415
```

```
   25.8000     0.0000    15.8257
   25.8000     0.0000    16.0100
 &BPNODE TNODE=3, TNPC=0, TINTC=0, &END
 &SECT1 STX=0.0, STY=0.0, STZ=0.0, SCALE=1.0, ALF=0.0, THETA=0.0, INMODE=4,
  TNODS=0, TNPS=0, TINTS=0, &END
   25.9300     0.5302    14.3377
   25.9300     0.5302    14.3753
   25.9300     0.5302    14.5558
   25.9300     0.5302    14.7362
   25.9300     0.5302    14.9167
   25.9300     0.5302    15.0971
   25.9300     0.5302    15.2776
   25.9300     0.5302    15.4581
   25.9300     0.5302    15.6385
   25.9300     0.5302    15.8190
   25.9300     0.5302    15.9995
 &BPNODE TNODE=3, TNPC=0, TINTC=0, &END
 &SECT1 STX=0.0, STY=0.0, STZ=0.0, SCALE=1.0, ALF=0.0, THETA=0.0, INMODE=4,
  TNODS=0, TNPS=0, TINTS=0, &END
   26.3144     0.9601    14.4108
   26.3144     0.9601    14.4384
   26.3144     0.9601    14.6089
   26.3144     0.9601    14.7793
   26.3144     0.9601    14.9497
   26.3144     0.9601    15.1201
   26.3144     0.9601    15.2905
   26.3144     0.9601    15.4609
   26.3144     0.9601    15.6313
   26.3144     0.9601    15.8017
   26.3144     0.9601    15.9721
 &BPNODE TNODE=3, TNPC=0, TINTC=0, &END
 &SECT1 STX=0.0, STY=0.0, STZ=0.0, SCALE=1.0, ALF=0.0, THETA=0.0, INMODE=4,
  TNODS=0, TNPS=0, TINTS=0, &END
   26.9363     1.2810    14.5052
   26.9363     1.2810    14.5199
   26.9363     1.2810    14.6773
   26.9363     1.2810    14.8348
   26.9363     1.2810    14.9922
   26.9363     1.2810    15.1496
   26.9363     1.2810    15.3070
   26.9363     1.2810    15.4644
   26.9363     1.2810    15.6219
   26.9363     1.2810    15.7793
   26.9363     1.2810    15.9367
 &BPNODE TNODE=3, TNPC=0, TINTC=0, &END
 &SECT1 STX=0.0, STY=0.0, STZ=0.0, SCALE=1.0, ALF=0.0, THETA=0.0, INMODE=4,
  TNODS=0, TNPS=0, TINTS=0, &END
   27.7687     1.4893    14.5940
   27.7687     1.4893    14.6034
   27.7687     1.4893    14.7408
   27.7687     1.4893    14.8859
   27.7687     1.4893    15.0309
   27.7687     1.4893    15.1759
   27.7687     1.4893    15.3210
   27.7687     1.4893    15.4660
   27.7687     1.4893    15.6110
   27.7687     1.4893    15.7561
   27.7687     1.4893    15.9011
 &BPNODE TNODE=3, TNPC=0, TINTC=0, &END
 &SECT1 STX=0.0, STY=0.0, STZ=0.0, SCALE=1.0, ALF=0.0, THETA=0.0, INMODE=4,
  TNODS=0, TNPS=0, TINTS=0, &END
   28.7750     1.5866    14.6549
   28.7750     1.5866    14.6638
   28.7750     1.5866    14.7837
   28.7750     1.5866    14.9196
   28.7750     1.5866    15.0555
   28.7750     1.5866    15.1914
   28.7750     1.5866    15.3273
   28.7750     1.5866    15.4632
   28.7750     1.5866    15.5991
   28.7750     1.5866    15.7351
   28.7750     1.5866    15.8710
 &BPNODE TNODE=3, TNPC=0, TINTC=0, &END
 &SECT1 STX=0.0, STY=0.0, STZ=0.0, SCALE=1.0, ALF=0.0, THETA=0.0, INMODE=4,
  TNODS=0, TNPS=0, TINTS=0, &END
   29.9113     1.5803    14.6732
   29.9113     1.5803    14.6818
   29.9113     1.5803    14.7940
   29.9113     1.5803    14.9260
   29.9113     1.5803    15.0580
   29.9113     1.5803    15.1900
   29.9113     1.5803    15.3220
   29.9113     1.5803    15.4540
   29.9113     1.5803    15.5860
   29.9113     1.5803    15.7180
   29.9113     1.5803    15.8500
 &BPNODE TNODE=3, TNPC=0, TINTC=0, &END
 &SECT1 STX=0.0, STY=0.0, STZ=0.0, SCALE=1.0, ALF=0.0, THETA=0.0, INMODE=4,
  TNODS=0, TNPS=0, TINTS=0, &END
   31.1281     1.4826    14.6416
   31.1281     1.4826    14.6504
   31.1281     1.4826    14.7667
   31.1281     1.4826    14.9009
   31.1281     1.4826    15.0351
   31.1281     1.4826    15.1694
   31.1281     1.4826    15.3036
   31.1281     1.4826    15.4379
   31.1281     1.4826    15.5721
   31.1281     1.4826    15.7063
   31.1281     1.4826    15.8406
 &BPNODE TNODE=3, TNPC=0, TINTC=0, &END
 &SECT1 STX=0.0, STY=0.0, STZ=0.0, SCALE=1.0, ALF=0.0, THETA=0.0, INMODE=4,
  TNODS=0, TNPS=0, TINTS=0, &END
   32.3719     1.3110    14.5598
   32.3719     1.3110    14.5691
   32.3719     1.3110    14.7023
   32.3719     1.3110    14.8450
   32.3719     1.3110    14.9877
   32.3719     1.3110    15.1304
   32.3719     1.3110    15.2731
   32.3719     1.3110    15.4158
   32.3719     1.3110    15.5585
   32.3719     1.3110    15.7012
   32.3719     1.3110    15.8439
 &BPNODE TNODE=3, TNPC=0, TINTC=0, &END
 &SECT1 STX=0.0, STY=0.0, STZ=0.0, SCALE=1.0, ALF=0.0, THETA=0.0, INMODE=4,
  TNODS=0, TNPS=0, TINTS=0, &END
   33.5886     1.0866    14.4337
   33.5886     1.0866    14.4475
   33.5886     1.0866    14.6044
   33.5886     1.0866    14.7614
   33.5886     1.0866    14.9184
   33.5886     1.0866    15.0754
   33.5886     1.0866    15.2324
   33.5886     1.0866    15.3894
   33.5886     1.0866    15.5464
   33.5886     1.0866    15.7034
   33.5886     1.0866    15.8604
 &BPNODE TNODE=3, TNPC=0, TINTC=0, &END
 &SECT1 STX=0.0, STY=0.0, STZ=0.0, SCALE=1.0, ALF=0.0, THETA=0.0, INMODE=4,
  TNODS=0, TNPS=0, TINTS=0, &END
   34.7250     0.8337    14.2747
   34.7250     0.8337    14.3074
   34.7250     0.8337    14.4831
   34.7250     0.8337    14.6589
   34.7250     0.8337    14.8347
   34.7250     0.8337    15.0105
   34.7250     0.8337    15.1863
   34.7250     0.8337    15.3621
   34.7250     0.8337    15.5379
```

```
  34.7250    0.8337    15.7137
  34.7250    0.8337    15.8895
&BPNODE TNODE=3, TNPC=0, TINTC=0, &END
&SECT1 STX=0.0, STY=0.0, STZ=0.0, SCALE=1.0, ALF=0.0, THETA=0.0, INMODE=4,
 TNODS=0, TNPS=0, TINTS=0, &END
  35.7313    0.5784    14.0992
  35.7313    0.5784    14.1537
  35.7313    0.5784    14.3510
  35.7313    0.5784    14.5484
  35.7313    0.5784    14.7457
  35.7313    0.5784    14.9430
  35.7313    0.5784    15.1403
  35.7313    0.5784    15.3377
  35.7313    0.5784    15.5350
  35.7313    0.5784    15.7323
  35.7313    0.5784    15.9296
&BPNODE TNODE=3, TNPC=0, TINTC=0, &END
&SECT1 STX=0.0, STY=0.0, STZ=0.0, SCALE=1.0, ALF=0.0, THETA=0.0, INMODE=4,
 TNODS=0, TNPS=0, TINTS=0, &END
  36.5637    0.3462    13.9276
  36.5637    0.3462    14.0041
  36.5637    0.3462    14.2235
  36.5637    0.3462    14.4428
  36.5637    0.3462    14.6622
  36.5637    0.3462    14.8815
  36.5637    0.3462    15.1009
  36.5637    0.3462    15.3203
  36.5637    0.3462    15.5396
  36.5637    0.3462    15.7590
  36.5637    0.3462    15.9783
&BPNODE TNODE=3, TNPC=0, TINTC=0, &END
&SECT1 STX=0.0, STY=0.0, STZ=0.0, SCALE=1.0, ALF=0.0, THETA=0.0, INMODE=4,
 TNODS=0, TNPS=0, TINTS=0, &END
  37.1856    0.1609    13.7823
  37.1856    0.1609    13.8781
  37.1856    0.1609    14.1173
  37.1856    0.1609    14.3565
  37.1856    0.1609    14.5957
  37.1856    0.1609    14.8349
  37.1856    0.1609    15.0741
  37.1856    0.1609    15.3134
  37.1856    0.1609    15.5526
  37.1856    0.1609    15.7918
  37.1856    0.1609    16.0310
&BPNODE TNODE=3, TNPC=0, TINTC=0, &END
&SECT1 STX=0.0, STY=0.0, STZ=0.0, SCALE=1.0, ALF=0.0, THETA=0.0, INMODE=4,
 TNODS=0, TNPS=0, TINTS=0, &END
  37.5700    0.0413    13.6845
  37.5700    0.0413    13.7951
  37.5700    0.0413    14.0488
  37.5700    0.0413    14.3025
  37.5700    0.0413    14.5562
  37.5700    0.0413    14.8099
  37.5700    0.0413    15.0636
  37.5700    0.0413    15.3173
  37.5700    0.0413    15.5710
  37.5700    0.0413    15.8247
  37.5700    0.0413    16.0784
&BPNODE TNODE=3, TNPC=0, TINTC=0, &END
&SECT1 STX=0.0, STY=0.0, STZ=0.0, SCALE=1.0, ALF=0.0, THETA=0.0, INMODE=4,
 TNODS=3, TNPS=0, TINTS=0, &END
  37.7000    0.0000    13.6500
  37.7000    0.0000    13.7663
  37.7000    0.0000    14.0256
  37.7000    0.0000    14.2849
  37.7000    0.0000    14.5442
  37.7000    0.0000    14.8035
  37.7000    0.0000    15.0628
  37.7000    0.0000    15.3221
  37.7000    0.0000    15.5814
  37.7000    0.0000    15.8407
  37.7000    0.0000    16.1000
&BPNODE TNODE=3, TNPC=0, TINTC=0, &END


&PATCH1 IREV=0, IDPAT=2, MAKE=0, KCOMP=1, KASS=1, IPATSYM=1, IPATCOP=0, &END
  FOG_ENGINE_POD
&SECT1 STX=0.0, STY=0.0, STZ=0.0, SCALE=1.0, ALF=0.0, THETA=0.0, INMODE=4,
 TNODS=0, TNPS=0, TINTS=0, &END
  16.5000    0.0000    20.4000
  16.5000    0.0000    20.4000
  16.5000    0.0000    20.4000
  16.5000    0.0000    20.4000
  16.5000    0.0000    20.4000
  16.5000    0.0000    20.4000
  16.5000    0.0000    20.4000
  16.5000    0.0000    20.4000
  16.5000    0.0000    20.4000
  16.5000    0.0000    20.4000
  16.5000    0.0000    20.4000
&BPNODE TNODE=3, TNPC=0, TINTC=0, &END
&SECT1 STX=0.0, STY=0.0, STZ=0.0, SCALE=1.0, ALF=0.0, THETA=0.0, INMODE=4,
 TNODS=0, TNPS=0, TINTS=0, &END
  16.7895    0.0000    19.7036
  16.7895    0.1802    19.7381
  16.7895    0.3338    19.8311
  16.7895    0.4530    19.9692
  16.7895    0.5342    20.1491
  16.7895    0.5642    20.3542
  16.7895    0.5363    20.5590
  16.7895    0.4556    20.7374
  16.7895    0.3349    20.8747
  16.7895    0.1800    20.9661
  16.7895    0.0000    20.9995
&BPNODE TNODE=3, TNPC=0, TINTC=0, &END
&SECT1 STX=0.0, STY=0.0, STZ=0.0, SCALE=1.0, ALF=0.0, THETA=0.0, INMODE=4,
 TNODS=0, TNPS=0, TINTS=0, &END
  17.6455    0.0000    18.9621
  17.6455    0.4134    19.0316
  17.6455    0.7696    19.2229
  17.6455    1.0398    19.5042
  17.6455    1.2183    19.8707
  17.6455    1.2728    20.2955
  17.6455    1.1966    20.7383
  17.6455    1.0093    21.1240
  17.6455    0.7418    21.4169
  17.6455    0.3972    21.6150
  17.6455    0.0000    21.6870
&BPNODE TNODE=3, TNPC=0, TINTC=0, &END
&SECT1 STX=0.0, STY=0.0, STZ=0.0, SCALE=1.0, ALF=0.0, THETA=0.0, INMODE=4,
 TNODS=0, TNPS=0, TINTS=0, &END
  19.0305    0.0000    17.6702
  19.0305    0.7979    17.7380
  19.0305    1.3113    17.9554
  19.0305    1.6163    18.3439
  19.0305    1.7872    18.9932
  19.0305    1.8434    19.9738
  19.0305    1.7865    20.8477
  19.0305    1.5906    21.4633
  19.0305    1.2554    21.8603
  19.0305    0.7367    22.0950
  19.0305    0.0000    22.1718
&BPNODE TNODE=3, TNPC=0, TINTC=0, &END
&SECT1 STX=0.0, STY=0.0, STZ=0.0, SCALE=1.0, ALF=0.0, THETA=0.0, INMODE=4,
 TNODS=0, TNPS=0, TINTS=0, &END
  20.8840    0.0000    16.8347
  20.8840    1.3042    16.8570
  20.8840    1.8746    16.9602
  20.8840    2.0812    17.2524
  20.8840    2.1525    18.0117
```

```
  20.8840    2.1689   19.5462
  20.8840    2.1572   21.0957
  20.8840    2.0882   21.8715
  20.8840    1.8780   22.1653
  20.8840    1.3111   22.2650
  20.8840    0.0000   22.2869
&BPNODE TNODE=3, TNPC=0, TINTC=0, &END
&SECT1 STX=0.0, STY=0.0, STZ=0.0, SCALE=1.0, ALF=0.0, THETA=0.0, INMODE=4,
 TNODS=0, TNPS=0, TINTS=0, &END
  23.1250    0.0000   16.3511
  23.1250    1.4033   16.3708
  23.1250    2.0127   16.4691
  23.1250    2.2204   16.7715
  23.1250    2.2862   17.5999
  23.1250    2.2999   19.2276
  23.1250    2.2915   20.8939
  23.1250    2.2329   21.7791
  23.1250    2.0307   22.0844
  23.1250    1.4246   22.1766
  23.1250    0.0000   22.1945
&BPNODE TNODE=3, TNPC=0, TINTC=0, &END
&SECT1 STX=0.0, STY=0.0, STZ=0.0, SCALE=1.0, ALF=0.0, THETA=0.0, INMODE=4,
 TNODS=0, TNPS=0, TINTS=0, &END
  25.6555    0.0000   16.0481
  25.6555    1.4141   16.0679
  25.6555    2.0188   16.1668
  25.6555    2.2226   16.4703
  25.6555    2.2870   17.3089
  25.6555    2.2999   18.9446
  25.6555    2.2912   20.6132
  25.6555    2.2327   21.5039
  25.6555    2.0316   21.8124
  25.6555    1.4305   21.9057
  25.6555    0.0000   21.9240
&BPNODE TNODE=3, TNPC=0, TINTC=0, &END
&SECT1 STX=0.0, STY=0.0, STZ=0.0, SCALE=1.0, ALF=0.0, THETA=0.0, INMODE=4,
 TNODS=0, TNPS=0, TINTS=0, &END
  28.3650    0.0000   15.8494
  28.3650    1.4144   15.8682
  28.3650    2.0199   15.9622
  28.3650    2.2237   16.2532
  28.3650    2.2875   17.0611
  28.3650    2.3000   18.6632
  28.3650    2.2900   20.2862
  28.3650    2.2287   21.1215
  28.3650    2.0240   21.4109
  28.3650    1.4190   21.4999
  28.3650    0.0000   21.5175
&BPNODE TNODE=3, TNPC=0, TINTC=0, &END
&SECT1 STX=0.0, STY=0.0, STZ=0.0, SCALE=1.0, ALF=0.0, THETA=0.0, INMODE=4,
 TNODS=0, TNPS=0, TINTS=0, &END
  31.1350    0.0000   15.7474
  31.1350    1.3961   15.7637
  31.1350    2.0103   15.8456
  31.1350    2.2203   16.1006
  31.1350    2.2865   16.8111
  31.1350    2.3000   18.3044
  31.1350    2.2888   19.8200
  31.1350    2.2242   20.5497
  31.1350    2.0130   20.8000
  31.1350    1.3979   20.8773
  31.1350    0.0000   20.8925
&BPNODE TNODE=3, TNPC=0, TINTC=0, &END
&SECT1 STX=0.0, STY=0.0, STZ=0.0, SCALE=1.0, ALF=0.0, THETA=0.0, INMODE=4,
 TNODS=0, TNPS=0, TINTS=0, &END
  33.8445    0.0000   15.8093
  33.8445    1.3627   15.8218
  33.8445    1.9940   15.8864
  33.8445    2.2152   16.0907
  33.8445    2.2852   16.6649
  33.8445    2.3000   17.9747
  33.8445    2.2868   19.3038
  33.8445    2.2166   19.8875
  33.8445    1.9942   20.0845
  33.8445    1.3615   20.1457
  33.8445    0.0000   20.1575
&BPNODE TNODE=3, TNPC=0, TINTC=0, &END
&SECT1 STX=0.0, STY=0.0, STZ=0.0, SCALE=1.0, ALF=0.0, THETA=0.0, INMODE=4,
 TNODS=0, TNPS=0, TINTS=0, &END
  36.3750    0.0000   15.9892
  36.3750    1.3053   15.9975
  36.3750    1.9691   16.0428
  36.3750    2.2080   16.1903
  36.3750    2.2835   16.6129
  36.3750    2.3000   17.6647
  36.3750    2.2844   18.7297
  36.3750    2.2062   19.1542
  36.3750    1.9627   19.2941
  36.3750    1.2912   19.3366
  36.3750    0.0000   19.3443
&BPNODE TNODE=3, TNPC=0, TINTC=0, &END
&SECT1 STX=0.0, STY=0.0, STZ=0.0, SCALE=1.0, ALF=0.0, THETA=0.0, INMODE=4,
 TNODS=0, TNPS=0, TINTS=0, &END
  38.6160    0.0000   16.2138
  38.6160    1.1972   16.2181
  38.6160    1.9280   16.2456
  38.6160    2.1972   16.3400
  38.6160    2.2813   16.6192
  38.6160    2.3000   17.3609
  38.6160    2.2827   18.1311
  38.6160    2.1968   18.4163
  38.6160    1.9293   18.5068
  38.6160    1.2029   18.5335
  38.6160    0.0000   18.5378
&BPNODE TNODE=3, TNPC=0, TINTC=0, &END
&SECT1 STX=0.0, STY=0.0, STZ=0.0, SCALE=1.0, ALF=0.0, THETA=0.0, INMODE=4,
 TNODS=0, TNPS=0, TINTS=0, &END
  40.4695    0.0000   16.4386
  40.4695    1.0541   16.4404
  40.4695    1.8638   16.4540
  40.4695    2.1814   16.5048
  40.4695    2.2786   16.6646
  40.4695    2.3000   17.1216
  40.4695    2.2796   17.6011
  40.4695    2.1790   17.7620
  40.4695    1.8677   17.8097
  40.4695    1.0610   17.8229
  40.4695    0.0000   17.8247
&BPNODE TNODE=3, TNPC=0, TINTC=0, &END
&SECT1 STX=0.0, STY=0.0, STZ=0.0, SCALE=1.0, ALF=0.0, THETA=0.0, INMODE=4,
 TNODS=0, TNPS=0, TINTS=0, &END
  41.8545    0.0000   16.6286
  41.8545    0.8776   16.6291
  41.8545    1.7102   16.6332
  41.8545    2.1282   16.6520
  41.8545    2.2589   16.7231
  41.8545    2.2846   16.9507
  41.8545    2.2559   17.1850
  41.8545    2.1229   17.2486
  41.8545    1.7061   17.2659
  41.8545    0.8776   17.2699
  41.8545    0.0000   17.2703
&BPNODE TNODE=3, TNPC=0, TINTC=0, &END
&SECT1 STX=0.0, STY=0.0, STZ=0.0, SCALE=1.0, ALF=0.0, THETA=0.0, INMODE=4,
 TNODS=0, TNPS=0, TINTS=0, &END
  42.7105    0.0000   16.7554
  42.7105    0.6609   16.7566
  42.7105    1.2924   16.7619
  42.7105    1.7606   16.7743
  42.7105    2.0332   16.7974
```

```
 42.7105    2.1274   16.8434
 42.7105    2.0340   16.8795
 42.7105    1.7674   16.9014
 42.7105    1.3047   16.9135
 42.7105    0.6710   16.9187
 42.7105    0.0000   16.9198
&BPNODE TNODE=3, TNPC=0, TINTC=0, &END
&SECT1 STX=0.0, STY=0.0, STZ=0.0, SCALE=1.0, ALF=0.0, THETA=0.0, INMODE=4,
 TNODS=5, TNPS=0, TINTS=0, &END
 43.0000    0.0000   16.8000
 43.0000    0.0000   16.8000
 43.0000    0.0000   16.8000
 43.0000    0.0000   16.8000
 43.0000    0.0000   16.8000
 43.0000    0.0000   16.8000
 43.0000    0.0000   16.8000
 43.0000    0.0000   16.8000
 43.0000    0.0000   16.8000
 43.0000    0.0000   16.8000
 43.0000    0.0000   16.8000
&BPNODE TNODE=3, TNPC=0, TINTC=0, &END


&PATCH1 IREV=0, IDPAT=1, MAKE=0, KCOMP=1, KASS=1, IPATSYM=0, IPATCOP=0, &END
 RIGHT_AIL - 5 DEG UP
&SECT1 STX=0.0, STY=0.0, STZ=0.0, SCALE=1.0, ALF=0.0, THETA=0.0, INMODE=4,
 TNODS=0, TNPS=0, TINTS=0, &END
 44.5896   31.5000   11.5308
 44.3717   31.5000   11.4932
 43.7277   31.5000   11.4770
 42.6855   31.5000   11.4565
 41.2909   31.5000   11.4290
 39.6047   31.5000   11.4032
 37.7006   31.5000   11.3871
 35.6619   31.5000   11.3790
 33.5777   31.5000   11.3991
 31.5390   31.5000   11.4614
 29.6349   31.5000   11.5647
 27.9487   31.5000   11.7283
 26.5541   31.5000   11.9690
 25.5119   31.5000   12.2862
 24.8679   31.5000   12.6691
 24.6500   31.5000   13.1000
&BPNODE TNODE=1, TNPC=0, TINTC=0, &END
 24.8679   31.5000   13.5517
 25.5119   31.5000   13.9485
 26.5541   31.5000   14.2646
 27.9487   31.5000   14.4706
 29.6349   31.5000   14.5367
 31.5390   31.5000   14.4449
 33.5777   31.5000   14.2088
 35.6619   31.5000   13.8627
 37.7006   31.5000   13.4473
 39.6047   31.5000   12.9980
 41.2909   31.5000   12.5573
 42.6855   31.5000   12.1606
 43.7277   31.5000   11.8400
 44.3717   31.5000   11.6336
 44.5896   31.5000   11.5308
&BPNODE TNODE=3, TNPC=0, TINTC=0, &END
&SECT1 STX=0.0, STY=0.0, STZ=0.0, SCALE=1.0, ALF=0.0, THETA=0.0, INMODE=4,
 TNODS=0, TNPS=0, TINTS=0, &END
 44.635    32.0261   11.83
 44.4810   32.0261   11.7835
 43.8389   32.0261   11.7108
 42.7994   32.0261   11.5989
 41.1500   32.0261   11.4266
 39.6500   32.0261   11.4037
 37.7402   32.0261   11.3873
```

```
 35.6953   32.0261   11.3790
 33.6047   32.0261   11.3986
 31.5598   32.0261   11.4606
 29.6500   32.0261   11.5637
 27.9587   32.0261   11.7270
 26.5598   32.0261   11.9677
 25.5145   32.0261   12.2851
 24.8685   32.0261   12.6685
 24.6500   32.0261   13.1000
&BPNODE TNODE=1, TNPC=0, TINTC=0, &END
 24.8685   32.0261   13.5524
 25.5145   32.0261   13.9496
 26.5598   32.0261   14.2658
 27.9587   32.0261   14.4714
 29.6500   32.0261   14.5366
 31.5598   32.0261   14.4431
 33.6047   32.0261   14.2049
 35.6953   32.0261   13.8565
 37.7402   32.0261   13.4385
 39.6500   32.0261   12.9867
 41.3112   32.0261   12.5589
 42.7396   32.0261   12.2831
 43.8090   32.0261   12.0529
 44.4706   32.0261   11.9025
 44.635    32.0261   11.83
&BPNODE TNODE=3, TNPC=0, TINTC=0, &END
&SECT1 STX=0.0, STY=0.0, STZ=0.0, SCALE=1.0, ALF=0.0, THETA=0.0, INMODE=4,
 TNODS=0, TNPS=0, TINTS=0, &END
 44.6369   33.5531   11.83
 44.4810   33.5531   11.7835
 43.8389   33.5531   11.7108
 42.7994   33.5531   11.5989
 41.1500   33.5531   11.4266
 39.6500   33.5531   11.4037
 37.7402   33.5531   11.3873
 35.6953   33.5531   11.3790
 33.6047   33.5531   11.3986
 31.5598   33.5531   11.4606
 29.6500   33.5531   11.5637
 27.9587   33.5531   11.7270
 26.5598   33.5531   11.9677
 25.5145   33.5531   12.2851
 24.8685   33.5531   12.6685
 24.6500   33.5531   13.1000
&BPNODE TNODE=1, TNPC=0, TINTC=0, &END
 24.8685   33.5531   13.5524
 25.5145   33.5531   13.9496
 26.5598   33.5531   14.2658
 27.9587   33.5531   14.4714
 29.6500   33.5531   14.5366
 31.5598   33.5531   14.4431
 33.6047   33.5531   14.2049
 35.6953   33.5531   13.8565
 37.7402   33.5531   13.4385
 39.6500   33.5531   12.9867
 41.3112   33.5531   12.5589
 42.7396   33.5531   12.2831
 43.8090   33.5531   12.0529
 44.4706   33.5531   11.9025
 44.635    33.5531   11.83
&BPNODE TNODE=3, TNPC=0, TINTC=0, &END
&SECT1 STX=0.0, STY=0.0, STZ=0.0, SCALE=1.0, ALF=0.0, THETA=0.0, INMODE=4,
 TNODS=0, TNPS=0, TINTS=0, &END
 44.635    35.9313   11.83
 44.4810   35.9313   11.7835
 43.8389   35.9313   11.7108
 42.7994   35.9313   11.5989
 41.1500   35.9313   11.4266
 39.6500   35.9313   11.4037
 37.7402   35.9313   11.3873
```

```
35.6953   35.9313   11.3790
33.6047   35.9313   11.3986
31.5598   35.9313   11.4606
29.6500   35.9313   11.5637
27.9587   35.9313   11.7270
26.5598   35.9313   11.9677
25.5145   35.9313   12.2851
24.8685   35.9313   12.6685
24.6500   35.9313   13.1000
&BPNODE TNODE=1, TNPC=0, TINTC=0, &END
24.8685   35.9313   13.5524
25.5145   35.9313   13.9496
26.5598   35.9313   14.2658
27.9587   35.9313   14.4714
29.6500   35.9313   14.5366
31.5598   35.9313   14.4431
33.6047   35.9313   14.2049
35.6953   35.9313   13.8565
37.7402   35.9313   13.4385
39.6500   35.9313   12.9867
41.3112   35.9313   12.5589
42.7396   35.9313   12.2831
43.8090   35.9313   12.0529
44.4706   35.9313   11.9025
44.635    35.9313   11.83
&BPNODE TNODE=3, TNPC=0, TINTC=0, &END
&SECT1 STX=0.0, STY=0.0, STZ=0.0, SCALE=1.0, ALF=0.0, THETA=0.0, INMODE=4,
 TNODS=0, TNPS=0, TINTS=0, &END
44.635    38.9281   11.8013
44.4810   38.9281   11.7835
43.8389   38.9281   11.7108
42.7994   38.9281   11.5989
41.1500   38.9281   11.4266
39.6500   38.9281   11.4037
37.7402   38.9281   11.3873
35.6953   38.9281   11.3790
33.6047   38.9281   11.3986
31.5598   38.9281   11.4606
29.6500   38.9281   11.5637
27.9587   38.9281   11.7270
26.5598   38.9281   11.9677
25.5145   38.9281   12.2851
24.8685   38.9281   12.6685
24.6500   38.9281   13.1000
&BPNODE TNODE=1, TNPC=0, TINTC=0, &END
24.8685   38.9281   13.5524
25.5145   38.9281   13.9496
26.5598   38.9281   14.2658
27.9587   38.9281   14.4714
29.6500   38.9281   14.5366
31.5598   38.9281   14.4431
33.6047   38.9281   14.2049
35.6953   38.9281   13.8565
37.7402   38.9281   13.4385
39.6500   38.9281   12.9867
41.3112   38.9281   12.5589
42.7396   38.9281   12.2831
43.8090   38.9281   12.0529
44.4706   38.9281   11.9025
44.635    38.9281   11.83
&BPNODE TNODE=3, TNPC=0, TINTC=0, &END
&SECT1 STX=0.0, STY=0.0, STZ=0.0, SCALE=1.0, ALF=0.0, THETA=0.0, INMODE=4,
 TNODS=0, TNPS=0, TINTS=0, &END
44.635    42.2500   11.83
44.4810   42.2500   11.7835
43.8389   42.2500   11.7108
42.7994   42.2500   11.5989
41.1500   42.2500   11.4266
39.6500   42.2500   11.4037
37.7402   42.2500   11.3873
```

```
35.6953   42.2500   11.3790
33.6047   42.2500   11.3986
31.5598   42.2500   11.4606
29.6500   42.2500   11.5637
27.9587   42.2500   11.7270
26.5598   42.2500   11.9677
25.5145   42.2500   12.2851
24.8685   42.2500   12.6685
24.6500   42.2500   13.1000
&BPNODE TNODE=1, TNPC=0, TINTC=0, &END
24.8685   42.2500   13.5524
25.5145   42.2500   13.9496
26.5598   42.2500   14.2658
27.9587   42.2500   14.4714
29.6500   42.2500   14.5366
31.5598   42.2500   14.4431
33.6047   42.2500   14.2049
35.6953   42.2500   13.8565
37.7402   42.2500   13.4385
39.6500   42.2500   12.9867
41.3112   42.2500   12.5589
42.7396   42.2500   12.2831
43.8090   42.2500   12.0529
44.4706   42.2500   11.9025
44.635    42.2500   11.83
&BPNODE TNODE=3, TNPC=0, TINTC=0, &END
&SECT1 STX=0.0, STY=0.0, STZ=0.0, SCALE=1.0, ALF=0.0, THETA=0.0, INMODE=4,
 TNODS=0, TNPS=0, TINTS=0, &END
44.635    45.5719   11.83
44.4810   45.5719   11.7835
43.8389   45.5719   11.7108
42.7994   45.5719   11.5989
41.1500   45.5719   11.4266
39.6500   45.5719   11.4037
37.7402   45.5719   11.3873
35.6953   45.5719   11.3790
33.6047   45.5719   11.3986
31.5598   45.5719   11.4606
29.6500   45.5719   11.5637
27.9587   45.5719   11.7270
26.5598   45.5719   11.9677
25.5145   45.5719   12.2851
24.8685   45.5719   12.6685
24.6500   45.5719   13.1000
&BPNODE TNODE=1, TNPC=0, TINTC=0, &END
24.8685   45.5719   13.5524
25.5145   45.5719   13.9496
26.5598   45.5719   14.2658
27.9587   45.5719   14.4714
29.6500   45.5719   14.5366
31.5598   45.5719   14.4431
33.6047   45.5719   14.2049
35.6953   45.5719   13.8565
37.7402   45.5719   13.4385
39.6500   45.5719   12.9867
41.3112   45.5719   12.5589
42.7396   45.5719   12.2831
43.8090   45.5719   12.0529
44.4706   45.5719   11.9025
44.635    45.5719   11.83
&BPNODE TNODE=3, TNPC=0, TINTC=0, &END
&SECT1 STX=0.0, STY=0.0, STZ=0.0, SCALE=1.0, ALF=0.0, THETA=0.0, INMODE=4,
 TNODS=0, TNPS=0, TINTS=0, &END
44.635    48.5687   11.83
44.4810   48.5687   11.7835
43.8389   48.5687   11.7108
42.7994   48.5687   11.5989
41.1500   48.5687   11.4266
39.6500   48.5687   11.4037
37.7402   48.5687   11.3873
```

```
 35.6953   48.5687   11.3790
 33.6047   48.5687   11.3986
 31.5598   48.5687   11.4606
 29.6500   48.5687   11.5637
 27.9587   48.5687   11.7270
 26.5598   48.5687   11.9677
 25.5145   48.5687   12.2851
 24.8685   48.5687   12.6685
 24.6500   48.5687   13.1000
&BPNODE TNODE=1, TNPC=0, TINTC=0, &END
 24.8685   48.5687   13.5524
 25.5145   48.5687   13.9496
 26.5598   48.5687   14.2658
 27.9587   48.5687   14.4714
 29.6500   48.5687   14.5366
 31.5598   48.5687   14.4431
 33.6047   48.5687   14.2049
 35.6953   48.5687   13.8565
 37.7402   48.5687   13.4385
 39.6500   48.5687   12.9867
 41.3112   48.5687   12.5589
 42.7396   48.5687   12.2831
 43.8090   48.5687   12.0529
 44.4706   48.5687   11.9025
 44.635    48.5687   11.83
&BPNODE TNODE=3, TNPC=0, TINTC=0, &END
&SECT1 STX=0.0, STY=0.0, STZ=0.0, SCALE=1.0, ALF=0.0, THETA=0.0, INMODE=4,
 TNODS=0, TNPS=0, TINTS=0, &END
 44.635    50.9469   11.83
 44.4810   50.9469   11.7835
 43.8389   50.9469   11.7108
 42.7994   50.9469   11.5989
 41.1500   50.9469   11.4266
 39.6500   50.9469   11.4037
 37.7402   50.9469   11.3873
 35.6953   50.9469   11.3790
 33.6047   50.9469   11.3986
 31.5598   50.9469   11.4606
 29.6500   50.9469   11.5637
 27.9587   50.9469   11.7270
 26.5598   50.9469   11.9677
 25.5145   50.9469   12.2851
 24.8685   50.9469   12.6685
 24.6500   50.9469   13.1000
&BPNODE TNODE=1, TNPC=0, TINTC=0, &END
 24.8685   50.9469   13.5524
 25.5145   50.9469   13.9496
 26.5598   50.9469   14.2658
 27.9587   50.9469   14.4714
 29.6500   50.9469   14.5366
 31.5598   50.9469   14.4431
 33.6047   50.9469   14.2049
 35.6953   50.9469   13.8565
 37.7402   50.9469   13.4385
 39.6500   50.9469   12.9867
 41.3112   50.9469   12.5589
 42.7396   50.9469   12.2831
 43.8090   50.9469   12.0529
 44.4706   50.9469   11.9025
 44.6339   50.9469   11.83
&BPNODE TNODE=3, TNPC=0, TINTC=0, &END
&SECT1 STX=0.0, STY=0.0, STZ=0.0, SCALE=1.0, ALF=0.0, THETA=0.0, INMODE=4,
 TNODS=0, TNPS=0, TINTS=0, &END
 44.635    52.4739   11.83
 44.4810   52.4739   11.7835
 43.8389   52.4739   11.7108
 42.7994   52.4739   11.5989
 41.1500   52.4739   11.4266
 39.6500   52.4739   11.4037
 37.7402   52.4739   11.3873
 35.6953   52.4739   11.3790
 33.6047   52.4739   11.3986
 31.5598   52.4739   11.4606
 29.6500   52.4739   11.5637
 27.9587   52.4739   11.7270
 26.5598   52.4739   11.9677
 25.5145   52.4739   12.2851
 24.8685   52.4739   12.6685
 24.6500   52.4739   13.1000
&BPNODE TNODE=1, TNPC=0, TINTC=0, &END
 24.8685   52.4739   13.5524
 25.5145   52.4739   13.9496
 26.5598   52.4739   14.2658
 27.9587   52.4739   14.4714
 29.6500   52.4739   14.5366
 31.5598   52.4739   14.4431
 33.6047   52.4739   14.2049
 35.6953   52.4739   13.8565
 37.7402   52.4739   13.4385
 39.6500   52.4739   12.9867
 41.3112   52.4739   12.5589
 42.7396   52.4739   12.2831
 43.8090   52.4739   12.0529
 44.4706   52.4739   11.9025
 44.635    52.4739   11.83
&BPNODE TNODE=3, TNPC=0, TINTC=0, &END
&SECT1 STX=0.0, STY=0.0, STZ=0.0, SCALE=1.0, ALF=0.0, THETA=0.0, INMODE=4,
 TNODS=3, TNPS=0, TINTS=0, &END
 44.5896   53.0000   11.5308
 44.3717   53.0000   11.4932
 43.7277   53.0000   11.4770
 42.6855   53.0000   11.4565
 41.2909   53.0000   11.4290
 39.6047   53.0000   11.4032
 37.7006   53.0000   11.3871
 35.6619   53.0000   11.3790
 33.5777   53.0000   11.3991
 31.5390   53.0000   11.4614
 29.6349   53.0000   11.5647
 27.9487   53.0000   11.7283
 26.5541   53.0000   11.9690
 25.5119   53.0000   12.2862
 24.8679   53.0000   12.6691
 24.6500   53.0000   13.1000
&BPNODE TNODE=1, TNPC=0, TINTC=0, &END
 24.8679   53.0000   13.5517
 25.5119   53.0000   13.9485
 26.5541   53.0000   14.2646
 27.9487   53.0000   14.4706
 29.6349   53.0000   14.5367
 31.5390   53.0000   14.4449
 33.5777   53.0000   14.2088
 35.6619   53.0000   13.8627
 37.7006   53.0000   13.4473
 39.6047   53.0000   12.9980
 41.2909   53.0000   12.5573
 42.6855   53.0000   12.1606
 43.7277   53.0000   11.8400
 44.3717   53.0000   11.6336
 44.5896   53.0000   11.5308
&BPNODE TNODE=3, TNPC=0, TINTC=0, &END


&PATCH1 IREV=-1, IDPAT=1, MAKE=0, KCOMP=1, KASS=1, IPATSYM=0, IPATCOP=0, &END
 LEFT_AIL - 5 DEG DOWN
&SECT1 STX=0.0, STY=0.0, STZ=0.0, SCALE=1.0, ALF=0.0, THETA=0.0, INMODE=4,
 TNODS=0, TNPS=0, TINTS=0, &END
 44.5896  -31.5000   11.5308
 44.3717  -31.5000   11.4932
 43.7277  -31.5000   11.4770
```

```
  42.6855  -31.5000   11.4565
  41.2909  -31.5000   11.4290
  39.6047  -31.5000   11.4032
  37.7006  -31.5000   11.3871
  35.6619  -31.5000   11.3790
  33.5777  -31.5000   11.3991
  31.5390  -31.5000   11.4614
  29.6349  -31.5000   11.5647
  27.9487  -31.5000   11.7283
  26.5541  -31.5000   11.9690
  25.5119  -31.5000   12.2862
  24.8679  -31.5000   12.6691
  24.6500  -31.5000   13.1000
&BPNODE TNODE=1, TNPC=0, TINTC=0, &END
  24.8679  -31.5000   13.5517
  25.5119  -31.5000   13.9485
  26.5541  -31.5000   14.2646
  27.9487  -31.5000   14.4706
  29.6349  -31.5000   14.5367
  31.5390  -31.5000   14.4449
  33.5777  -31.5000   14.2088
  35.6619  -31.5000   13.8627
  37.7006  -31.5000   13.4473
  39.6047  -31.5000   12.9980
  41.2909  -31.5000   12.5573
  42.6855  -31.5000   12.1606
  43.7277  -31.5000   11.8400
  44.3717  -31.5000   11.6336
  44.5896  -31.5000   11.5308
&BPNODE TNODE=3, TNPC=0, TINTC=0, &END
&SECT1 STX=0.0, STY=0.0, STZ=0.0, SCALE=1.0, ALF=0.0, THETA=0.0, INMODE=4,
 TNODS=0, TNPS=0, TINTS=0, &END
  44.5136  -32.0261   11.232
  44.3570  -32.0261   11.2115
  43.7120  -32.0261   11.2514
  42.6688  -32.0261   11.3217
  41.1500  -32.0261   11.4266
  39.6500  -32.0261   11.4037
  37.7402  -32.0261   11.3873
  35.6953  -32.0261   11.3790
  33.6047  -32.0261   11.3986
  31.5598  -32.0261   11.4606
  29.6500  -32.0261   11.5637
  27.9587  -32.0261   11.7270
  26.5598  -32.0261   11.9677
  25.5145  -32.0261   12.2851
  24.8685  -32.0261   12.6685
  24.6500  -32.0261   13.1000
&BPNODE TNODE=1, TNPC=0, TINTC=0, &END
  24.8685  -32.0261   13.5524
  25.5145  -32.0261   13.9496
  26.5598  -32.0261   14.2658
  27.9587  -32.0261   14.4714
  29.6500  -32.0261   14.5366
  31.5598  -32.0261   14.4431
  33.6047  -32.0261   14.2049
  35.6953  -32.0261   13.8565
  37.7402  -32.0261   13.4385
  39.6500  -32.0261   12.9867
  41.3699  -32.0261   12.5256
  42.7287  -32.0261   12.0059
  43.7419  -32.0261   11.5935
  44.3674  -32.0261   11.3305
  44.518   -32.0261   11.232
&BPNODE TNODE=3, TNPC=0, TINTC=0, &END
&SECT1 STX=0.0, STY=0.0, STZ=0.0, SCALE=1.0, ALF=0.0, THETA=0.0, INMODE=4,
 TNODS=0, TNPS=0, TINTS=0, &END
  44.518   -33.5531   11.232
  44.3570  -33.5531   11.2115
  43.7120  -33.5531   11.2514
  42.6688  -33.5531   11.3217
  41.1500  -33.5531   11.4266
  39.6500  -33.5531   11.4037
  37.7402  -33.5531   11.3873
  35.6953  -33.5531   11.3790
  33.6047  -33.5531   11.3986
  31.5598  -33.5531   11.4606
  29.6500  -33.5531   11.5637
  27.9587  -33.5531   11.7270
  26.5598  -33.5531   11.9677
  25.5145  -33.5531   12.2851
  24.8685  -33.5531   12.6685
  24.6500  -33.5531   13.1000
&BPNODE TNODE=1, TNPC=0, TINTC=0, &END
  24.8685  -33.5531   13.5524
  25.5145  -33.5531   13.9496
  26.5598  -33.5531   14.2658
  27.9587  -33.5531   14.4714
  29.6500  -33.5531   14.5366
  31.5598  -33.5531   14.4431
  33.6047  -33.5531   14.2049
  35.6953  -33.5531   13.8565
  37.7402  -33.5531   13.4385
  39.6500  -33.5531   12.9867
  41.3699  -33.5531   12.5256
  42.7287  -33.5531   12.0059
  43.7419  -33.5531   11.5935
  44.3674  -33.5531   11.3305
  44.518   -33.5531   11.232
&BPNODE TNODE=3, TNPC=0, TINTC=0, &END
&SECT1 STX=0.0, STY=0.0, STZ=0.0, SCALE=1.0, ALF=0.0, THETA=0.0, INMODE=4,
 TNODS=0, TNPS=0, TINTS=0, &END
  44.518   -35.9313   11.232
  44.3570  -35.9313   11.2115
  43.7120  -35.9313   11.2514
  42.6688  -35.9313   11.3217
  41.1500  -35.9313   11.4266
  39.6500  -35.9313   11.4037
  37.7402  -35.9313   11.3873
  35.6953  -35.9313   11.3790
  33.6047  -35.9313   11.3986
  31.5598  -35.9313   11.4606
  29.6500  -35.9313   11.5637
  27.9587  -35.9313   11.7270
  26.5598  -35.9313   11.9677
  25.5145  -35.9313   12.2851
  24.8685  -35.9313   12.6685
  24.6500  -35.9313   13.1000
&BPNODE TNODE=1, TNPC=0, TINTC=0, &END
  24.8685  -35.9313   13.5524
  25.5145  -35.9313   13.9496
  26.5598  -35.9313   14.2658
  27.9587  -35.9313   14.4714
  29.6500  -35.9313   14.5366
  31.5598  -35.9313   14.4431
  33.6047  -35.9313   14.2049
  35.6953  -35.9313   13.8565
  37.7402  -35.9313   13.4385
  39.6500  -35.9313   12.9867
  41.3699  -35.9313   12.5256
  42.7287  -35.9313   12.0059
  43.7419  -35.9313   11.5935
  44.3674  -35.9313   11.3305
  44.518   -35.9313   11.232
&BPNODE TNODE=3, TNPC=0, TINTC=0, &END
&SECT1 STX=0.0, STY=0.0, STZ=0.0, SCALE=1.0, ALF=0.0, THETA=0.0, INMODE=4,
 TNODS=0, TNPS=0, TINTS=0, &END
  44.518   -38.9281   11.232
  44.3570  -38.9281   11.2115
  43.7120  -38.9281   11.2514
```

```
 42.6688   38.9281   11.3217
 41.1500  -38.9281   11.4266
 39.6500  -38.9281   11.4037
 37.7402  -38.9281   11.3873
 35.6953  -38.9281   11.3790
 33.6047  -38.9281   11.3986
 31.5598  -38.9281   11.4606
 29.6500  -38.9281   11.5637
 27.9587  -38.9281   11.7270
 26.5598  -38.9281   11.9677
 25.5145  -38.9281   12.2851
 24.8685  -38.9281   12.6685
 24.6500  -38.9281   13.1000
&BPNODE TNODE=1, TNPC=0, TINTC=0, &END
 24.8685  -38.9281   13.5524
 25.5145  -38.9281   13.9496
 26.5598  -38.9281   14.2658
 27.9587  -38.9281   14.4714
 29.6500  -38.9281   14.5366
 31.5598  -38.9281   14.4431
 33.6047  -38.9281   14.2049
 35.6953  -38.9281   13.8565
 37.7402  -38.9281   13.4385
 39.6500  -38.9281   12.9867
 41.3699  -38.9281   12.5256
 42.7287  -38.9281   12.0059
 43.7419  -38.9281   11.5935
 44.3674  -38.9281   11.3305
 44.518   -38.9281   11.232
&BPNODE TNODE=3, TNPC=0, TINTC=0, &END
&SECT1 STX=0.0, STY=0.0, STZ=0.0, SCALE=1.0, ALF=0.0, THETA=0.0, INMODE=4,
 TNODS=0, TNPS=0, TINTS=0, &END
 44.518   -42.2500   11.232
 44.3570  -42.2500   11.2115
 43.7120  -42.2500   11.2514
 42.6688  -42.2500   11.3217
 41.1500  -42.2500   11.4266
 39.6500  -42.2500   11.4037
 37.7402  -42.2500   11.3873
 35.6953  -42.2500   11.3790
 33.6047  -42.2500   11.3986
 31.5598  -42.2500   11.4606
 29.6500  -42.2500   11.5637
 27.9587  -42.2500   11.7270
 26.5598  -42.2500   11.9677
 25.5145  -42.2500   12.2851
 24.8685  -42.2500   12.6685
 24.6500  -42.2500   13.1000
&BPNODE TNODE=1, TNPC=0, TINTC=0, &END
 24.8685  -42.2500   13.5524
 25.5145  -42.2500   13.9496
 26.5598  -42.2500   14.2658
 27.9587  -42.2500   14.4714
 29.6500  -42.2500   14.5366
 31.5598  -42.2500   14.4431
 33.6047  -42.2500   14.2049
 35.6953  -42.2500   13.8565
 37.7402  -42.2500   13.4385
 39.6500  -42.2500   12.9867
 41.3699  -42.2500   12.5256
 42.7287  -42.2500   12.0059
 43.7419  -42.2500   11.5935
 44.3674  -42.2500   11.3305
 44.518   -42.2500   11.232
&BPNODE TNODE=3, TNPC=0, TINTC=0, &END
&SECT1 STX=0.0, STY=0.0, STZ=0.0, SCALE=1.0, ALF=0.0, THETA=0.0, INMODE=4,
 TNODS=0, TNPS=0, TINTS=0, &END
 44.518   -45.5719   11.232
 44.3570  -45.5719   11.2115
 43.7120  -45.5719   11.2514
```

```
 42.6688  -45.5719   11.3217
 41.1500  -45.5719   11.4266
 39.6500  -45.5719   11.4037
 37.7402  -45.5719   11.3873
 35.6953  -45.5719   11.3790
 33.6047  -45.5719   11.3986
 31.5598  -45.5719   11.4606
 29.6500  -45.5719   11.5637
 27.9587  -45.5719   11.7270
 26.5598  -45.5719   11.9677
 25.5145  -45.5719   12.2851
 24.8685  -45.5719   12.6685
 24.6500  -45.5719   13.1000
&BPNODE TNODE=1, TNPC=0, TINTC=0, &END
 24.8685  -45.5719   13.5524
 25.5145  -45.5719   13.9496
 26.5598  -45.5719   14.2658
 27.9587  -45.5719   14.4714
 29.6500  -45.5719   14.5366
 31.5598  -45.5719   14.4431
 33.6047  -45.5719   14.2049
 35.6953  -45.5719   13.8565
 37.7402  -45.5719   13.4385
 39.6500  -45.5719   12.9867
 41.3699  -45.5719   12.5256
 42.7287  -45.5719   12.0059
 43.7419  -45.5719   11.5935
 44.3674  -45.5719   11.3305
 44.518   -45.5719   11.232
&BPNODE TNODE=3, TNPC=0, TINTC=0, &END
&SECT1 STX=0.0, STY=0.0, STZ=0.0, SCALE=1.0, ALF=0.0, THETA=0.0, INMODE=4,
 TNODS=0, TNPS=0, TINTS=0, &END
 44.518   -48.5687   11.232
 44.3570  -48.5687   11.2115
 43.7120  -48.5687   11.2514
 42.6688  -48.5687   11.3217
 41.1500  -48.5687   11.4266
 39.6500  -48.5687   11.4037
 37.7402  -48.5687   11.3873
 35.6953  -48.5687   11.3790
 33.6047  -48.5687   11.3986
 31.5598  -48.5687   11.4606
 29.6500  -48.5687   11.5637
 27.9587  -48.5687   11.7270
 26.5598  -48.5687   11.9677
 25.5145  -48.5687   12.2851
 24.8685  -48.5687   12.6685
 24.6500  -48.5687   13.1000
&BPNODE TNODE=1, TNPC=0, TINTC=0, &END
 24.8685  -48.5687   13.5524
 25.5145  -48.5687   13.9496
 26.5598  -48.5687   14.2658
 27.9587  -48.5687   14.4714
 29.6500  -48.5687   14.5366
 31.5598  -48.5687   14.4431
 33.6047  -48.5687   14.2049
 35.6953  -48.5687   13.8565
 37.7402  -48.5687   13.4385
 39.6500  -48.5687   12.9867
 41.3699  -48.5687   12.5256
 42.7287  -48.5687   12.0059
 43.7419  -48.5687   11.5935
 44.3674  -48.5687   11.3305
 44.518   -48.5687   11.232
&BPNODE TNODE=3, TNPC=0, TINTC=0, &END
&SECT1 STX=0.0, STY=0.0, STZ=0.0, SCALE=1.0, ALF=0.0, THETA=0.0, INMODE=4,
 TNODS=0, TNPS=0, TINTS=0, &END
 44.518   -50.9469   11.232
 44.3570  -50.9469   11.2115
 43.7120  -50.9469   11.2514
```

```
   42.6688  -50.9469   11.3217
   41.1500  -50.9469   11.4266
   39.6500  -50.9469   11.4037
   37.7402  -50.9469   11.3873
   35.6953  -50.9469   11.3790
   33.6047  -50.9469   11.3986
   31.5598  -50.9469   11.4606
   29.6500  -50.9469   11.5637
   27.9587  -50.9469   11.7270
   26.5598  -50.9469   11.9677
   25.5145  -50.9469   12.2851
   24.8685  -50.9469   12.6685
   24.6500  -50.9469   13.1000
&BPNODE TNODE=1, TNPC=0, TINTC=0, &END
   24.8685  -50.9469   13.5524
   25.5145  -50.9469   13.9496
   26.5598  -50.9469   14.2658
   27.9587  -50.9469   14.4714
   29.6500  -50.9469   14.5366
   31.5598  -50.9469   14.4431
   33.6047  -50.9469   14.2049
   35.6953  -50.9469   13.8565
   37.7402  -50.9469   13.4385
   39.6500  -50.9469   12.9867
   41.3699  -50.9469   12.5256
   42.7287  -50.9469   12.0059
   43.7419  -50.9469   11.5935
   44.3674  -50.9469   11.3305
   44.5216  -50.9469   11.232
&BPNODE TNODE=3, TNPC=0, TINTC=0, &END
&SECT1 STX=0.0, STY=0.0, STZ=0.0, SCALE=1.0, ALF=0.0, THETA=0.0, INMODE=4,
 TNODS=0, TNPS=0, TINTS=0, &END
   44.518   -52.4739   11.232
   44.3570  -52.4739   11.2115
   43.7120  -52.4739   11.2514
   42.6688  -52.4739   11.3217
   41.1500  -52.4739   11.4266
   39.6500  -52.4739   11.4037
   37.7402  -52.4739   11.3873
   35.6953  -52.4739   11.3790
   33.6047  -52.4739   11.3986
   31.5598  -52.4739   11.4606
   29.6500  -52.4739   11.5637
   27.9587  -52.4739   11.7270
   26.5598  -52.4739   11.9677
   25.5145  -52.4739   12.2851
   24.8685  -52.4739   12.6685
   24.6500  -52.4739   13.1000
&BPNODE TNODE=1, TNPC=0, TINTC=0, &END
   24.8685  -52.4739   13.5524
   25.5145  -52.4739   13.9496
   26.5598  -52.4739   14.2658
   27.9587  -52.4739   14.4714
   29.6500  -52.4739   14.5366
   31.5598  -52.4739   14.4431
   33.6047  -52.4739   14.2049
   35.6953  -52.4739   13.8565
   37.7402  -52.4739   13.4385
   39.6500  -52.4739   12.9867
   41.3699  -52.4739   12.5256
   42.7287  -52.4739   12.0059
   43.7419  -52.4739   11.5935
   44.3674  -52.4739   11.3305
   44.518   -52.4739   11.232
&BPNODE TNODE=3, TNPC=0, TINTC=0, &END
&SECT1 STX=0.0, STY=0.0, STZ=0.0, SCALE=1.0, ALF=0.0, THETA=0.0, INMODE=4,
 TNODS=3, TNPS=0, TINTS=0, &END
   44.5896  -53.0000   11.5308
   44.3717  -53.0000   11.4932
   43.7277  -53.0000   11.4770
   42.6855  -53.0000   11.4565
   41.2909  -53.0000   11.4290
   39.6047  -53.0000   11.4032
   37.7006  -53.0000   11.3871
   35.6619  -53.0000   11.3790
   33.5777  -53.0000   11.3991
   31.5390  -53.0000   11.4614
   29.6349  -53.0000   11.5647
   27.9487  -53.0000   11.7283
   26.5541  -53.0000   11.9690
   25.5119  -53.0000   12.2862
   24.8679  -53.0000   12.6691
   24.6500  -53.0000   13.1000
&BPNODE TNODE=1, TNPC=0, TINTC=0, &END
   24.8679  -53.0000   13.5517
   25.5119  -53.0000   13.9485
   26.5541  -53.0000   14.2646
   27.9487  -53.0000   14.4706
   29.6349  -53.0000   14.5367
   31.5390  -53.0000   14.4449
   33.5777  -53.0000   14.2088
   35.6619  -53.0000   13.8627
   37.7006  -53.0000   13.4473
   39.6047  -53.0000   12.9980
   41.2909  -53.0000   12.5573
   42.6855  -53.0000   12.1606
   43.7277  -53.0000   11.8400
   44.3717  -53.0000   11.6336
   44.5896  -53.0000   11.5308
&BPNODE TNODE=3, TNPC=0, TINTC=0, &END


&PATCH1 IREV=0, IDPAT=1, MAKE=0, KCOMP=1, KASS=1, IPATSYM=1, IPATCOP=0, &END
  ELEVATOR +5 DEG (TED) 10X16
&SECT1 STX=0.0, STY=0.0, STZ=0.0, SCALE=1.0, ALF=0.0, THETA=0.0, INMODE=4,
 TNODS=0, TNPS=0, TINTS=0, &END
   95.988     0.0000    7.85
   95.8588    0.0000    7.8439
   95.4739    0.0000    7.8513
   94.8489    0.0000    7.8651
   94.0082    0.0000    7.8870
   93.2460    0.0000    7.9099
   91.8331    0.0000    7.8370
   90.5669    0.0000    7.7806
   89.2500    0.0000    7.7327
   87.9331    0.0000    7.6989
   86.6669    0.0000    7.6850
   85.4999    0.0000    7.6952
   84.4770    0.0000    7.7316
   83.6376    0.0000    7.7933
   83.0138    0.0000    7.8771
   82.6297    0.0000    7.9775
   82.5000    0.0000    8.0900
&BPNODE TNODE=1, TNPC=0, TINTC=0, &END
   82.6297    0.0000    8.2025
   83.0138    0.0000    8.3029
   83.6376    0.0000    8.3867
   84.4770    0.0000    8.4484
   85.4999    0.0000    8.4848
   86.6669    0.0000    8.4950
   87.9331    0.0000    8.4811
   89.2500    0.0000    8.4473
   90.5669    0.0000    8.3994
   91.8331    0.0000    8.3430
   93.2460    0.0000    8.2701
   94.0318    0.0000    8.1575
   94.8636    0.0000    8.0332
   95.4815    0.0000    7.9382
   95.8618    0.0000    7.8786
   95.988     0.0000    7.85
```

```
&BPNODE TNODE=3, TNPC=0, TINTC=0, &END
&SECT1 STX=0.0, STY=0.0, STZ=0.0, SCALE=1.0, ALF=0.0, THETA=0.0, INMODE=4,
 TNODS=0, TNPS=0, TINTS=0, &END
  95.9907    0.4864    7.851
  95.8609    0.4864    7.8432
  95.4787    0.4864    7.8506
  94.8583    0.4864    7.8642
  94.0236    0.4864    7.8861
  93.2391    0.4864    7.9097
  91.8642    0.4864    7.8388
  90.6070    0.4864    7.7828
  89.2996    0.4864    7.7352
  87.9921    0.4864    7.7017
  86.7349    0.4864    7.6879
  85.5763    0.4864    7.6980
  84.5608    0.4864    7.7342
  83.7273    0.4864    7.7954
  83.1080    0.4864    7.8787
  82.7267    0.4864    7.9783
  82.5979    0.4864    8.0900
&BPNODE TNODE=1, TNPC=0, TINTC=0, &END
  82.7267    0.4864    8.2017
  83.1080    0.4864    8.3013
  83.7273    0.4864    8.3846
  84.5608    0.4864    8.4458
  85.5763    0.4864    8.4820
  86.7349    0.4864    8.4921
  87.9921    0.4864    8.4783
  89.2996    0.4864    8.4448
  90.6070    0.4864    8.3972
  91.8642    0.4864    8.3412
  93.2391    0.4864    8.2703
  94.0471    0.4864    8.1546
  94.8729    0.4864    8.0312
  95.4863    0.4864    7.9369
  95.8639    0.4864    7.8777
  95.9907    0.4864    7.851
&BPNODE TNODE=3, TNPC=0, TINTC=0, &END
&SECT1 STX=0.0, STY=0.0, STZ=0.0, SCALE=1.0, ALF=0.0, THETA=0.0, INMODE=4,
 TNODS=0, TNPS=0, TINTS=0, &END
  95.9941    1.8979    7.847
  95.8671    1.8979    7.8415
  95.4929    1.8979    7.8487
  94.8854    1.8979    7.8621
  94.0682    1.8979    7.8834
  93.2212    1.8979    7.9091
  91.9543    1.8979    7.8441
  90.7234    1.8979    7.7892
  89.4434    1.8979    7.7426
  88.1633    1.8979    7.7098
  86.9324    1.8979    7.6963
  85.7980    1.8979    7.7062
  84.8038    1.8979    7.7416
  83.9878    1.8979    7.8015
  83.3814    1.8979    7.8831
  83.0080    1.8979    7.9806
  82.8820    1.8979    8.0900
&BPNODE TNODE=1, TNPC=0, TINTC=0, &END
  83.0080    1.8979    8.1994
  83.3814    1.8979    8.2969
  83.9878    1.8979    8.3785
  84.8038    1.8979    8.4384
  85.7980    1.8979    8.4738
  86.9324    1.8979    8.4837
  88.1633    1.8979    8.4702
  89.4434    1.8979    8.4374
  90.7234    1.8979    8.3908
  91.9543    1.8979    8.3359
  93.2212    1.8979    8.2709
  94.0912    1.8979    8.1464
  94.8997    1.8979    8.0255
  95.5003    1.8979    7.9332
  95.8701    1.8979    7.8753
  95.9941    1.8979    7.847
&BPNODE TNODE=3, TNPC=0, TINTC=0, &END
&SECT1 STX=0.0, STY=0.0, STZ=0.0, SCALE=1.0, ALF=0.0, THETA=0.0, INMODE=4,
 TNODS=0, TNPS=0, TINTS=0, &END
  95.9996    4.0964    7.845
  95.8768    4.0964    7.8394
  95.5150    4.0964    7.8463
  94.9278    4.0964    7.8592
  94.1378    4.0964    7.8799
  93.2001    4.0964    7.9086
  92.0947    4.0964    7.8523
  90.9048    4.0964    7.7992
  89.6674    4.0964    7.7542
  88.4299    4.0964    7.7224
  87.2400    4.0964    7.7094
  86.1434    4.0964    7.7190
  85.1822    4.0964    7.7532
  84.3934    4.0964    7.8111
  83.8073    4.0964    7.8900
  83.4463    4.0964    7.9843
  83.3244    4.0964    8.0900
&BPNODE TNODE=1, TNPC=0, TINTC=0, &END
  83.4463    4.0964    8.1957
  83.8073    4.0964    8.2900
  84.3934    4.0964    8.3689
  85.1822    4.0964    8.4268
  86.1434    4.0964    8.4610
  87.2400    4.0964    8.4706
  88.4299    4.0964    8.4576
  89.6674    4.0964    8.4258
  90.9048    4.0964    8.3808
  92.0947    4.0964    8.3277
  93.2001    4.0964    8.2714
  94.1600    4.0964    8.1341
  94.9416    4.0964    8.0172
  95.5222    4.0964    7.9280
  95.8796    4.0964    7.8720
  95.9996    4.0964    7.845
&BPNODE TNODE=3, TNPC=0, TINTC=0, &END
&SECT1 STX=0.0, STY=0.0, STZ=0.0, SCALE=1.0, ALF=0.0, THETA=0.0, INMODE=4,
 TNODS=0, TNPS=0, TINTS=0, &END
  96.004     6.8667    7.843
  95.8870    6.8667    7.8378
  95.5410    6.8667    7.8445
  94.9792    6.8667    7.8568
  94.2234    6.8667    7.8766
  93.1853    6.8666    7.9088
  92.2716    6.8666    7.8626
  91.1334    6.8666    7.8119
  89.9496    6.8666    7.7688
  88.7659    6.8666    7.7384
  87.6276    6.8666    7.7259
  86.5786    6.8666    7.7351
  85.6591    6.8666    7.7678
  84.9046    6.8666    7.8233
  84.3438    6.8666    7.8987
  83.9986    6.8666    7.9889
  83.8820    6.8666    8.0900
&BPNODE TNODE=1, TNPC=0, TINTC=0, &END
  83.9986    6.8666    8.1911
  84.3438    6.8666    8.2813
  84.9046    6.8666    8.3567
  85.6591    6.8666    8.4122
  86.5786    6.8666    8.4449
  87.6276    6.8666    8.4541
  88.7659    6.8666    8.4416
  89.9496    6.8666    8.4112
```

```
   91.1334     6.8666     8.3681
   92.2716     6.8666     8.3174
   93.3333     6.8666     8.2516
   94.2447     6.8666     8.1197
   94.9924     6.8666     8.0080
   95.5478     6.8667     7.9226
   95.8897     6.8667     7.8690
   96.004      6.8667     7.843
 &BPNODE TNODE=3, TNPC=0, TINTC=0, &END
 &SECT1 STX=0.0, STY=0.0, STZ=0.0, SCALE=1.0, ALF=0.0, THETA=0.0, INMODE=4,
  TNODS=0, TNPS=0, TINTS=0, &END
   96.0126     9.9375     7.843
   95.9010     9.9375     7.8373
   95.5724     9.9375     7.8436
   95.0389     9.9375     7.8553
   94.3211     9.9375     7.8741
   93.1841     9.9375     7.9099
   92.4677     9.9375     7.8740
   91.3867     9.9375     7.8258
   90.2625     9.9375     7.7849
   89.1383     9.9375     7.7561
   88.0573     9.9375     7.7442
   87.0610     9.9375     7.7530
   86.1878     9.9375     7.7840
   85.4712     9.9375     7.8367
   84.9386     9.9375     7.9083
   84.6107     9.9375     7.9939
   84.5000     9.9375     8.0900
 &BPNODE TNODE=1, TNPC=0, TINTC=0, &END
   84.6107     9.9375     8.1861
   84.9386     9.9375     8.2717
   85.4712     9.9375     8.3433
   86.1878     9.9375     8.3960
   87.0610     9.9375     8.4270
   88.0573     9.9375     8.4358
   89.1383     9.9375     8.4239
   90.2625     9.9375     8.3951
   91.3867     9.9375     8.3542
   92.4677     9.9375     8.3060
   93.4757     9.9375     8.2302
   94.3414     9.9375     8.1050
   95.0514     9.9375     7.9989
   95.5789     9.9375     7.9178
   95.9036     9.9375     7.8669
   96.0126     9.9375     7.843
 &BPNODE TNODE=3, TNPC=0, TINTC=0, &END
 &SECT1 STX=0.0, STY=0.0, STZ=0.0, SCALE=1.0, ALF=0.0, THETA=0.0, INMODE=4,
  TNODS=0, TNPS=0, TINTS=0, &END
   96.0208    13.0084     7.843
   95.9151    13.0084     7.8382
   95.6039    13.0084     7.8441
   95.0986    13.0084     7.8553
   94.4189    13.0084     7.8730
   93.1989    13.0084     7.9121
   92.6638    13.0084     7.8855
   91.6401    13.0084     7.8398
   90.5754    13.0084     7.8011
   89.5107    13.0084     7.7738
   88.4869    13.0084     7.7626
   87.5434    13.0084     7.7708
   86.7165    13.0084     7.8002
   86.0378    13.0084     7.8501
   85.5334    13.0084     7.9179
   85.2229    13.0084     7.9990
   85.1180    13.0084     8.0900
 &BPNODE TNODE=1, TNPC=0, TINTC=0, &END
   85.2229    13.0084     8.1810
   85.5334    13.0084     8.2621
   86.0378    13.0084     8.3299
   86.7165    13.0084     8.3798
   87.5434    13.0084     8.4092
   88.4869    13.0084     8.4174
   89.5107    13.0084     8.4062
   90.5754    13.0084     8.3789
   91.6401    13.0084     8.3402
   92.6638    13.0084     8.2945
   93.6182    13.0083     8.2103
   94.4380    13.0083     8.0917
   95.1105    13.0084     7.9912
   95.6100    13.0084     7.9144
   95.9175    13.0084     7.8662
   96.0208    13.0084     7.843
 &BPNODE TNODE=3, TNPC=0, TINTC=0, &END
 &SECT1 STX=0.0, STY=0.0, STZ=0.0, SCALE=1.0, ALF=0.0, THETA=0.0, INMODE=4,
  TNODS=0, TNPS=0, TINTS=0, &END
   96.029     15.7786     7.844
   95.9286    15.7786     7.8401
   95.6331    15.7786     7.8458
   95.1533    15.7786     7.8563
   94.5079    15.7786     7.8732
   93.7217    15.7786     7.8975
   93.2260    15.7786     7.9148
   91.8686    15.7786     7.8524
   90.8576    15.7786     7.8157
   89.8467    15.7786     7.7897
   88.8745    15.7786     7.7791
   87.9786    15.7786     7.7869
   87.1934    15.7786     7.8148
   86.5489    15.7786     7.8622
   86.0700    15.7786     7.9266
   85.7751    15.7786     8.0036
   85.6756    15.7786     8.0900
 &BPNODE TNODE=1, TNPC=0, TINTC=0, &END
   85.7751    15.7786     8.1764
   86.0700    15.7786     8.2534
   86.5489    15.7786     8.3178
   87.1934    15.7786     8.3652
   87.9786    15.7786     8.3931
   88.8745    15.7786     8.4009
   89.8467    15.7786     8.3903
   90.8576    15.7786     8.3643
   91.8686    15.7786     8.3276
   93.2260    15.7786     8.2652
   93.7476    15.7786     8.1935
   94.5261    15.7786     8.0809
   95.1646    15.7786     7.9854
   95.6389    15.7786     7.9125
   95.9310    15.7786     7.8668
   96.029     15.7786     7.844
 &BPNODE TNODE=3, TNPC=0, TINTC=0, &END
 &SECT1 STX=0.0, STY=0.0, STZ=0.0, SCALE=1.0, ALF=0.0, THETA=0.0, INMODE=4,
  TNODS=0, TNPS=0, TINTS=0, &END
   96.0347    17.9771     7.847
   95.9385    17.9771     7.8425
   95.6554    17.9771     7.8480
   95.1959    17.9771     7.8581
   94.5776    17.9771     7.8742
   93.8246    17.9771     7.8975
   93.2568    17.9771     7.9175
   92.0500    17.9771     7.8625
   91.0816    17.9771     7.8272
   90.1133    17.9771     7.8024
   89.1821    17.9771     7.7922
   88.3240    17.9771     7.7997
   87.5718    17.9771     7.8264
   86.9546    17.9771     7.8718
   86.4959    17.9771     7.9335
   86.2134    17.9771     8.0073
   86.1180    17.9771     8.0900
 &BPNODE TNODE=1, TNPC=0, TINTC=0, &END
```

```
  86.2134   17.9771   8.1727
  86.4959   17.9771   8.2465
  86.9546   17.9771   8.3082
  87.5718   17.9771   8.3536
  88.3240   17.9771   8.3803
  89.1821   17.9771   8.3878
  90.1133   17.9771   8.3776
  91.0816   17.9771   8.3528
  92.0500   17.9771   8.3175
  93.2568   17.9771   8.2625
  93.8494   17.9771   8.1810
  94.5950   17.9771   8.0731
  95.2067   17.9771   7.9817
  95.6610   17.9771   7.9119
  95.9407   17.9771   7.8681
  96.0347   17.9771   7.847
&BPNODE TNODE=3, TNPC=0, TINTC=0, &END
&SECT1 STX=0.0, STY=0.0, STZ=0.0, SCALE=1.0, ALF=0.0, THETA=0.0, INMODE=4,
 TNODS=0, TNPS=0, TINTS=0, &END
  96.0382   19.3886   7.848
  95.9448   19.3886   7.8444
  95.6698   19.3887   7.8497
  95.2232   19.3887   7.8595
  94.6224   19.3887   7.8753
  93.8907   19.3887   7.8979
  93.2810   19.3886   7.9195
  92.1664   19.3886   7.8689
  91.2254   19.3886   7.8347
  90.2845   19.3886   7.8105
  89.3796   19.3886   7.8006
  88.5457   19.3886   7.8079
  87.8148   19.3886   7.8339
  87.2150   19.3886   7.8780
  86.7693   19.3886   7.9379
  86.4948   19.3886   8.0096
  86.4021   19.3886   8.0900
&BPNODE TNODE=1, TNPC=0, TINTC=0, &END
  86.4948   19.3886   8.1704
  86.7693   19.3886   8.2421
  87.2150   19.3886   8.3020
  87.8148   19.3886   8.3461
  88.5457   19.3886   8.3721
  89.3796   19.3886   8.3794
  90.2845   19.3886   8.3695
  91.2254   19.3886   8.3453
  92.1664   19.3886   8.3111
  93.2810   19.3886   8.2605
  93.9148   19.3886   8.1733
  94.6394   19.3886   8.0685
  95.2337   19.3886   7.9797
  95.6752   19.3886   7.9118
  95.9470   19.3886   7.8693
  96.0382   19.3886   7.848
&BPNODE TNODE=3, TNPC=0, TINTC=0, &END
&SECT1 STX=0.0, STY=0.0, STZ=0.0, SCALE=1.0, ALF=0.0, THETA=0.0, INMODE=4,
 TNODS=3, TNPS=0, TINTS=0, &END
  96.0395   19.8750   7.849
  95.9470   19.8750   7.8452
  95.6747   19.8750   7.8504
  95.2326   19.8750   7.8601
  94.6379   19.8750   7.8757
  93.9135   19.8750   7.8980
  93.2900   19.8750   7.9202
  92.2066   19.8750   7.8711
  91.2750   19.8750   7.8372
  90.3434   19.8750   7.8133
  89.4477   19.8750   7.8035
  88.6222   19.8750   7.8107
  87.8986   19.8750   7.8365
  87.3047   19.8750   7.8801
  86.8635   19.8750   7.9394
  86.5918   19.8750   8.0104
  86.5000   19.8750   8.0900
&BPNODE TNODE=1, TNPC=0, TINTC=0, &END
  86.5918   19.8750   8.1696
  86.8635   19.8750   8.2406
  87.3047   19.8750   8.2999
  87.8986   19.8750   8.3435
  88.6222   19.8750   8.3693
  89.4477   19.8750   8.3765
  90.3434   19.8750   8.3667
  91.2750   19.8750   8.3428
  92.2066   19.8750   8.3089
  93.2900   19.8750   8.2598
  93.9374   19.8750   8.1708
  94.6546   19.8750   8.0670
  95.2430   19.8750   7.9791
  95.6801   19.8750   7.9119
  95.9492   19.8750   7.8697
  96.0395   19.8750   7.849
&BPNODE TNODE=3, TNPC=0, TINTC=0, &END

&PATCH1 IREV=0, IDPAT=1, MAKE=0, KCOMP=1, KASS=1, IPATSYM=0, IPATCOP=0, &END
  RUDDER  +5 DEG (TEL) 10X12
&SECT1 STX=0.0, STY=0.0, STZ=0.0, SCALE=1.0, ALF=0.0, THETA=0.0, INMODE=4,
 TNODS=0, TNPS=0, TINTS=0, &END
  97.4877   -0.413    10.4049
  97.1510   -0.3501   10.4038
  96.1610   -0.2008   10.4006
  94.5854    0.0287   10.3958
  92.5000    0.3161   10.4000
  90.0882    0.4315   10.4000
  87.5000    0.5294   10.4000
  84.9118    0.5900   10.4000
  82.5000    0.5942   10.4000
  80.4289    0.5310   10.4000
  78.8397    0.4015   10.4000
  77.8407    0.2183   10.4000
  77.5000    0.0000   10.4000
&BPNODE TNODE=1, TNPC=0, TINTC=0, &END
  77.8407   -0.2183   10.4000
  78.8397   -0.4015   10.4000
  80.4289   -0.5310   10.4000
  82.5000   -0.5942   10.4000
  84.9118   -0.5900   10.4000
  87.5000   -0.5294   10.4000
  90.0882   -0.4315   10.4000
  92.4786   -0.3151   10.4070
  94.5521   -0.3721   10.4067
  96.1439   -0.4057   10.4062
  97.1451   -0.4218   10.4058
  97.4877   -0.413    10.4056
&BPNODE TNODE=3, TNPC=0, TINTC=0, &END
&SECT1 STX=0.0, STY=0.0, STZ=0.0, SCALE=1.0, ALF=0.0, THETA=0.0, INMODE=4,
 TNODS=0, TNPS=0, TINTS=0, &END
  97.6057   -0.4180   10.7661
  97.2733   -0.3558   10.7650
  96.2954   -0.2083   10.7618
  94.7391    0.0183   10.7570
  92.5590    0.3185   10.7610
  90.2976    0.4262   10.7610
  87.7410    0.5229   10.7610
  85.1845    0.5828   10.7610
  82.8022    0.5869   10.7610
  80.7565    0.5245   10.7610
  79.1868    0.3966   10.7610
  78.2000    0.2157   10.7610
  77.8634    0.0000   10.7610
&BPNODE TNODE=1, TNPC=0, TINTC=0, &END
  78.2000   -0.2157   10.7610
```

```
  79.1868   -0.3966   10.7610
  80.7565   -0.5245   10.7610
  82.8022   -0.5869   10.7610
  85.1845   -0.5828   10.7610
  87.7410   -0.5229   10.7610
  90.2976   -0.4262   10.7610
  92.6581   -0.3212   10.7682
  94.7062   -0.3775   10.7679
  96.2786   -0.4108   10.7674
  97.2674   -0.4267   10.7669
  97.6057   -0.4180   10.7668
&BPNODE TNODE=3, TNPC=0, TINTC=0, &END
&SECT1 STX=0.0, STY=0.0, STZ=0.0, SCALE=1.0, ALF=0.0, THETA=0.0, INMODE=4,
 TNODS=0, TNPS=0, TINTS=0, &END
  97.9488   -0.432    11.8141
  97.6283   -0.3710   11.8131
  96.6855   -0.2288   11.8100
  95.1852   -0.0103   11.8054
  92.7472    0.3243   11.8085
  90.9052    0.4109   11.8085
  88.4406    0.5041   11.8085
  85.9760    0.5618   11.8085
  83.6793    0.5658   11.8085
  81.7071    0.5056   11.8085
  80.1938    0.3823   11.8085
  79.2425    0.2079   11.8085
  78.9180    0.0000   11.8085
&BPNODE TNODE=1, TNPC=0, TINTC=0, &END
  79.2425   -0.2079   11.8085
  80.1938   -0.3823   11.8085
  81.7071   -0.5056   11.8085
  83.6793   -0.5658   11.8085
  85.9760   -0.5618   11.8085
  88.4406   -0.5041   11.8085
  90.9052   -0.4109   11.8085
  93.1790   -0.3377   11.8161
  95.1534   -0.3919   11.8159
  96.6693   -0.4240   11.8154
  97.6226   -0.4393   11.8149
  97.9488   -0.432    11.8148
&BPNODE TNODE=3, TNPC=0, TINTC=0, &END
&SECT1 STX=0.0, STY=0.0, STZ=0.0, SCALE=1.0, ALF=0.0, THETA=0.0, INMODE=4,
 TNODS=0, TNPS=0, TINTS=0, &END
  98.4834   -0.448    13.4464
  98.1815   -0.3905   13.4454
  97.2935   -0.2565   13.4426
  95.8803   -0.0507   13.4382
  93.0906    0.3301   13.4401
  91.8516    0.3871   13.4401
  89.5302    0.4748   13.4401
  87.2087    0.5292   13.4401
  85.0454    0.5330   13.4401
  83.1878    0.4763   13.4401
  81.7624    0.3601   13.4401
  80.8663    0.1958   13.4401
  80.5607    0.0000   13.4401
&BPNODE TNODE=1, TNPC=0, TINTC=0, &END
  80.8663   -0.1958   13.4401
  81.7624   -0.3601   13.4401
  83.1878   -0.4763   13.4401
  85.0454   -0.5330   13.4401
  87.2087   -0.5292   13.4401
  89.5302   -0.4748   13.4401
  91.8516   -0.3871   13.4401
  93.9906   -0.3591   13.4483
  95.8504   -0.4102   13.4480
  97.2782   -0.4404   13.4476
  98.1762   -0.4548   13.4472
  98.4834   -0.448    13.4470
&BPNODE TNODE=3, TNPC=0, TINTC=0, &END
&SECT1 STX=0.0, STY=0.0, STZ=0.0, SCALE=1.0, ALF=0.0, THETA=0.0, INMODE=4,
 TNODS=0, TNPS=0, TINTS=0, &END
  99.1565   -0.460    15.5033
  98.8781   -0.4077   15.5024
  98.0591   -0.2842   15.4998
  96.7556   -0.0944   15.4958
  95.0561    0.1422   15.4908
  93.6103    0.3318   15.4960
  90.9031    0.4380   15.4960
  88.7620    0.4881   15.4960
  86.7668    0.4916   15.4960
  85.0535    0.4393   15.4960
  83.7389    0.3321   15.4960
  82.9124    0.1806   15.4960
  82.6305    0.0000   15.4960
&BPNODE TNODE=1, TNPC=0, TINTC=0, &END
  82.9124   -0.1806   15.4960
  83.7389   -0.3321   15.4960
  85.0535   -0.4393   15.4960
  86.7668   -0.4916   15.4960
  88.7620   -0.4881   15.4960
  90.9031   -0.4380   15.4960
  93.6103   -0.3318   15.4960
  95.0128   -0.3788   15.5051
  96.7281   -0.4259   15.5048
  98.0450   -0.4538   15.5044
  98.8731   -0.4671   15.5040
  99.1565   -0.460    15.5039
&BPNODE TNODE=3, TNPC=0, TINTC=0, &END
&SECT1 STX=0.0, STY=0.0, STZ=0.0, SCALE=1.0, ALF=0.0, THETA=0.0, INMODE=4,
 TNODS=0, TNPS=0, TINTS=0, &END
  99.9086   -0.465    17.7815
  99.6562   -0.4178   17.7807
  98.9136   -0.3058   17.7783
  97.7319   -0.1337   17.7746
  96.1911    0.0808   17.7702
  94.3000    0.3265   17.7750
  92.4250    0.3971   17.7750
  90.4839    0.4425   17.7750
  88.6750    0.4456   17.7750
  87.1217    0.3982   17.7750
  85.9298    0.3011   17.7750
  85.1806    0.1637   17.7750
  84.9250    0.0000   17.7750
&BPNODE TNODE=1, TNPC=0, TINTC=0, &END
  85.1806   -0.1637   17.7750
  85.9298   -0.3011   17.7750
  87.1217   -0.3982   17.7750
  88.6750   -0.4456   17.7750
  90.4839   -0.4425   17.7750
  92.4250   -0.3971   17.7750
  94.3420   -0.3280   17.7829
  96.1519   -0.3915   17.7831
  97.7070   -0.4342   17.7828
  98.9009   -0.4595   17.7825
  99.6517   -0.4716   17.7821
  99.9086   -0.465    17.7820
&BPNODE TNODE=3, TNPC=0, TINTC=0, &END
&SECT1 STX=0.0, STY=0.0, STZ=0.0, SCALE=1.0, ALF=0.0, THETA=0.0, INMODE=4,
 TNODS=0, TNPS=0, TINTS=0, &END
 100.657    -0.461    20.0608
 100.4305   -0.4177   20.0601
  99.7645   -0.3173   20.0579
  98.7045   -0.1629   20.0547
  97.3224    0.0295   20.0507
  95.1090    0.3144   20.0540
  93.9469    0.3562   20.0540
  92.2057    0.3969   20.0540
  90.5832    0.3997   20.0540
  89.1899    0.3572   20.0540
```

```
  88.1208     0.2701    20.0540
  87.4487     0.1469    20.0540
  87.2195     0.0000    20.0540
&BPNODE TNODE=1, TNPC=0, TINTC=0, &END
  87.4487    -0.1469    20.0540
  88.1208    -0.2701    20.0540
  89.1899    -0.3572    20.0540
  90.5832    -0.3997    20.0540
  92.2057    -0.3969    20.0540
  93.9469    -0.3562    20.0540
  95.6638    -0.3372    20.0621
  97.2872    -0.3942    20.0622
  98.6821    -0.4325    20.0620
  99.7530    -0.4552    20.0617
 100.4265    -0.4660    20.0614
 100.657     -0.461     20.0613
&BPNODE TNODE=3, TNPC=0, TINTC=0, &END
&SECT1 STX=0.0, STY=0.0, STZ=0.0, SCALE=1.0, ALF=0.0, THETA=0.0, INMODE=4,
 TNODS=0, TNPS=0, TINTS=0, &END
 101.3318    -0.447     22.1171
 101.1288    -0.4092    22.1164
 100.5318    -0.3191    22.1145
  99.5816    -0.1808    22.1116
  98.3427    -0.0083    22.1080
  96.8990     0.1815    22.1041
  95.9413     0.2981    22.1099
  93.7590     0.3558    22.1099
  92.3046     0.3583    22.1099
  91.0556     0.3202    22.1099
  90.0972     0.2421    22.1099
  89.4948     0.1317    22.1099
  89.2893     0.0000    22.1099
&BPNODE TNODE=1, TNPC=0, TINTC=0, &END
  89.4948    -0.1317    22.1099
  90.0972    -0.2421    22.1099
  91.0556    -0.3202    22.1099
  92.3046    -0.3583    22.1099
  93.7590    -0.3558    22.1099
  95.9413    -0.2981    22.1099
  96.8559    -0.3370    22.1183
  98.3111    -0.3881    22.1184
  99.5615    -0.4224    22.1182
 100.5215    -0.4427    22.1179
 101.1252    -0.4524    22.1176
 101.3318    -0.447     22.1175
&BPNODE TNODE=3, TNPC=0, TINTC=0, &END
&SECT1 STX=0.0, STY=0.0, STZ=0.0, SCALE=1.0, ALF=0.0, THETA=0.0, INMODE=4,
 TNODS=0, TNPS=0, TINTS=0, &END
 101.869     -0.432     23.7484
 101.6846    -0.3967    23.7478
 101.1423    -0.3149    23.7461
 100.2793    -0.1893    23.7434
  99.1540    -0.0326    23.7402
  97.8427     0.1397    23.7366
  96.6709     0.2815    23.7415
  94.9917     0.3232    23.7415
  93.6707     0.3255    23.7415
  92.5363     0.2908    23.7415
  91.6658     0.2199    23.7415
  91.1186     0.1196    23.7415
  90.9320     0.0000    23.7415
&BPNODE TNODE=1, TNPC=0, TINTC=0, &END
  91.1186    -0.1196    23.7415
  91.6658    -0.2199    23.7415
  92.5363    -0.2908    23.7415
  93.6707    -0.3255    23.7415
  94.9917    -0.3232    23.7415
  96.6709    -0.2815    23.7415
  97.8035    -0.3312    23.7495
  99.1253    -0.3776    23.7496
 100.2610    -0.4088    23.7494
 101.1330    -0.4272    23.7492
 101.6813    -0.4360    23.7489
 101.869     -0.432     23.7488
&BPNODE TNODE=3, TNPC=0, TINTC=0, &END
&SECT1 STX=0.0, STY=0.0, STZ=0.0, SCALE=1.0, ALF=0.0, THETA=0.0, INMODE=4,
 TNODS=0, TNPS=0, TINTS=0, &END
 102.214     -0.419     24.7958
 102.0415    -0.3861    24.7952
 101.5344    -0.3096    24.7936
 100.7273    -0.1920    24.7911
  99.6750    -0.0456    24.7881
  98.4487     0.1156    24.7848
  97.1716     0.2692    24.7890
  95.7832     0.3022    24.7890
  94.5478     0.3044    24.7890
  93.4869     0.2720    24.7890
  92.6729     0.2057    24.7890
  92.1611     0.1118    24.7890
  91.9866     0.0000    24.7890
&BPNODE TNODE=1, TNPC=0, TINTC=0, &END
  92.1611    -0.1118    24.7890
  92.6729    -0.2057    24.7890
  93.4869    -0.2720    24.7890
  94.5478    -0.3044    24.7890
  95.7832    -0.3022    24.7890
  97.1716    -0.2692    24.7890
  98.4121    -0.3248    24.7968
  99.6481    -0.3681    24.7969
 100.7103    -0.3973    24.7967
 101.5257    -0.4146    24.7965
 102.0385    -0.4228    24.7962
 102.214     -0.419     24.7961
&BPNODE TNODE=3, TNPC=0, TINTC=0, &END
&SECT1 STX=0.0, STY=0.0, STZ=0.0, SCALE=1.0, ALF=0.0, THETA=0.0, INMODE=4,
 TNODS=5, TNPS=0, TINTS=0, &END
 102.3341    -0.413     25.1563
 102.1658    -0.3820    25.1557
 101.6708    -0.3073    25.1541
 100.8830    -0.1926    25.1517
  99.8558    -0.0496    25.1487
  98.6588     0.1077    25.1455
  97.3500     0.2647    25.1500
  96.0559     0.2950    25.1500
  94.8500     0.2971    25.1500
  93.8145     0.2655    25.1500
  93.0199     0.2007    25.1500
  92.5204     0.1092    25.1500
  92.3500     0.0000    25.1500
&BPNODE TNODE=1, TNPC=0, TINTC=0, &END
  92.5204    -0.1092    25.1500
  93.0199    -0.2007    25.1500
  93.8145    -0.2655    25.1500
  94.8500    -0.2971    25.1500
  96.0559    -0.2950    25.1500
  97.3293    -0.2638    25.1568
  98.6230    -0.3221    25.1572
  99.8296    -0.3645    25.1573
 100.8663    -0.3930    25.1572
 101.6623    -0.4098    25.1569
 102.1628    -0.4178    25.1567
 102.3341    -0.413     25.1566
&BPNODE TNODE=3, TNPC=0, TINTC=0, &END


&PATCH1 IREV=0, IDPAT=2, MAKE=0, KCOMP=1, KASS=1, IPATSYM=1, IPATCOP=0, &END
 FOG_UAV_BOOM (10X12) CLOSED ENDS
&SECT1 STX=0.0, STY=0.0, STZ=0.0, SCALE=1.0, ALF=0.0, THETA=0.0, INMODE=4,
 TNODS=0, TNPS=0, TINTS=0, &END
  53.5000     0.0000     9.3750
```

```
  53.5000    0.0000    9.3750
  53.5000    0.0000    9.3750
  53.5000    0.0000    9.3750
  53.5000    0.0000    9.3750
  53.5000    0.0000    9.3750
  53.5000    0.0000    9.3750
  53.5000    0.0000    9.3750
  53.5000    0.0000    9.3750
  53.5000    0.0000    9.3750
  53.5000    0.0000    9.3750
&BPNODE TNODE=3, TNPC=0, TINTC=0, &END
&SECT1 STX=0.0, STY=0.0, STZ=0.0, SCALE=1.0, ALF=0.0, THETA=0.0, INMODE=4,
 TNODS=0, TNPS=0, TINTS=0, &END
  53.5000    0.0000    8.5178
  53.5000    0.2731    8.5625
  53.5000    0.5094    8.6857
  53.5000    0.6900    8.8665
  53.5000    0.8127    9.1024
  53.5000    0.8572    9.3738
  53.5000    0.8121    9.6495
  53.5000    0.6885    9.8855
  53.5000    0.5074   10.0658
  53.5000    0.2712   10.1882
  53.5000    0.0000   10.2322
&BPNODE TNODE=3, TNPC=0, TINTC=0, &END
&SECT1 STX=0.0, STY=0.0, STZ=0.0, SCALE=1.0, ALF=0.0, THETA=0.0, INMODE=4,
 TNODS=0, TNPS=0, TINTS=0, &END
  55.1002    0.0000    8.5000
  55.1002    0.2785    8.5455
  55.1002    0.5195    8.6711
  55.1002    0.7046    8.8564
  55.1002    0.8296    9.0971
  55.1002    0.8750    9.3739
  55.1002    0.8290    9.6548
  55.1002    0.7031    9.8956
  55.1002    0.5175   10.0804
  55.1002    0.2766   10.2051
  55.1002    0.0000   10.2500
&BPNODE TNODE=3, TNPC=0, TINTC=0, &END
&SECT1 STX=0.0, STY=0.0, STZ=0.0, SCALE=1.0, ALF=0.0, THETA=0.0, INMODE=4,
 TNODS=0, TNPS=0, TINTS=0, &END
  57.1102    0.0000    8.5000
  57.1102    0.2785    8.5455
  57.1102    0.5195    8.6711
  57.1102    0.7046    8.8564
  57.1102    0.8296    9.0971
  57.1102    0.8750    9.3739
  57.1102    0.8290    9.6548
  57.1102    0.7031    9.8956
  57.1102    0.5175   10.0804
  57.1102    0.2766   10.2051
  57.1102    0.0000   10.2500
&BPNODE TNODE=3, TNPC=0, TINTC=0, &END
&SECT1 STX=0.0, STY=0.0, STZ=0.0, SCALE=1.0, ALF=0.0, THETA=0.0, INMODE=4,
 TNODS=0, TNPS=0, TINTS=0, &END
  59.9757    0.0000    8.5000
  59.9757    0.2785    8.5455
  59.9757    0.5195    8.6711
  59.9757    0.7046    8.8564
  59.9757    0.8296    9.0971
  59.9757    0.8750    9.3739
  59.9757    0.8290    9.6548
  59.9757    0.7031    9.8956
  59.9757    0.5175   10.0804
  59.9757    0.2766   10.2051
  59.9757    0.0000   10.2500
&BPNODE TNODE=3, TNPC=0, TINTC=0, &END
&SECT1 STX=0.0, STY=0.0, STZ=0.0, SCALE=1.0, ALF=0.0, THETA=0.0, INMODE=4,
 TNODS=0, TNPS=0, TINTS=0, &END
  63.8927    0.0000    8.5000
  63.8927    0.2785    8.5455
  63.8927    0.5195    8.6711
  63.8927    0.7046    8.8564
  63.8927    0.8296    9.0971
  63.8927    0.8750    9.3739
  63.8927    0.8290    9.6548
  63.8927    0.7031    9.8956
  63.8927    0.5175   10.0804
  63.8927    0.2766   10.2051
  63.8927    0.0000   10.2500
&BPNODE TNODE=3, TNPC=0, TINTC=0, &END
&SECT1 STX=0.0, STY=0.0, STZ=0.0, SCALE=1.0, ALF=0.0, THETA=0.0, INMODE=4,
 TNODS=0, TNPS=0, TINTS=0, &END
  71.0000    0.0000    8.5000
  71.0000    0.2785    8.5455
  71.0000    0.5195    8.6711
  71.0000    0.7046    8.8564
  71.0000    0.8296    9.0971
  71.0000    0.8750    9.3739
  71.0000    0.8290    9.6548
  71.0000    0.7031    9.8956
  71.0000    0.5175   10.0804
  71.0000    0.2766   10.2051
  71.0000    0.0000   10.2500
&BPNODE TNODE=3, TNPC=0, TINTC=0, &END
&SECT1 STX=0.0, STY=0.0, STZ=0.0, SCALE=1.0, ALF=0.0, THETA=0.0, INMODE=4,
 TNODS=0, TNPS=0, TINTS=0, &END
  78.1073    0.0000    8.5000
  78.1073    0.2785    8.5455
  78.1073    0.5195    8.6711
  78.1073    0.7046    8.8564
  78.1073    0.8296    9.0971
  78.1073    0.8750    9.3739
  78.1073    0.8290    9.6548
  78.1073    0.7031    9.8956
  78.1073    0.5175   10.0804
  78.1073    0.2766   10.2051
  78.1073    0.0000   10.2500
&BPNODE TNODE=3, TNPC=0, TINTC=0, &END
&SECT1 STX=0.0, STY=0.0, STZ=0.0, SCALE=1.0, ALF=0.0, THETA=0.0, INMODE=4,
 TNODS=0, TNPS=0, TINTS=0, &END
  82.0243    0.0000    8.5000
  82.0243    0.2785    8.5455
  82.0243    0.5195    8.6711
  82.0243    0.7046    8.8564
  82.0243    0.8296    9.0971
  82.0243    0.8750    9.3739
  82.0243    0.8290    9.6548
  82.0243    0.7031    9.8956
  82.0243    0.5175   10.0804
  82.0243    0.2766   10.2051
  82.0243    0.0000   10.2500
&BPNODE TNODE=3, TNPC=0, TINTC=0, &END
&SECT1 STX=0.0, STY=0.0, STZ=0.0, SCALE=1.0, ALF=0.0, THETA=0.0, INMODE=4,
 TNODS=0, TNPS=0, TINTS=0, &END
  84.8898    0.0000    8.5000
  84.8898    0.2785    8.5455
  84.8898    0.5195    8.6711
  84.8898    0.7046    8.8564
  84.8898    0.8296    9.0971
  84.8898    0.8750    9.3739
  84.8898    0.8290    9.6548
  84.8898    0.7031    9.8956
  84.8898    0.5175   10.0804
  84.8898    0.2766   10.2051
  84.8898    0.0000   10.2500
&BPNODE TNODE=3, TNPC=0, TINTC=0, &END
&SECT1 STX=0.0, STY=0.0, STZ=0.0, SCALE=1.0, ALF=0.0, THETA=0.0, INMODE=4,
 TNODS=0, TNPS=0, TINTS=0, &END
  86.8998    0.0000    8.5000
```

```
   86.8998    0.2785    8.5455
   86.8998    0.5195    8.6711
   86.8998    0.7046    8.8564
   86.8998    0.8296    9.0971
   86.8998    0.8750    9.3739
   86.8998    0.8290    9.6548
   86.8998    0.7031    9.8956
   86.8998    0.5175   10.0804
   86.8998    0.2766   10.2051
   86.8998    0.0000   10.2500
 &BPNODE TNODE=3, TNPC=0, TINTC=0, &END
 &SECT1 STX=0.0, STY=0.0, STZ=0.0, SCALE=1.0, ALF=0.0, THETA=0.0, INMODE=4,
  TNODS=0, TNPS=0, TINTS=0, &END
   88.5002    0.0000    8.5178
   88.5002    0.2731    8.5625
   88.5002    0.5094    8.6857
   88.5002    0.6900    8.8665
   88.5002    0.8127    9.1024
   88.5002    0.8572    9.3738
   88.5002    0.8121    9.6495
   88.5002    0.6885    9.8855
   88.5002    0.5074   10.0658
   88.5002    0.2712   10.1882
   88.5002    0.0000   10.2322
 &BPNODE TNODE=3, TNPC=0, TINTC=0, &END
 &SECT1 STX=0.0, STY=0.0, STZ=0.0, SCALE=1.0, ALF=0.0, THETA=0.0, INMODE=4,
  TNODS=5, TNPS=0, TINTS=0, &END
   88.5000    0.0000    9.3750
   88.5000    0.0000    9.3750
   88.5000    0.0000    9.3750
   88.5000    0.0000    9.3750
   88.5000    0.0000    9.3750
   88.5000    0.0000    9.3750
   88.5000    0.0000    9.3750
   88.5000    0.0000    9.3750
   88.5000    0.0000    9.3750
   88.5000    0.0000    9.3750
   88.5000    0.0000    9.3750
 &BPNODE TNODE=3, TNPC=0, TINTC=0, &END


 &PATCH1 IREV=0, IDPAT=1, MAKE=0, KCOMP=1, KASS=1, IPATSYM=0, IPATCOP=0, &END
   VERT STAB 0 deg / NO DEFLECTION (10X12)
 &SECT1 STX=0.0, STY=0.0, STZ=0.0, SCALE=1.0, ALF=0.0, THETA=0.0, INMODE=4,
  TNODS=0, TNPS=0, TINTS=0, &END
   97.5000    0.0      10.4000
   97.1593    0.0360   10.4000
   96.1603    0.1029   10.4000
   94.5711    0.2011   10.4000
   92.5000    0.3161   10.4000
   90.0882    0.4315   10.4000
   87.5000    0.5294   10.4000
   84.9118    0.5900   10.4000
   82.5000    0.5942   10.4000
   80.4289    0.5310   10.4000
   78.8397    0.4015   10.4000
   77.8407    0.2183   10.4000
   77.5000    0.0000   10.4000
 &BPNODE TNODE=1, TNPC=0, TINTC=0, &END
   77.8407   -0.2183   10.4000
   78.8397   -0.4015   10.4000
   80.4289   -0.5310   10.4000
   82.5000   -0.5942   10.4000
   84.9118   -0.5900   10.4000
   87.5000   -0.5294   10.4000
   90.0882   -0.4315   10.4000
   92.5000   -0.3161   10.4000
   94.5711   -0.2011   10.4000
   96.1603   -0.1029   10.4000
   97.1593   -0.0360   10.4000
   97.5000    0.0      10.4000
 &BPNODE TNODE=3, TNPC=0, TINTC=0, &END
 &SECT1 STX=0.0, STY=0.0, STZ=0.0, SCALE=1.0, ALF=0.0, THETA=0.0, INMODE=4,
  TNODS=0, TNPS=0, TINTS=0, &END
   97.6187    0.000    10.7610
   97.2821    0.0356   10.7610
   96.2953    0.1016   10.7610
   94.7256    0.1987   10.7610
   92.5590    0.3185   10.7610
   90.2976    0.4262   10.7610
   87.7410    0.5229   10.7610
   85.1845    0.5828   10.7610
   82.8022    0.5869   10.7610
   80.7565    0.5245   10.7610
   79.1868    0.3966   10.7610
   78.2000    0.2157   10.7610
   77.8634    0.0000   10.7610
 &BPNODE TNODE=1, TNPC=0, TINTC=0, &END
   78.2000   -0.2157   10.7610
   79.1868   -0.3966   10.7610
   80.7565   -0.5245   10.7610
   82.8022   -0.5869   10.7610
   85.1845   -0.5828   10.7610
   87.7410   -0.5229   10.7610
   90.2976   -0.4262   10.7610
   92.6799   -0.3122   10.7610
   94.7256   -0.1987   10.7610
   96.2953   -0.1016   10.7610
   97.2821   -0.0356   10.7610
   97.6187    0.0      10.7610
 &BPNODE TNODE=3, TNPC=0, TINTC=0, &END
 &SECT1 STX=0.0, STY=0.0, STZ=0.0, SCALE=1.0, ALF=0.0, THETA=0.0, INMODE=4,
  TNODS=0, TNPS=0, TINTS=0, &END
   97.9631    0.0      11.8085
   97.6387    0.0343   11.8085
   96.6874    0.0980   11.8085
   95.1740    0.1915   11.8085
   92.7472    0.3243   11.8085
   90.9052    0.4109   11.8085
   88.4406    0.5041   11.8085
   85.9760    0.5618   11.8085
   83.6793    0.5658   11.8085
   81.7071    0.5056   11.8085
   80.1938    0.3823   11.8085
   79.2425    0.2079   11.8085
   78.9180    0.0000   11.8085
 &BPNODE TNODE=1, TNPC=0, TINTC=0, &END
   79.2425   -0.2079   11.8085
   80.1938   -0.3823   11.8085
   81.7071   -0.5056   11.8085
   83.6793   -0.5658   11.8085
   85.9760   -0.5618   11.8085
   88.4406   -0.5041   11.8085
   90.9052   -0.4109   11.8085
   93.2019   -0.3010   11.8085
   95.1740   -0.1915   11.8085
   96.6874   -0.0980   11.8085
   97.6387   -0.0343   11.8085
   97.9631    0.0      11.8085
 &BPNODE TNODE=3, TNPC=0, TINTC=0, &END
 &SECT1 STX=0.0, STY=0.0, STZ=0.0, SCALE=1.0, ALF=0.0, THETA=0.0, INMODE=4,
  TNODS=0, TNPS=0, TINTS=0, &END
   98.4996    0.0      13.4401
   98.1940    0.0323   13.4401
   97.2979    0.0923   13.4401
   95.8725    0.1804   13.4401
   93.0906    0.3301   13.4401
   91.8516    0.3871   13.4401
   89.5302    0.4748   13.4401
   87.2087    0.5292   13.4401
```

```
 85.0454    0.5330   13.4401
 83.1878    0.4763   13.4401
 81.7624    0.3601   13.4401
 80.8663    0.1958   13.4401
 80.5607    0.0000   13.4401
&BPNODE TNODE=1, TNPC=0, TINTC=0, &END
 80.8663   -0.1958   13.4401
 81.7624   -0.3601   13.4401
 83.1878   -0.4763   13.4401
 85.0454   -0.5330   13.4401
 87.2087   -0.5292   13.4401
 89.5302   -0.4748   13.4401
 91.8516   -0.3871   13.4401
 94.0149   -0.2835   13.4401
 95.8725   -0.1804   13.4401
 97.2979   -0.0923   13.4401
 98.1940   -0.0323   13.4401
 98.4996    0.0      13.4401
&BPNODE TNODE=3, TNPC=0, TINTC=0, &END
&SECT1 STX=0.0, STY=0.0, STZ=0.0, SCALE=1.0, ALF=0.0, THETA=0.0, INMODE=4,
 TNODS=0, TNPS=0, TINTS=0, &END
 99.1756    0.0      15.4960
 98.8938    0.0298   15.4960
 98.0673    0.0851   15.4960
 96.7527    0.1664   15.4960
 95.0394    0.2615   15.4960
 93.6103    0.3318   15.4960
 90.9031    0.4380   15.4960
 88.7620    0.4881   15.4960
 86.7668    0.4916   15.4960
 85.0535    0.4393   15.4960
 83.7389    0.3321   15.4960
 82.9124    0.1806   15.4960
 82.6305    0.0000   15.4960
&BPNODE TNODE=1, TNPC=0, TINTC=0, &END
 82.9124   -0.1806   15.4960
 83.7389   -0.3321   15.4960
 85.0535   -0.4393   15.4960
 86.7668   -0.4916   15.4960
 88.7620   -0.4881   15.4960
 90.9031   -0.4380   15.4960
 93.6103   -0.3318   15.4960
 95.0394   -0.2615   15.4960
 96.7527   -0.1664   15.4960
 98.0673   -0.0851   15.4960
 98.8938   -0.0298   15.4960
 99.1756    0.0      15.4960
&BPNODE TNODE=3, TNPC=0, TINTC=0, &END
&SECT1 STX=0.0, STY=0.0, STZ=0.0, SCALE=1.0, ALF=0.0, THETA=0.0, INMODE=4,
 TNODS=0, TNPS=0, TINTS=0, &END
 99.9250    0.00     17.7750
 99.6694    0.0270   17.7750
 98.9202    0.0772   17.7750
 97.7283    0.1509   17.7750
 96.1750    0.2371   17.7750
 94.3000    0.3265   17.7750
 92.4250    0.3971   17.7750
 90.4839    0.4425   17.7750
 88.6750    0.4456   17.7750
 87.1217    0.3982   17.7750
 85.9298    0.3011   17.7750
 85.1806    0.1637   17.7750
 84.9250    0.0000   17.7750
&BPNODE TNODE=1, TNPC=0, TINTC=0, &END
 85.1806   -0.1637   17.7750
 85.9298   -0.3011   17.7750
 87.1217   -0.3982   17.7750
 88.6750   -0.4456   17.7750
 90.4839   -0.4425   17.7750
 92.4250   -0.3971   17.7750
 94.3661    0.3236   17.7750
 96.1750   -0.2371   17.7750
 97.7283   -0.1509   17.7750
 98.9202   -0.0772   17.7750
 99.6694   -0.0270   17.7750
 99.9250    0.00     17.7750
&BPNODE TNODE=3, TNPC=0, TINTC=0, &END
&SECT1 STX=0.0, STY=0.0, STZ=0.0, SCALE=1.0, ALF=0.0, THETA=0.0, INMODE=4,
 TNODS=0, TNPS=0, TINTS=0, &END
 100.6744   0.00     20.0540
 100.4451   0.0242   20.0540
 99.7731    0.0692   20.0540
 98.7039    0.1353   20.0540
 97.3106    0.2126   20.0540
 95.1090    0.3144   20.0540
 93.9469    0.3562   20.0540
 92.2057    0.3969   20.0540
 90.5832    0.3997   20.0540
 89.1899    0.3572   20.0540
 88.1208    0.2701   20.0540
 87.4487    0.1469   20.0540
 87.2195    0.0000   20.0540
&BPNODE TNODE=1, TNPC=0, TINTC=0, &END
 87.4487   -0.1469   20.0540
 88.1208   -0.2701   20.0540
 89.1899   -0.3572   20.0540
 90.5832   -0.3997   20.0540
 92.2057   -0.3969   20.0540
 93.9469   -0.3562   20.0540
 95.6881   -0.2903   20.0540
 97.3106   -0.2126   20.0540
 98.7039   -0.1353   20.0540
 99.7731   -0.0692   20.0540
 100.4451  -0.0242   20.0540
 100.6744   0.00     20.0540
&BPNODE TNODE=3, TNPC=0, TINTC=0, &END
&SECT1 STX=0.0, STY=0.0, STZ=0.0, SCALE=1.0, ALF=0.0, THETA=0.0, INMODE=4,
 TNODS=0, TNPS=0, TINTS=0, &END
 101.3504   0.00     22.1099
 101.1449   0.0217   22.1099
 100.5424   0.0620   22.1099
 99.5841    0.1213   22.1099
 98.3351    0.1906   22.1099
 96.8807    0.2602   22.1099
 95.9413    0.2981   22.1099
 93.7590    0.3558   22.1099
 92.3046    0.3583   22.1099
 91.0556    0.3202   22.1099
 90.0972    0.2421   22.1099
 89.4948    0.1317   22.1099
 89.2893    0.0000   22.1099
&BPNODE TNODE=1, TNPC=0, TINTC=0, &END
 89.4948   -0.1317   22.1099
 90.0972   -0.2421   22.1099
 91.0556   -0.3202   22.1099
 92.3046   -0.3583   22.1099
 93.7590   -0.3558   22.1099
 95.9413   -0.2981   22.1099
 96.8807   -0.2602   22.1099
 98.3351   -0.1906   22.1099
 99.5841   -0.1213   22.1099
 100.5424  -0.0620   22.1099
 101.1449  -0.0217   22.1099
 101.3504   0.00     22.1099
&BPNODE TNODE=3, TNPC=0, TINTC=0, &END
&SECT1 STX=0.0, STY=0.0, STZ=0.0, SCALE=1.0, ALF=0.0, THETA=0.0, INMODE=4,
 TNODS=0, TNPS=0, TINTS=0, &END
 101.8869   0.00     23.7415
 101.7002   0.0197   23.7415
 101.1530   0.0564   23.7415
```

```
 100.2826    0.1102    23.7415
  99.1481    0.1731    23.7415
  97.8271    0.2364    23.7415
  96.6709    0.2815    23.7415
  94.9917    0.3232    23.7415
  93.6707    0.3255    23.7415
  92.5363    0.2908    23.7415
  91.6658    0.2199    23.7415
  91.1186    0.1196    23.7415
  90.9320    0.0000    23.7415
&BPNODE TNODE=1, TNPC=0, TINTC=0, &END
  91.1186   -0.1196    23.7415
  91.6658   -0.2199    23.7415
  92.5363   -0.2908    23.7415
  93.6707   -0.3255    23.7415
  94.9917   -0.3232    23.7415
  96.6709   -0.2815    23.7415
  97.8271   -0.2364    23.7415
  99.1481   -0.1731    23.7415
 100.2826   -0.1102    23.7415
 101.1530   -0.0564    23.7415
 101.7002   -0.0197    23.7415
 101.8869    0.00      23.7415
&BPNODE TNODE=3, TNPC=0, TINTC=0, &END
&SECT1 STX=0.0, STY=0.0, STZ=0.0, SCALE=1.0, ALF=0.0, THETA=0.0, INMODE=4,
 TNODS=0, TNPS=0, TINTS=0, &END
 102.2313    0.00      24.7890
 102.0568    0.0184    24.7890
 101.5450    0.0527    24.7890
 100.7310    0.1030    24.7890
  99.6701    0.1619    24.7890
  98.4347    0.2210    24.7890
  97.1716    0.2692    24.7890
  95.7832    0.3022    24.7890
  94.5478    0.3044    24.7890
  93.4869    0.2720    24.7890
  92.6729    0.2057    24.7890
  92.1611    0.1118    24.7890
  91.9866    0.0000    24.7890
&BPNODE TNODE=1, TNPC=0, TINTC=0, &END
  92.1611   -0.1118    24.7890
  92.6729   -0.2057    24.7890
  93.4869   -0.2720    24.7890
  94.5478   -0.3044    24.7890
  95.7832   -0.3022    24.7890
  97.1716   -0.2692    24.7890
  98.4347   -0.2210    24.7890
  99.6701   -0.1619    24.7890
 100.7310   -0.1030    24.7890
 101.5450   -0.0527    24.7890
 102.0568   -0.0184    24.7890
 102.2313    0.00      24.7890
&BPNODE TNODE=3, TNPC=0, TINTC=0, &END
&SECT1 STX=0.0, STY=0.0, STZ=0.0, SCALE=1.0, ALF=0.0, THETA=0.0, INMODE=4,
 TNODS=5, TNPS=0, TINTS=0, &END
 102.3500    0.00      25.1500
 102.1796    0.0180    25.1500
 101.6801    0.0514    25.1500
 100.8855    0.1006    25.1500
  99.8500    0.1580    25.1500
  98.6441    0.2158    25.1500
  97.3500    0.2647    25.1500
  96.0559    0.2950    25.1500
  94.8500    0.2971    25.1500
  93.8145    0.2655    25.1500
  93.0199    0.2007    25.1500
  92.5204    0.1092    25.1500
  92.3500    0.0000    25.1500
&BPNODE TNODE=1, TNPC=0, TINTC=0, &END
  92.5204   -0.1092    25.1500
  93.0199   -0.2007    25.1500
  93.8145   -0.2655    25.1500
  94.8500   -0.2971    25.1500
  96.0559   -0.2950    25.1500
  97.3500   -0.2647    25.1500
  98.6441   -0.2158    25.1500
  99.8500   -0.1580    25.1500
 100.8855   -0.1006    25.1500
 101.6801   -0.0514    25.1500
 102.1796   -0.0180    25.1500
 102.3500    0.00      25.1500
&BPNODE TNODE=3, TNPC=0, TINTC=0, &END

&WAKE1   IDWAK=1,        IFLXW=1,       ITRFTZ= 1,      INTRW= 0,        &END
WING_WAKE_tip_to_tip
&WAKE2   KWPACH=18,       KWSIDE=4,      KWLINE=0,       KWPAN1=0,
           KWPAN2=0,       NODEW=0,       INITIAL=0,                     &END
&WAKE2   KWPACH=16,       KWSIDE=4,      KWLINE=0,       KWPAN1=0,
           KWPAN2=0,       NODEW=0,       INITIAL=0,                     &END
&WAKE2   KWPACH=14,       KWSIDE=4,      KWLINE=0,       KWPAN1=0,
           KWPAN2=0,       NODEW=0,       INITIAL=0,                     &END
&WAKE2   KWPACH=8,        KWSIDE=3,      KWLINE=15,      KWPAN1=1,
           KWPAN2=1,       NODEW=0,       INITIAL=0,                     &END
&WAKE2   KWPACH=10,       KWSIDE=2,      KWLINE=3,       KWPAN1=1,
           KWPAN2=5,       NODEW=0,       INITIAL=0,                     &END
&WAKE2   KWPACH=12,       KWSIDE=2,      KWLINE=3,       KWPAN1=1,
           KWPAN2=7,       NODEW=0,       INITIAL=0,                     &END
&WAKE2   KWPACH=12,       KWSIDE=3,      KWLINE=7,       KWPAN1=13,
           KWPAN2=15,      NODEW=0,       INITIAL=0,                     &END
&WAKE2   KWPACH=11,       KWSIDE=3,      KWLINE=7,       KWPAN1=1,
           KWPAN2=3,       NODEW=0,       INITIAL=0,                     &END
&WAKE2   KWPACH=11,       KWSIDE=4,      KWLINE=13,      KWPAN1=2,
           KWPAN2=8,       NODEW=0,       INITIAL=0,                     &END
&WAKE2   KWPACH=9,        KWSIDE=4,      KWLINE=13,      KWPAN1=1,
           KWPAN2=5,       NODEW=0,       INITIAL=0,                     &END
&WAKE2   KWPACH=7,        KWSIDE=3,      KWLINE=15,      KWPAN1=4,
           KWPAN2=4,       NODEW=0,       INITIAL=0,                     &END
&WAKE2   KWPACH=13,       KWSIDE=2,      KWLINE=0,       KWPAN1=0,
           KWPAN2=0,       NODEW=0,       INITIAL=0,                     &END
&WAKE2   KWPACH=15,       KWSIDE=2,      KWLINE=0,       KWPAN1=0,
           KWPAN2=0,       NODEW=0,       INITIAL=0,                     &END
&WAKE2   KWPACH=17,       KWSIDE=2,      KWLINE=0,       KWPAN1=0,
           KWPAN2=0,       NODEW=5,       INITIAL=0,                     &END


&WAKE1   IDWAK=1,        IFLXW=1,       ITRFTZ= 1,      INTRW= 0,        &END
 ENGINE_PYLON_WAKE
&WAKE2   KWPACH=22,       KWSIDE=3,      KWLINE=0,       KWPAN1=0,
           KWPAN2=0,       NODEW=3,       INITIAL=0,                     &END


&WAKE1   IDWAK=1,        IFLXW=1,       ITRFTZ= 1,      INTRW= 0,        &END
 RIGHT_HORIZ_TAIL_WAKE
&WAKE2   KWPACH=21,       KWSIDE=4,      KWLINE=1,       KWPAN1=0,
           KWPAN2=0,       NODEW=3,       INITIAL=0,                     &END

&WAKE1   IDWAK=1,        IFLXW=1,       ITRFTZ= 1,      INTRW= 0,        &END
LEFT_HORIZ_TAIL_WAKE
&WAKE2   KWPACH=22,       KWSIDE=4,      KWLINE=1,       KWPAN1=0,
           KWPAN2=0,       NODEW=3,       INITIAL=0,                     &END

&WAKE1   IDWAK=1,        IFLXW=1,       ITRFTZ= 1,      INTRW= 1,        &END
 VERT_TAIL_WAKE
&WAKE2   KWPACH=23,       KWSIDE=4,      KWLINE=1,       KWPAN1=0,
           KWPAN2=0,       NODEW=5,       INITIAL=0,                     &END


&ONSTRM  NONSL =0,  KPSL =     1,                                        &END
```

```
&BLPARAM RN =929000,    VISC = 0.022641, NSLBL = 1,                    &END

&VS1     NVOLR= 0,        NVOLC= 0,                                     &END
&VS2     X0=     -0.1000, Y0=     1.5000, Z0=    -0.1000, INTVSR= 1,    &END
&VS3     X1=     -0.1000, Y1=     1.5000, Z1=     0.1000, NPT1=  0,     &END
&VS4     X2=     -0.1000, Y2=     1.5000, Z2=     0.1000, NPT2= 20,     &END
&VS5     X3=      1.1000, Y3=     1.5000, Z3=    -0.1000, NPT3= 25,     &END

&VS6     XR0=     2.0000, YR0=    2.0000, ZR0=    0.0000, INTVSC= 1,    &END
&VS7     XR1=     4.0000, YR1=    2.0000, ZR1=    0.0000,
           XR2=    2.0000, YR2=    2.0000, ZR2=    1.0000,              &END
&VS8     R1=      0.1000, R2=     1.0000, PHI1=  0.0,     PHI2=360.0,   &END
&VS9     NRAD=   5,       NPHI=  12,       NLEN=  3,                    &END


&SLIN1   NSTLIN=4,                                                      &END
&SLIN2   SX0=    -6.5000, SY0=    2.50000, SZ0=   7.5000,
           SU=      2.0000, SD=    2.0000, DS=     0.100, INTSL= 1,     &END
&SLIN2   SX0=    -8.25000, SY0=    0.00000, SZ0=   7.5000,
           SU=      2.0000, SD=    2.0000, DS=     0.100, INTSL= 1,     &END

&SLIN2   SX0=    -6.5000, SY0=    2.50000, SZ0=   7.5000,
           SU=     15.0000, SD=   100.0000, DS=     0.500, INTSL= 1,    &END
&SLIN2   SX0=    -8.25000, SY0=    0.00000, SZ0=   7.5000,
           SU=     15.0000, SD=   100.0000, DS=     0.500, INTSL= 1,    &END
```

APPENDIX D

MATLAB SCRIPT FOR DYNAMIC MODE ANALYSIS

```
% froguav.m: This MATLAB script calculates FROG UAV dynamics.  Eigenvalue modal analysis
%            and response to control input is obtained for three aerodynamic models.
%
clear

%  Calculate trim lift and drag coefficients

% FROG Trim condition

       W = 67.73;                     % lbs
       m = W/32.2;                    % slugs
       S =  2530/144;                 % ft^2, 2530 in^2
       V = 88;                        % ft/s = 1056 in/s
       M = V/1118;                    % trim mach number
       cbar = 20/12;                  % ft = 20 in
       b = 126.5/12;                  % ft = 124 in
       rho = 0.002327;                % slugs/ft^3 800 ft MSL std day
       cruise_HP = 5;
       etaP = 0.35;
       L_D=7;
       CL0 = 0.4295;
       Ixx = 12.52; Iyy = 8.43; Izz = 18.55; Ixz=0; %slugs-ft^2
       q = 0.5*rho*(V)^2;
       CL = W/(q*S);

%  Input the non-dimensional stab derivatives:

% ******************************************************************************************
for i = 1:3

 if i==1

   source='CMARC'

   %   Longitudinal Stability Derivatives
   D_L_D=W/L_D;CD_L_D = D_L_D/(q*S);               % Drag from Lift to Drag Ratio
   Tr=cruise_HP*etaP*550/V; CD_Tr=Tr/(q*S);        % Drag from thrust required calculation
   CD=(CD_L_D +CD_Tr)/2;                           % CD averaged from both methods
   CLalpha = 4.845; CDalpha = 0.2664; CMalpha = -0.4126;
   CLalphadot = 1.420; CMalphadot = -6.264; CDalphadot = 0;         % Assumed to be small
   alphatrim = 0;                      % radians
   theta0 = alphatrim;
   CLmach = 0; CDmach = 0; CMmach = 0;
   CLq = 6.82; CMq = -11.78; CDq = 0;                               % Assumed to be small
   CLde = 0.4378; CMde = -1.199; CDde = 0.0092;                     % Induced drag contribution only

   %   Lateral - Directional Stability Derivatives

   CYbeta = -0.2493; Clbeta = -0.0630;Cnbeta = 0.0630;
   Clp = -0.4514; Cnp = -0.0220; CYp = 0.0488;
   Clr = 0.1210; Cnr = -0.1210; CYr = 0.3370;
   Cldr = 0.0040; Cndr = -0.0453; CYdr = 0.0928;
   Clda = 0.1943; Cnda = -0.0121; CYda = -0.0206;

  elseif i==2

   source='Classical_Analysis'

   %   Longitudinal Stability Derivatives
   D_L_D=W/L_D;CD_L_D = D_L_D/(q*S);               % Drag from Lift to Drag Ratio
   Tr=cruise_HP*etaP*550/V; CD_Tr=Tr/(q*S);        % Drag from thrust required calculation
   CD=(CD_L_D +CD_Tr)/2;                           % CD averaged from both methods

   CLalpha = 4.82; CDalpha = 0.253; CMalpha = -0.70 % d_epsilon/d_alpha = 0.40

   CLalphadot = 1.56; CMalphadot = -4.14; CDalphadot = 0;           % Assumed to be small
   alphatrim = 0;                                                   % radians
   theta0 = alphatrim;
   CLmach = 0; CDmach = 0; CMmach = 0;
   CLq = 3.89; CMq = -11.39; CDq = 0;                               % Assumed to be small
   CLde = 0.39; CMde = -1.04; CDde = 0.00;
```

```
%   Lateral - Directional Stability Derivatives

CYbeta = -0.511; Clbeta = -0.055;Cnbeta = 0.051;
Clp = -0.300; Cnp = -0.072; CYp = 0;                               % Assumed to be small
Clr = 0.168; Cnr = -0.0762; CYr = 0.140;
Cldr = 0.0056; Cndr = -0.0341; CYdr = 0.081;
Clda = 0.213; Cnda = -0.0236; CYda = -0.00;

else

    source='Parameter_Analysis'

%   Longitudinal Stability Derivatives
CL = 0.4295; CD = 0.0614;
CLalpha = 4.0907; CDalpha = 0.23; CMalpha = -0.4174;
CLalphadot = 1.3877; CMalphadot = -3.7115; CDalphadot = 0;        % Assumed to be small
alphatrim = 0;                          % radians
theta0 = alphatrim;
CLmach = 0; CDmach = 0; CMmach = 0;
CLq = 3.35; CMq = -8.8818; CDq = 0;                                % Assumed to be small
CLde = 1.1249; CMde = -1.6208; CDde = 0.0676;

%   Lateral - Directional Stability Derivatives

CYbeta = -0.9867; Clbeta = -0.0942;Cnbeta = 0.1755;
Clp = -0.4483; Cnp = -0.1077; CYp = 0;                             % Assumed to be small
Clr = 0.2078; Cnr = -0.1212; CYr = 0.1096;
Cldr = 0.0004; Cndr = -0.0785; CYdr = 0.0926;
Clda = 0.2387; Cnda = -0.0261; CYda = 0;


end

% Calculate the Dimensional Stability Derivatives

Xu = -q*S/(m*V)*(2*CD+M*CDmach);          % Xu - 1/sec , assumes dCD/dM=0 (ie no Mach effect)
Xalpha = q*S/m*(CL-CDalpha);              % Xalpha - ft/sec^2
Xalphadot = -q*S/m*cbar/(2*V)*CDalphadot; % Xalphadot - ft/sec
Xq = -q*S/m*cbar/(2*V)*CDq;               % Xq - ft/sec
Xde = -q*S/m*CDde;                        % Xde - ft/sec^2

Zu = -q*S/(m*V)*(2*CL+M*CLmach);          % Zu - 1/sec , assumes dCL/dM=0 (ie no Mach effect)
    Zalpha = -q*S/m*(CD+CLalpha);         % Zalpha - ft/sec^2
    Zalphadot = -q*S/m*cbar/(2*V)*CLalphadot;    % Zalphadot - ft/sec
Zq = -q*S/m*cbar/(2*V)*CLq ;                     % Zq - ft/sec
Zde = -q*S/m*CLde;                               % Zde - ft/sec^2

Mu = q*S*cbar/(Iyy*V)*CMmach;                    % Mu - ft/sec
Malpha = q*S*cbar/Iyy*CMalpha;                   % Malpha - 1/sec^2
Malphadot = q*S*cbar/Iyy*cbar/(2*V)*CMalphadot;  % Malphadot - 1/sec
Mq = q*S*cbar/Iyy*cbar/(2*V)*CMq;                % Mq - 1/sec
Mde = q*S*cbar/Iyy*CMde;                         % Mde - 1/sec^2


% Linearized Longitudinal 4x4 Plant Matrix

% Form the An Bn and In plant matrices

An = [V*Xu Xalpha 0 -32.17*cos(theta0); V*Zu Zalpha (V+Zq) -32.17*sin(theta0);
V*Mu Malpha Mq 0; 0 0 1 0];
Bn = [Xde Zde Mde 0]';
In = [V 0 0 0; 0 (V-Zalphadot) 0 0; 0 -Malphadot 1 0; 0 0 0 1];

A = inv(In)*An;
B = inv(In)*Bn;

% Find Short and Long Period Natural Frequency and damping

out=source
out='Longitudinal mode E-values'
P = poly(A);
```

```
  R = roots(P)
  out='Short Period'
  phi = angle(R);
  Z1(i) = (1/(1+tan(phi(1))^2))^.5
  Wn1(i) = real(R(1))/(-Z1(i))
  Wd1(i) = (1-Z1(i)^2)^.5*Wn1(i);
  Td1(i) = 2*pi/Wd1(i);

 out='Long Period'

  Z3(i) = (1/(1+tan(phi(3))^2))^.5
  Wn3(i) = real(R(3))/(-Z3(i))
  Wd3(i) = (1-Z3(i)^2)^.5*Wn3(i);
  Td3(i) = 2*pi/Wd3(i);

 out='Step response'

  C1=[1 0 0 0;0 1 0 0;0 0 1 0; 0 0 0 1]; D1=0;
  U=zeros(1001,1);
  U(101:1001)=-2/57.3;
  t=(0:.01:10);
  SYS=ss(A,B,C1,D1);
  [Y,T]=lsim(SYS,U,t);
  tl=t;
  de_s=U*57.3;
  alpha_s(:,i)=Y(:,2)*57.3;
  pr_s(:,i)=Y(:,3)*57.3;
  theta_s(:,i)=Y(:,4)*57.3;

  C1=[1 0 0 0;0 1 0 0;0 0 1 0; 0 0 0 1]; D1=0;
  U=zeros(1001,1);
  U(101:160)=-5/57.3;
  U(161:220)=5/57.3;
  t=(0:.01:10);
  SYS=ss(A,B,C1,D1);
  [Y,T]=lsim(SYS,U,t);
  tl=t;
  de_d=U*57.3;
  alpha_d(:,i)=Y(:,2)*57.3;
  pr_d(:,i)=Y(:,3)*57.3;
  theta_d(:,i)=Y(:,4)*57.3;


% Lateral-Directional 4x4 Plant Matrix


 % Calculate the Dimensional Stability Derivatives

  Ybeta = q*S/m*(CYbeta);                          % Ybeta - ft/sec^2
  Yp = q*S/m*b/(2*V)*CYp;                          % Yp - ft/sec
  Yr = q*S/m*b/(2*V)*CYr;                          % Yr - ft/sec
  Yda = q*S/m*CYda;                                % Yda - ft/sec^2
  Ydr = q*S/m*CYdr;                                % Ydr - ft/sec^2

  Lbeta = q*S*b/Ixx*(Clbeta);                      % Lbeta - 1/sec^2
  Lp = q*S*b/Ixx*b/(2*V)*Clp;                      % Lp - 1/sec
  Lr = q*S*b/Ixx*b/(2*V)*Clr;                      % Lr - 1/sec
  Lda = q*S*b/Ixx*Clda;                            % Lda - 1/sec^2
  Ldr = q*S*b/Ixx*Cldr;                            % Ldr - 1/sec^2

  Nbeta = q*S*b/Izz*(Cnbeta);                      % Nbeta - 1/sec^2
  Np = q*S*b/Izz*b/(2*V)*Cnp;                      % Np - 1/sec
  Nr = q*S*b/Izz*b/(2*V)*Cnr;                      % Nr - 1/sec
  Nda = q*S*b/Izz*Cnda;                            % Nda - 1/sec^2
  Ndr = q*S*b/Izz*Cndr;                            % Ndr - 1/sec^2


  % Linearized Longitudinal 4x4 Plant Matrix

  source
```

```
longmodes='Lateral Directional 4x4 Plant Matrix'

   % Form the An Bn and In plant matrices

   Cn = [Ybeta Yp 32.17*cos(theta0) (Yr-V); Lbeta Lp 0 Lr; 0 1 0 0; Nbeta Np 0 Nr];
   Dn = [Yda Lda 0 Nda; Ydr Ldr 0 Ndr]';
   IIn = [V 0 0 0; 0 1 0 -Ixz/Ixx; 0 0 1 0; 0 -Ixz/Izz 0 1];

   C = inv(IIn)*Cn;
   D = inv(IIn)*Dn;

   % Find Dutch roll, roll and spiral Natural Frequency and damping

   out='Lateral Directional mode E-values'

   P1 = poly(C);

   R1 = roots(P1)

 if i==1

   out='Dutch Roll Mode'

   phi = angle(R1);
   Z2(i) = (1/(1+tan(phi(2))^2))^.5
   Wn2(i) = real(R1(2))/(-Z2(i))
   Wd2(i) = (1-Z2(i)^2)^.5*Wn2(i);
   Td2(i) = 2*pi/Wd2(i);

  out='Roll Mode'
  roll(i) = (R1(1))
  out='Spiral Mode'
  Spiral(i) = (R1(4));

 elseif i==2

   out='Dutch Roll Mode'

   phi = angle(R1);
   Z2(i) = (1/(1+tan(phi(1))^2))^.5
   Wn2(i) = real(R1(1))/(-Z2(i))
   Wd2(i) = (1-Z2(i)^2)^.5*Wn2(i);
   Td2(i) = 2*pi/Wd2(i);
   out='Roll Mode'
   roll(i) = (R1(3))
   out='Spiral Mode'
   Spiral(i) = (R1(4));

 else

   out='Dutch Roll Mode'
   phi = angle(R1);
   Z2(i) = (1/(1+tan(phi(1))^2))^.5
   Wn2(i) = real(R1(1))/(-Z2(i))
   Wd2(i) = (1-Z2(i)^2)^.5*Wn2(i);
   Td2(i) = 2*pi/Wd2(i);
   out='Roll Mode'
   roll(i) = (R1(3))
   out='Spiral Mode'
   Spiral(i) = (R1(4))

end
% Aileron step

   C1=[1 0 0 0;0 1 0 0;0 0 1 0; 0 0 0 1]; D1=0;
   U=zeros(1001,2);
   U(101:1001,1)=2/57.3;
   t=(0:.01:10);
   SYS=ss(C,D,C1,D1);
   [Y,T]=lsim(SYS,U,t);
```

```
    tld=t;
    da_sa=U*57.3;
    rr_sa(:,i)=Y(:,2)*57.3;
    phi_sa(:,i)=Y(:,3)*57.3;
    beta_sa(:,i)=Y(:,1)*57.3;

    % Aileron doublet


    C1=[1 0 0 0;0 1 0 0;0 0 1 0; 0 0 0 1]; D1=0;
    U=zeros(1001,2);
    U(101:175,1)=-5/57.3;
    U(176:250,1)=5/57.3;
    t=(0:.01:10);
    SYS=ss(C,D,C1,D1);
    [Y,T]=lsim(SYS,U,t);
    tld=t;
    da_da=U*57.3;
    rr_da(:,i)=Y(:,2)*57.3;
    phi_da(:,i)=Y(:,3)*57.3;
    beta_da(:,i)=Y(:,1)*57.3;


% Rudder step

    C1=[1 0 0 0;0 1 0 0;0 0 1 0; 0 0 0 1]; D1=0;
    U=zeros(101,2);
    U(101:1001,2)=2/57.3;
    t=(0:.01:10);
    SYS=ss(C,D,C1,D1);
    [Y,T]=lsim(SYS,U,t);
    tld=t;
    dr_sr=U*57.3;
    beta_sr(:,i)=Y(:,1)*57.3;
    lr_sr(:,i)=Y(:,2)*57.3;
    rr_sr(:,i)=Y(:,4)*57.3;

    % Rudder doublet

    C1=[1 0 0 0;0 1 0 0;0 0 1 0; 0 0 0 1]; D1=0;
    U=zeros(1001,2);
    U(101:175,2)=-5/57.3;
    U(176:250,2)=5/57.3;
    t=(0:.01:10);
    SYS=ss(C,D,C1,D1);
    [Y,T]=lsim(SYS,U,t);
    tld=t;
    dr_dr=U*57.3;
    beta_dr(:,i)=Y(:,1)*57.3;
    lr_dr(:,i)=Y(:,2)*57.3;
    rr_dr(:,i)=Y(:,4)*57.3;

end
%**********************************************************************************************
% Plot Responses
% Plot Elevator Step Response
figure
 subplot(4,1,1), plot(tl,de_s),title('LONGITUDINAL RESPONSE TO A 2 DEGREE ELEVATOR STEP
INPUT'),ylabel('Elevator (deg)'),axis([0 5 -4 4]),grid
 subplot(4,1,2), plot(tl,alpha_s(:,1),'-.',tl,alpha_s(:,2),'--',tl,alpha_s(:,3),'-'),ylabel('A.O.A
(deg)'),axis([0 5 -5 10]),grid
 subplot(4,1,3), plot(tl,pr_s(:,1),'-.',tl,pr_s(:,2),'--',tl,pr_s(:,3),'-'),ylabel('q
(deg/s)'),axis([0 5 -20 20]),grid
 subplot(4,1,4), plot(tl,theta_s(:,1),'-.',tl,theta_s(:,2),'--',tl,theta_s(:,3),'-'),ylabel('Theta
(deg)'),grid
 xlabel('Time (sec)') ,axis([0 5 -10 50]), pause,
 legend('CMARC','Classical','Parameter Est      ',0)

 % Plot Elevator Doublet Response
 figure
```

```
 subplot(4,1,1), plot(tl,de_d),title('LONGITUDINAL RESPONSE TO A 5 DEGREE ELEVATOR
DOUBLET'),ylabel('Elevator (deg)'),axis([0 5 -10 10]),grid
 subplot(4,1,2), plot(tl,alpha_d(:,1),'-.',tl,alpha_d(:,2),'--',tl,alpha_d(:,3),'-'),ylabel('A.O.A
(deg)'),axis([0 5 -12 12]),grid
 subplot(4,1,3), plot(tl,pr_d(:,1),'-.',tl,pr_d(:,2),'--',tl,pr_d(:,3),'-'),ylabel('q
(deg/s)'),axis([0 5 -60 50]),grid
 subplot(4,1,4), plot(tl,theta_d(:,1),'-.',tl,theta_d(:,2),'--',tl,theta_d(:,3),'-'),ylabel('Theta
(deg)'),grid
 xlabel('Time (sec)'),,axis([0 5 -10 30]),pause
 legend('CMARC','Classical','Parameter Est      ',0)

 % Plot Aileron Step Response
figure
 subplot(4,1,1), plot(tld,da_sa(:,1)),title('LATERAL-DIRECTIONAL RESPONSE TO A 2 DEGREE AILERON
STEP INPUT'),ylabel('Aileron (deg)'),axis([0 5 -4 4]),grid
 subplot(4,1,2), plot(tld,rr_sa(:,1),'-.',tld,rr_sa(:,2),'--',tld,rr_sa(:,3),'-'),ylabel('p
(deg/s)'),axis([0 5 -10 25]),grid
 subplot(4,1,3), plot(tld,phi_sa(:,1),'-.',tld,phi_sa(:,2),'--',tld,phi_sa(:,3),'-'),ylabel('Bank
Angle (deg)'),axis([0 5 -10 70]),grid
 subplot(4,1,4), plot(tld,beta_sa(:,1),'-.',tld,beta_sa(:,2),'--',tld,beta_sa(:,3),'-
'),ylabel('Beta (deg)'),grid
 xlabel('Time (sec)') ,axis([0 5 -5 10]), pause,
 legend('CMARC','Classical','Parameter Est      ',0)

 % Plot Aileron Doublet Response
figure
 subplot(4,1,1), plot(tld,da_da(:,1)),title('LATERAL-DIRECTIONAL RESPONSE TO A 5 DEGREE AILERON
DOUBLET'),ylabel('Aileron (deg)'),axis([0 8 -10 10]),grid
 subplot(4,1,2), plot(tld,rr_da(:,1),'-.',tld,rr_da(:,2),'--',tld,rr_da(:,3),'-'),ylabel('p
(deg/s)'),axis([0 8 -50 60]),grid
 subplot(4,1,3), plot(tld,phi_da(:,1),'-.',tld,phi_da(:,2),'--',tld,phi_da(:,3),'-'),ylabel('Bank
Angle (deg)'),axis([0 8 -30 10]),grid
 subplot(4,1,4), plot(tld,beta_da(:,1),'-.',tld,beta_da(:,2),'--',tld,beta_da(:,3),'-
'),ylabel('Beta (deg)'),grid
 xlabel('Time (sec)'),axis([0 8 -10 15]), pause,
 legend('CMARC','Classical','Parameter Est      ',0)

  % Plot Rudder Step Response
figure
 subplot(4,1,1), plot(tld,dr_sr(:,2)),title('LATERAL-DIRECTIONAL RESPONSE TO A 2 DEGREE RUDDER STEP
INPUT'),ylabel('Rudder (deg)'),axis([0 8 -4 4]),grid
 subplot(4,1,2), plot(tld,beta_sr(:,1),'-.',tld,beta_sr(:,2),'--',tld,beta_sr(:,3),'-
'),ylabel('Beta (deg)'),axis([0 8 -1 3]),grid
 subplot(4,1,3), plot(tld,rr_sr(:,1),'-.',tld,rr_sr(:,2),'--',tld,rr_sr(:,3),'-'),ylabel('r
(deg/s)'),axis([0 8 -10 5]),grid
 subplot(4,1,4), plot(tld,lr_sr(:,1),'-.',tld,lr_sr(:,2),'--',tld,lr_sr(:,3),'-'),ylabel('p
(deg/s)'),grid
 xlabel('Time (sec)'),axis([0 8 -5 10]), pause,
 legend('CMARC','Classical','Parameter Est      ',0)

 % Plot Rudder Doublet Response
figure
 subplot(4,1,1), plot(tld,dr_dr(:,2)),title('LATERAL-DIRECTIONAL RESPONSE TO A 5 DEGREE RUDDER
DOUBLET'),ylabel('Rudder (deg)'),axis([0 8 -10 10]),grid
 subplot(4,1,2), plot(tld,beta_dr(:,1),'-.',tld,beta_dr(:,2),'--',tld,beta_dr(:,3),'-
'),ylabel('Beta (deg)'),axis([0 8 -10 10]),grid
 subplot(4,1,3), plot(tld,rr_dr(:,1),'-.',tld,rr_dr(:,2),'--',tld,rr_dr(:,3),'-'),ylabel('r
(deg/s)'),axis([0 8 -30 30]),grid
 subplot(4,1,4), plot(tld,lr_dr(:,1),'-.',tld,lr_dr(:,2),'--',tld,lr_dr(:,3),'-'),ylabel('p
(deg)'),grid
 xlabel('Time (sec)'), ,axis([0 8 -20 20]),pause,
 legend('CMARC','Classical','Parameter Est      ',0)
```

LIST OF REFERENCES

1. Pollard, S., "*Evaluation of the CMARC Panel Code Software Suite for the Development of a UAV Aerodynamic Model*," Master's Thesis, Naval Postgraduate School, Monterey, CA, June 1997.

2. Papageorgiou, E., "*Development of a Dynamic Model for a UAV*," Master's Thesis, Naval Postgraduate School, Monterey, CA, March 1997.

3. Garrison, P., and Pinella, D., *CMARC User's Guide*, AeroLogic, Inc, http://www.iac.net/~aerol, 1996.

4. Bertin, J. J., and Smith, M. L., *Aerodynamics for Engineers*, Prentice Hall, 1989.

5. Ashby, D. L., Dudley, M. R., Iguchi, S. K., Browne, L., and Katz, J., *Potential Flow Theory and Operation Guide for the Panel Code PMARC_12*, NASA TM-102851, Ames Research Center, Moffet Field, CA., December 1992.

6. Anderson, J. D., *Fundamentals of Aerodynamics*, McGraw-Hill, Inc., 1991.

7. Lambert, M. A., *Evaluation of the NASA-AMES Panel Method (PMARC) for Aerodynamic Missile Design*, Master's Thesis, Naval Postgraduate School, CA, September, 1995.

8. Tuncer, I. H., and Platzer, M. F., *PMARC Potential Flow Solutions with Wakes Over an Ogive Cylinder at High Incidence*, AIAA Paper No. 97-1968, American Institute of Aeronautics and Astronautics, June 1997.

9. Cebeci, T., "*Computation of Three-Dimensional Boundary Layers Including Separation*," VKI Lecture Series, Douglas Aircraft Company, April 1986.

10. Young, A. D., *Boundary Layers*, American Institute of Aeronautics, 1989.

11. *Performance Phase Textbook-Volume I*, USAF Test Pilot School, Edwards AFB, CA., June 1988.

12. Roskam, J., *Airplane Flight Dynamics and Automatic Flight Controls*, Roskam Aviation and Engineering Corporation, 1979.

13. Etkin, B., *Dynamics of Flight - Stability and Control*, John Wiley & Sons, Inc., 1959.

14. Schmidt, L, V., *Introduction to Aircraft Flight Dynamics*, American Institute of Aeronautics and Astronautics, 1998.

15. Roskam, J., *Methods for Estimating Stability and Control Derivatives of Conventional Subsonic Airplanes*, Roskam Aviation and Engineering Corporation, 1971.

16. Nicolai, L. M., *Fundamentals of AIRCRAFT DESIGN*, METs, Inc., 1984.

17. Walden, A. B., van Dam, C. P., and Brandon, J. M., *Modeling of the Interaction Between a Lifting Wing and a Following Aircraft and Comparison with Experimental Results*, AIAA 96-0771, 34th Aerospace Sciences Meeting and Exhibit, Reno, NV, January 1996.

INITIAL DISTRIBUTION LIST

1. Defense Technical Information Center..2
   8725 John J. Kingman Road, Ste 0944
   Ft. Belvoir, VA 22060-6218

2. Dudley Knox Library..2
   Naval Postgraduate School
   411 Dyer Rd.
   Monterey, CA 93943-5101

3. Chairman...1
   Department of Aeronautics and Astronautics, Code AA
   Naval Postgraduate School
   699 Dyer Road, Room 137
   Monterey, CA 93943-5106

4. Dr. Max F. Platzer...4
   Department of Aeronautics and Astronautics, Code AA/PL
   Naval Postgraduate School
   699 Dyer Road, Room 137
   Monterey, CA 93943-5106

5. Dr. Louis. V. Schmidt...1
   Department of Aeronautics and Astronautics, Code AA
   Naval Postgraduate School
   699 Dyer Road, Room 137
   Monterey, CA 93943-5106

6. Dr. Isaac I. Kaminer...1
   Department of Aeronautics and Astronautics, Code AA
   Naval Postgraduate School
   699 Dyer Road, Room 137
   Monterey, CA 93943-5106

7. Dr. Kevin Jones..1
   Department of Aeronautics and Astronautics, Code AA
   Naval Postgraduate School
   699 Dyer Road, Room 137
   Monterey, CA 93943-5106

8. CDR Stephen J. Pollard.. 2
Department of Aviation Safety
Naval Postgraduate School
1588 Cunningham Road, Room E-303
Monterey, CA 93943-5202

9. Peter Garrison... 1
AeroLogic, Inc.
1613 Altivo Way
Los Angeles, CA 90026